19th International Symposium on "Yacht Design and Yacht Construction"

Amsterdam, 13 & 14 November 2006

PROCEEDINGS

Edited by Piet W. de Heer

November 2006

Organized by HISWA - National Association of Watersport Industries in The Netherlands,
The International Trade Show of Marine Equipment METS 2006
Delft University of Technology

Delft University of Technology
Ship Hydromechanics Laboratory

Printed by:

CENDRIS CMC DELFT
Leeghwaterstraat 42
2628 CA Delft

Phone: +31 (0)15 2786012
Fax: +31 (0)15 2781749

KONINKLIJKE BIBLIOTHEEK, DEN HAAG

19th International Symposium on "Yacht Design and Yacht Construction": Proceedings of the19th International Symposium on "Yacht Design and Yacht Construction", Amsterdam, 13 & 14 November 2006 – Delft University of Technology, Ship Hydromechanics laboratory, The Netherlands.
ISBN: 90-811322-1-0
Subject headings: Yacht Design, Yacht Construction

TABLE OF CONTENTS

Program Monday November 13, 2006

Moderator: **Jack Somer**

08:30 – 10:00	Registration
10:00 – 10:30	Opening
10:30 – 11:00	**Session 1:** The "Axe Bow Concept": The shape of ships to come - Jaap Gelling
11:00 – 11:30	Coffee Break
11:30 – 12:00	**Session 2:** The Modern Super-yacht - James Roy
12:00 – 12:30	**Session 3:** Investigation of sustainable technologies for the design, construction, operation and decommissioning of recreational craft - Richard Birmingham and Melanie Landamore
12:30 – 14:30	Lunch Break
14:30 – 15:00	**Session 4:** An investigation of aerodynamic force modeling for IMS rule using wind tunnel techniques - Fabio Fossati
15:00 – 15:30	**Session 5:** The Carbon and PBO RIG for the „Sailovation" – Finite Element Analysis - Guenter Grabe
15:30 – 16:00	Tea Break
16:00 – 16:30	**Session 6:** Interactions between Yacht-Crew Systems and Racing Scenarios combining behavioral models with VPPs - Ajit Shenoi
16:30 – 17:00	**Session 7:** Does it pay to play with the construction? Comparative analysis of a sailing yacht performance due to the building materials - Balázs Hunyadi
17:00 – 17:30	Welcome Reception
18:00 – 18:15	Boarding to Symposium Dinner
18:30 – 21:00	Symposium Dinner at Restaurant d'Vijff Vlieghen in Amsterdam

Program Tuesday November 14, 2006

Moderator: **Jack Somer**

08:30 – 09:00	Registration
09:00 – 09:30	**Session 8:** Development of the structural requirements in the Volvo Open 70 rule version 2 - Ian Campbell
09:30 – 10:00	**Session 9:** An experimental study of the hydrodynamics of a yacht with a canting keel and forward rudder - Florent Maes
10:00 – 10:30	Coffee Break
10:30 – 11:00	**Session 10:** The influence of the shape of the keel on the forces on the rudder of a sailing yacht - Jan Alexander Keuning
11:00 – 11:15	Closing

Introduction

Here for the 19th time in front of you lie the Proceedings of the International HISWA Symposium on Yacht Design and Construction.

The Organizing Committee is proud that the HISWA Symposium may be held now for the 19th time, meaning that it is the oldest and the longest existing symposium in this field on the world.
As such it has always drawn the attention of all who are active in the world of yachting and certainly contributed to the excellent the name of the Dutch designers and builders as leading in the field of Innovation, Research and Development.
It has also shown that, certainly during this period, the liaison between “the theory” and “the practice” in the Netherlands is very strong, apparent fruitful and quite alive. The short “lines” and the short “distances” between all kind of interesting industries, research institutes and technical highly developed parties makes the field in the Netherlands very interesting and very innovative. In this field the Symposium has always played an important role.

The partners that organize the Symposium, i.e. the HISWA Association, the METS Marine Equipment Trade Show and the Shiphydromechanics Department of the Delft University of Technology, all three find the symposium of strong interest for their constituencies: the industry, the trade, the research field and the education . For the third time now the Symposium is organized in cooperation with the Royal Institute of Naval Architects (RINA) of London, which strengthens it’s role in the international arena.

To select the right topics of interest and to guard over the quality of the papers the Paper Committee has played an important role again. The members of this Committee perform their task out of the spotlights, but take it very seriously and they earn the full gratitude for their efforts by both the organizers and the delegates. There is a good mix of topics now with special interest to some new areas.

Finally I would like to express our gratitude to our sponsors: MARIN, FEADSHIP and GDNP. Without their support the Symposium would be difficult to organize. And in particular it would not be possible to ask for such a low fee for students. In addition to this by connecting their names to the Symposium they underline and appreciate its importance.

I hope you will enjoy the material supplied and the gathering at the symposium itself. I hope you will be able to meet a lot of interesting people, who are attending the symposium. This time and the times to come!

Jan Alexander Keuning
Chairman Symposium Organizing Committee

Session 1

Jaap Gelling

The Axe Bow: The Shape of Ships to Come

by

J.L. Gelling, Product Director High Speed & Naval Craft, Damen Shipyards Gorinchem
jlg@damen.nl

Introduction

Damen Shipyards has been involved in the Fast Workboats market for over 30 years. In this period, a lot has changed. The ongoing demand for higher speed through the years has in many cases resulted in the replacement of steel as a hull construction material by aluminium and composites. Also, totally new markets have developed in the past decades. Initially, only law enforcing authorities required high speed workboats for their patrol tasks. Nowadays, all kind of commercial and non-profit organizations make use of high speed boats, e.g. Crew Boats, Fast Suppliers, Survey Boats and Life Boats.
In many cases Fast Workboats are used for 5000-6000 hours per year, whatever the sea conditions. Flat water performance therefore is not the yardstick. It is the speed that can be reached in adverse conditions that really counts in the design of Fast Workboats. The limiting factor in this respect is not determined by propulsion or resistance characteristics, but by the behaviour of the ship in waves. Too high vertical acceleration levels will impede work and life on board, cause sea sickness, wear out the crew and eventually will damage the ship's structure.

Realizing the importance of sea-keeping characteristics, the Product Group "High Speed & Naval Craft" of Damen Shipyards has for a long time co-operated closely with the Delft Shiphydromechanics Department (Delft University). As a result of extensive research projects, some significant successes were achieved in the past ten years. In the following chapters, the "Enlarged Ship Concept" and the "Axe Bow Concept" are described. Finally an analysis is made of possible application of the Axe Bow in yacht design.

The Enlarged Ship Concept

In 1995, Delft University and Damen Shipyards carried out a desk study on the influence of hull lengthening on the "practical characteristics" of a ship. In this study, a 26 m Damen Patrol Boat was taken as the "parent ship". In two steps the hull of this design was lengthened respectively by 25% and 50%, See Figure 1. Similar studies were carried out before, but in this case it was decided to keep the functionality of the two lengthened versions completely equal to the original design. In other words, only the hull length was varied, the accommodation, superstructure, speed and range were all untouched. For the three designs, the following "practical characteristics" were determined:

- Building cost
- Operational cost (i.e. mainly fuel)
- Transport efficiency
- Operability (i.e. sea-keeping characteristics)

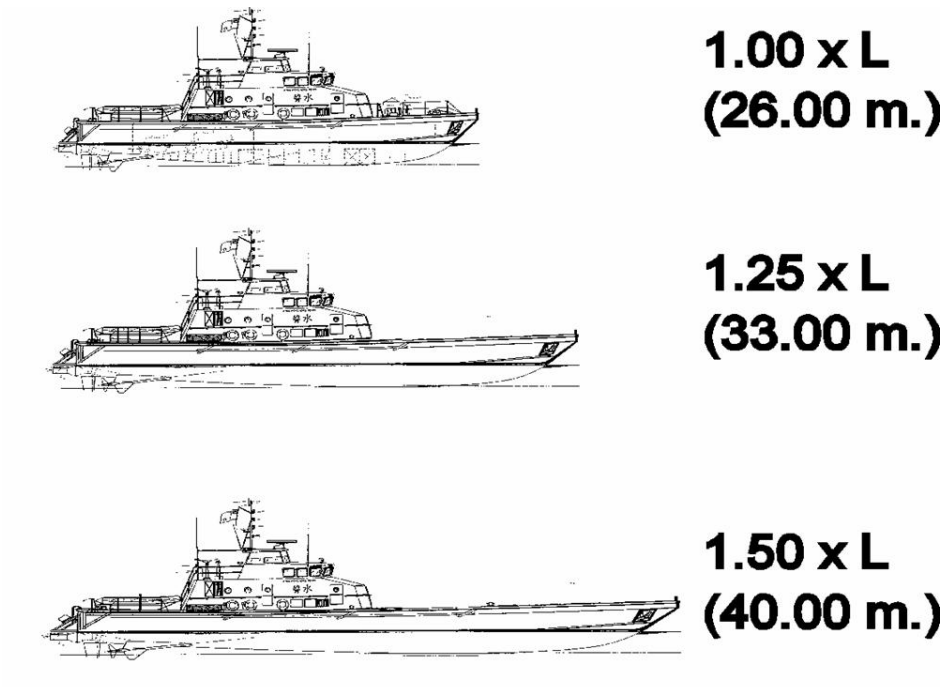

Figure 1: The Designs in the Enlarged Ship Concept (ESC) study

Comparing the results of the three variants, some very interesting conclusions were drawn for the lengthened designs:

- Building costs are only influenced marginally by the hull length, due to the fact that the extra length is “empty”.
- Operational costs decrease, due to lower resistance
- Transport Efficiency increases significantly
- Operability increases significantly

In Table 1, the results of this analysis are summarized. For comparison reasons, the reference characteristics of the parent design are defined as 100% in Table 1.

	26 m parent design	25% enlarged hull	50% enlarged hull
Building costs	100%	103%	106%
Operational costs	100%	94%	93%
Transport Efficiency	100%	154%	167%
Operability	100%	135%	168%

Table 1: Comparison of “practical characteristics” of a 26m patrol boat with 2 enlarged variants

The final conclusion of the “Enlarged Ship” desk study was that – at equal functionality - a ship significantly profits from lengthening the hull.

In the study, the hulls were lengthened by simply increasing frame spacing. Realizing that the forward part of an enlarged ship is relatively empty, it was concluded that some of the volume and the deck area could be sacrificed in order to optimize the fore ship for sea-keeping characteristics. This was done in 1997, during the design of Patrol Boats for the Coastguard of the Netherlands Antilles and Aruba. A conventional 35 m design was enlarged to 42 m and the fore ship was designed to minimize vertical accelerations. IN Figure 2, the linesplans of the non-optimized and of the optimized Enlarged Ship design are shown.

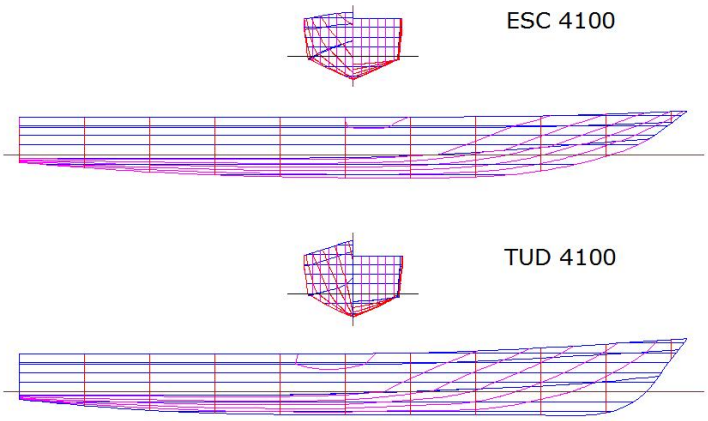

Figure 2: Line plans of the ESC 4100 and the TUD 4100 with improved bow shape

Extensive towing tank tests were carried out, which confirmed the forecast superior sea-keeping characteristics of the 42 m design. See Figure 3 for the comparison of the "vertical acceleration distribution" between the original 35 m design and the 42 m "Enlarged Ship".

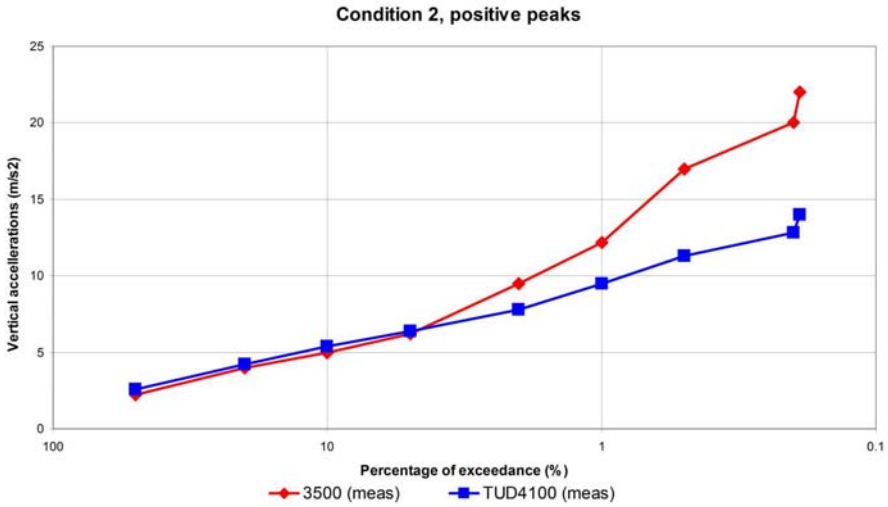

Figure 3: Distribution of peaks in the vertical accelerations in the wheelhouse for the ESC 4100 and the TUD 4100

In 1999 the first Patrol Boat (Stan Patrol 4207) of the enlarged design was delivered. The ship showed the expected excellent sea-keeping characteristics, both in the North Sea and the Caribbean. Figure 4 shows a picture of this first "Enlarged Ship".
For a more elaborate explanation of the Enlarged Ship Concept, see Keuning e.a. Ref [1].

Figure 4 : The first Stan Patrol 4207

The Axe Bow Concept

Prediction of the operability of surface ships commonly is carried out with the use of linear theory based calculation methods. In the standard procedure, the seakeeping behaviour of a ship in a specific operating area is obtained by combining the Response Amplitude Operators (RAO's) of the motions with the wave spectra derived from scatter diagrams. The performance of a design is then determined on the basis of the "root-mean-square" (rms) or the "significant values" ($a_{1/3}$) of the calculated motions and accelerations.
This standard procedure however is not really applicable for fast craft, due to the strong non linearity's in the response of high speed ships to incoming waves.
According to Keuning e.a. (Ref [2]), the limiting criteria for safe operations of fast ships should be based on the actual distribution of the peaks and troughs of the responses (motions, accelerations) in irregular waves rather than on the average or significant values. In this procedure extensive time simulations have to be made in order to determine whether the limiting criteria for the safe operation of the ship under consideration are superseded or not. This is much more time consuming than the "linear" operability analyses carried out using the RAO's.

In order to determinate realistic limiting criteria for the operation of fast ships in irregular waves, the Delft Shiphydromechanics Department has carried out extensive series of full-scale experiments with fast patrol boats and SAR vessels on the North Sea. These were not limited purely to objective measurements, but also the opinion of the crews was taken into account.

Some very interesting conclusions were drawn from these studies:

- All crews decided for a voluntary speed reduction at roughly the same conditions on board the ship.
- The reason for voluntary speed reduction was not the magnitude of the significant amplitude of motions or vertical accelerations, but the occurrence of high vertical acceleration peaks.
- The voluntary speed reduction after a very big peak in vertical accelerations had just one reason: to prevent a repeat of such a high peak.

Clearly, most people react to “extremes” and not to “averages”. Therefore, it is apparent that research on optimization of sea-keeping behaviour should not be focussed on “significant values”, but on decreasing the high peaks in the response of a ship in irregular waves. For this goal, in 2003 a research project was started with the following participants:

- Delft Shiphydromechanics Department
- Royal Netherlands Navy
- US Coast Guard
- Maritime Research Institute Netherlands
- Royal Schelde (Damen Shipyards Group)
- High Speed & Naval Craft product group of Damen Shipyards Gorinchem

Based on an “Enlarged Ship” design, two hull forms were derived with significantly different fore body shapes.

The first variant is a Wave Piercer, designed to go through - instead of over – the waves, thereby limiting vertical accelerations.

The second variant was called the “Axe Bow Concept”, due to the peculiar Axe-shaped bow. As a first step in the design of what would become the “Axe Bow”, the pitching motion equation was analyzed. It was concluded that the level of vertical accelerations will decrease when the bow has a relatively low and non-progressive increase of buoyancy in pitching. This can be reached when the bow has a very fine entry, the sections are extremely narrow V-shaped and the flare above the waterline is limited as much as possible. In analogy with a mass-spring system, compared to a conventional bow the Axe Bow “softens” the spring and thereby decreases the vertical accelerations. The result however is that the pitching amplitude itself will increase somewhat due to the “softer spring” behaviour. For this reason the bow is very high (to forestall deck wetness) and extremely deep, in order to exclude the risk of slamming.

The same principles had been applied already (although to a lesser extent) in the optimization of the Enlarged Ship Concept in 1997. The Axe Bow design therefore could be regarded as an extreme version of the Enlarged Ship Concept.
Figures 5a, 5b and 5c, respectively show the models of the parent Enlarged Ship, the Wave Piercer and the Axe Bow Concept.

The following model test series were carried out with the three models:

- resistance tests (0 to 50 knots)
- head waves (25, 35 and 50 knots)
- following waves (25, 35 and 50 knots)
- free running with stern quartering waves (25, 35 and 50 knots)

Figure 5a: Model according to the Enlarged Ship Concept (ESC)

Figure 5b: Model according to the Wave Piercer Concept (WPC)

Figure 5c: Model according to the AXE Bow Concept (ABC)

All tests in waves were carried out in irregular waves, presenting a JONSWAP wave spectrum shape. The significant wave heights were 2, 2.5, 3, 3.5 and 4 m. The other integral wave parameters were constant: mean zero crossing period 6 s, peak period 7.8 s and gamma 3.3.

Compared to the performance of the “Enlarged Ship” parent model, the following conclusions were drawn for the Wave Piercer and the Axe Bow Concept:

Conclusions for the Wave Piercer:

- The flat water resistance of the Wave Piercer was the lowest of the three models. This probably is the result of the fact that the Wave Piercer had the longest underwater body (at the same waterline length) and the finest entry of the three models.
- In head seas the Wave Piercer performed quite well – as long as only focussing on the measurement results. Viewing the model test videos however, the picture changes dramatically. The model took so much water over the bow, even at lower speeds, that it

was decided not to test the Wave Piercer at the highest speed. The chance of loosing the model due to nose-diving was considered too high.

- Free running tests in quartering waves were not carried out with the Wave Piercer model, as the partners in the research project agreed that these expensive tests were of limited value, considering the disappointing performance of the Wave Piercer model in head waves.

Conclusions for the Axe Bow Concept:

- The highest measured vertical accelerations on the Axe Bow Concept proved to be 50% below those of the Enlarged Ship Concept. This notable improvement in sea-keeping performance becomes even more significant when realizing that the Enlarged Ship Concept already decreased peak vertical accelerations with 50% over conventional hull forms.
  In Figure 6 the sea-keeping performance of the Axe Bow is compared to the Enlarged Ship. This graph shows the probability of exceeding peak vertical accelerations in Sea State 5.
- Up to a speed of 35 knots, compared to the Enlarged Ship Concept, the flat water resistance of the Axe Bow is approximately 5% lower.
- During the free running tests in stern quartering waves, the necessary steering corrections for keeping track were very similar for the Axe Bow and the Enlarged Ship model. Both models did not broach, despite the very serious wave conditions.

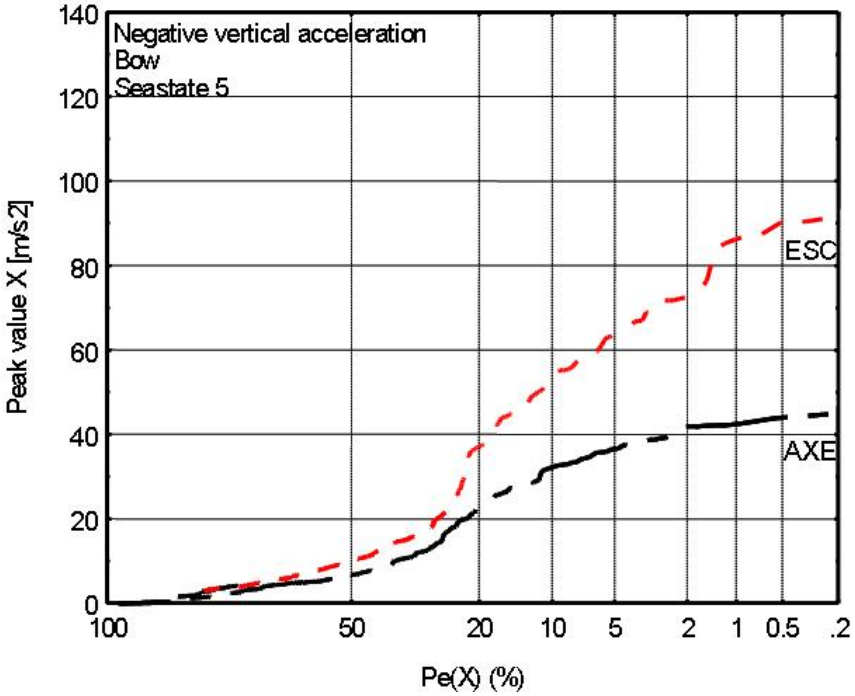

Figure 6: Distribution of peaks in the vertical accelerations at the bow Of the model according to the ESC and ABC

Based on the favourable characteristics of the Axe Bow Concept, Damen has designed a series of Fast Crew Suppliers and Patrol Boats. Figure 7 shows a 33 m Fast Crew Supplier in service in Mexico, appropriately named “Axebow 101” by the owner.

Figure 7: Fast Crew Supplier build according to the AXE Bow Concept

Axe Bows on Yachts?

In the design of Fast Workboats, optimization of functionality is the main objective. Only at a much lower priority, attention is given to styling. “Form follows function” clearly is the guiding principle for Fast Workboats. As a matter of fact this not only holds for the designers, but also for the users.

In general, the emphasis in yacht design is much more on styling than on pure functionality. This however does not obstruct application of the Axe Bow Concept in yacht design – but the owner clearly has to be interested in modern styling.

A yacht will particularly benefit from an Axe Bow, when it combines the following characteristics:

- Relatively high speed
  At relatively high speed, semi-displacement yachts with conventional hull forms will suffer from slamming at moderate to high sea states. This will be totally excluded with an Axe Bow hull shape.
- Long offshore cruising (or transits)
  In case a yacht is offshore for longer periods, it is impossible to shelter during adverse weather. Therefore, the hull design of these yachts should be focused on sea-keeping characteristics. The Axe Bow will significantly decrease the level of vertical accelerations and thereby will make life on board much more comfortable.

As mentioned earlier, the Axe Bow is an extreme version of the Enlarged Ship Concept. An Axe Bow yacht therefore should be relatively slender and light, in order not to spoil the hydrodynamic concept. This implies that an Axe Bow yacht has limited available volume for its length. As well as this, the volume should not be completely used in order to keep the ship light enough. Roughly, it can be concluded that a 50 m Axe Bow yacht should be compared with a 43-44 m conventional yacht. This however should not be regarded as a drawback, as the extra meters come at a low price and bring some very interesting features:

- Superior sea-keeping characteristics with total absence of slamming.
- Lower resistance at high speed due to longer waterline and slender lines plan. Apart from obvious merits as higher speed or less power, the low resistance hull shape yields the possibility of using steel as the hull construction material. This will have positive effects on stability and will decrease fatigue issues for larger sized yachts.
- Notably lower resistance at cruising/transit speed compared to more conventional semi-displacement and planing hull forms. This clearly has a very positive effect on the fuel consumption and thereby on the maximum range of a yacht.

In Figure 8 an artist's impression is given of a 50 m Axe Bow yacht.

Figure 8: AXE Bow Yacht artist impression.

Conclusions

In general, the following can be concluded for the Axe Bow Concept:

- The Axe Bow Concept decreases the level of peak vertical accelerations by 50% compared to the Enlarged Ship Concept (which already decreased peak vertical accelerations by 50% over conventional hull forms).
- Up to a speed of 35 knots, the flat water resistance of the Axe Bow is approximately 5% lower compared to the Enlarged Ship Concept (which already decreased flat water resistance significantly over conventional hull forms).
- Despite the deep fore foot, the Axe Bow Concept does not show a tendency to broach, when fitted with the right appendages.

Although developed for Fast Workboats like Fast Crew Suppliers and Patrol Boats, the Axe Bow Concept could be interesting for yachts. Particularly at relatively high speeds, and when used for serious offshore cruising, a yacht could clearly benefit from an Axe Bow. It must be realized however that an Axe Bow design should be relatively slender and light, in order not to spoil the hydrodynamic concept. Therefore, a 50 m Axe Bow yacht should be compared with a 43-44 m conventional yacht. This should not be regarded as a drawback, as these extra meters come at a low price, make life on board much more comfortable, and will reduce fuel consumption as a further bonus

References:

[1] Keuning, J.A. and Walree, F van
The Comparison of the hydrodynamic behavior of three fast patrol boats with special hull geometries
Proceedings of the HIPER 2006 Conference on high performance marine vehicles, Launceston Tasmania November 2006

[2] Keuning, J A and Pinkster J (1995)
"Optimization of the seakeeping behaviour of a fast monohull",
Proceedings Of Fifth International Conference on Fast Sea Transportation (FAST 1995) pp. 179-193

[3] Keuning, J A and Pinkster, J. (1997):
"Further Designs and Seakeeping Investigations in the Enlarged Ship Design"
Proceedings of 6th International Conference on Fast Sea Transportation (FAST 1997) Sydney, pp 201-209

[4] Keuning, J A , Pinkster J and Van Walree, F. (2002):
"Further Investigations into the Hydrodynamic Performance of the AXE Bow Concept"
Proc. of the 6th Symposium on High Speed Marine Vehicles (WEMT 2002),Castello di Baia, Italy 2002 pp II 25-II 38

Session 2

James Roy

The Modern Superyacht ; Enlarged Yacht or Smaller Ship?

James Roy, Yacht Design Manager, BMT Nigel Gee and Associates Ltd

Summary

The increasing size of the modern superyacht is pushing the boundaries of traditional yacht architecture. Large yachts are now more akin to small ships and the naval architecture, engineering and procurement of such vessels demands an increasingly rigorous approach. Coupled with ever increasing requirements for increased range, reduced noise levels and good seakeeping ability the engineering of these vessels requires a multi-disciplined approach with increasingly higher level technical input essential from the early conceptual design stage.

Within this paper the Author will examine a number of areas where mature technology developed within the commercial shipping industry is now being adopted in the yacht market and where some requirements specific to the large motor yachts are leading to adaptation of existing technology.

Introduction

Yacht design is often referred to as a careful blend of art and science. Historically the role of the yacht designer has encompassed both these disciplines with the successful designers of yesteryear possessing a good eye for style whilst integrating the latest technology through sound engineering skills.

Today the situation has changed somewhat with the role of the designer /stylist often separated from that of the naval architect. Projects generally begin life on the drawing board of the stylist and whilst he may have a good judgement for engineering aspects, the fact is that as yachts get larger and more technically complex there is an ever growing need for fundamental multi-disciplined engineering input from the earliest design stages. Whilst this separation of disciplines can often stimulate innovation with the creativity of the designer/stylist pushing the engineering boundaries, it also often leads to un-necessary compromise in some fundamental engineering aspects.

The size of the modern superyacht has grown rapidly in the last 10 years with vessels of 80m now being common place and yachts of up to 162m have been successfully constructed.

The technical demands required of these large motor yachts are generally encapsulated in the following fundamental requirements;

- Increased range capability and good seakeeping through close attention to optimisation of hull and propulsion system
- Stabilisation at rest
- Exceptionally low noise and vibration levels
- Good manoeuvrability and increasingly a requirement for DP capability

It is these fundamental requirements that are driving the leading naval architects and builders to adopt and adapt technology normally found in the commercial ship market.

Hullform Development

Examination of the trends in large (circa 80m) modern displacement motor yacht characteristics indicates that the majority operate with a length displacement of between 5 and 7 and a Froude number of up to 0.36. Given these two parameters the modern fleet shares some similar characteristics with the modern commercial ro-pax vessel.

These vessels mostly operate at a sub-hump Froude number of around 0.35. Hull forms are therefore more traditional displacement forms and the uniform operational profile results in most vessels utilising a bulbous bow. The current state the art hull-forms incorporate twin screws (either conventional props or podded drives) with wide-radius tunnels over the propellers and "gooseneck" type bulbous bows. Bulbous bow technology is largely mature yet a variety of different forms still prevail whilst differences in geometry are subtle.

Stern forms developed incorporate generally quite shallow buttock angles with wide and flatter stern sections. One form developed, termed a so-called "wave damping" afterbody, incorporates refinements of these features. The "wave damping" effect is reportedly achieved by careful hull form development featuring a long flat run aft, and a section shape which promotes buttock flow with optimised hull form coefficients and curve of sectional areas. Essentially this from is describing a properly optimised after body which results in a low wave making resistance component by limiting running trim without recourse to excessive trim wedges, whilst ensuring a good uniform flow into the propulsors.

Ducktails are also incorporated in many modern commercial forms. Typical improvements in resistance of over 5% are possible with the use of a ducktail. As Froude number increases the ducktails should ideally incorporate a slight trim wedge to control dynamic running trim. On yacht forms this is often observed as a discreet trim wedge but in the Authors experience it is better integrated as a return in the buttock lines. Return angles of not more than 2-3 degrees should be required to control running trim on a properly optimised form. Ducktails in effect offer an increase in length and many yachts essentially feature these as there is often a large, low freeboard bathing / boarding platform which serves the same purpose hydrodynamically as a ducktail as described.

Despite the requirement for increased range, a significant number of yachts do not utilise bulbous bows for practical reasons as they can cause problems when at anchor. Additionally given the operational profile of some yachts there may be little practical benefit from fitting a bulb with regard to overall fuel economy. At service speed however a bulb can offer a resistance reduction of up to 15% and should always be considered. Stern geometry is often constrained by the volumetric requirements of the large lazarette that feature on all yachts and often this results in a greater transom immersion and steeper buttock angles than are desirable hydrodynamically.

A specific example in the development of an 80m yacht is presented where a conventional yacht from, derived principally from smaller yachts and progressively scaled over a series of vessels of increasing size, was optimised utilising some of the aforementioned features. A parent form and resistance characteristics were provided to BMT Nigel Gee and Associates as a basis and the task set to conduct lines development and optimisation.

The initial optimisation process suggested by the yard involved testing a single model with multiple interchangeable bulbous bows including tests without a bulb. The Author does not however recommend this approach as the fitment of a bulb to a hullform demands refinement of the waterlines forward in close association with each bulb derivative. Additionally the bulb gives careful control over the LCB characteristics of a hullform and to remove an interchangeable bulb and replace with a non bulbous form leads to a non comparative analysis of LCB values and consequentially requires a different stern geometry to be used.

A revised optimisation process was proposed as follows;

- Optimise sectional area curve as far as possible within current state of the art practice
- Undertake comparative CFD studies on three different bulbous bow forms
- Perform model tests on the best form
- From model test observations and results refine lines further
- Test final form

The initial process involved optimisation of the sectional area curve and principal characteristics. From this a first iteration of the hull lines was derived (Iteration 1, Figure 1). These were largely derived from proven Ro-Pax and yacht forms within the main parameters of the parent hull. The lines incorporated the aforementioned gooseneck type bulbous bows featuring a slender neck and reverse form with the volume distribution concentrated near the DWL. The stern form adopted was partially based on the features previously described, however the constrains imposed by the requirement for a large and deep lazarette for tender stowage prohibited optimisation of the stern as much as would have been liked. A shallow trim wedge of 2 degrees was integrated by introduction of return in the buttocks.

From iteration 1 two further forms were developed; iteration 2 has the bulb volume raised somewhat so that the upper surface of the bulb is in contact with the DWL and the neck of the bulb has been narrowed slightly further. Iteration 3 has the bulb lengthened by around 1.5% LWL and a steeper return profile on the centerline buttock. It should be appreciated that these changes are only subtle, modification to the yachts bow profile was prohibited for styling reasons and this imposed subsequent limitations on the extent of geometric variations that could be explored. The principal characteristics of the variants and those of the parent from are presented in Figure 2.

CFD analysis was undertaken at three ship speeds, 12, 14 and 16 knots. The analysis consisted of inviscid free-surface calculations providing the wave pattern and wave resistance. The pressure distribution on the hull in the bulb/bow area at speed 14 kn are shown in Figure 3. The streamline originating at the bulb/stem intersection is also visualized in these figures.

Figure 4 illustrates that there are small differences in computed resistance between the three designs, however the bulb design of iteration 1 was slightly better than iteration 2 or 3. It was concluded that the knuckle line of iteration three was more optimum as it was better aligned with the local streamline.

Following the CFD analysis a final form, iteration 4 was developed based on a marriage of the iteration 1 and 3 forms. This was tested at Marintek in Norway. A comparison of the CR values across the speed range is presented in Figure 5. It can be seen that at a Froude number of 0.31 (relating to 16 knots) the achieved improvement in CR is in the region of 25% over the parent from. A further form was developed (iteration 5) as a result of testing which incorporated some stern modifications to reduce the trim wedge by straightening of the aft buttocks to almost completely remove the integrated stern wedge, leading to a further resistance reduction.

Whilst most significant yachts received this type of hullform optimisation process it is in many cases normal for this to be carried out fairly late in the design process (either post contract or very near to contract signature) with the result that the hydrodynamic package is often severely constrained by the arrangements agreed between the stylist and the owner. A better design process is to have the naval architect involved early in the design so that the hullform can be developed in parallel with the vessels arrangement and the right level of compromise achieved between the need to maximise interior volume and obtain a good hydrodynamic package.

Dynamic Positioning

Whilst the size of yachts grow, the size of the ports which they use remain largely static and become ever more crowded. This drives the need for improved manoeuvrability on larger yachts. Additionally many of these vessels now visit areas where anchoring may not be an ecologically sensitive activity.

These factors are leading to a number of yachts now requesting some form of dynamic positioning (DP) capability. The level of DP sought by modern yachts is (in most cases) not significant when compared with commercial vessels but the power requirements to achieve a reasonable level of capability can have a significant impact on the power demand. Hotel loads on modern yachts are relatively high with a typical 80m demanding around 600kW.

Figure 6 presents a plot of power required for DP vs vessel length. This is based on a simplified case for holding station in a beam wind of 15 knots for typical modern yacht windage profiles utilising thrusters. The power level required depends heavily on the type of thruster unit utilised. It can be seen that for an 80m vessel achieving station keeping in these conditions could double the hotel load.

Tunnel thrusters offer the greatest efficiency however these must be utilised in conjunction with the main propulsion system for DP capability as they have no azimuthing capability. Resiliently mounted units are now available with this development driven by the need for low noise and vibration levels. Retractable azimuthing units are occasionally used but as these can increase draught they are not generally favourable. Use of the main propulsion system in DP mode is preferably avoided as there is an associated increased in noise and vibration.

The use of pump jets is also becoming increasingly common. Whilst less efficient these units offer many benefits. Firstly, as they are mounted flush to the hull surface there is no additional appendage resistance. Secondly as they have full azimuthing capability they can offer DP capability without the need to run the main propulsion system. However these can be difficult to fit in the bow sections without imposing geometric constraint on the hullform.

The requirement for DP is one reason why a number of significant new builds have made the change to diesel electric propulsion systems.

Propulsion

The greater majority of the world's super yacht fleet are fitted with conventional propulsion systems comprising of CP or FP props driven by high or medium speed diesels. A very limited number employ a hybrid propulsion system comprising a gas turbine to provide a boost capability. However the demand for increased operational speed in the large yacht market is generally a niche requirement. Increased range and manoeuvrability are commonly of greater importance.

These two factors have led a number of recent new builds to specify diesel electric propulsion (DEP) systems coupled to podded electric drives. Three significant new builds between 65 and 90m launched in the last 2 years have seen this system utilised and they appear to offer solutions to many of the requirements discussed thus far.

Diesel electric systems are now fully mature technology and have been under continuous development since they were first introduced in the early 1900's (yes that long ago). Whilst a mature technology there is still a wide scope for refinement of DEP systems and advancements in computer control, switching technology and motor design are the key areas for advancement in a bid to reduce system losses and reduce weight. System losses are now as low as 8-10% between generator and propeller.

DEP systems afford greater flexibility in the positioning of the engine room and generally better utilisation of the onboard space. Additionally given the high hotel loads the ability to swing and manage power around the vessel is greater and more efficient. When used with a conventional prop arrangement they are certainly more space demanding and in all cases more expensive and complex. Recent reports however indicate that the cost issue is not as great as is widely believed with a diesel electric system reportedly adding approximately 1 - 2% on the build price when compared to a conventional system on a typical 80m yacht.

For vessels where there is a large variation in load demand, DEP systems can offer improved life cycle costs. With yachts now featuring DP in conjunction with high hotel loads the ability to manage this load variation is better achieved and improved life cycle costs can be achieved by reduced fuel consumption through optimised loading of generators.

To fully exploit the DEP concept the use of electric podded drives are now being utilised in large yachts. The podded, electric propulsor was first developed in the late 1980's and have since then matured to a proven product (not without some significant problems). Development has mainly taken place in the cruise ship market and the units have proven to be of major importance as a means to reduce cavitation, noise and vibration. In the case of the yacht these are critical factors and when married with the requirements for DP capability and increased manoeuvrability the podded drive appears an ideal choice.

The use of pods removes the associated appendage drag from shafts, brackets, rudders and stern thrusters. With appendage drag contributing to perhaps a much as 15% on large yachts (with the inclusion of anti roll fins and bilge keels) podded propulsors can lead to an overall power saving. The podded configuration utilises pulling propellers which allow good uniformity of the ship wave velocities resulting in extremely good cavitation characteristics of the propellers and reduce significantly propeller induced vibration and noise. Additionally given that the electric motor is mounted outside of the hull shell envelope the increased space associated with diesel electric systems is regained and generators can now be mounted on flexible rafts to reduce structural borne vibration. Recently a leading cruise operator has reported that the use of podded drives has, when carefully monitored over a seven day period, resulted in a 7% fuel saving, and when monitored purely in an at sea period (i.e. at service speed) the saving was around 10%.

Coupled with the flexibility in location of thruster devices and main propulsors that diesel electric affords, there is greater freedom in the hydrodynamic design of the hull form. The flat aft forms previously discussed are generally favourable from a resistance point of view and create a very uniform flow into the pod. However care should obviously be taken with regard to stern slamming.

Amongst this seemingly endless list of benefits, improved crash stopping characteristics can also be added to the list with crash stop distances of around 1.5 ship lengths being achievable from full speed. Reduced installation times are also claimed for podded drives with one recent 80m new build claiming that the use of pods cut up to 20 weeks of the build programme. The cost increase for a full DEP system coupled with podded drives is also claimed to be less expensive than might be anticipated with a recently reported cost increase of around 5% on the build price.

Hybrid systems are now being explored in the commercial market and CODED (combined diesel electric and diesel mechanical) are now in service linked to contra-rotating podded systems. In this case a conventional mechanically driven propeller is placed in front of an electrically driven pod, contra rotating to the main propeller. Efficiency gains of up to 15% are claimed and the pioneering customer of the arrangement has claimed an operational fuel saving of 20%. A number of very large yachts are currently under construction which utilise podded drives in combination with conventional propellers to offer a hybrid solution to more closely meet the specific needs of the yacht.

All of these apparent benefits do however come at the cost of increased complexity requiring a higher level of on-board skills to maintain and operate the systems. The high profile press coverage of pod failures in the cruise ship industry have served to leave many sceptical as to the reliability of this technology. These failures related mainly to bearings and seals and these appear to now be largely resolved. Commercial operator opinion is that the smaller units, typically below 14MW, are now problem free.

It is unlikely that the large yacht market is going to move wholesale to the use of either DEP or / and podded drives but the benchmark projects have now been launched which will surely lead to a steady move towards increased confidence in their use.

Stabilisation At Rest

Stabilisation of modern yachts is one area where technology derived from the commercial shipping sector has been adapted to meet the specific needs of yachts. An ever increasing number of manufacturers are now developing and selling at rest stabilisation systems and it is now more uncommon to hear of new builds which *don't* have a system fitted.

Modern motor yachts tend to be driven to higher GM values than is necessarily desirable. The deadweight faction of these vessels is typically quite low at around 15% -20% with the fuel load typically constituting 60 – 80% of the deadweight. The result of this is that the large consumable load, located low in the vessel, results in light arrival conditions becoming challenging with regard to stability criteria. Consequentially the GM values which the designer has within his control are often more limited than he may like. Natural roll periods tend to vary between 8 and 15 seconds and consequently motions in longer swells where the period is typically 7 – 14 seconds increases the probability of synchronous roll.

Given the operational profile of a typical yacht will be to spend a significant portion of time at anchor, the requirement for stabilisation systems that work when at rest has resulted and a wide range of solutions are being developed.

A number of equipment suppliers have developed fin stabilisers which require no forward motion to generate sufficient damping forces. Essentially a development of the conventional roll fin these systems use fins of increased area in a paddle fashion to create roll moments under at rest conditions. In order to create large enough forces at rest the fins require typically 30-40% more area than conventional roll fins and consequently a lower aspect ratio than is normal on conventional fins. Model test data indicates that reductions in significant roll amplitude in beam seas of up to 90% can be achieved (depending on the GM and natural roll period characteristics of the yacht). The operational feedback from yacht owners, and as reported in various public domain technical publications, is that these systems work well. These are now a mature and well proven product having been first utilised in 1999.

However as yachts get larger practical limitations are beginning to appear which is driving the need for new solutions. The fitment of anti roll fins is wholly scaleable with regard to vessel size but as length grows so too does the required size of the fins. Coupled with forms become fuller and speed increasing due to increased length so the use of fins becomes impractical. It is becoming increasingly difficult to fit the required fin area within the beam / keel envelope of the hull forms and the appendage drag increases to unfavourable levels.

A typical 80m will require approximately 25 sq.m of fin area whilst a 120m might require approximately 50 sq.m fin area. It is quickly realised whilst this technology is scaleable it becomes impractical much beyond this size of vessel. Where the exact limit is can be somewhat of a grey area as the fin area requirement for each project will depend heavily on the GM and natural roll period characteristics of the yacht, but it can be surmised that it is in the region of 120m.

Manufacturers of fin based zero speed systems are now exploring further developments and partially retractable and variable geometry fin area systems are just becoming available. The latter system offers a true dual purpose capability with relatively small fins utilised for the underway condition which employ a variable geometry system to increase the fin area for the at rest condition. It is reported by the systems manufacturer (Quantum) that a 30 – 35% increase in the fin size can result is as much as doubling of the roll damping capabilities. The first of these systems are due to be trialed in service in early 2007.

Fin based systems require about twice the power consumption of conventional fins and the installation cost is typically reported to be approximately 30-50% higher than conventional stabilisers. In practice these drawbacks are however far outweighed by the benefits and this is fully borne out by the number of owners specifying their use.

Fin based systems are not the only solutions available. Anti-roll tanks have been utilised in the past on yachts and these systems are well understood from application in the commercial field. The passive tank is designed such that roll moments from the tank are out of phase with the wave induced roll moments such that the ship roll motions are reduced. An active roll tank essentially performs the same task however being active the system is effective over a larger range of wave periods. Active and passive roll tanks work underway and at zero ship speed. These systems take up more internal volume and are therefore perhaps less suitable for yachts much below 80m where space is at a premium.

Anti-roll gyroscopes are also under development for yacht applications and are currently offered by one leading yacht manufacturer as standard on vessels up to approximately 30m. These were first explored in marine applications in the 1930's on various vessel types with varying degrees of success. Anti roll gyros make a compelling case for application as they can be easily installed and offer no appendage drag. However the major drawback with the current state of the technology is the size, weight and power requirements for these systems. Further development is currently being undertaken and one manufacturer reports to have a product range now available for yachts up to 100m.

Perhaps one of the most interesting products to come to the market recently is that of the rotary fin stabiliser. These utilise slewing rotating cylinders, deployed in a similar manner to retractable stabilisers, to create lift by the MAGNUS effect. Model test results with these systems on large yachts (over 120m) indicate that a reduction in significant roll angle of well over 80% can be achieved at zero speed. In practice it is believed that the largest vessel fitted with such a system is currently approximately 40m although it is known that systems are currently being supplied for yachts of over 150m for new build and retro fit applications. Whilst these systems are likely to be more complex mechanically they offer a practical alternative for larger vessels where as discussed, fitment of fins can become impractical.

A qualitative summary of the technical aspects surrounding the various systems described is presented in Figure 7, together with quantitative model test data (courtesy of Quantum) for zero speed fins, rotary fin stabilisers and variable geometry fins.

There are in summary an ever increasing number of options available to the modern yacht for at rest stabilisation. Suppliers are innovating new products to meet the challenges posed by ever increasing vessel size. Combining devices to achieve an acceptable level of motion both at rest and whilst underway may also become common place in the future.

Conclusions

As the size of the modern motor yacht continues to grow there is an ever increasing demand to employ technology developed in the commercial shipping industry. This transfer of technology is serving the technical requirements of the modern yacht. Additionally system suppliers are adapting existing technology to meet demands specific to modern yachts. Hullfrom development, dynamic positioning, propulsion and stabilisation at rest have been discussed, but the list is more extensive and topics such as the modern regulatory framework, safety aspects and lifesaving are other areas where large yachts are pushing the boundaries of previously established practices.

The increase in vessel size coupled with the adoption of this technology demands a higher level of technical input at the early design stages, especially with an increasing trend for the styling and engineering aspects of modern motor yachts to be distinctly separated disciplines. Whilst the wishes of the designer and stylist are often conflicting with those of the engineer, an early design stage collaboration and careful integration of technology and style will lead to yachts that, whilst looking ground breaking will also incorporate the right level of engineering optimisation to ensure that they do justice to the adage that yacht design is both art and science.

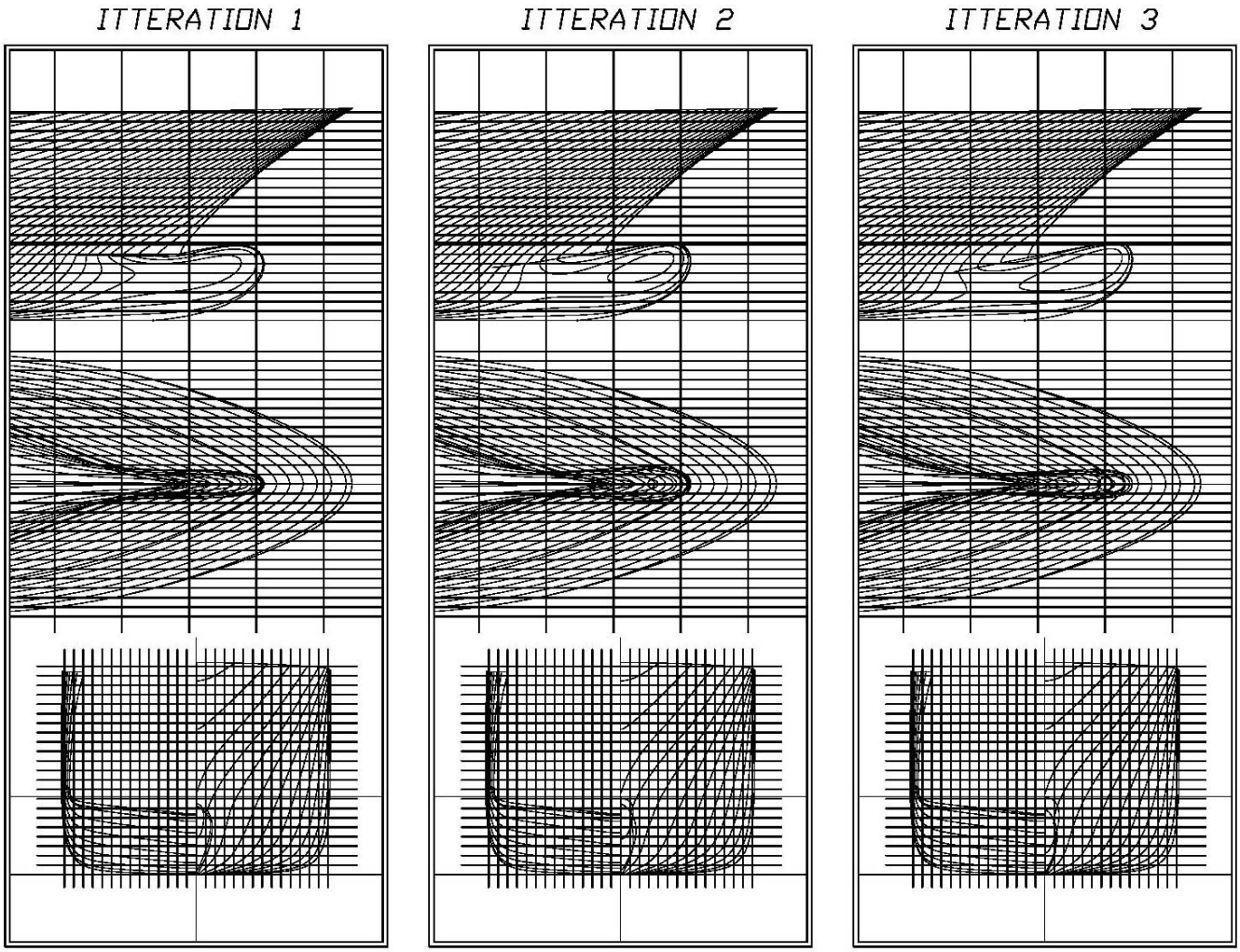

Figure 1 – Comparison of Forms Developed

	Parent Form	Iteration 1	Iteration 2	Iteration 3
Cp	0.626	0.593	0.597	0.596
CB	0.510	0.507	0.551	0.550
CM	0.836	0.855	0.923	0.923
LCB [% aft]	-2.676	-0.805	-0.871	-0.917
L/Vol$^{1/3}$	6.934	6.994	6.994	6.994
WSA/Vol$^{2/3}$	7.310	6.624	6.621	6.650

Figure 2 – Comparison of Principal Characteristics

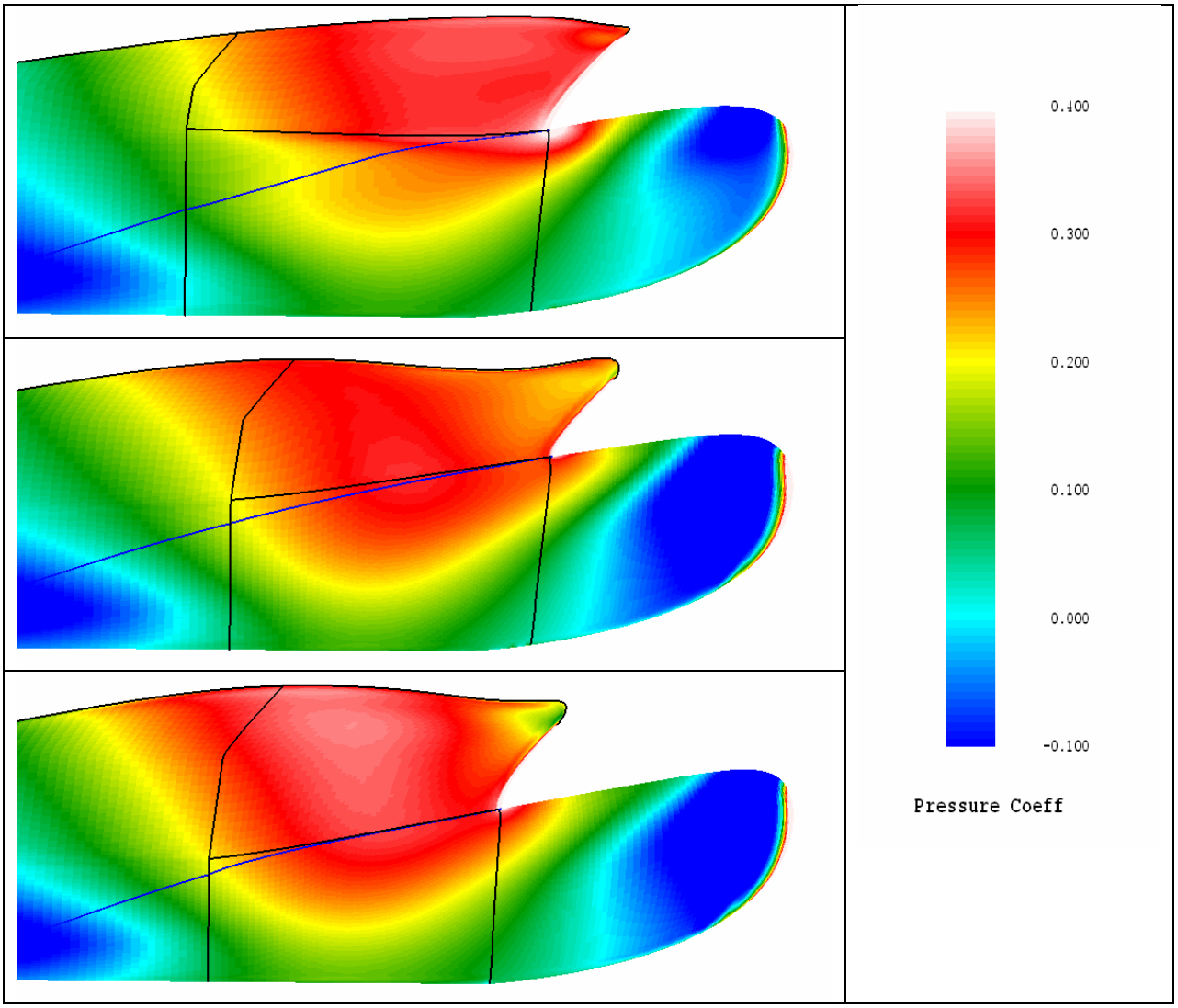

Figure 3 Pressure distribution with streamline at Vs =14 kn.

Speed [kn]	FN	C_R Itt1	C_R Itt2	C_R Itt3
12	0.233	1.92E-03	2.05E-03	1.96E-03
14	0.272	1.84E-03	1.99E-03	1.96E-03
16	0.311	1.94E-03	2.12E-03	2.14E-03

Figure 4 Computed Resistance Coefficients, C_R

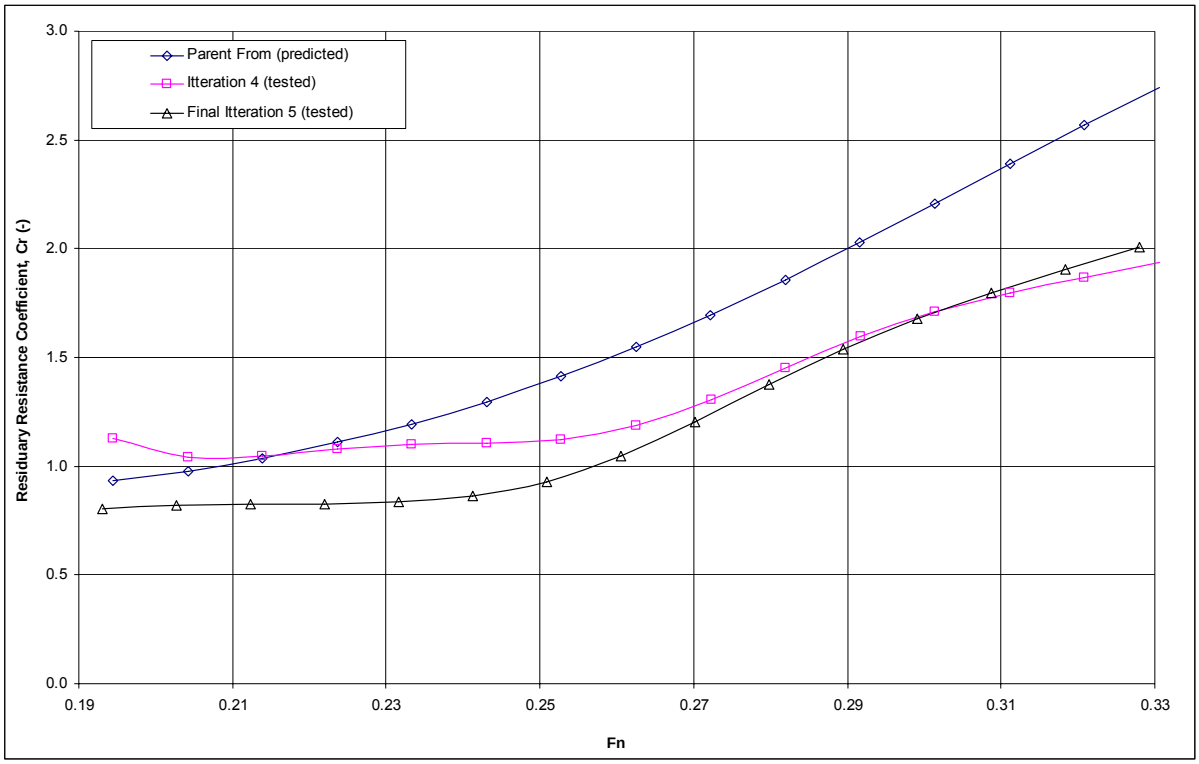

Figure 5 Final Measured Resistance Coefficients, C_R

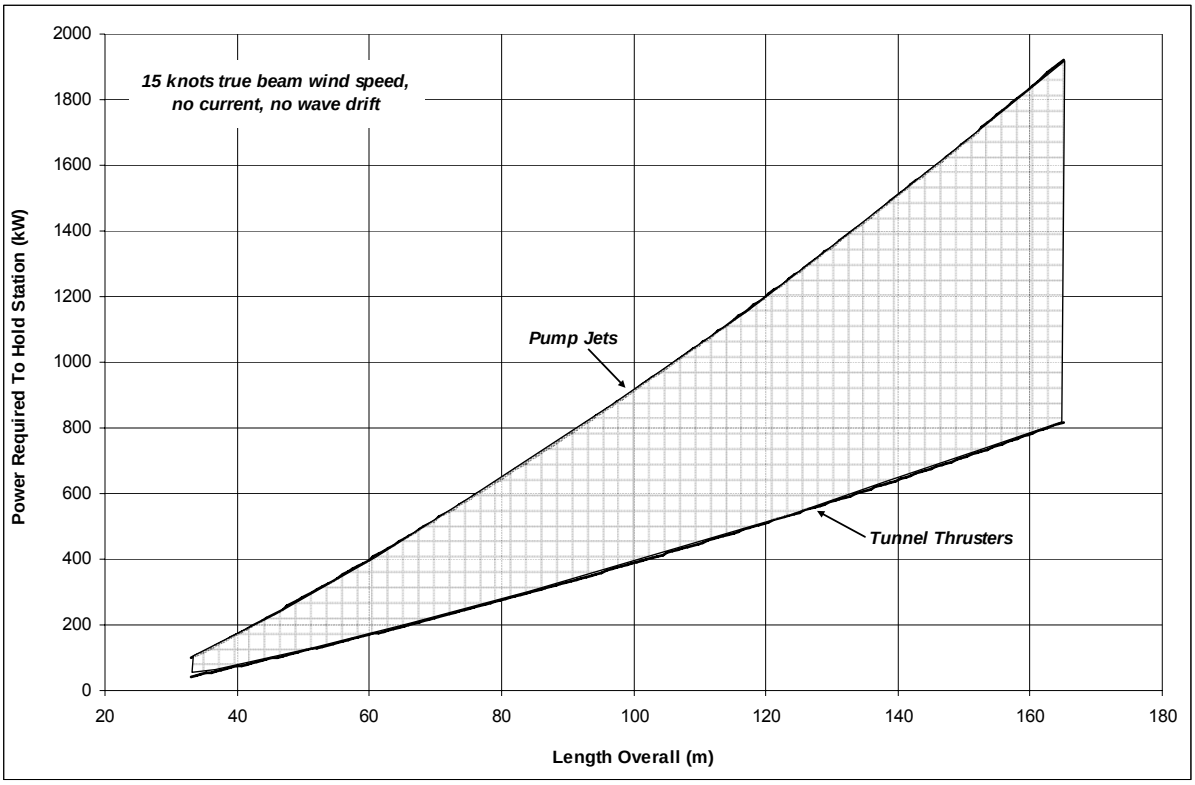

Figure 6, Power Demand To Hold Station, 15 knots True Wind Speed

Roll Reduction System Comparisons

	Conventional Roll Fins	At Anchor / Zero Speed Roll Fins	At Anchor / Zero Speed Rotary Fins	Bilge Keels	Roll Tanks	Anti-Roll Gyroscopes
Effictiveness at Anchor	– Low	+ Very Good	+ Very Good	+/- Moderate / Low	+ Good	+ Moderate
Effectiveness Underway	+ Good	+ Good	+/- Moderate / Low	+/- Moderate	+ Good	– Low
Internal Space Required	+/- Moderate	+/- Moderate	+/- Moderate	+ None	– Relatively Large	+/- Moderate / High
Ease of Retrofit	+/- Moderate	+/- Moderate	+/- Moderate	+ Easy	– Difficult	+ Easy
Impact On Displacement[1]	+/- Moderate / Low	+/- Moderate / Low	+/- Moderate / Low	– None	+/- Moderate	+/- Moderate
Impact on Power[2]	+/- Relatively Small	+/- Moderate	+/- Moderate / High	+ None	+/- Relatively Small	+/- Moderate / High
Noise and Vibration[3]	– Relatively Small	+/- Moderate / Small	+/- Moderate (no hard data)	+ None	+/- Moderate	+/- Moderate
Complexity / Ease of Maintanance	+/- Moderate	+/- Moderate	+/- Moderate	+ Low	+ Low	+/- Moderate
Cost of Installation	+/- Moderate	– Higher	– Higher	+ Low	+/- Moderate	– High
Technology Maturity	+ High	+ High	+/- Moderate	+ High	+ High	– Moderate / Low
Largest Application Available	+ 345m	+/- Approx 120m	+ 150m+	+ No Limit	+ No Limit	– 30m (modern gyro)[4]

Notes
1. - Depending on installation configuration. Retractable fins can lead to a large loss in buoyancy, coupled with system weight can lead to relatively high increase in displcaement
2. - Impact on power is intended to be general and include additional propulsive power and power to run the system
3. - All systems have been applied to yacht applications. With correct selection of equipment and sound treatments all systems can be made to operate to acceptablt noise levels
4. - Gyros have been installed on vessels up to 249m but using older, heavier, technology

Roll Reduction Systems Model Test Results

Significant Wave Height [m]	Standard Fins (Zero Speed™) Roll Reduction [%]	Magnus Effect MagLift™ Roll Reduction [%]	Variable Geometry Fin XT™ Roll Reduction [%]
0.50	78 - 92%	84 - 93%	82 - 90%
1.00	69 - 90%	78 - 92%	78 - 84%
1.50	58 - 81%	69 - 82%	

Note - Test in beam seas at resonant roll frequency, JONSWAP spectrum.

Figure 7, Qualitative and Quantitative Stabilisation System Comparisons

Session 3

Richard Birmingham & Melanie Landamore

INVESTIGATION OF SUSTAINABLE TECHNOLOGIES FOR THE DESIGN, CONSTRUCTION, OPERATION AND DECOMMISSIONING OF RECREATIONAL CRAFT

R W Birmingham, M J Landamore, P N H Wright and **M J Downie**, University of Newcastle, UK

Summary

To ensure that boating can become both environmentally sustainable and economically viable the principles of sustainable engineering must be closely observed. This paper investigates sustainable technologies and methodologies potentially available for transfer into the inland craft market, and the applicable timescales and environmental and economic implications of such. In the case study area the charter boat market is well established and important to the local economy and environmental considerations are of importance to the area in general. An initial review of the international state of the art and elicitation of local stakeholder knowledge was validated by a summary analysis of the ecological, economic and social implications of the considered technologies. Further detailed analysis of selected technologies was undertaken in the form of environmental life cycle, life cycle costing, and cost-benefit analyses.

Nomenclature

BD: Biodiesel-Electric System
BM_S: Individual Benchmark System Cost
BM_T: Total Benchmark System Cost (= $\Sigma\{BM_S\}$)
D: Diesel Engine
DEFC: Direct Ethanol Fuel Cell
EOL: End of Life Scenario
FC: Fuel Cell-Electric System
GRP: Glass Reinforced Plastic
GW: Greywater
GWC: Greywater Collection and Mains Discharge
GWD: Greywater Direct Discharge
GWF: Greywater Filter
IC: Incinerated at End of Life
ICE: Internal Combustion Engine
LF: Landfilled at End of Life
NPV: Net Present Value
RE: Recycled at End of Life
SPW: Series Present Worth
T: Taxed: Domestic Fossil Diesel (incorporating the relevant UK tax regime)
UT: Untaxed: Commercial Fossil Diesel (known as “red diesel”, subject to tax relief in UK)
WE: Wood-Epoxy Hull

1 INTRODUCTION

This paper looks at the issues of environmental, economic and social sustainability in the small craft sector, in the context of the inland charter boat market, and specifically, the Norfolk Broads. The work presented in this paper was undertaken by Newcastle University in 2005 on behalf of the Norfolk and Suffolk Boatbuilders Association [1,2]. The Norfolk Broads is a useful case study area for this industry in Europe. It is recognised as an area of environmental importance, having National Park status, and the charter boat market is well established and widespread throughout the region. The Broads is one of the fastest growing tourist regions in the UK, and in complying with the associated regulations, both those in existence and those anticipated, the local boating industry is looking to assume the position of market leaders in sustainable waterborne tourism and boating in general.

Sustainability can be summarised as development which meets the needs of the present without compromising the ability of future generations to meet their own needs [3]. Sustaining the Norfolk Broads environment against the pressures of modern use has become increasingly important. To ensure that boating can become both environmentally sustainable and economically viable the principles of sustainable engineering have been closely observed in this analysis. In the context of this paper, a sustainable design must balance the economic, environmental and social costs and needs of the area and industry overall. Total system life cycle emissions should be reduced, or their effect nullified, as much as is economically viable with due attention paid to the social implications of any decisions.
In the first instance, it was necessary to look at the current best practice employed in all the major areas of sustainable design, production, operation and decommissioning. In order to encompass the widest possible solution envelope, enabling technologies were drawn from across all fields embracing concepts of sustainable engineering. The report looked at the latest international innovations in sustainable design, and how they could be applied to a specific area: small inland charter and private craft operating on the Norfolk Broads.

2 State of the Art

2.1 Technologies for reduced carbon emissions from propulsion systems

Technologies related to the powering of the craft and propulsion system are considered, including: biodiesel, fuel cells, electric, solar/PV, wind, gas and human-power. Utilisation of waste heat in co-generation and tri-generation is becoming popular due to the limited space available onboard. Wind power encompasses sailpower (traditional and innovative rig configurations), as well as wind turbines. The economic and social costs of a number of the systems are considerable and therefore reduce their applicability. The use of biodiesel offers significant advantages in terms of required labour skills and technology, since the technology involved is basically the same as that used by the majority of motorised small craft. However the fuel itself is considerably more expensive than the tax-relieved ‘red’ diesel available to pleasure craft operating in the UK [4].

The use of solar power or hydrogen fuel cells are highly environmentally sustainable, and the positive public perception of photovoltaics as a ‘green’ technology is a major benefit; however drawbacks include expense and lack of operating expertise. Fuel cells [5] produce electricity via a chemical reaction, greatly reducing emissions, but fuel cell technology (and the availability of hydrogen) is not yet sufficiently robust to replace onboard power systems for a motorcraft of this size.

2.2 Technologies for handling and treating waste

All blackwater (sewage) and greywater (drainage) handling and treatment systems are considered here. The systems are designated as either onboard or onshore, depending on where the active treatment occurs, and include: greywater reuse, membrane separation/bioreaction, reverse osmosis, anaerobic septic system, aerobic septic system, reedbed filtration and composting toilets.

The limited options for waste handling and treatment leave few alternatives. Ideally treatment of black water would occur onboard [6], but space is an issue. To improve the sustainability of the current system of storing waste and disposing of or treating it ashore, and make this a viable alternative, a system such as reedbed filtration could be introduced. The collection and storage of greywater raises the issue of available tank space; onboard filtering is a more realistic proposal in this instance.

2.3 Sustainable materials for lower resource use, and increased recycling and reuse

The construction of the hull and subsequent disposal of spent hulls, as well as waste from the production process is a major area of concern when attempting to reduce the environmental impact of the system as a whole. There are a number of options available with varying levels of sustainability. GRP, the most widely used material in Broads craft, does not have a high level of sustainability. The use of low styrene resins, low emission processes such as infusion, and recycling can increase this [7].

The more traditional material, wood, can be sustainable if it is sourced appropriately, despite the requirement to coat the hull to prevent moisture ingress and rot. The associated manufacturing technology for thermoplastic composites is not yet sufficiently mature, and the use of biocomposite materials and resins [8] is still in development, there are currently many issues with reliability, strength, and water absorption. Steel and aluminium processing is highly energy intensive, and steel hulls also require coating for corrosion protection.

2.4 Novel propulsion technologies

Vast improvements in efficiency over a single screw propeller are available, usually at the expense of simplicity, for example: waterjet, PDX marine drive, low speed foils, podded drive, whale tail wheel and the flapping foil vehicle. Increased propulsive efficiency generates greater fuel efficiency, thereby reducing

dependence on fuel supplies, and the associated emissions. Propeller fouling can be avoided by selecting systems which minimise underwater moving parts.

Developments have led to improved efficiency and reduced disturbance of the waterbody. The Whale Tail Wheel [9], for example, offers a significant potential increase in efficiency, as well as being ideally suited to wide, flat, shallow draft craft. These systems may be applicable in specialised circumstances; however, none are well enough developed to be applicable at the moment.

2.5 Design for minimum impact on waterways

The factors identified here: wash [10], air, noise and water pollution, riverbed disturbance, foul release systems [11], propeller fouling and biofouling, must all be carefully examined when preparing a sustainable design. The cumulative effect of degradation to waterways can be significant and it is vital that in the production of a sustainable boat these environmental factors are recognised and steps are significant in preventing further detriment to the environment.

The recognition of simple technologies and lifestyle choices as part of sustainable design as a whole and limiting waste and resource depletion is an important part of sustainability. Much of this technology will transfer from existing domestic and other industry markets.

3 Local Elicitation – Addressing the social aspect of sustainable design

The elicitation of local knowledge included the views of local boatbuilders and hire operators. The objective was to better understand the current business of the interviewees, their views upon, and understanding of, various environmental and sustainability issues, and to elicit their expertise in terms of practical restraints, and knowledge of any existing projects in the area which may fall under the banner of sustainability.

It was thought that more considerate, environment-aware tourists will pay more for a quality holiday. Customers in general need to be better educated as to the effect they have on their surroundings; air and noise pollution, and wash caused by excessive speed, should be better controlled through education of users and stricter controls. If an existing technology works well,

then an industry will be reluctant to replace it with an alternative system if no immediate tangible benefits are available. Whilst respondents were open to suggestions of new technology routes, cost was a barrier in many cases. Lack of reliability and new technical knowledge requirement of systems were also raised as issues.

Overall, some respondents already operate in a manner similar to ecotourism; although they do not explicitly market their activities as such; this may be a profitable future market for the industry. The respondents were generally receptive to the idea of environmentally sustainable boating; existing schemes included fleets of electric- and biodiesel-powered boats. Several solutions were considered to be technically viable, but concerns were raised over their economic implications.

4 ANALYSIS and RESULTS

4.1 Initial Analysis

This initial analysis brings together the technologies identified in the state of the art review with the local expertise and opinions of the boatbuilders and operators in the Norfolk and Suffolk area, and the expertise of the academic team, to evaluate the most appropriate technologies for the advancement of sustainable boating in the area. All identified technologies were reviewed and assigned a score to enable competitive ranking. The scores are based on expert opinion and derived from the state of the art review and the elicitation exercise. The technologies are ranked with respect to: applicability to the Broads (now or in the longer term); acceptability to the stakeholders; local and global environmental impact; and economic viability. The sensitivity of the rankings to the weighting applied to these three factors (local and global environment, and economic) is explored.

Three main results sets were analysed:

- Set 1 considers all technologies applicable now and in the foreseeable future, and does not take account of the acceptability to the local boatbuilders.
- Set 2 takes account of the ability to implement the technology now (the applicability filter), but does not apply the acceptability filter.
- Set 3 applies both this applicability filter and the acceptance of the stakeholders (acceptability filter).

The key results are presented in Figure 1; these are for the average weighted condition, the most useful case for analysis. The choice of weighting system had little effect on many of the rankings, and almost never altered the ‘best and worst’ candidates; thus demonstrating the robustness of the results to conflicting attitudes and prejudices. A complete discussion of the results can be found in Landamore et al [1]. It should be recognised that these results do not include any factor for the social acceptability to the customers (hirers), this information not being part of the scope of this study.

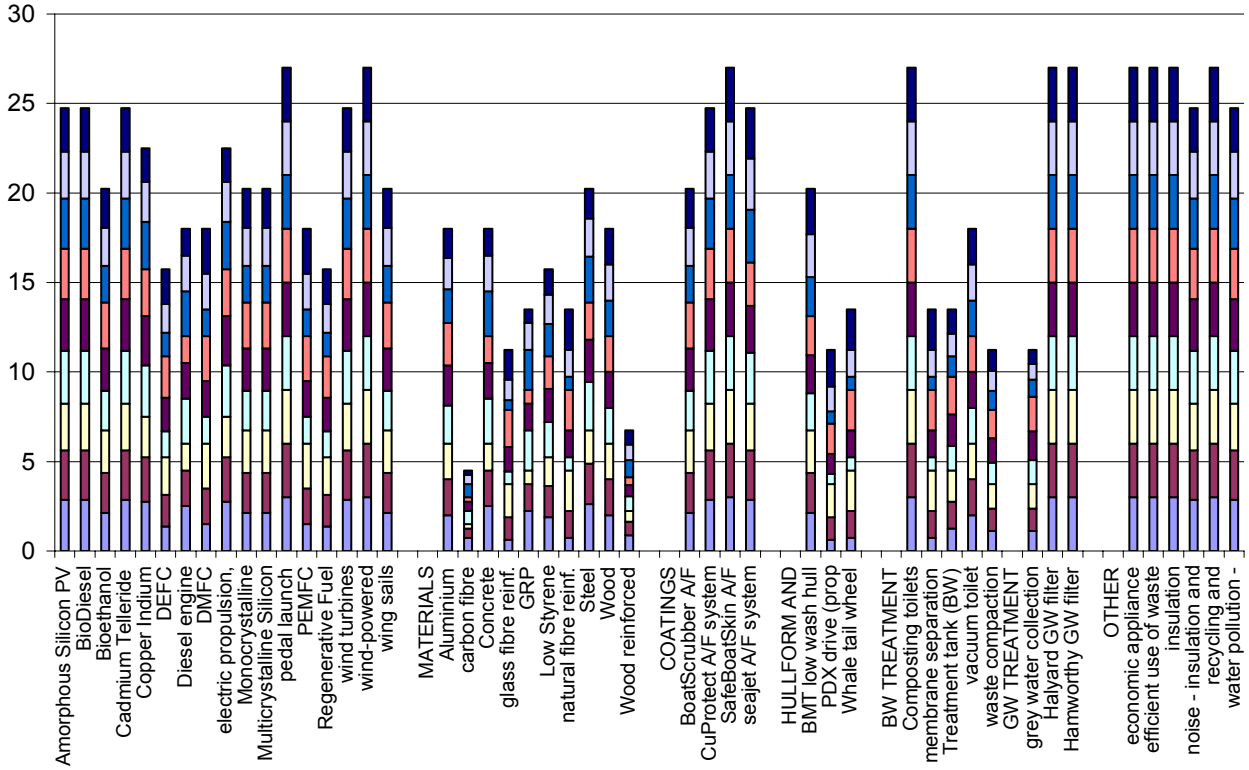

Figure 1: Initial Analysis: All Weighting Systems (Series 1-9), Stacked Columns

4.3 environmental Life Cycle Analysis

This section focuses on more detailed life cycle analyses of selected technologies. The technologies chosen by the stakeholders for further analysis against the benchmark fall into three categories:

- Powering: direct ethanol fuel cell-electric (DEFC) and biodiesel-electric systems; compared with the benchmark system, a standard direct drive diesel internal combustion engine (ICE).
- Hull Matieral: steel and wood-epoxy composite; compared with the benchmark technology, basic lay-up glass reinforced plastic (GRP).
- Greywater Treatment: filtering for 'clean' discharge overboard (or collection, discharge later); or a system which collects the greywater for disposal (untreated) into the mains drainage system; compared with the benchmark system, direct discharge to the waterways.

Life Cycle Assessment (LCA) is a technique for assessing the environmental aspects associated with a product over its life cycle. In general, an LCA study consists of four main steps:

- Defining the goal and scope of the study;
- Making a model of the product life cycle with all the environmental inflows and outflows, the life cycle inventory (LCI) stage;
- Understanding the environmental relevance of all the inflows and outflows, the life cycle impact assessment (LCIA) phase;
- The interpretation of the study.

Results are normalised to the impact category indicators for Western Europe during a year; these are shown in terms of 'Ecopoints', enabling comparison against the standard of one

Ecopoint/area/year; highlighting significant contributions to an overall environmental problem. A benchmark system designation (see 4.4.1) enables meaningful comparison of impacts across all categories.

Powering - the largest impacts associated with the biodiesel-electric and diesel systems are almost entirely located within the usage phase of the life cycle. The DEFC system has a very low environmental impact in all categories considered.

Hull material - the three competing hull systems exhibit no impact during the usage phase. The steel hull impacts considerably more environmentally than the other systems. Wood-epoxy scores significantly better than GRP in a number of categories.

Greywater treatment: All greywater systems demonstrate major impacts from the production phase due to the manufacture of the steel tanks. The overall results show little variation; and choice may rely on individual bias toward impact category, for example, the filter system delivers minimum impact to local water quality.

A steel hull has the largest impact on the environment, the diesel engine power system after that. The next largest impact overall is the biodiesel-electric system; the choice of end of life scenario is relatively unimportant, it does not move the system's overall ranking position with the exception of DEFC. Landfilling rather than recycling this system has a relatively large impact, because there is almost no discernible impact from the usage phase, but on average 5 fuel cells are used and disposed of over the 30 year life compared to one diesel engine.

4.4 Life Cycle Costing Analysis

The case study fleet size is approximately 800 boats. The established base system requirement, to ensure results could be meaningfully compared, is:

- Generic 12.2m 4 berth motor-cruiser design, lifespan of 30 years, 30 weeks active use per year;
- Standard single skin hand lay-up GRP hull with marine ply bulkheads;
- Powered by a direct drive diesel engine (32KW, lifespan 30 years) on an average loading cycle;
- 100 litre fuel tank capacity, standard starter domestic backup batteries (life span approximately 6 years);
- Direct discharge of greywater into the river system, one freshwater tank.

All hull and tank materials have a 30 year lifespan. This benchmark system designation enables meaningful comparison of impacts across all categories, as well as within a category; it also enables comparison with other external systems, regulations and benchmarks.

All material, labour, overhead and end of life disposal costs must be considered for all components of all systems. Each system is costed over the predicted average life of the craft, using Net Present Value [12]. Some costs are difficult to define, especially where innovative technology is constantly evolving. Some costs fluctuate continuously with market influences, for example, fossil fuels. The cost of a DEFC capable of powering this system is currently unknown as these are not yet commercially available. Estimated current and future costs, assuming market success of this product, have been included, to give an idea of the potential for this technology at a later date.

4.5 Life Cycle Cost Breakdown Results

The average cost of each system is broken down into build, operation and end of life costs. Cost inputs are calculated for a range of values; some fluctuate regularly, while for others the input parameter must be estimated due to a lack of solid information from which to source the data. The powering systems (figure 2) display very little effect from end of life costs. The biodiesel-electric and fuel cell-electric systems cost more than the diesel engine to build and operate.

	Build inc materials	Op inc materials	End of life LF	TOTAL
Diesel(UT) BENCHMARK	**5740**	**20136.536**	**0.80**	**25877.34**
Biodiesel	7081.5	47441.52	0.82	54523.84
Fuel Cell	203149.5	190699.83	0.93	393850.26
Diesel(T)	5740	49344.963	0.80	55085.76

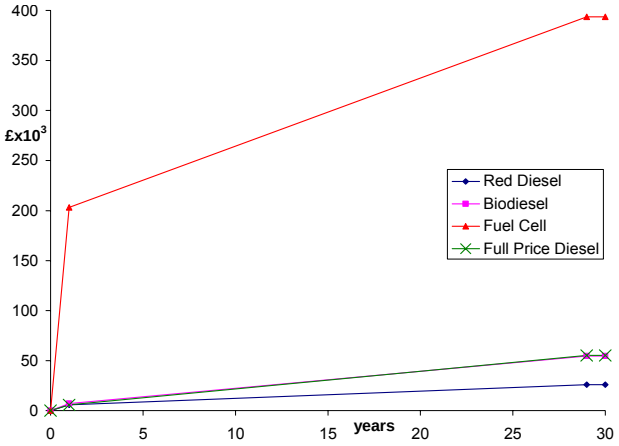

Figure 2 – Powering Life Cycle Cost Breakdown

The steel hull is cheaper to build, operate and recycle than the GRP (incinerated) benchmark system, but slightly more expensive to landfill. The wood-epoxy system is more expensive than the GRP in all three phases (figure 3). The greywater filter system is much more expensive to build and operate than the benchmark, but incurs the same end of life cost. The GW collect system is marginally more expensive initially and at end of life, and the same cost to operate, as the benchmark.

	Build inc materials	Op inc materials	End of life RE/IC	TOTAL
GRP BENCHMARK	**26478.13**	**1189.12**	**80.00**	**27747.24**
Steel	12350.00	8063.16	-750.00	19663.16
Wood-Epoxy	33262.91	2378.23	85.25	35726.40
GW Disch. BENCHMARK	**287.00**	**250.43**	**0.25**	**537.68**
GW Collect	322.00	250.43	0.50	572.93
GW Filter	1164.00	4936.99	0.25	6101.24

Figure 3 – Hull Material and GW Cost Breakdowns (in £)

4.6 Cost-benefit Analysis

Realistic comparison of technologies for adoption by industry must consider the economic and environmental implications of such a choice. The lifecycle cost can be compared against the environmental effects of each system to give an analysis of the cost versus benefit. Those systems demonstrating worse environmental performance than the benchmark are discounted from any further analysis as there is no environmental improvement available; they are: Steel hull (landfilled and recycled); GW Collect and Mains Discharge System (landfilled) and GW Filter (landfilled).

An assumption can be made whereby an acceptable level of cost increase exists for a unit reduction in environmental impact. The cost per ecopoint environmental improvement required to implement the system has been calculated; the value of an environmental impact reduction to the business, and the system cost required to meet that value, can be judged. The environmental score is measured in ecopoints saved, and represents the impact of the craft over its assumed 30 year life.

4.7 Cost-benefit analysis Results

Effective analysis of the two data fields (LCC and LCA) can identify cost-efficient and environmentally-sound solutions [2]. The cost per ecopoint saved is a comparison of the environmental improvement of the system against the technology benchmark (BM_S) (measured in ecopoints saved), and the additional cost of the system above the benchmark. If the system is cheaper than the benchmark (a negative cost), then it is deemed viable at this level (figure 4). The next levels assume that an additional cost premium of 1% or 5% benchmark system cost per ecopoint environmental improvement is acceptable. Evaluating the systems in this way, against BM_S, provides information relevant to the inclusion of that system into any craft.
In order to be able to compare the relative merit of alternative systems in different technology groups an analysis is needed that uses as its base the entire combination of technologies defined as the benchmark case. The required cost premium as a percentage of the entire benchmark cost (BM_T) for these three systems is calculated. The additional cost of each alternative is compared with the environmental improvement and the total benchmark cost.

	POWER 1			POWER 2			HULL		GREYWATER		
	D Re	BD Re	FC Re	D Re	BD Re	FC Re	GRP Lf	WE Lf	GWD Re	GWC Re	GWF Re
COST(£)/ ECOPT SAVED	**-11.33**	264	1,767	**-11.33**	**-6.90**	1,626	**-145**	2,036	**-8.85**	689	92,691
1% premium	**Yes**	No	No	**Yes**	**Yes**	No	**Yes**	No	**Yes**	No	No
5% premium	**Yes**	**Yes**	No	**Yes**	**Yes**	**Yes**	**Yes**	No	**Yes**	No	No

Figure 4: Cost (£) /Ecopoint and Viability of Systems under Different Acceptable Cost Premiums

Key:
D: diesel engine
BD: biodiesel-electric system
FC: fuel cell-electric system
WE: wood-epoxy hull
GWD: greywater direct discharge
GWC: greywater collection and mains discharge
GWF: greywater filter
Re: Recycled at end of life
Lf: Landfilled at end of life

POWER 1 Benchmark:	Diesel powered internal combustion engine using 'untaxed' diesel, components landfilled at end of life.
POWER 2 Benchmark:	Diesel powered internal combustion engine using 'taxed' (UK regime) diesel, components landfilled at end of life.
HULL Benchmark:	GRP hull, incinerated at end of life.
GREYWATER Benchmark:	Greywater discharged directly into surrounding waterways untreated, components landfilled at end of life.

The systems which show a reduction in cost against benchmark are:

- Diesel engine (recycled) against 'untaxed' and 'taxed' diesel benchmark;
- Biodiesel-electric (landfilled and recycled) against 'taxed' diesel;
- GRP hull (landfilled);
- GW direct discharge (recycled).

There are a number of technologies which fall close to the '1% benchmark cost per ecopoint saved' limit:

- Biodiesel-electric (recycled and landfilled, against 'untaxed' diesel) requires 1.02% and 1.03% benchmark cost premium, respectively;
- DEFC-electric systems (recycled and landfilled, against 'taxed' diesel) requires 2.94% and 3.02% benchmark cost premium, respectively.

5 discussion

5.1 Initial Analysis

This outcome provides a ranking of all the technologies considered, analysed in a systematic manner. The technologies to be adopted in a design are a matter of subjective choice but should logically belong to the groups with the highest rankings. The highest ranking technologies, which score well under any value system, present themselves clearly. The more interesting analysis involves the 'mid-range' results, where the selection of value system (weighting) alters the score of a technology.

5.2 Life Cycle Analysis

Powering - the biodiesel and fuel cell systems incur almost all their impact during the production phase; these impacts also exist for the diesel engine, but are overwhelmed by the usage phase. Aside from the production phase, there are few impacts associated with the use of DEFC; the LCA supports the use of this, providing the suggested system can be developed commercially for power generation on this scale.

Hull Materials - there are major environmental effects from the production of steel, this system shows the largest impacts across all categories and in total, whereas the GRP and wood-epoxy systems rank 4th and equal 5th respectively in terms of total impacts. The impacts of GRP are more than double those of the wood-epoxy hull.

Greywater Systems - the benchmark greywater system shows minor impacts related to the discharge of the polluted water, and major impacts from the manufacture of the steel tanks. The greywater collection and filtering systems show little difference overall and are small impacts when compared to the effect of the powering systems or hull materials; in terms of overall environmental impact, any changes to the greywater treatment system have a relatively insignificant impact. These results recommend the direct discharge system overall, but if the impact of building the tanks is ignored, it is likely the filter system would score best.

5.3 Life Cycle Costing and Cost Benefit Analysis

Although the biodiesel-electric system requires an additional input of just 1.02% BM_S (or 0.49% BM_T) per ecopoint environmental improvement, this is a significant absolute cost because of the net environmental improvement gained. It is clear from this analysis that some systems, e.g. the GW filter (recycled), will never represent good value; this system would require an extra 171% BM_T per ecopoint improvement.

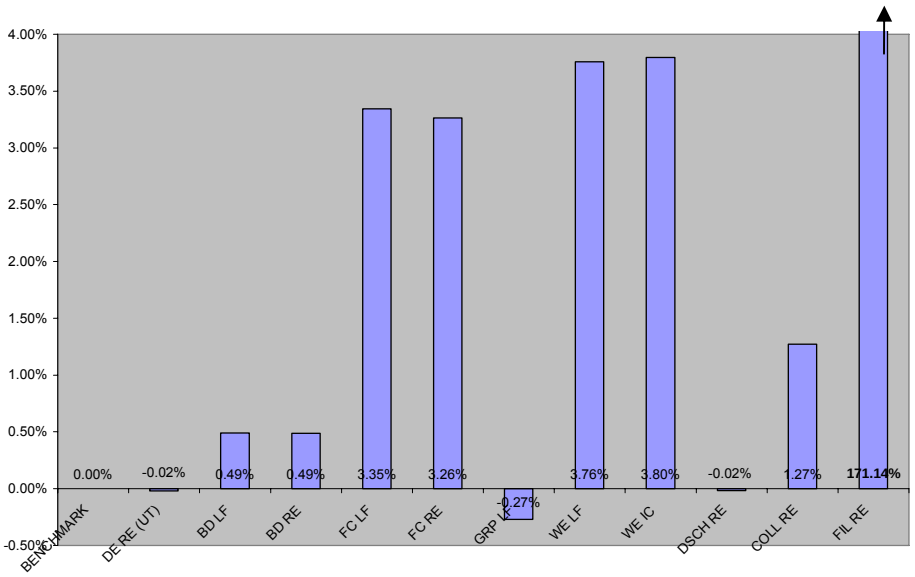

DE: diesel engine
BD: biodiesel-electric
FC: direct ethanol fuel cell-electric
GRP: GRP hull
WE: wood-epoxy hull
DSCH: GW direct discharge
COLL: GW collect & discharge
FIL: GW filter
(UT): untaxed diesel
(T): taxed diesel
LF: landfilled
RE: recycled
IC: incinerated

Figure 5– Cost Premium required/Ecopoint saved as Percentage of the Total Benchmark System Cost

Figure 5 shows the distribution of the cost premium required per ecopoint improvement for each technology against the total benchmark base cost (BM_T): the three benchmark systems summed. Lower column height represents greater environmental benefit per £ additional investment. Negative figures represent cheaper than benchmark options demonstrating environmental improvement which therefore hold no barriers to implementation.

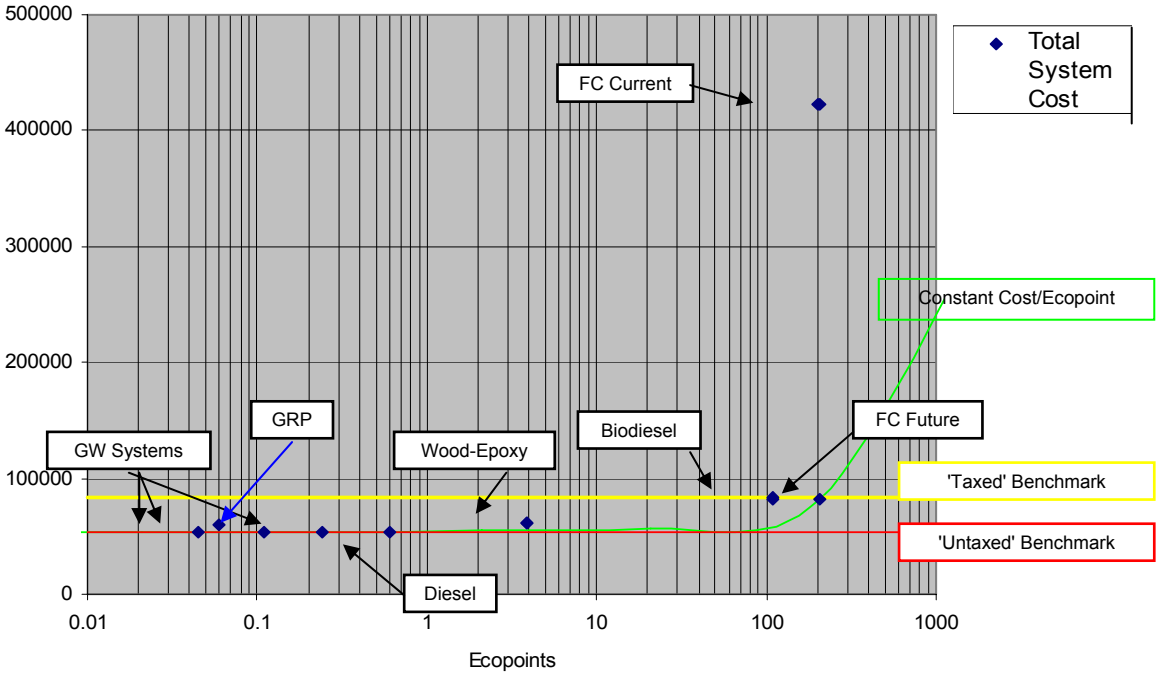

Figure 6 – Representation with x axis plotted as a logarithmic scale (base 10): Absolute Cost of Systems plotted against Ecopoints Saved

The direct ethanol fuel cell-electric (DEFC) has an average system cost of £393,850. This unproven and currently unavailable (for this application) technology has been attributed a high cost of £100,000 per fuel cell, however successful development and market implementation of this technology should see costs fall dramatically. Therefore the 'FC Future' figure of £10,000 per cell has been included (figure 6). The lower system cost is greater than the benchmark with 'untaxed' diesel, but £879 less than the 'taxed' diesel benchmark, with a lifecycle environmental benefit of 208.2 ecopoints. The exact costs of DEFC units of this size are very difficult to predict; assuming the unit price falls to near £10,000, this system can become cost efficient against 'taxed' diesel. It is highly likely that this cost could fall even further.

Figure 6 shows all technologies plotted against absolute cost of system and number of ecopoints saved (against benchmark) with the x-axis plotted as a logarithmic (base 10) scale. Minimum cost with maximum ecopoints saved is desirable. The contour (figure 6) is equivalent to the DEFC system cost: 'FC Future'. Any technologies falling on or below this cost/ecopoint contour exhibit environmental properties per £ extra investment similar to or better than this; and of the current technology costs, Biodiesel-electric clearly exhibits the greatest environmental improvement. Compared with the 'taxed' (UK regime) BM_T, there is a small saving if this system is used. The remaining technologies exhibit little environmental improvement in comparison.

The wood-epoxy system exhibits greater environmental improvement, at a greater absolute cost and cost/ecopoint saved than the GRP, Diesel Engine (recycled, 'untaxed' diesel) or GW collect or discharge systems: these all fall within the 0.25% BM_T/ecopoint contour. Better performing technologies will be preferred for equivalent cost/ecopoint saved.

If a finite level of additional funding were available, lower scoring technologies may be reintroduced into the decision-making process. For example, if £10,000 funding were available to improve the overall environmental performance of a fleet of 50 boats, the optimum solution would be introducing one wood-epoxy hull (figure 7).

System	Additional system Cost (£)	Ecopoints saved	No. of systems	'Fleet Cost' (£)	'Fleet' ecopoints saved
Wood-epoxy	7,962	3.91	1	7,962	**3.91**
GW collect	31	0.045	50	1,550	2.25
GW discharge	5,561	0.06	1	5,561	0.06

Figure 7: £10,000 (3.7% fleet BM_T) additional funding available, fleet of 50 boats

Equally, if a fleet of 100 craft were considered, a £10,000 additional budget (1.85% fleet BM_T) provides a different optimum solution: installing 100 GW collection systems for 4.5 ecopoints improvement. Assuming the owner (fleet size ≥1) could spend an additional £30,000, then 1 biodiesel-electric system would provide the greatest benefit. For a fleet of 100 boats, £30,000 equates to only 5.5% fleet BM_T.

These are through life costs, and as such the total cost may not be borne by one person or company; the cost is also spread over the entire 30 year life of the craft (figure 2). If the current UK tax regime is considered (ignoring the dispensation for pleasure craft to use 'red' tax-relieved diesel), then the performance of the biodiesel-electric system improves dramatically against this 'taxed' diesel benchmark.

The cost of environmental improvement in one particular category per ecopoint is also calculated. However, considering one category in isolation can give misleading results. If a particular area is of specific interest, possibly to facilitate the achievement of National, European or International standards, then this method may be valid as a comparison of different options.

6 Conclusions

The technologies considered have varied impacts upon the environment which are not always intuitive. The smaller impacts should not be ignored; when balanced against the cost of implementation these may become efficient methods for reducing a craft's impact on the environment whilst remaining commercially viable. Overall, the life cycle analysis demonstrates that environmentally the best technologies are the wood-epoxy hull, direct ethanol fuel cell-electric powering system and the direct discharge GW system; with biodiesel-electric, GRP and the remaining GW systems also scoring well. Excepting steel as a hull material, the major impacts are within the powering system.

The inclusion of economic factors produces an alternative set of results: the high cost of the most environmentally effective technologies (fuel cell-electric and wood-epoxy) makes them an ineffective way to spend resources at this time. This cost benefit analysis demonstrates that the most cost effective use of resources is firstly, the implementation of the 'cheaper than benchmark' systems which still exhibit an environmental improvement (all benchmark systems with alternative end of life {EOL} scenario). In addition, both biodiesel-electric (landfilled and recycled) systems cost less than the 'taxed' diesel benchmark, whilst still exhibiting an environmental improvement.

If it is accepted that additional costs can be incurred to reduce environmental impact, then systems incurring the smallest cost penalties per ecopoint improvement should be used. These are the biodiesel-electric system (both EOL, against 'untaxed' diesel benchmark), and the GW collection system (recycled EOL). All other systems, with the exception of the GW filter and those demonstrating no environmental benefit, fall within 3.8% additional BM_T per ecopoint improvement (see Figure 5). This analysis against entire combined benchmark cost (BM_T) does not include the 'taxed' diesel option, as this would alter the benchmark case. However, when comparisons are made against a 'taxed' diesel benchmark system, the biodiesel-electric systems are 'cheaper than benchmark' and the DEFC systems score significantly better than when

compared with the 'untaxed' diesel system; they also fall within an additional 3.8% 'taxed' BM_T/ecopoint improvement range.

Any technologies falling on or below the marked contour (See Figure 6) exhibit environmental properties per £ extra investment similar to or better than "FC Future"; of the lower scoring technologies, the wood-epoxy system exhibits the greatest environmental improvement. The other systems fall below this contour due to low cost, but exhibit minimal environmental improvement.

A finite level of additional funding could revalidate lower scoring technologies. The optimum solution if £10,000 is available to improve the overall environmental performance of a fleet of 50 boats is one hull replaced with wood-epoxy. For a fleet of 100 craft, an additional £10,000 would install 100 GW collection systems. For an additional £30,000, the optimum solution becomes 1 biodiesel-electric system.

To improve the environmental performance of a small charter craft for use on the Norfolk Broads for today's market:

- Powering - biodiesel-electric, recycled at end of life or diesel engine (recycled). However, if the red diesel concession were removed, the biodiesel-electric (recycled) would become the cheapest system overall, the fuel cell-electric systems (landfilled and recycled) would also then incur a relatively lower premium;
- Hull material - a GRP hull, landfilled at end of life should be used;
- Greywater - should be discharged directly into the waterways, and the system components recycled at end of life. As an alternative, the greywater collection system also represents good value at 1.27% total system cost/ecopoint.

In conclusion, a number of systems can be implemented without extra cost to the builder/operator, and the majority of systems can be implemented if a premium of a small percentage of system cost is applied per ecopoint environmental improvement gained. It is clear that environmental improvements can be made without additional total cost, often simply by changing end of life strategy.

7 References

1 Landamore, M.J. Birmingham, R.W. Downie, M.J. Wright, P.N.H. “ECOBOAT – Boat for a Sustainable Future on the Norfolk and Suffolk Broads”, Newcastle University, May 2005.
2 Landamore, M.J. Birmingham, R.W. Downie, M.J. Mesbahi, E. “Life Cycle and Cost Benefit Analysis of Selected Technologies for Sustainable Inland Boating”, Newcastle University, January 2006.
3 Garner, R. “Environmental Politics” Prentice Hall, 1996.
4 Zhou, P.L. Fet, A.M. Michelsen, O. Fet, K. “A Feasibility Study of the Use of Biodiesel in Recreational Boats in the United Kingdom” IMechE Proceedings Vol. 217, Part M:J. Engineering for the Maritime Environment, 2003.
5 Hengst, S. van Boonstra, H. der Wegt, J. Schmal, D. Mallant, R. “Design and Development of a Prototype Inland Vessel provided with Fuel Cell Power generation”, ENSUS Conference Proceedings, 2000.
6 Bentley, A. and Ballard, E. “Black and greywater treatment solutions using membrane bioreactors”, The Naval Architect, February 2003.
7 Hayashi, S. Yamane, K. “Study on the Development of the Recycling Technology of Waste FRP Boats” Papers of Ship Research Institute, v. 35, n. 3, 1998.
8 Gurram, S., J.L. Julson, K. Muthukumarrapan, D.D. Stokke, and A. K. Mahapatra. “Application of Biorenewable Fibres in Composites”, ASAE/CSAE North Central Intersectional Conference, 2002.
9 van Manen, J. and van Terswiga, T. “A New Way of Simulating Whale Tail Propulsion”, Twenty-first symposium on Naval Hydrodynamics, 1997.
10 Gadd, G. “The Development of an Energy Efficient Low Wash Cabin Cruiser Hull Form”, BMT Seatech Ltd., BRAP Seminar, 1997.
11 Candries, M. Atlar, M. Anderson, C. “Considering the use of alternative antifoulings: The advantages of foul-release systems”, ENSUS 2000 Conference Proceedings, September 2000.
12 Buxton I.L. “Engineering Economics and Ship Design”, BMT Ltd, 1987.

Session 4

Fabio Fossati

19th International HISWA Symposium on Yacht Design and Yacht Construction
13 and 14 November 2006, Amsterdam, The Netherlands, Amsterdam RAI Convention Centre

AN INVESTIGATION OF AERODYNAMIC FORCE MODELLING FOR IMS RULE USING WIND TUNNEL TECHNIQUES

Fabio Fossati[1], fabio.fossati@polimi.it
Sara Muggiasca[2]
Ignazio Maria Viola[3]

ABSTRACT

Aim of this paper is to describe research activities carried out at Politecnico di Milano Twisted Flow Wind Tunnel with partial funding from the ORC in order to investigate the performance of upwind sails: in particular a series of rig planform variations in mainsail roach and jib overlap have been tested in order to overcome some perceived inequities in the ratings of boats of various rig design racing under the International Measurement System (IMS).The results of these investigation are used to assist the International Technical Committee (ITC) in changing the formulations in the IMS sail aerodynamic model.

INTRODUCTION

As well know the International Measurement System (IMS) is an handicap rule which provides elapsed time corrections for a broad range of sailing yacht types utilizing speed prediction from a velocity prediction program based on fundamental principles of hydrodynamics and aerodynamics: then the problem of properly modelling sail forces is a topic of the utmost importance.
The IMS Rule uses a Velocity Prediction Program (VPP) in which sail forces are represented by algorithms that are based on a combination of science and reverse engineering from the measured sailing performance of real boats.
Generally speaking in velocity prediction programs for yachts the problem of modelling sail forces is a fundamental focus. Two major topics have to be considered: several sailplan geometries must be taken into account and on the other side for given sailplan sails shapes are not fixed: alteration in sail trim produce a wide range of combination of lift, drag and heeling moment.
With reference to IMS VPP, the basis of IMS aerodynamic model is mainly derived from the aerodynamic model well known as Kerwin model.
Basically the IMS Rule does not measure sail shapes but sail size. The loads on each sail are found by multiplying the area of that sail by dynamic pressure and by the force coefficient for that kind of sail at the specified apparent wind angle. For each sail type there are curves of maximum lift and parasitic drag coefficient versus apparent wind angle. It is very important to point out that these coefficients do not represent the aerodynamic characteristics those sails would have if they were flying by themselves but when summed together the total force coefficients should accurately represent the aerodynamics of all the sails flying at any given apparent wind angle.
There are large fleets of boats successfully racing under the IMS Rule but from racing experience some inequities in the ratings of boats of various rig design sailing are perceived.
Aim of this paper is to describe research activities carried out at Politecnico di Milano Twisted Flow Wind Tunnel with partial funding from the ORC in order to investigate the performance of upwind sails: in particular a series of rig planform variations in mainsail roach and jib overlap have

[1] Full Professor, PhD, Sailing Yacht Testing Scientific Coordinator CIRIVE – Wind Tunnel - Politecnico di Milano; Research Associate, ORC International Technical Committee
[2] PhD, CIRIVE – Wind Tunnel - Politecnico di Milano
[3] PhD student, Department of Mechanical Engineering, Politecnico di Milano

been tested in response to the above mentioned perceived inequities under the International Measurement System (IMS). The results of this investigation are used to assist the International Technical Committee (ITC) in changing the formulations in the IMS sail aerodynamic model. A large amount of work has been recently carried out by researchers [8] and more tests are planned in the next future in order to investigate also the fractionality effects on the planform aerodynamics.
This paper in the first part presents test arrangements, procedures and methodologies that have been carried out both for systematic gathering of wind tunnel data and subsequent analysis in order to describe aerodynamic behaviour of different sailplans.
Some interesting results and trends are presented and discussed.
Then a brief review of aerodynamic models available up to-date for VPP use is outlined; in particular an investigation of the methods of modelling the depowering of sails in VPP is considered.
Finally some basic ideas to provide a more suitable aero-model for upwind sails as required by IMS VPP to predict the performance of yacht for rating purposes are outlined. The new approach which is at the moment under ITC discussion is strongly based on the availability of an experimental data base according to the ITC research program guidelines.

POLITECNICO DI MILANO UPWIND TESTS PROGRAM

THE FACILITY

At the purpose of supporting with a state of the art facility the world-wide recognised excellence of Politecnico di Milano research in the field Wind Engineering as well as general Aerodynamics, Politecnico di Milano decided to design and build a new large Wind Tunnel having a very wide spectrum of applications and very high standards of flow quality and testing facilities. The Wind Tunnel is fully operative since September 2001 and in the first year of operations has been fully booked for applications in both fields of Wind Engineering and Aerospace applications.
Figure 1 shows an overview of the Wind Tunnel: it's a closed circuit facility in vertical arrangement having two test sections, a 4x4 high speed low turbulence and a 14x4 low speed boundary layer test section. The overall wind tunnel characteristics are summarised in Table 1. Peculiarity of the facility is the presence of two test sections of very different characteristics, offering a very wide spectrum of flow conditions from very low turbulence and high speed in the contracted 4x4m section (I_u<0.15% - V_{Matex}=55 m/s) to earth boundary layer simulation in the large wind engineering test section. Focusing on the boundary layer test section, its overall size of 36m length, 14m width and 4m height allows for very large scale wind engineering simulations, as well as for setting up scale models of very large structures including wide portions of the surrounding territory. The relevant height of the test section and its very large total area (4m, 56m^2) allows for very low blockage effects even if large models are included. The flow quality in smooth flow shows 1.5% along wind turbulence and $\pm$3% mean velocity oscillations in the measuring section. A very large 13m-diameter turntable lifted by air-film technology allows for fully automatic rotation of very large and heavy models fitted over it (max load 100.000 N).
The wind tunnel has a floating floor allowing for very clean model set-up, living all the instrumentation cable connections out of the flow. The very long upwind chamber is designed in order to develop a stable boundary layer and the flow conditions are very stable also in terms of temperature due to the presence of a heat exchanger linked in the general control loop of the facility. The Wind Tunnel is operated through an array of 14 axial fans organised in two rows of seven 2x2m independent cells. 14 independent inverters drive the fans allowing for continuous and independent control of the rotation speed of each fan. This fully computer controlled facility can help in easily obtaining, joined to the traditional spires & roughness technique, a very large range of wind profiles simulating very different flow conditions and very different geometrical scales. The wind tunnel process is fully controlled by a PLC and a computer network (ABB control system), monitoring through more than 100 transducers all the most important flow parameters in terms of wind speeds, pressures, temperatures, humidity, vibrations of the fans and the structure, door opening etc., and allowing for feedback control on the flow temperature and speed. The flow conditions were found very stable and a confirm of that is the very low turbulence level in smooth

flow. All the typical various set of spires have been developed in order to simulate the different wind profiles and an original facility has been recently installed allowing for active turbulence control in the low frequency range. Concerning the low-turbulence high-speed section, the large dimensions (4x4m) and the quite high wind speed (55 m/s) enable to reach quite high Reynolds numbers. Table 1 shows the very low levels of turbulence reached in this section, giving to the facility a very wide spectrum of possible applications. A very wide range of transducers, instrumentation and data acquisition systems are available allowing for all the typical boundary layer wind tunnel measuring applications in the wind-engineering field. More details on the facility can be found in [2] and [9].

Politecnico di Milano Wind Tunnel				
Tunnel Overall Dimensions			$50\times15\times15\ [m]$	
Maximum Power (Fans only)			$1.5\ [MW]$	
Test Section	**Size** $[m]$	**Max Speed** $[m/s]$	$\Delta U/U$ %	**Turb. Int.** I_u %
Boundary Layer	14×4	16	$<\pm2$	<2
Low Turbulence	4×4	55	$<\pm0.2$	< 0.2

Table 1: Overall wind tunnel characteristics

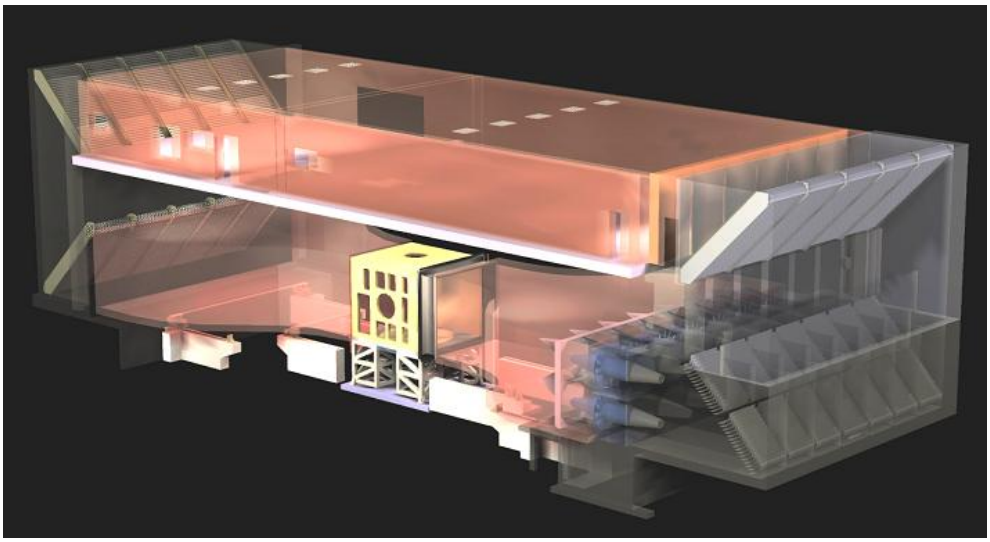

Figure 1: Politecnico di Milano Wind Tunnel 3D transparent rendering; the 14 2m diameter axial fans array is recognizable on the right lower side

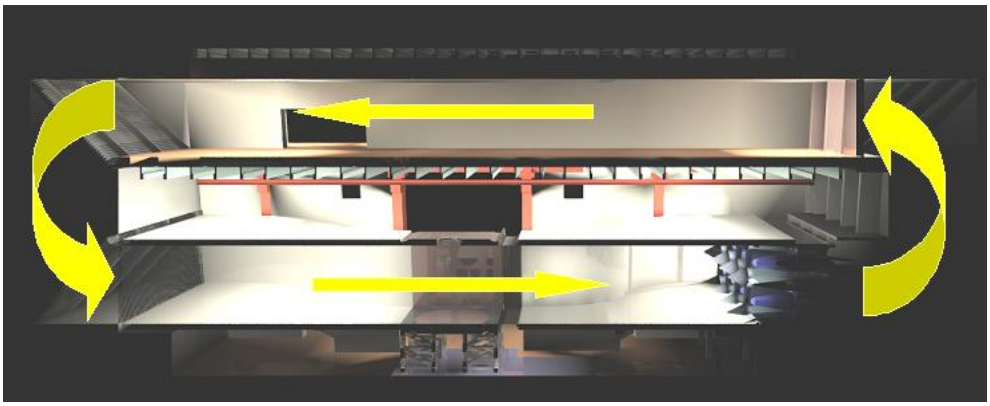

Figure 2: Longitudinal section showing the flow circuit; on the upper side is the boundary layer test section – on the lower side centre is the high speed low-turbulence test section – on the lower side at right is the 14 axial fans array

TEST ARRANGEMENTS AND MEASUREMENTS SETUP

A complete model, consisting of yacht hull body (above the waterline) with deck, mast, rigging and sails is mounted on a six component balance, which is fitted on the turntable of the wind tunnel. The turntable is automatically operated from the control room enabling a 360° range of headings.
The large size of the low speed test section enables yacht models of quite large size to be used, so that the sails are large enough to be made using normal sail making techniques, the model can be rigged using standard model yacht fittings and small dinghy fittings without the work becoming too small to handle, commercially available model yacht sheet winches can be used and, most important, deck layout can be reproduced around the sheet winch, allowing all the sails to be trimmed as in real life. Moreover the model yacht sheets winches are operated through a 7 channel proportional control system, by a console with a 7 multi-turn control knobs that allow winch drum positions to be recorded and re-established if necessary. The sheet trims are controlled by the sail trimmer who operates from the wind tunnel control room.
A high performance strain gage dynamic conditioning system is used for balance signal conditioning purposes.
The balance is placed inside the yacht hull in such a way that X axis is always aligned with the yacht longitudinal axis while the model can be heeled with respect to the balance.
Data acquisition can be performed in several ways: the usual procedure provides direct digital data acquisition by means of National Instruments Data Acquisition Boards (from 12 to 16 bits, from 8 differential channels up to 64 single ended) and suitably in-house written programs according to or Matlab standards.
The data acquisition software calculates the forces and moments using a calibration matrix. The forces are shown on the screen in real time so that the sail trim can be optimised. Actual measurements are obtained by sampling the data over a period specified by the test manager (generally 30 seconds) with a sample frequency specified too.
The raw data are stored in files that are used for the detailed data analysis.

SAIL PLANS TESTED

According to the overall activities program a series of sails was designed to investigate main girth and jib overlap. In particular 3 different main sails (with the same actual and IMS area but different roach) and 3 different jibs with different overlap were manufactured by North Sails Italia.
Politecnico di Milano CIRIVE Department provided a scale model of a sailing hull with mast and rigging. The dimension of the rig are as follows:

EHM		2.160 [m]
P		1.950 [m]
HBI		0.145 [m]
BAS		0.210 [m]
J		0.600 [m]
I		1.970 [m]
LPG	G100	0.580 [m]
LPG	G135	0.810 [m]
LPG	G150	0.900 [m]

Table 2

Table 3 shows different sails code with relevant roach and overlapping values

	Mims	Mhr	Mtri
Roach = MainAreaIMS/(1/2*P*E)-1	0.193	0.335	0.097

	G100	G135	G150
Overlap = LPG/J	1.00	1.35	1.5

Table 3:

The *"Mims"* code means that this mainsail girth is the maximum allowed by IMS Rule.
Considering the wind tunnel available time for testing only 5 different sets of upwind model sails have been tested.
In particular it was decided to test the 100% jib with all the 3 mainsails available and the IMS mainsail with the 135% and 150% overlap genoas.
Moreover all tests were performed in upright condition and at 30° heeling too.
Only the IMS mainsail+135% jib have been tested at 15° heeled condition too.
Apparent wind angles tested were chosen to be 22°, 27°, 32° and 42° in order to cover the upwind range.
Pictures of Figure 3 show model tested.

Mims G100

Mims G135

Mims G150

Mhr G100

Mtri G100

Figure 3

TESTING PROCEDURE

The yacht model is set at an apparent wind angle and at a fixed heel. After a sail trim has been explored, actual measurements are obtained by sampling the data over a period specified by the test manager (generally 30 seconds) with a sample frequency specified too.
The tunnel always runs at a constant dynamic pressure but, by trimming the sails in certain ways, the effect of different wind strength can be simulated.
An important feature of wind testing procedure is that the model should be easily visible during the tests so that the sail tell-tales can be seen by the sail trimmer. At this purposes four cameras are placed in the wind tunnel as well as onboard in order to help sails trimming procedure with sails view similar to the real life situation.
In particular a camera was placed on the floor looking at the yacht stern, another one was placed on the roof looking along the mast direction in order to check the mainsail flying shape, another one looks jib from deck and the last was used in order to control the genoa and jib car position.
The first task is to try to reach the maximum driving force consistent with light wind sailing. From there, the sails have to be either over trimmed, to get the part of the curve where stall is clearly evident, and sistemayically de-powered to collect data consistent with stronger wind conditions.
In Figure 4 a typical variation of the driving force coefficient Cx with heeling force coefficient Cy is reported.

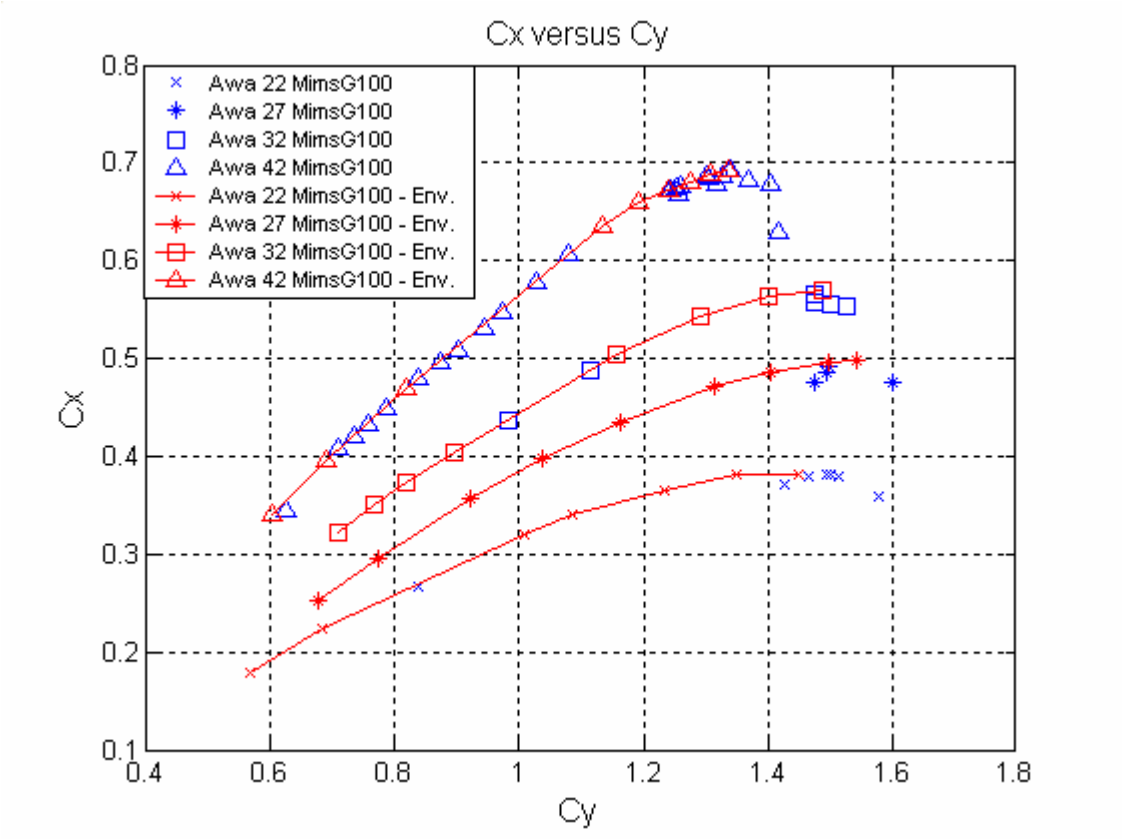

Figure 4

They are given by the expressions:

$$Cx = \frac{Fx}{\frac{1}{2}\rho S v^2} \quad (1)$$

$$Cy = \frac{Fy}{\frac{1}{2}\rho S v^2} \quad (2)$$

It can be seen that there are some settings at the highest values of heeling force coefficients where the driving force is lower than the maximum value. These non optimum values were obtained by oversheeting the sails such that the mainsail generally had a tight leech and the airflow separated in the head of the sail.

Envelope curves have been drawn through the test points with the greatest driving force at a given heeling force (Figure 4). In particular we are interested only on the envelope of all the sails trimming performed in order to exclude the non optimum sail setting position for the post processing which are non representative (see Figure 4).

Therefore a selection was made to choose those points that formed the envelope curves (maximum Cx for a given Cy value) for each apparent wind angle (Figure 4).

Trimming the sails to obtain optimum sailing points, i.e. points on the envelope curve proved to be the most challenging task of the test process. Attempts were made to carry out the job as systematically as possible. Firstly, the maximum drive point was found by trimming the sails to the best using the cameras views, the tufts on the sails and the force measurements output data.

From there, the heeling force would be reduced to simulate the trim of the sails for windier conditions: infact in windy conditions, to keep the optimum heeling angle, heeling force has to be reduced.

Once a specific trimming condition is obtained using the real time force and moments values displayed by the data acquisition system, a 30 seconds acquisition sampling has been performed with 100Hz sample frequency, and both time histories and mean values of each measured quantity can be stored in a file.
With reference to sails maximum camber configuration the decision was to adopt design camber values.
Some runs have been performed on the bare hull and rigging only (without sails) at different apparent wind angles to be able to evaluate windage. This has been subtracted from the measured data points in order to study the effect of the sail plan only.

DATA ANALYSIS PROCEDURE

The usual way of analysing data is to compare non dimensional coefficients, to be able to compare the efficiency of sails of different total area at different conditions of dynamic pressure.
The first analysis performed is the variation of driving force coefficient Cx with heeling force coefficient Cy as shown in Figure 4.
Also the plot of the Cx to Cy ratio versus Cy is very interesting. As an example with reference to the MimsG100 sail plan testing, Figure 5 shows a comparative plot of the Cx to Cy ratio versus Cy for the four apparent wind angles tested. Envelope curves have been drawn again through the test points with the greatest driving force at a given heeling force (Figure 4)

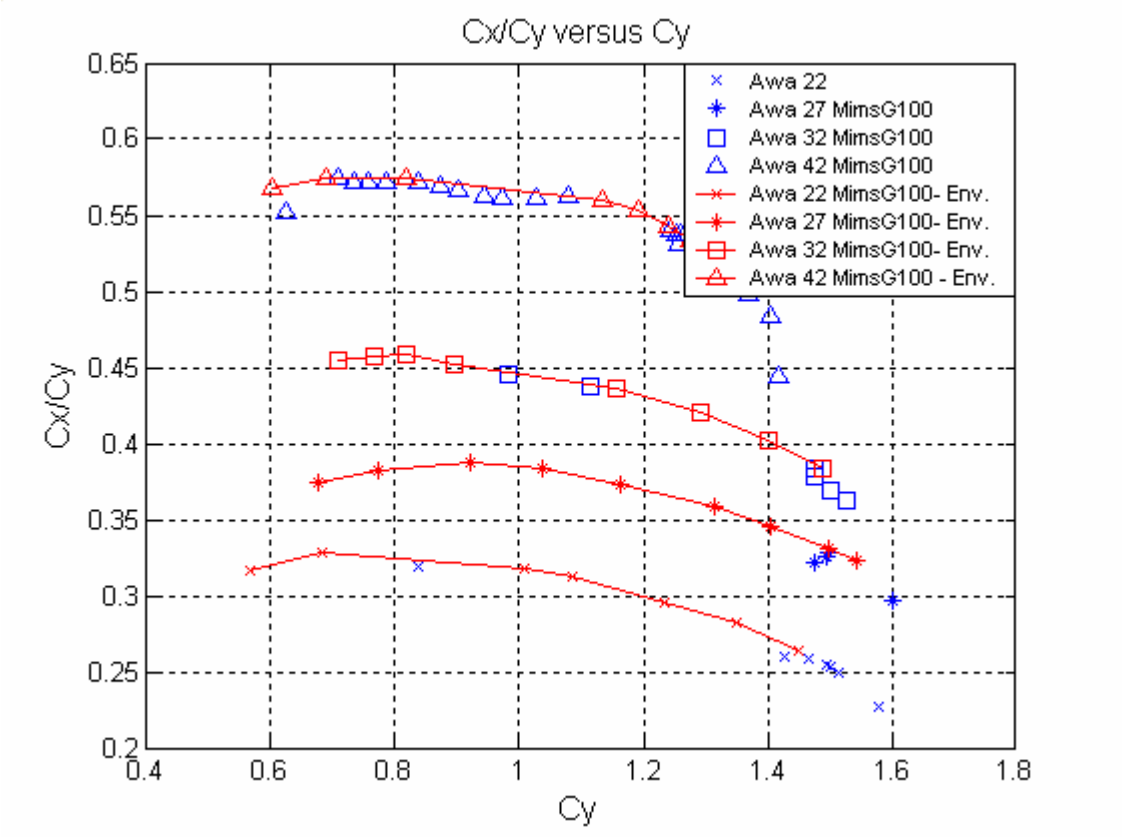

Figure 5

From the study of these plots some comments can be made:

- For a determined AWA and a given Cy the higher Cx, the more efficiently sail plan is operating
- For a given AWA the greatest efficiency of the sails is achieved when the Cx to Cy ratio is maximum
- From the comparison between the plots, it is observed that the max efficiency corresponds to a point with a lower driving force than the maximum. The translation of that in sailing performance terms is that, in light conditions when the maximum driving force is sought from the sails, there is some reduction in the rig efficiency that may be also affect boat speed. In medium wind, the sails are operating at their maximum efficiency. Finally in strong winds, where the sails are set to restrict the heeling force, the sail efficiency is reduced and some reduction in the sail are may enable the sails o be re-sheeted to operate near the maximum efficiency.
- It is noted that for the same heeling force, the driving force increases with AWA. This reveals that it would be necessary to operate with the sails eased in order to sail with the rig at optimum efficiency at closer apparent wind angles
- Also Cx/Cy increases with AWA. When the yacht is sailing in steady conditions that ratio has to be matched by the resistance to side force ratio, therefore it is important to note that the more efficient hull will be able to sail closer to the wind.

The centre of effort height, Ceh, can be obtained by dividing the roll moment by the heeling force component in the yacht body reference system:

$$Ceh = \frac{Mx}{Fy} \tag{3}$$

As an example, a plot of its variation with heeling force for all angles can be seen in Figure 6. Both all the measured values and the envelope of the points corresponding to maximum driving force at each heeling force are reported. The results are given in terms of ratio between centre of effort height from boat deck and must length. For the purpose of the analysis only envelope curves through the test points with the greatest driving force at a given heeling force have been used.

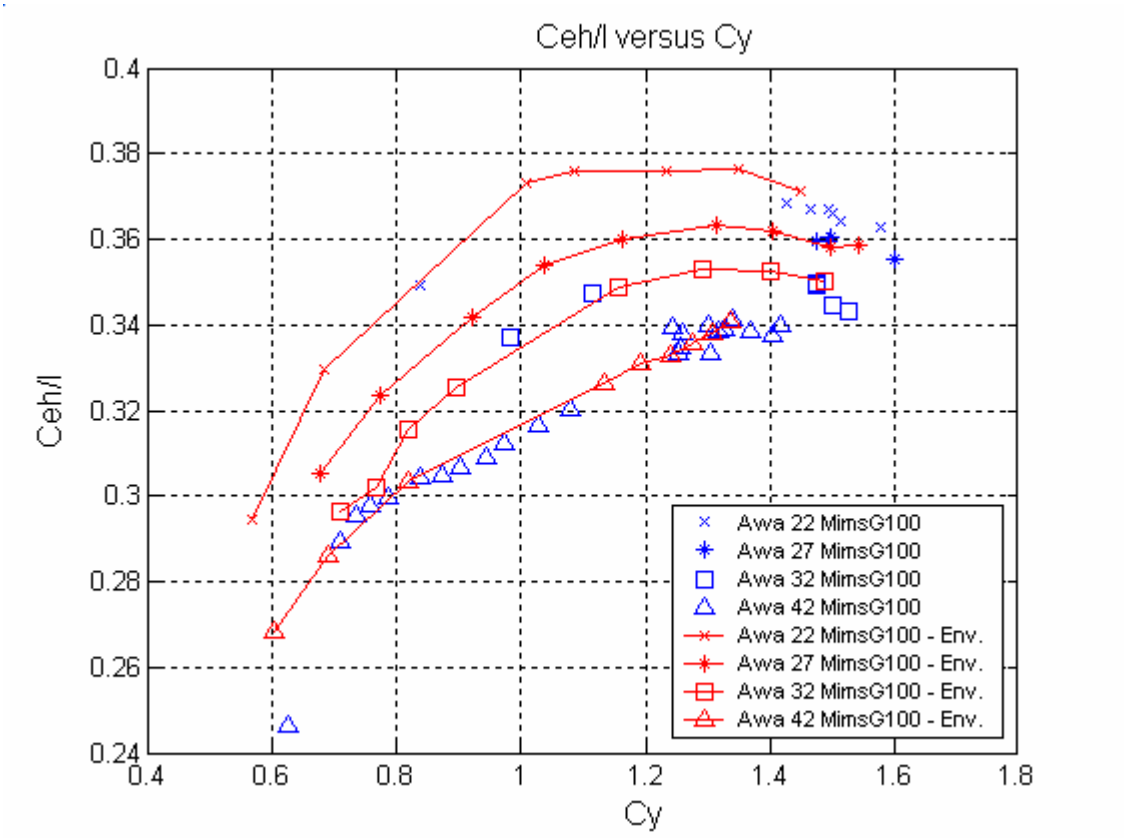

Figure 6

From the analysis of Figure 6 some comments are:

- The centre of effort height tends to reduce as the heeling force coefficients reduces. This is explained by the way in which the sails are de-powered to reduce Cy.
- The smaller the AWA is, the higher centre of effort is.
- The data show a quite big scatter due to the sensitivity of the Ceh to sail trim. Different trim position can have the same overall driving and heeling force but different Ceh because of a different span wise distribution of the forces.

The centre of effort longitudinal position, Cea, can obtained by dividing the yaw moment by the heeling force component in the yacht body reference system:

$$Cea = \frac{Mz}{Fy} \tag{4}$$

As an example, a plot of its variation with heeling force for all angles can be seen in Figure 7. Both all the measured values and the envelope of the points corresponding to maximum driving force at each heeling force are reported.

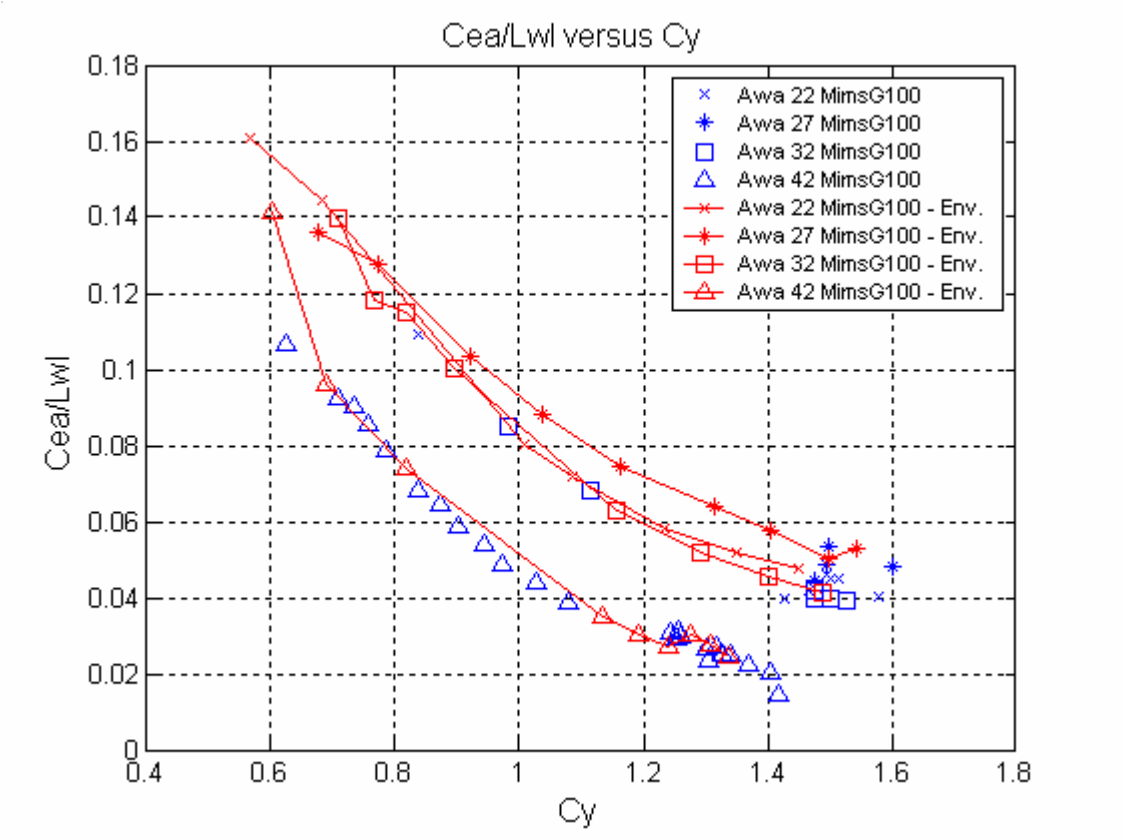

Figure 7

The results are given in terms of ratio between centre of effort longitudinal position from balance origin and yacht model length at waterline. Cea is measured from the origin of the balance which is placed behind the mast. It can be seen that Cea moves forward as Cy reduces. This is explained by the way the sails are de-powered.
Using the driving and heeling aerodynamic force Fx and Fy component in the yacht body reference system the corresponding drag and lift forces components can be obtained as follows:

$$DRAG = -F_x \cos(AWA) + F_y \sin(AWA) \tag{5}$$

$$LIFT = F_x \sin(AWA) + F_y \cos(AWA) \tag{6}$$

Then the corresponding drag and lift coefficients C_D and C_L can be evaluated:

$$DRAG = \frac{1}{2}\rho V_a^2 C_D(AWA) S \tag{7}$$

$$LIFT = \frac{1}{2}\rho V_a^2 C_L(AWA) S \tag{8}$$

The apparent wind speed V_a and apparent wind angle are evaluated in the heeled plane perpendicular to the mast according to:

$$V_a = \sqrt{\left(-V_t \cos\gamma\right)^2 + \left(V_t \sin\gamma \cos\phi\right)^2} \tag{9}$$

$$AWA = \text{arctg}\left(\frac{V_t \sin\gamma \cos\phi}{-V_t \cos\gamma}\right) \tag{10}$$

where represent the true wind angle (yaw angle), V_t is the wind tunnel flow velocity corresponding to the mean dynamic pressure at each run and is the heel angle.
As an example in Figure 8 and Figure 9 the C_D and C_L measured values at different AWA for MimsG100 upright test condition are reported. At each AWA, values corresponding to each run performed are reported and red full dots correspond to the maximum driving force condition trimming point.

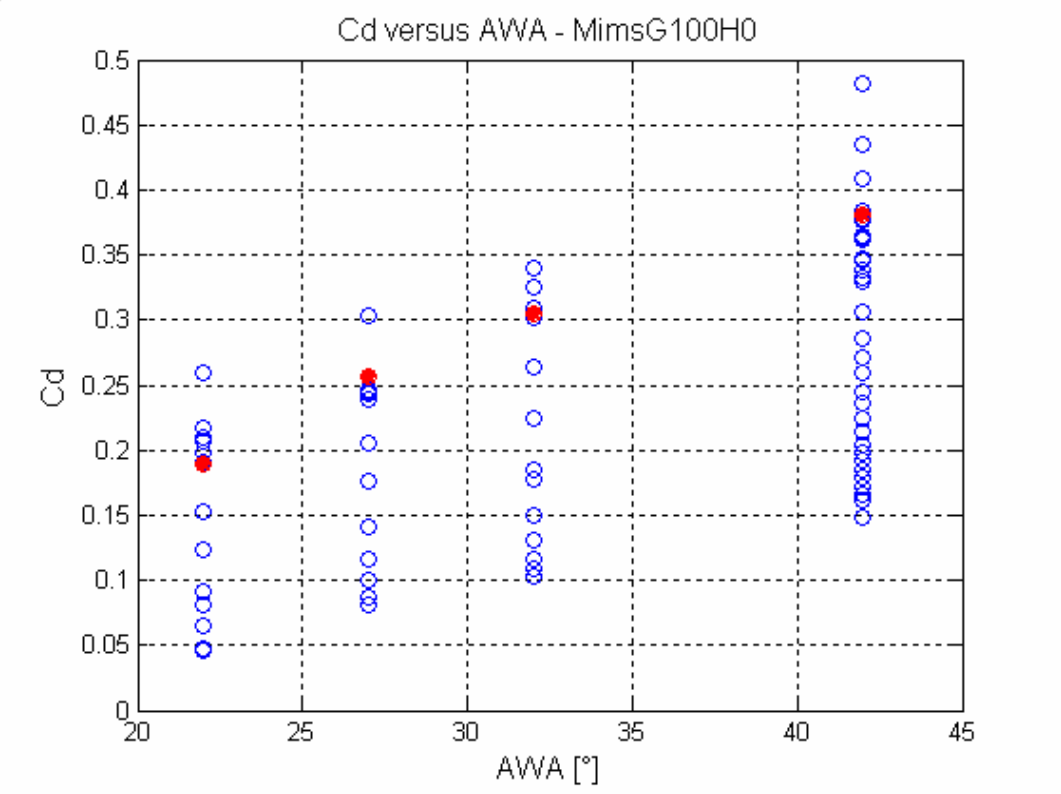

Figure 8

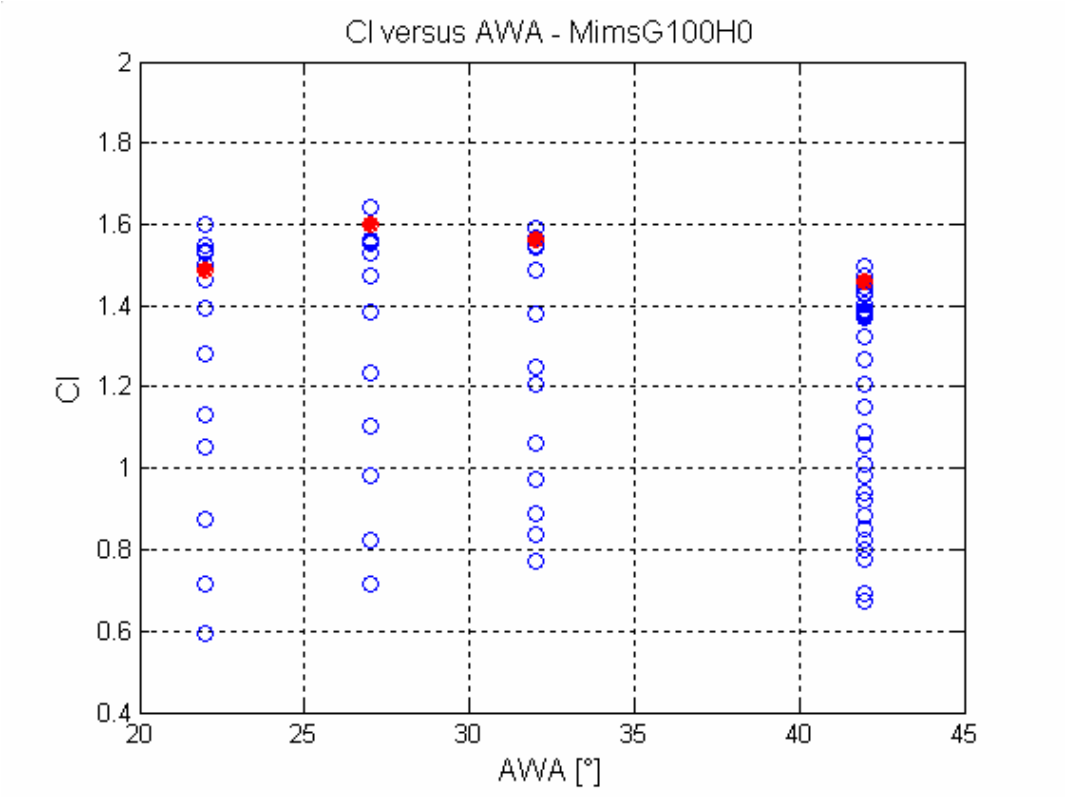

Figure 9

More information from the sail plan can be obtained from lift and drag coefficients because both the induced drag and quadratic profile drag vary with the square of lift.
By plotting the drag coefficients against lift coefficient squared the components of sail drag can be identified. That will be extremely informative and give the required input data for the current IMS VPP aero-model.
As an example in Figure 10 the drag coefficients against lift coefficient squared for each run performed at different AWA in upright condition is reported. Red line correspond to the maximum drive force condition trimming point envelope. As can be seen the envelope line fit points associated to the minimum drag at each lift produced by the sail plan.

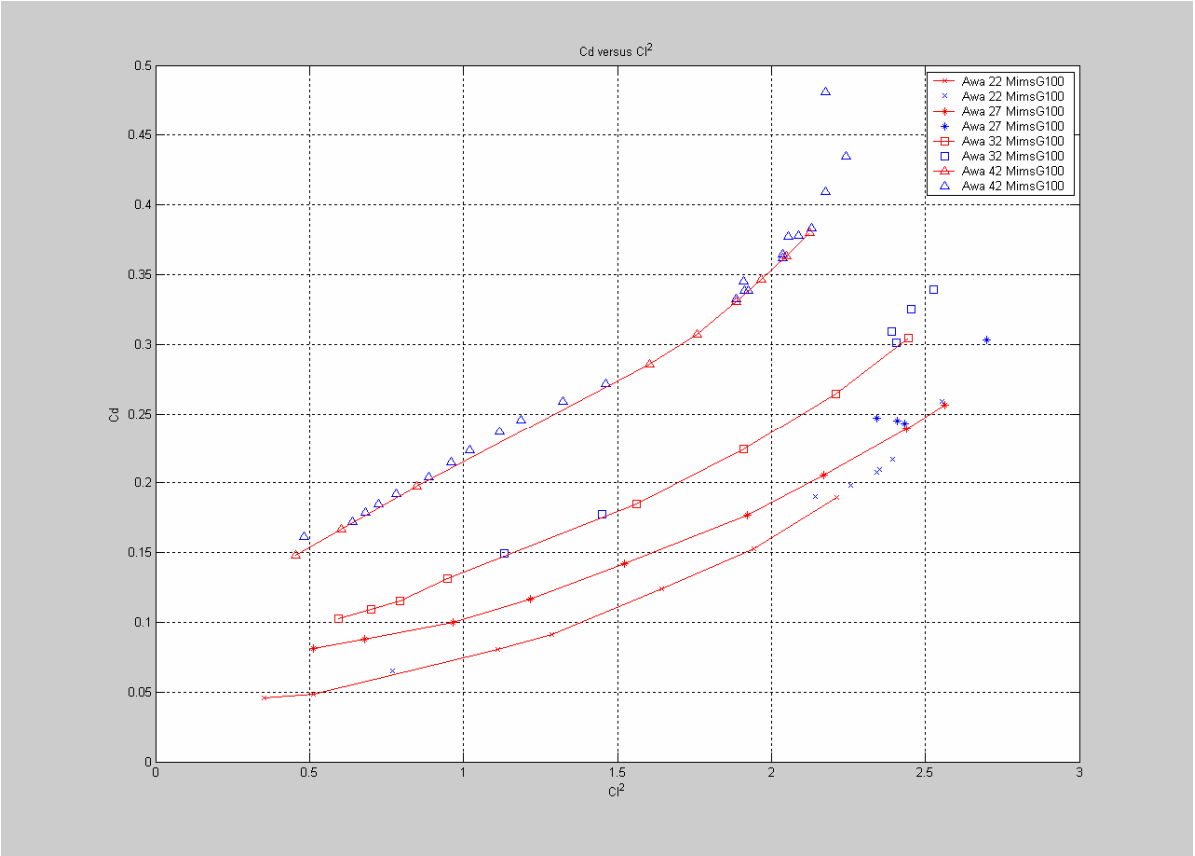

Figure 10

It is important to note that some data points within the low range of lift are above the induced line drag. This does not means that the testing accuracy is not good but that the sail setting of those points were not the optimum. For some reason the drag was higher than it could have been typically because there is some flow separation (in particular backwind on mainsail).
It can be seen that for lower values ofC_L^2 the data tend to collapse to a straight line, whereby C_D increases linearly with C_L^2.
This linear increase is attributable to the induced drag. The effective height Heff which is a measure of the efficiency of the rig can be determined from the slope of the straight line applying simple aerodynamic theory.
For higher values of C_L^2 the CD values increase more rapidly with C_L^2. This additional drag can be attributed to flow separation from the sails, particularly from the upper mainsail leech.
It can be seen that the intercept of the straight line with the zero lift axis through data from the lowest apparent wind angle is conveniently zero but at higher apparent wind angles there remains a residual base drag, not accounted for by windage which increases with the angle.
The intercept of the straight line with the zero lift axis directly represent the parasitic drag coefficient C_{DO} in the IMS model.

For each sail plan tested and for each AWA the effective height can be evaluated considering the linear regression between points that seem to be on a straight line: then the effective height is evaluated according to the following equation:

$$Heff = \sqrt{\frac{SailArea}{\pi Slope}} \tag{11}$$

As an example of this procedure see Figure 11.
Green line represent the linear best fit considering only 5 runs and the slope this straight line is used for effective height evaluation.

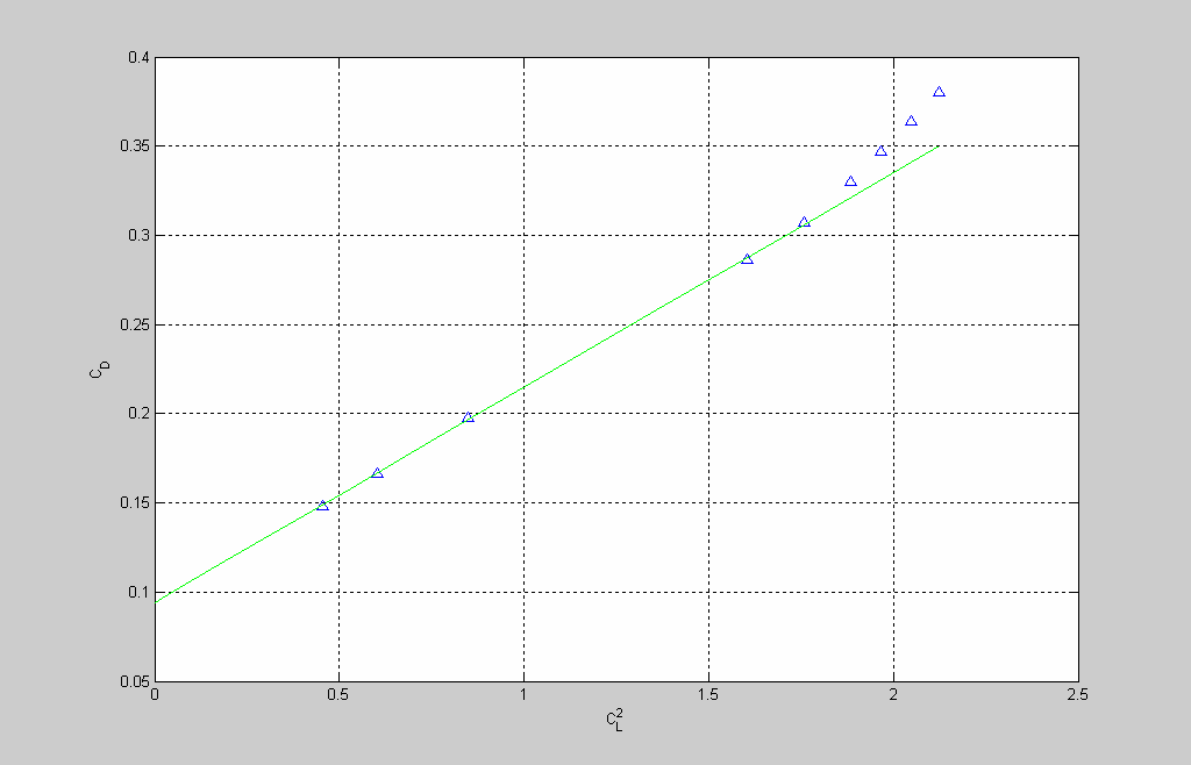

Figure 11

SOME RESULTS

In the following main results obtained in the upright condition are reported.
The relative performance of various rigs tested can be compared without recourse to full VPP calculations by comparing the driving force at similar apparent wind angle and heeling moments. A rig which produce a higher driving force for a given heeling moment, irrespective of the sail settings required to achieve this, will drive the yacht faster.
In Figure 12 the driving force area coefficient [m^2] versus heeling moment area coefficient [m^3] is reported for all the sail-plan considered at each of the AWA tested.
Different colours used refer to different sailplan (for instance blue corresponds to high roach main and 100% overlap jib) and different symbols are related to AWA.
It can be seen that genoas with overlapping have less induced drag (which is confirmed by the effective height as shown in the following) and produce a higher driving force for a given heeling moment.
At the same overlap IMS max roach seems to give better performance except at higher apparent wind angle tested.

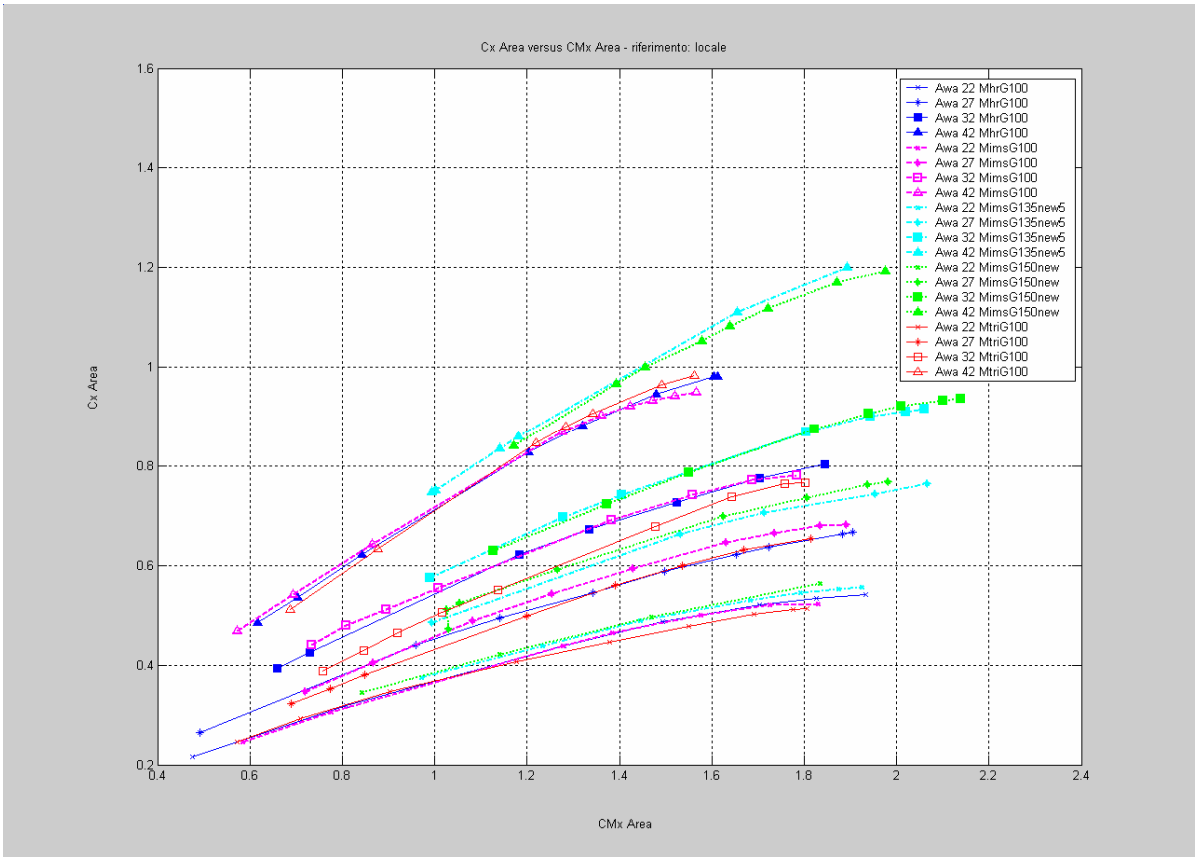

Figure 12

In Figure 13 the plot of the Cx to Cy ratio versus Cy is reported for all the sail-plan considered at each of the AWA tested.
Different colours used refer to different sail plan (for instance blue corresponds to high roach main and 100% overlap jib) and different symbols are related to AWA.

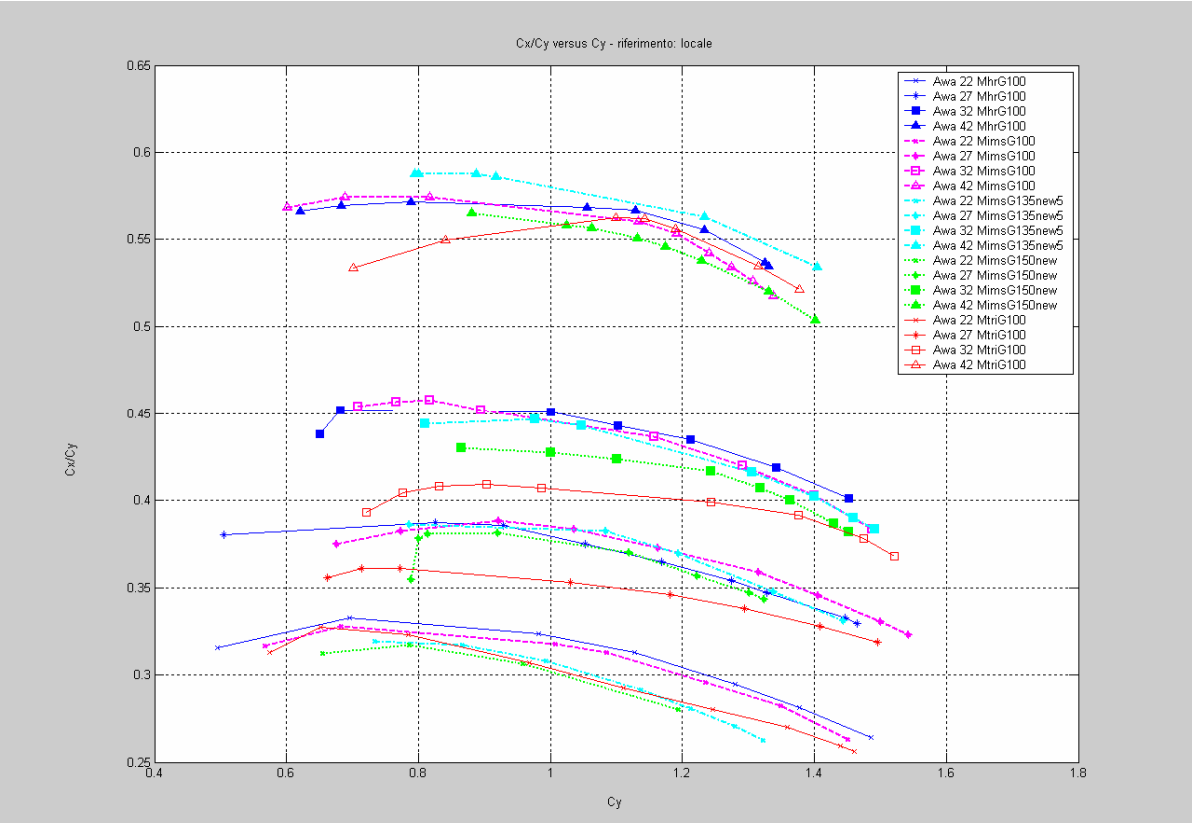

Figure 13

For a given AWA the greatest efficiency of the sails is achieved when the Cx to Cy ratio is maximum.
Mainsail roach gives better performance at each apparent wind angle tested (as confirmed by the effective height trend as shown in the following).
Figure 14 shows the centre of effort height above deck with respect to the mast height for different sail plan for the upright condition.
In particular for each sail plan the measured value at different AWA is reported and the relevant mean value (named “media”) is reported too.

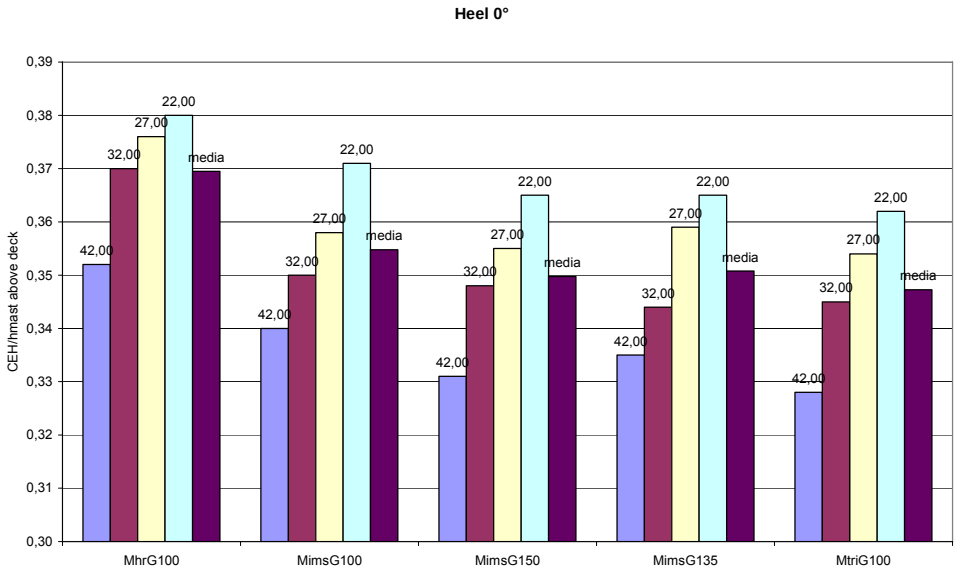

Figure 14

A number of comments can be made on the information given by this plot:

- The smaller the apparent wind angle is, the higher CEH is.
- Increasing mainsail roach (with the same overlap) CEH becomes higher.
- At the same mainsail roach, the smaller the overlap is, the higher CEH is. This is explained by the fact that increasing overlap sail plan has less area high up in the genoa.
- In any case this variation is quite inappreciable.

Following graphs summarise these comments.

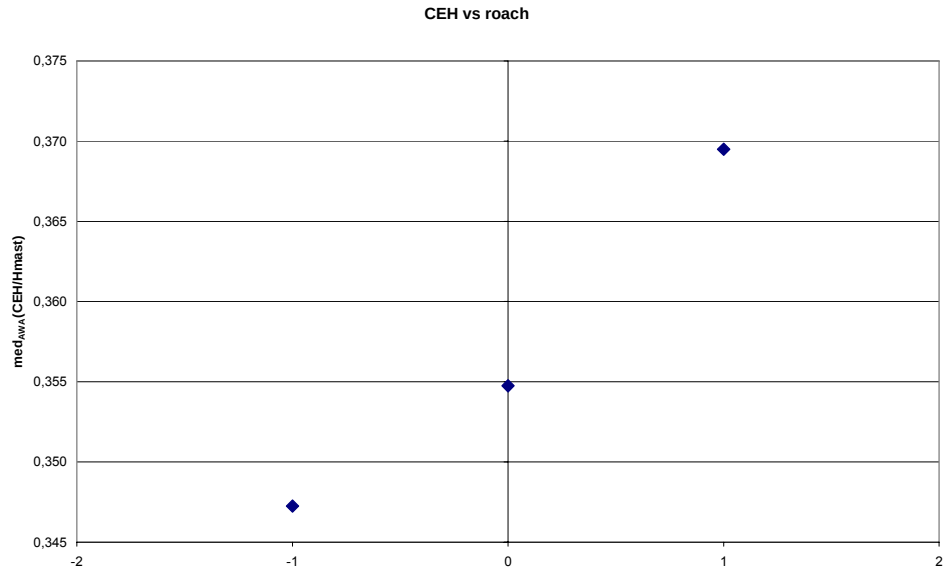

Figure 15

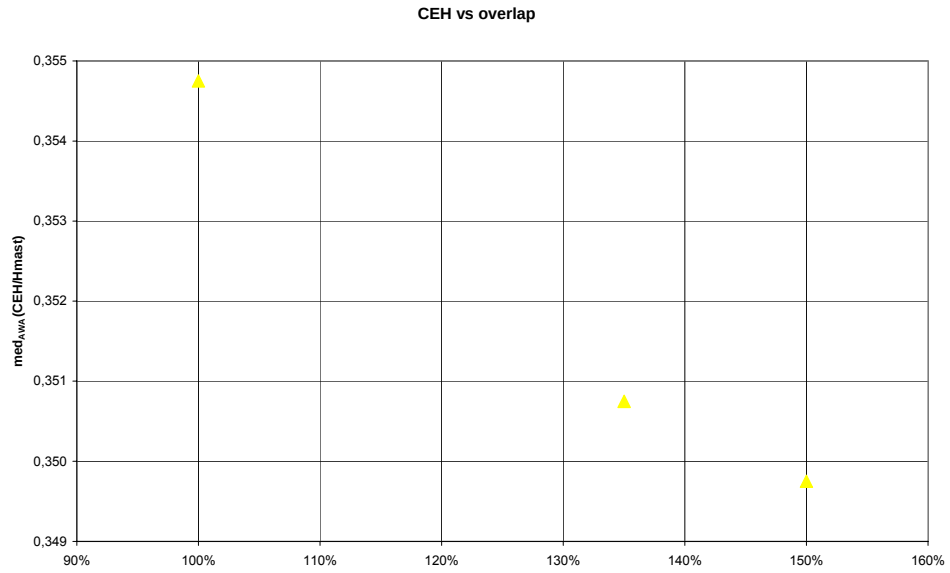

Figure 16

Figure 17 shows the ratio of the Effective rig height to the mast height for different sailplan in upright condition. In particular for each sail plan the evaluated effective height at different AWA is reported and the relevant mean value for each sail plan is reported too. It can be seen that generally the effective height decreases with respect to the AWA.

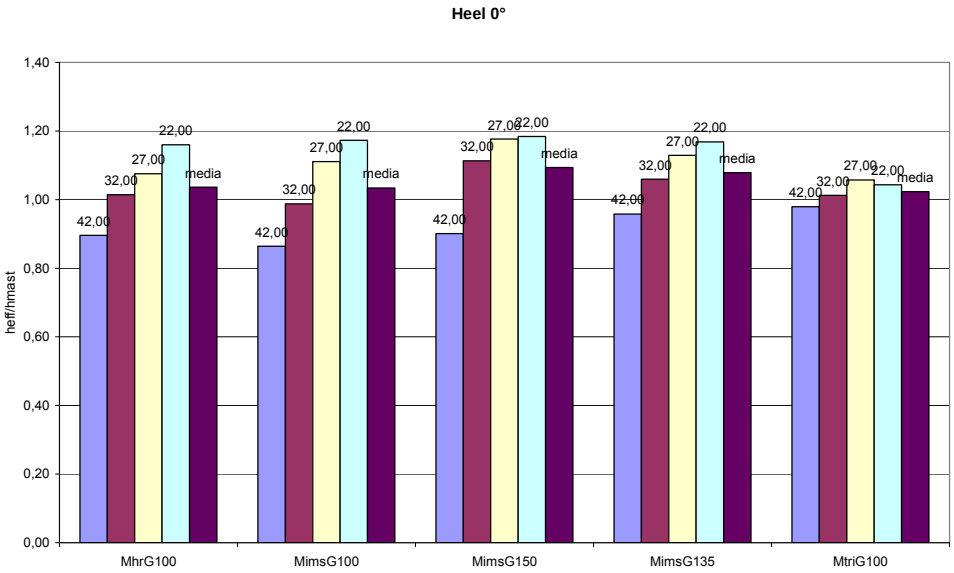

Figure 17

Following figure shows the change in effective rig height (mean value of different AWA results for each sail plan) with varying overlap.
The results show that there is a greater effective height, and less induced drag, with the jib overlapping increase.
In the same figure the Effective height for different mainsail roach is shown at the only available overlap (100%) for all of the mainsails tested.

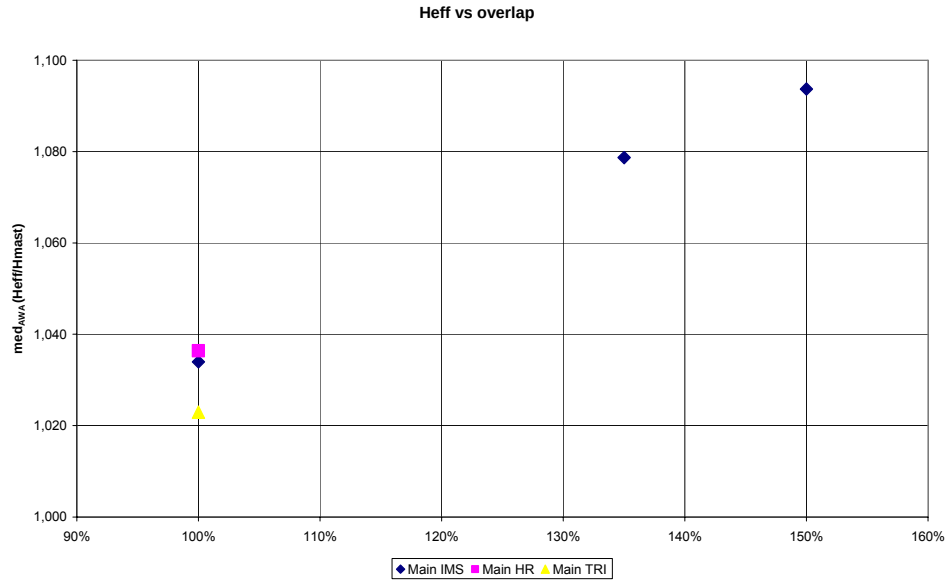

Figure 18

This roach effect is more detailed in Figure 19

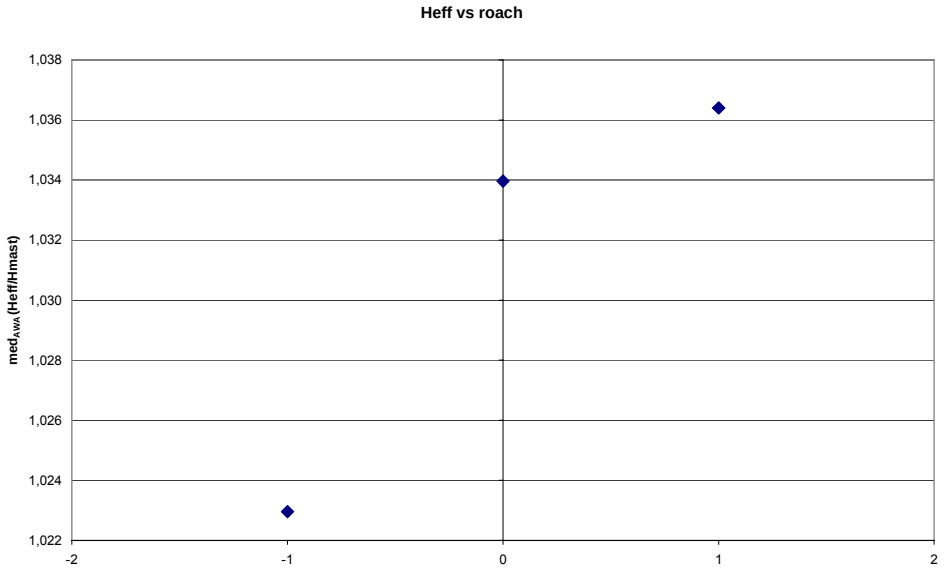

Figure 19

It seems to be some influence of roach but this should be more investigated also for other sailplan combination (i.e. with other jibs available). It should also be remembered that the calculation of effective rig height is very sensitive to variation in the data; in any case the obtained results have the same trend outlined in previous tests performed at the Wolfson Unit in 2002 [8].

GENERAL REVIEW OF AERODYNAMIC MODELS

In this paragraph a brief review of models for the aerodynamics of upwind sails available up to-date for VPP use is outlined with particular reference to the methods of modelling the depowering of sails.
Some remarks (based on the last ITC meetings discussions) on the current IMS aero model are summarised and a proposal for a new approach to model sail forces is outlined.
In velocity prediction programs suitable models must account for the effects of hull speed, heel angle, wind speed and direction and sail area and planform and shape. Generally this is accomplished by force and moments coefficients which provide aerodynamic and hydrodynamic forces and moments: the yacht performance may be predicted by solving the equilibrium equations.
More in details performance prediction requires a complete set of equation which is cabable of predicting the lift, drag and overturning moment of multiple interacting sails at any apparent wind angle and at any sail trim.
The principles of fluid dynamics require each of the various force coefficients (for instance with reference to lift produced by the sails)to depend on different factors as follows:

$$C_L = \frac{Lift}{qA} = C_L(AWA, heel, sailplan, shape) \tag{12}$$

where in particular

- *Sailplan* is the set of ratios describing sail shape which are fixed for a given set of sails
- *Shape* is the additional set needed to represent their flying shape, that is all of those changes which can be made by sail trimmers.

From a general point of view two different approaches can be used in order to manage the flying shape role in the above mentioned formulation which are basically devoted to find explicit expressions for the effects of these sail variables or to move from descriptions of sail shape to description of sail trim which may either explicit or implicit.
With particular reference to the former approach some workers have attempted to find explicit expressions for the effects of these sail variables directly by means of of incorporating CFD into design process and some other use direct methods making numerous CFD runs for various shapes of a given sail plan and feeding the results in the VPP [10], [11].
Within the limits of existing CFD and full scale or wind tunnel testing (at least up to date) it is most unlikely that the effects of every shape parameter on the force coefficients can be described with sufficient accuracy and even if it were possible, the sheer number of variables involved means that this approach is unlikely to find favour.
With reference to the subsequent approach based on explicit description of sails trim, it has the advantage of using variables which are readily measured in full scale or wind tunnel tests (like the position of mainsheet, jibsheet, traveller etc) but the disadvantage that they cannot easily be related to sail shape description.
Finally implicit measures of sail trim may be used which incorporate penalties for departing from an optimum sail setting, as embodied in the concept of reef and flat used in the Kerwin model and adopted currently in the IMS VPP.
The fundamental difference between this approach and the direct methods is that no attempt is made to explicitly link the aerodynamics of the sail with their shapes. In any case it is authors' view the only approach which is currently capable of realise a reasonable association between the parameters describing the shape of the sail and its corresponding aerodynamic performance is to use implicit measures of sails trim so extension to the current model will be suggested.

CURRENT IMS AERO-MODEL: SOME REMARKS

With reference to the current aerodynamic model of the IMS Rule a detailed description can be found in [5] and [8] provides thorough descriptions of subsequent aerodynamic model changes but essentially the basis of IMS aero model eqs is basically Kerwin model [2] (see also [12]):

$$C_L = flat * reef^2 C_{L\max}(AWA) \tag{13}$$

$$C_D = reef^2 (C_{D0}(AWA) + k * flat^2 C_{L\max}^2) \tag{14}$$

$$CEH = CEH(CEH_{geo}, flat) \tag{15}$$

$$k = kpp + \frac{1}{\pi Heff^2} \tag{16}$$

While the maximum lift CLmax the parasite drag CD_0 and the sailing centre of effort height CEH have to be supplied, this formulation cleverly avoids associating the sails forces with explicit features of sail trim and instead uses the reef and flat concepts to complete the system of equations for the force and moment balance.
The main topic of this approach is that sail shapes changes and their effects on aerodynamic properties are modelled using the well known reef and flat parameters.

In particular:

- Choosing flat<1 represents a deliberate reduction of lift in order to reduce the heeling moment or side force.
- Also the use of term flat indicates the reducing of sail camber would be one way of achieving this it is not necessary to say how this reduction is actually achieved in practice.
- Similarly the factor reef multiplies the sail size so that reef<1 represents the reduction on moment by a reduction of sail area (reefing) and consequent lowering the centre of effort and induced drag.

For a given apparent wind angle (AWA) the VPP chooses values of *reef* and *flat* to maximise yacht performance.
To have survived so long this model must *obviously work well*, which is interesting because looking at this model some obvious deficiencies are revealed: in particular first it is important to note that reef is a *geometric* rather than an *aerodynamic factor* (if the actual sail area is used to form the coefficients the reef factor would not appear). In addition we know that when the set of sails are trimmed to their optimum aerodynamic state (elliptic or semi-elliptic loading) but the resulting overturning moment is too great, then the optimum loading now becomes that which minimise drag for a given lift and for a given heeling moment. In this condition the corresponding induced drag must be greater than that of an unconstrained moment, that is as the centre of effort of sails is trimmed further away from the aerodynamic optimum at fixed lift, the induced drag must increase. This is not correctly modelled using reef since eqn 1b always has the drag reducing with the centre of effort.

THE JACKSON AERO-MODEL: SOME REMARKS

In order to overcome the above mentioned problems Jackson (1998) introduced a new parameter called *twist* which explicitly models the relationship between *Induced Drag*, *Lift* and *Centre of Effort Height*
Basic equation of Jackson model are the following:

$$C_L = C_{L\max}(AWA) \tag{17}$$

$$C_D = C_{D0}(AWA) + k * C_L^2 * (1 + ct^2) \tag{18}$$

$$t = 1 - \frac{Ceh}{Ceh_{opt}} \tag{19}$$

$$k = kpp + \frac{1}{\pi Heff^2} \tag{20}$$

$$Ceh = Ceh_{opt} * (1 - t) \tag{21}$$

where:

- t is called twist parameter
- t is zero when the centre of effort is at its optimum height Ceh_{opt}
- t^2 gives the required penalty in induced drag for not keeping the centre of effort height at the height corresponding to semi-elliptic loading
- c is the twist weight function

C_{D0}, Ceh_{opt} and k value can be obtained from experimental results fitting available drag and centre of effort data to the expression (eq.18).
As an example, Figure 20 shows a scatter plot of the predicted versus actual drag for IMS mainsail and 100% overlapping jib.

Ideally this will result in a plot with all the data on a 1:1 straight line, but the onset of separation cause data to diverge.
This unsuccessfully behaviour has been generally found considering also experimental data available from other sailplan tested: then a new approach, strongly based on the availability of an experimental data base according to the ITC research program guidelines will be outlined in the following.

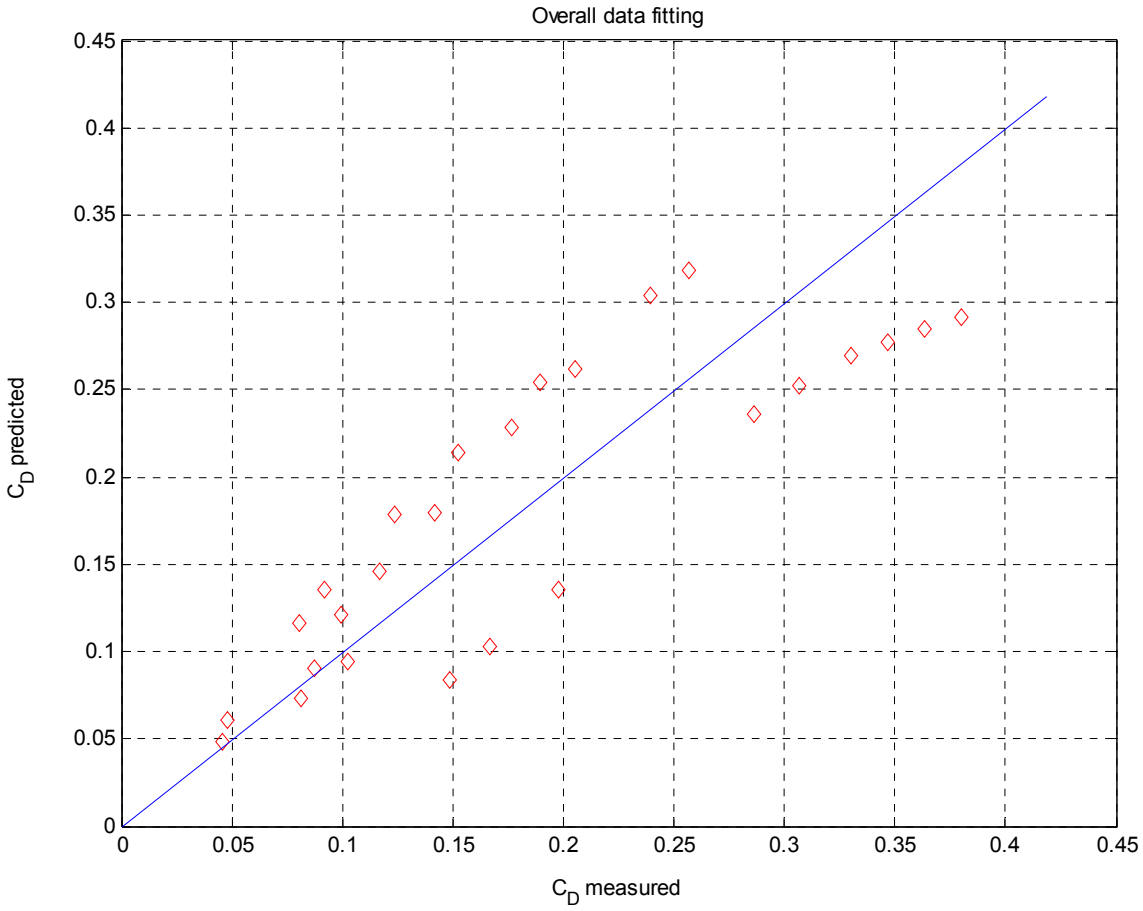

Figure 20

SOME BASIC IDEAS FOR A NEW UPWIND AERO-MODEL

With particular reference to the current IMS VPP aero-model, it should be also noted that some other obvious deficiencies are revealed. In particular:

- Once sailplan is decided, sail area changes occur in discrete steps and not necessarily by scaling all sails dimensions equally (see various headsail codes).

- Both overlap and roach (i.e. sail plan geometry) seem to affect effective height and aerodynamic coefficients

From tests results it seems that different C_D and C_L curve with respect to AWA could be considered for different sail plan. In the current IMS aero model this is accomplished by combining the individual sail's characteristics to produce a set of lift and drag coefficients that describe the aerodynamic behavior of the entire rig [5]. The drawback of this approach is that

mainsail roach does not affect the sail plan aero coefficients. As an example Figure 21 shows a comparison between experimental data and current IMS aero-model Drag and Lift predicted values for different main roach + non overlapping jib.
In Figure 21 the comparison in terms of effective height is reported too.

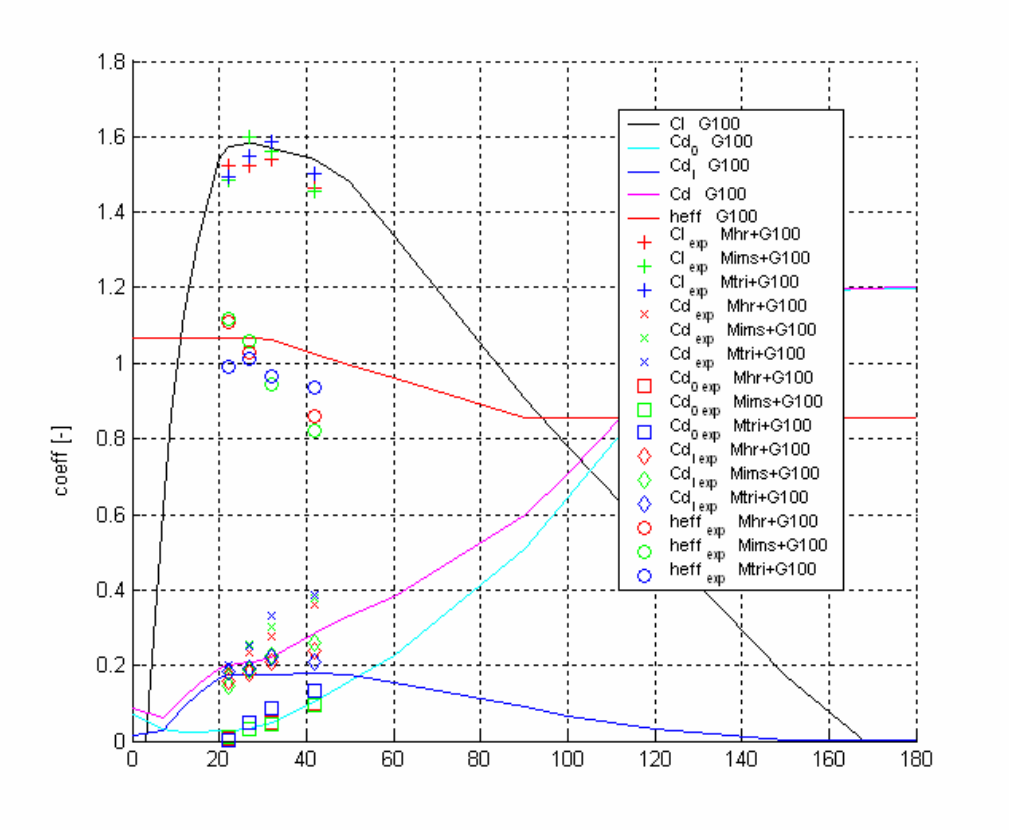

Figure 21

Figure 22 shows the comparison between experimental data and current IMS aero-model predicted values for sailplans with different overlap and the same mainsail.

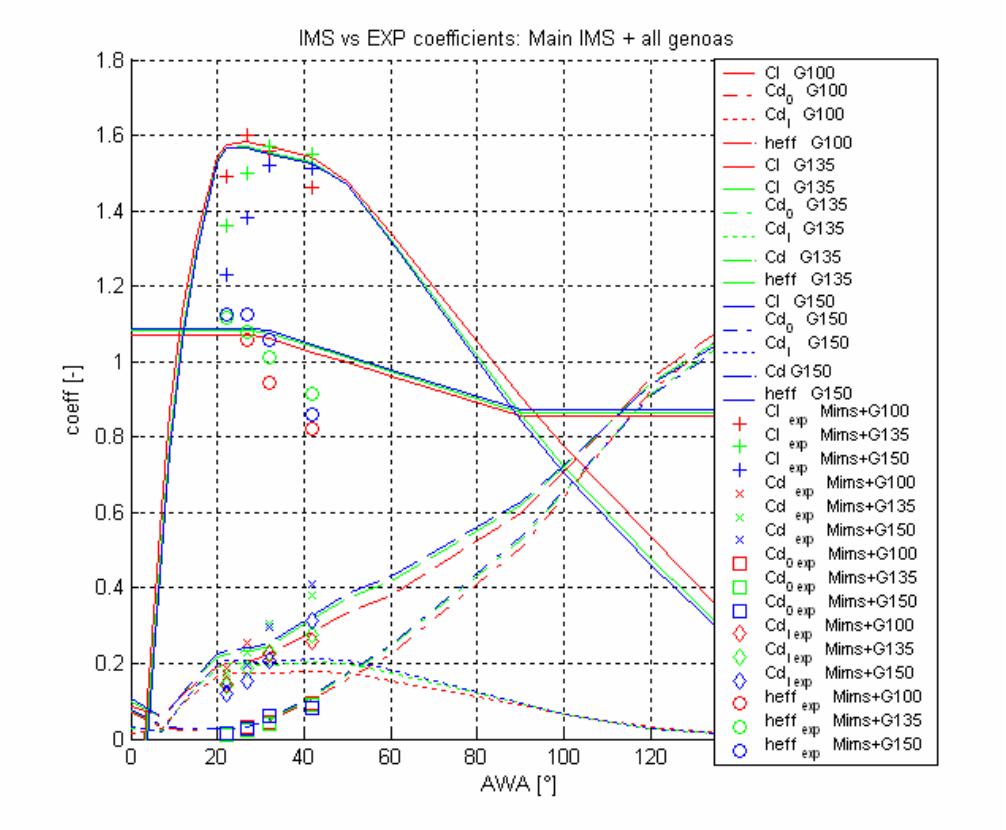

Figure 22

In this case great difference in terms of CL coefficients predicted by actual IMS formulation with larger overlapping at typical close hauled apparent wind angles is pointed out. This means in particular that boats with overlap are supposed faster than they are.
Taking into account that the CL max is directly obtained from the experimental measures and that it is simply an IMS VPP input, different coefficients sets should be considered for different overlapping sailplans.
Also the total drag of overlapping sails at typical close hauled apparent wind angles is under estimated too.
Moreover considering a typical C_D vs C_L^2 plot obtained from tests (Figure 23) emerged that:

- generally the maximum drive condition may be associated with some separated flow.
- effective height seems to be strongly dependent on apparent wind angle
- taking into account the (C_{Lmax}(AWA) and $C_{Dmaxdrive}$(AWA)) curve the actual decline of C_D, as C_{Lmax} is reduced, would follow the straight dotted line which means have a drag value higher than it should be.

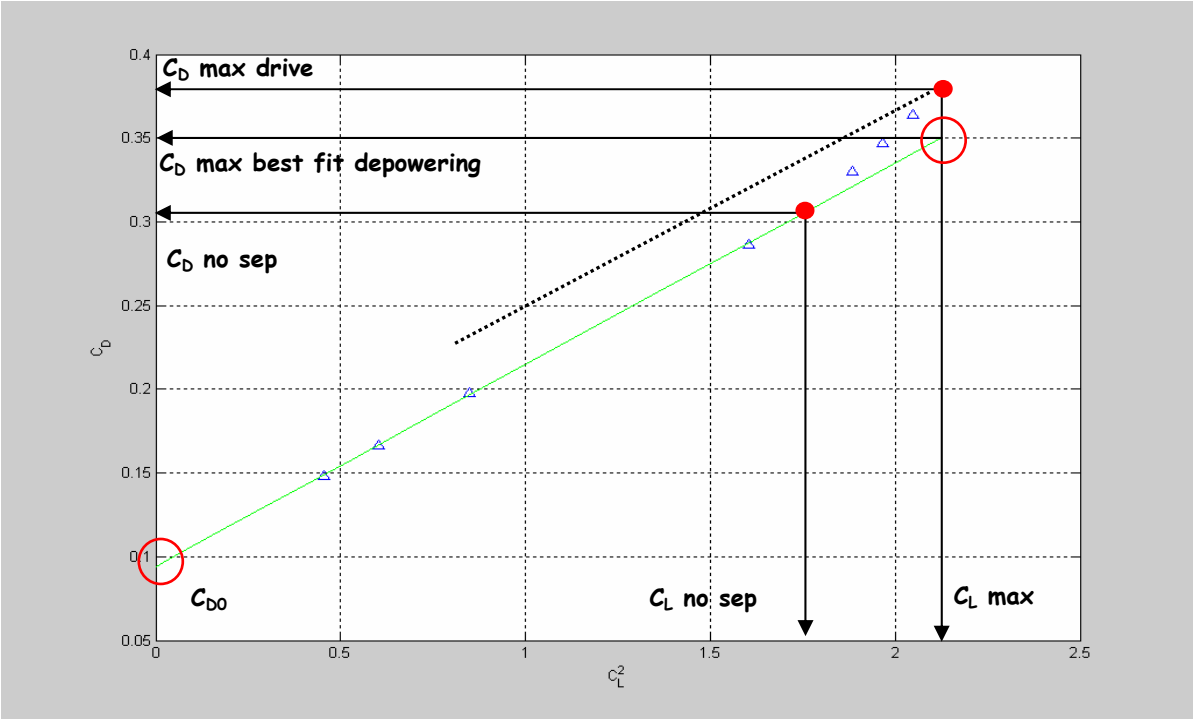

Figure 23

Assuming to have a set of realistic depowered trims from the wind tunnel tests this provides the opportunity to develop improved semi-empirical aerodynamic force model.
In particular the basic idea is that forces and centre of effort height can be modelled as *surfaces* dependent on the apparent wind angle and a newly defined trim parameter we will call in the following *"Power".*
Since the main reason for depowering the sails is to reduce the heeling moment, the level of depowering can be quantified by the reduction in heeling moment.
Then the trim parameter "Power" can be defined as the ratio between the heeling moment coefficient C_{Mx} and the maximum heeleng moment coefficient C_{Mxmax} for that apparent wind angle.

$$Power = \frac{C_{Mx}(awa)}{C_{Mxmax}(awa)} \tag{22}$$

A similar idea is briefly outlined also in [4].
This way the wind tunnel measurements are assigned at different level of depowering so that the VPP can use the depowered trims by optimising the trim "Power" parameter.
Using the experimental data obtained for each sailplan from wind tunnel tests aerodynamic forces (Lift and Drag) and centre of effort height the basic idea is try to match them using *Bezier Surfaces* which can be evaluated as functions of the *"apparent wind angle"* and *"Power"* parameters.
Using this approach we model the surface as a patch, that is a curve-bounded collection of points whose coordinates are given by continuous two – parameters single valued mathematical functions of the form:

$$x = x(u,w)$$
$$y = y(u,w)$$
$$z = z(u,w)$$

In other words we could define a surface that approximates or approaches the experimental points available from wind tunnel tests.
As well known Bezier surface is defined by means of a characteristic polyhedron which is defined using *(m+1) x (n+1)* control points where *m* and *n* are the Bezier patch degrees.
Bezier started with the principle that any point on a surface must be given by a parametric function if the following form:

$$\underline{p}(u,w) = \sum_{i=0}^{m}\sum_{j=0}^{n} \underline{p}_{ij} B_{i,m}(u) B_{j,n}(w) \qquad (23)$$
$$u, w \in [0,1]$$

where $\underline{p}_{ij}$ is a vector of 3D coordinates of the ij-th control point and $B_{i,m}(u)$ and $B_{j,n}(w)$ are Bernstein polynomials which act as shape function.
In particular with reference to wind tunnel results approximation bicubic Bezier patch have been choosen.
The 3D coordinates of the generic point which belongs to the surface are given by the following relationship:

$$\underline{p}(u,w) = \begin{bmatrix} x_{Sp}(u,w) \\ y_{Sp}(u,w) \\ z_{Sp}(u,w) \end{bmatrix} = \begin{bmatrix} (1-u)^3 & 3u(1-u)^2 & 3u^2(1-u) & u^3 \end{bmatrix} \begin{bmatrix} \underline{p}_{11} & \underline{p}_{12} & \underline{p}_{13} & \underline{p}_{14} \\ \underline{p}_{21} & \underline{p}_{22} & & \\ & & \underline{p}_{33} & \\ \underline{p}_{41} & & & \underline{p}_{44} \end{bmatrix} \begin{bmatrix} (1-w)^3 \\ 3w(1-w)^2 \\ 3w^2(1-w) \\ w^3 \end{bmatrix}$$

The matrix

$$\begin{bmatrix} \underline{p}_{11} & \underline{p}_{12} & \underline{p}_{13} & \underline{p}_{14} \\ \underline{p}_{21} & \underline{p}_{22} & & \\ & & \underline{p}_{33} & \\ \underline{p}_{41} & & & \underline{p}_{44} \end{bmatrix}$$

contains the position vectors of the surface control points which define the vertices of the characteristic polyhedron and thereby the Bezier surface patch (Figure 24).

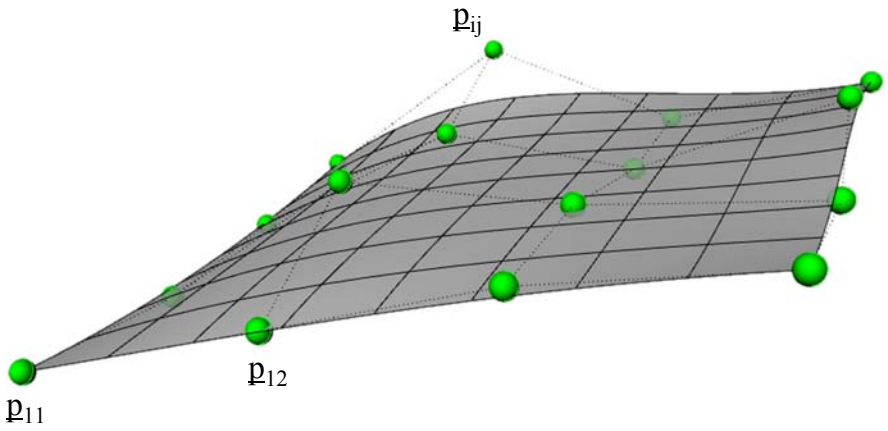

Figure 24

As an example with reference to CL surface the 3D coordinates are:

$$\underline{p}(u,w) = \begin{bmatrix} AWA(u,w) \\ Power(u,w) \\ CL(u,w) \end{bmatrix} \tag{24}$$

and u and w are nondimensional variables ($u, w \in [0,1]$) associated to *AWA* and *Power* values range corresponding to wind tunnel tests performed.
In order to identify the elements of P matrix, i.e the surface control points coordinates, we have to approximate CL values at each AWA as a function of Power values (available from the experimental depowering sequence) by means of a cubic Bezier curve which is a sort of a skeleton of the CL surface patch.
As an example Figure 25 shows the C_L surface and the corresponding control points location with reference to a particular sailplan.

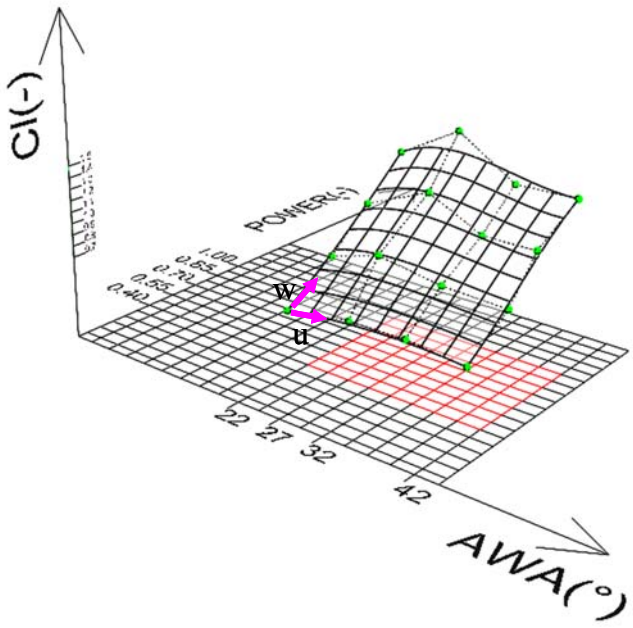

Figure 25

On the basis of the control points location knowledge, for a fixed u and w degree using equation (23) the C_L Bezier patch is univocally determined.
As an example in Figure 26 the Bezier CL surface and experimental measured CL values (red dots) corresponding to different *AWA* and depowering sequence tested are reported.

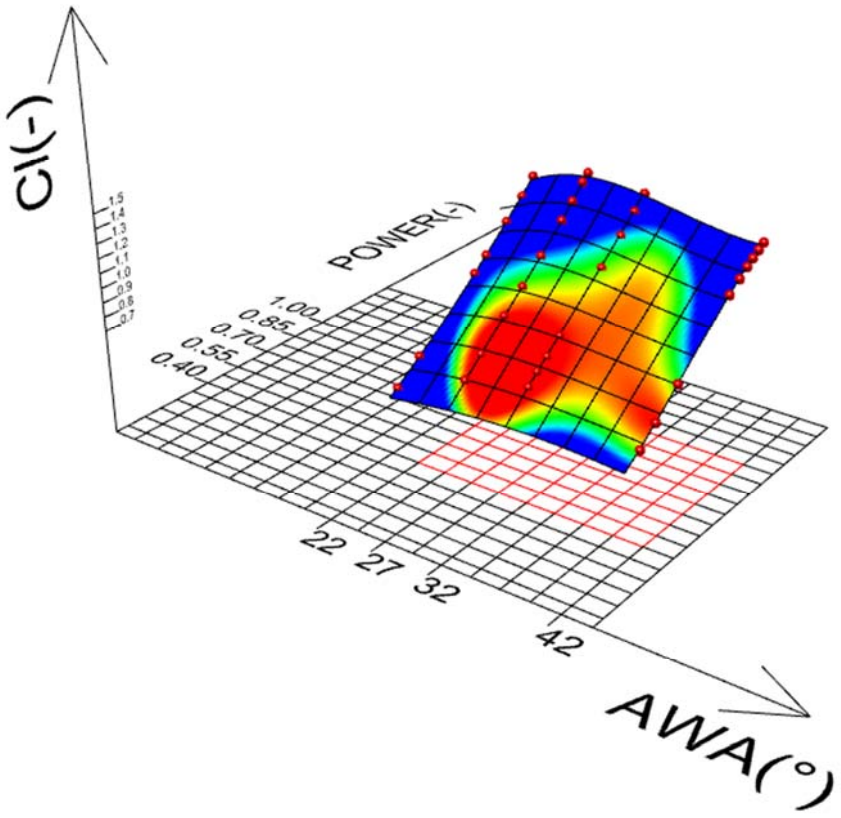

Figure 26

In the same way it's possible to include the dependency of the drag coefficient and centre of effort height from these parameters (Figure 27– Figure 28).

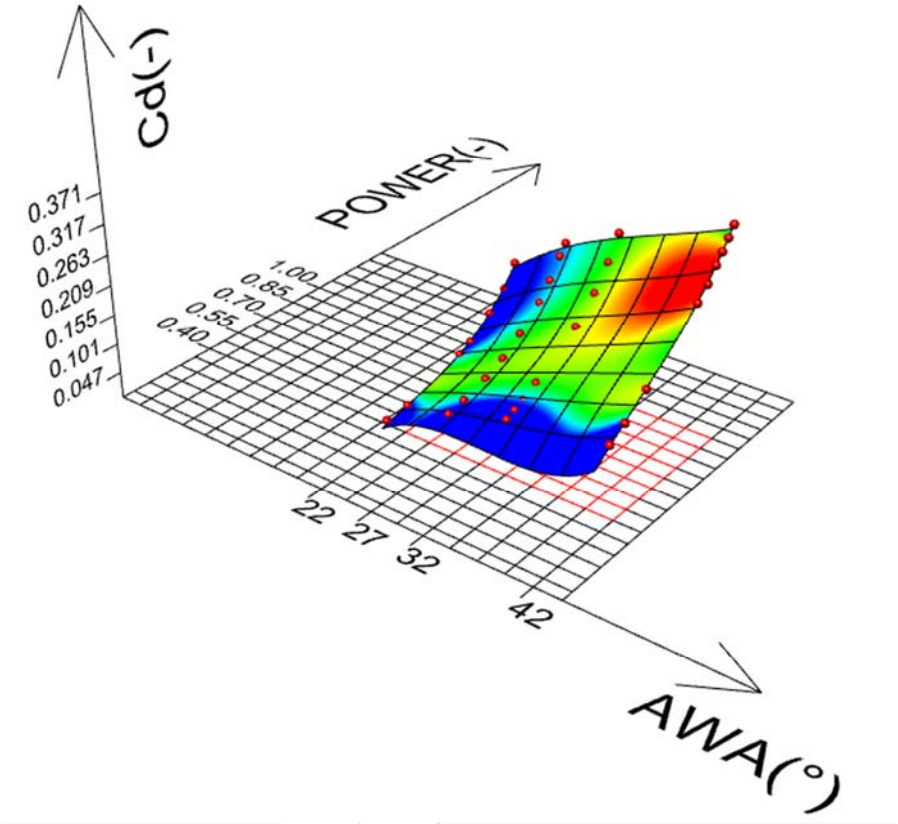
Cd(-)
0.371
0.317
0.263
0.209
0.155
0.101
0.047
POWER(-)
1.00
0.85
0.70
0.55
0.40
22
27
32
42
AWA(°)

Figure 27

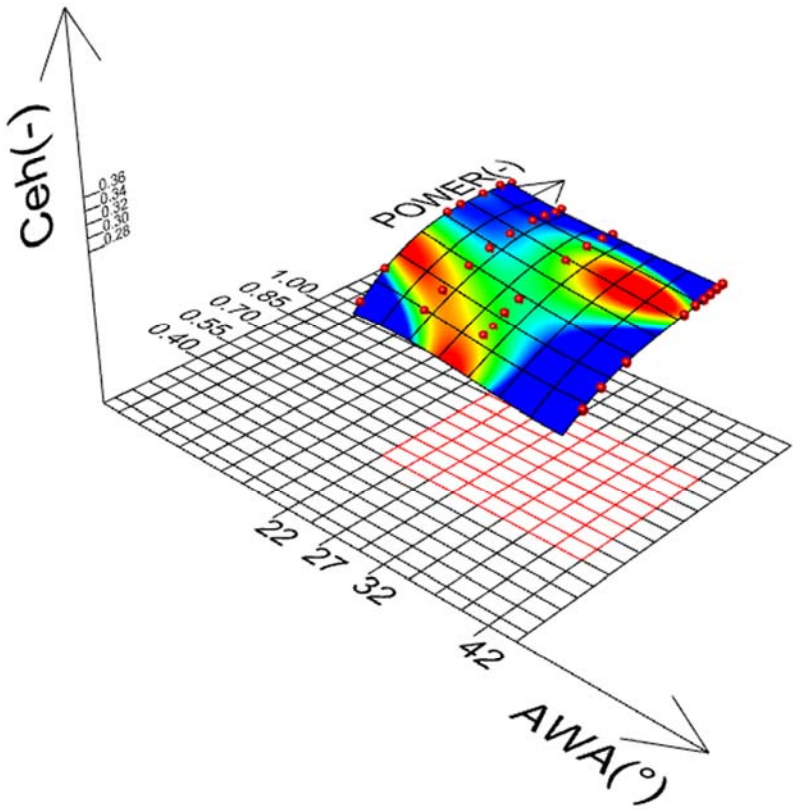

Figure 28

Using the above mentioned approach, for each sailplan tested it is possible to use the relevant C_D C_L and Centre of Effort height surfaces as a function of apparent wind angle *"awa"* and *Power*: in particular VPP procedure will take into account these surfaces as sails aerodynamic input data.
VPP solution iterative procedure is not affected by the new aero-model with the main advantage that the proposed formulation is based on *wind tunnel collected results only* without considering any drag superposition effects.
More in details for a given apparent wind angle (AWA) the VPP chooses values of *"Power"* parameter to maximise yacht performance.completing the system of equations for the force and moment balance in the same way of the reef and flat concepts.
The main advantage of the proposed formulation is that is based on *wind tunnel collected results only* without considering any drag superposition effects.

GENERIC SET OF SAILS

In order to include in the aero model the effects of jib overlap and mainsail roach, and in order to take into account that genoa overlap varies, for a given boat, with varying wind speed and the need of de-power, the right way to do could be to attempt to interpolate between the experimental available surfaces data base (which are related to discrete jib overlap and to discrete mainsails roach values).
As an example Figure 29 shows the C_L surface obtained for all the five tested sailplans.

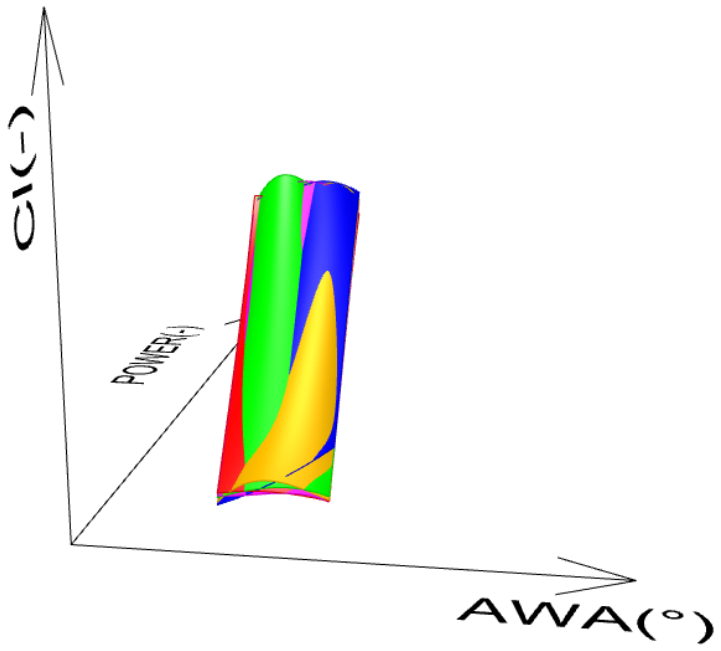

Figure 29

The basic concept has been an investigation of the Bezier Surface control points mathematical dependence on sailplan overlap and roach parameters.
Let's suppose we have an explicit function of the control points 3D coordinates by the sailplan overlap and roach parameters (Figure 30):

$$\underline{p}_{ij}(overlap, roach)$$

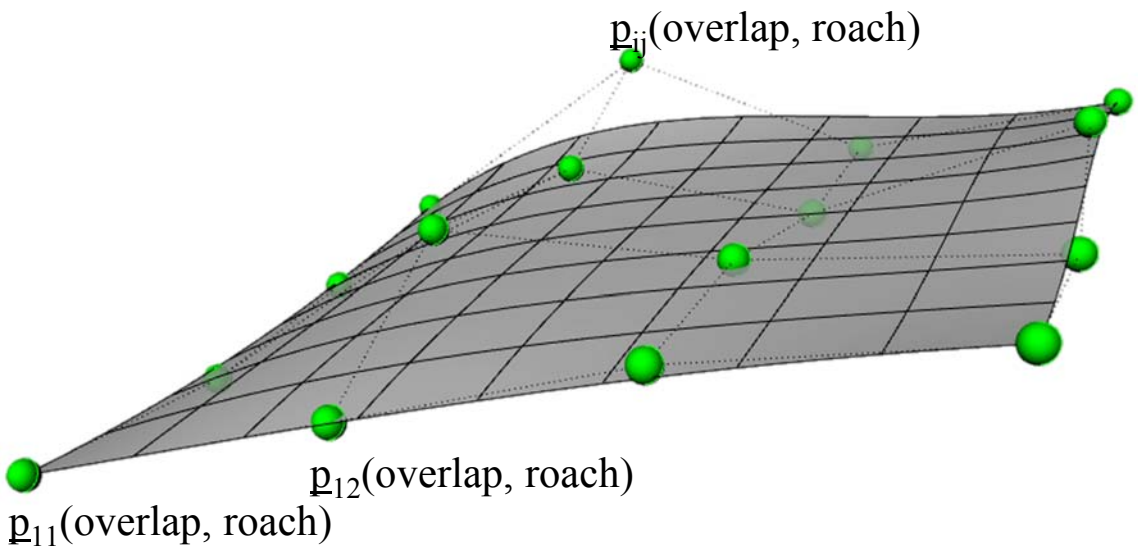

Figure 30

Then it is possible to evaluate the matrix that contains the position vectors of the surface control points which define the vertices of the characteristic polyhedron and thereby the Bezier surface patch relevant to a generic overlap and roach combination:

$$\begin{bmatrix} \underline{p}_{11}(overlap,roach) & \underline{p}_{12}(overlap,roach) & \underline{p}_{1j}(overlap,roach) & \underline{p}_{1N}(overlap,roach) \\ \underline{p}_{21}(overlap,roach) & \underline{p}_{2j}(overlap,roach) & & \\ & & \underline{p}_{ij}(overlap,roach) & \\ \underline{p}_{M1}(overlap,roach) & & & \underline{p}_{MN}(overlap,roach) \end{bmatrix}$$

As an example with reference to CL surface (Figure 30) the 3D coordinates are:

$$\underline{p}(u,w)=\begin{bmatrix} AWA(u,w) \\ Power(u,w) \\ CL(u,w) \end{bmatrix}=\begin{bmatrix}(1-u)^3 & 3u(1-u)^2 & 3u^2(1-u) & u^3\end{bmatrix}\begin{bmatrix} \underline{p}_{11}(overlap,roach) & \underline{p}_{12}(overlap,roach) & \underline{p}_{1j}(overlap,roach) & \underline{p}_{1N}(overlap,roach) \\ \underline{p}_{21}(overlap,roach) & \underline{p}_{2j}(overlap,roach) & & \\ & & \underline{p}_{ij}(overlap,roach) & \\ \underline{p}_{M1}(overlap,roach) & & & \underline{p}_{MN}(overlap,roach) \end{bmatrix}\begin{bmatrix}(1-w)^3 \\ 3w(1-w)^2 \\ 3w^2(1-w) \\ w^3\end{bmatrix}$$

and u and w are nondimensional variables ($u,w\in[0,1]$) associated to *AWA* and *Power* values range corresponding to wind tunnel tests performed.
With reference to the tested sailplan, it should be noted that vertices of the characteristic polyhedron aerodynamic coefficients and centre of effort height surfaces are defined by the same apparent wind angles for each sailplan (which means each overlap and roach combination) and by *"Power"* parameter values that are very closer (see Figure 31).

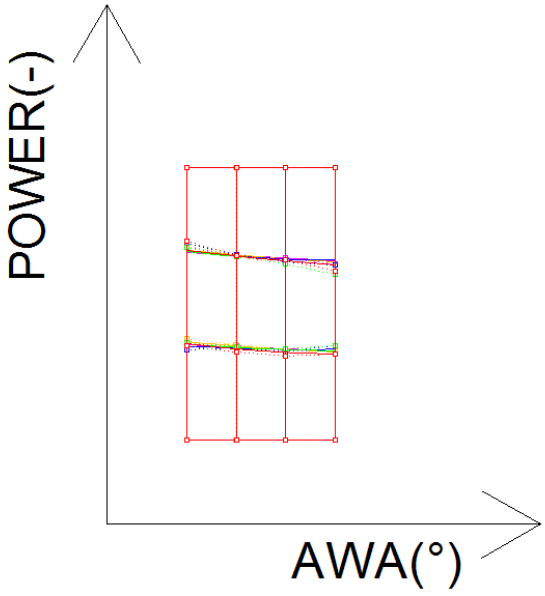

Figure 31

This means we can only consider the surface control points 3rd coordinate variation with respect to overlap and roach parameters combination neglecting the others two coordinates.
In other words we can look for explicit functions between the aerodynamic coefficients and centre of effort height surface 3rd coordinate control points (Zp_{ij}) and overlap and roach parameters:

$$Zp_{ij} = Zp_{ij}(overlap, roach)$$

which can be used during VPP iterations for evaluate the aerodynamic coefficients and centre of effort height for each apparent wind angle and "Power"parameter combination of the generic yacht sailplan.
Considering experimental results available from different sailplan tested (which means for each overlap and roach combination) for each *"apparent wind angle"* and *"Power" parameter* combination (which define the vertices of the characteristic polyhedron), in order to fit 3rd coordinate control points (Zp_{ij}) measured values, quadratic polynomial surfaces have been choosen:

$$Zp_{ij} = a_0 * overlap^2 + a_1 * roach^2 + a_2 * overlap * roach + a_3 * overlap + a_4 * roach + a_5$$

Coefficients a_0, a_1,….a_5 have been evaluated by means of a least square minimization procedure.

As an example Figure 32, Figure 33, Figure 34 show the surface for the C_D C_L and Ceh values for a fixed couple of apparent wind angle and Power values.
In the same figures experimental points are reported too (dots).

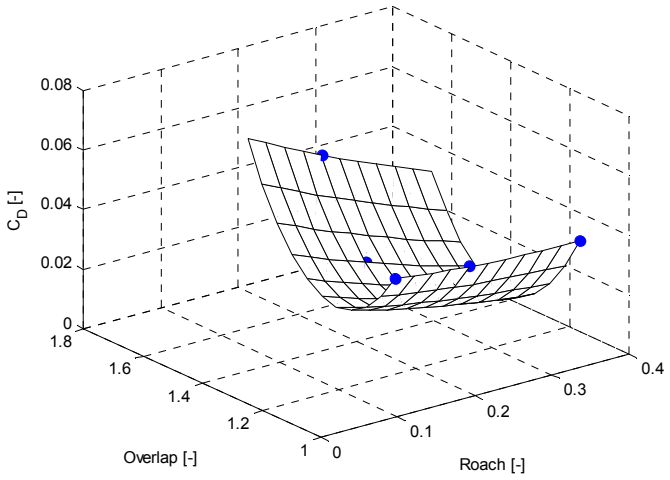

Figure 32

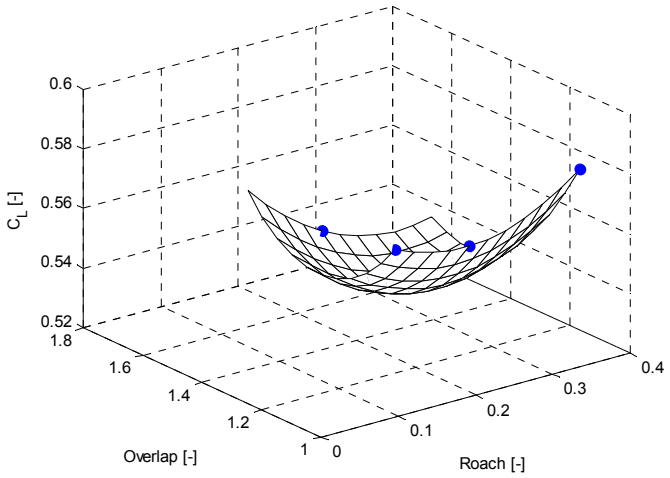

Figure 33

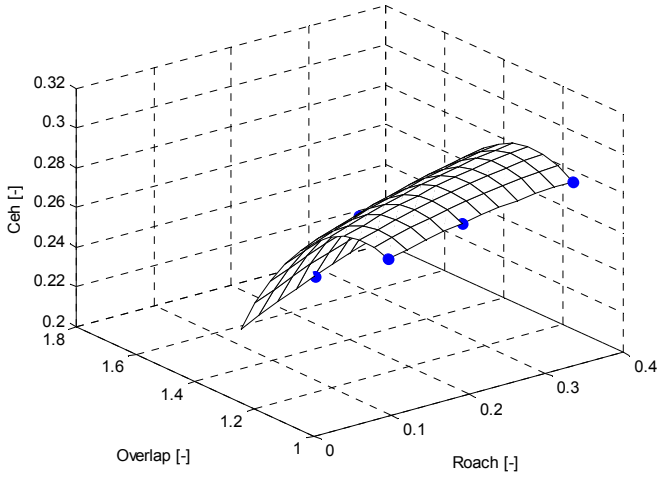

Figure 34

VPP procedure could easily take into account these surfaces as sails aerodynamic input data.
More in details the VPP will try to optimise the boat speed and the *"Power"* parameter concept will be used to complete the system of equations for the force and moment balance in the same way of the reef and flat concepts.
With reference to IMS VPP, the currently used solution iterative procedure should not be affected by the new aero-model with the main advantage that the proposed formulation should be based on *wind tunnel collected results only* without considering any drag superposition effects as the actual IMS aero model does.

CONCLUSION

In this paper research activities carried out at Politecnico di Milano Twisted Flow Wind Tunnel with partial funding from the ORC in order to investigate the performance of upwind sails have been summarised. In particular a series of rig planform variations in mainsail roach and jib overlap have been tested. The results of these investigation are used to assist the International Technical Committee (ITC) in upgrade the formulations in the IMS sail aerodynamic model.
Finally some basic ideas to provide a more suitable aero-model for upwind sails as required by IMS VPP to predict the performance of yacht for rating purposes are outlined. The new approach is strongly based on the availability of an experimental data base according to the ITC research program guidelines.
The proposed method is now under ITC analysis and in particular the effects are tested on a sample fleet that the ORC is still committed to handicapping correctly.
The aero model could be improved including also the sailplan fractionality as a geometric parameter affecting the aerodynamics of the sailplan. From this point of view some preliminary results from wind tunnel tests are available and more investigation are planned for the next future.

ACKNOWLEDGEMENTS

This wind tunnel testing have occurred with the financial assistance of the Offshore Racing Congress and the support of Politecnico di Milano CIRIVE Department.
North Sails Italy provided sails and trimming expertise to the program.

There are a number of individuals who contribute to the development of offshore handicapping rules. Authors would like to thank in particular the ITC members and ORC Chairman Bruno Finzi for their continued support.

REFERENCES

1. Kerwin, JE "A velocity Prediction Program for Ocean racing yachts", *Rep 78-11 MIT*, July 1978
2. Fossati, F.& Zasso, A.& Viola I., "Twisted Flow Wind Tunnel Design for Yacht Aerodynamic Studies", *Proc. of the 4th European and African Conference on Wind Engineering*, J. Naprstek & C. Fisher, Prague, 11-15 July, 2005.
3. J. M. C. Campbell, & A. R. Claughton – "Wind Tunnel Testing of Sailing Yacht Rigs" – *13th HISVA symposium* – Amsterdam 1994
4. P. S. Jackson P. Richards & H. Hansen – " An investigation of Aerodynamic Force Modelling for Yacht Sails Using Wind Tunnel" - *Proceedings of the 2nd High Performance Yacht Design Conference* Auckland, 14-16 February, 2006
5. Claughton A, "Development in the IMS VPP Formulations" – *SNAME 14th CSYS,* Annapolis, 1999
6. P. S. Jackson, "Modelling the Aerodynamics of Upwind Sails" – *Journal of Wind Eng. & Ind. Aerodyn.,* vol. 63 , 1996
7. P. S. Jackson, "An improved Upwind Sail Model for VPPs" – *SNAME 15th CSYS,* Annapolis, 2001
8. Teeters J & al., "Changes to Sail Aerodynamics in the IMS Rule", *SNAME 16th CSYS,* Annapolis, 2003
9. Fossati, F.& al., "Wind Tunnel Techniques for Investigation and Optimization of Sailing Yachts Aerodynamics", *Proceedings of the 2nd High Performance Yacht Design Conference* Auckland, 14-16 February, 2006
10. Day, A. "Sail Optimisation for Optimal Speed", *Journal of Wind Eng. & Ind. Aerodyn.,* vol. 63 , 1996
11. Euerle, SE & al, "Toward a rational Upwind Sail Force Model for Vpps" *SNAME 11th CSYS,* Annapolis, 1993
12. Hazen G. " A Model of Sail Aerodynamics for Diverse Rig Types", SNAME 1980

Session 5

Guenter Grabe

The Carbon and PBO Rig for the „sailOvation“
- Finite Element Analysis -

University of Applied Sciences Kiel

Prof. Dr.-Ing. Guenter Grabe

Guenter.Grabe@FH-Kiel.de

1. Introduction

The “sailOvation” is a German innovation bearer for the cruising yacht of the future. She is a 30 ft long canting keel yacht and bound to plane on a close reach. The project is sponsored by the German yachting magazine “segeln-magazin” and involved companies to build her.
The rig is a key term to enable the “sailOvation” to plane on a close reach. The aim is to design and to construct a rig that is strong and stiff enough to resist the big righting moment from the canting keel and that is also as light as possible. A global geometrical nonlinear finite element analysis is performed for the rig. Two load cases are investigated: dock tune and sailing close hauled. The rig is constructed out of carbon for the spars and out of PBO fibres for the transverse standing rigging.
Results of first trial runs show that the “sailOvation” is able to start semi-planing on a close reach and that there is still a potential to raise speeds by optimizing rig and sail trim.

2. The sailing yacht “sailOvation” and her rig

The sailing yacht „sailOvation“ is designed by M. O. v.Ahlen and constructed by the boatyard Janssen and Renkhoff. The design is in the tension field of the contradicting demands of cruising and planing on a close reach. The main numbers are:

L = 9.00 m	D = 2.00 m
LWL = 8.92 m	Depl. = 1.7 t light weight, 1.9 t loaded
B = 3.43 m	Keel weight = 0.7 t
BWL = 2.00	RM25 = 2,775 kgm

Everything possible was done to reduce drag and weight. The hull is built in carbon-SPRINT sandwich. The big carbon and PBO rig has a lot of power (**figure 1**). A special feature is the so called X-keel arrangement (**figure 2**). The “sailOvation” has two keels that can be canted individually. The forward keel carries the bulb. It is canted to windward up to 50° to enhance the righting moment. The aft keel is canted to leeward as much as the yacht heels. It will be adjusted vertical to produce optimal side force. Two asymmetric dagger boards were no alternative, for they would reduce the space under deck for cruising accommodations. Two hydraulic rams move the keels. The “sailOvation” has no engine. The energy to move the keels comes from a bank of 12 V batteries. 180 tacks are possible with fully charged batteries.

Semi-planing on a close reach is only possible with the ability to carry a large sail area for propulsion force combined with a small total weight. Racing dinghies like a Flying Dutchman can semi-plane on a close reach. They have a length/displacement ratio of about 7.5 and higher. The length/displacement ratio and the sail carrying number of the “sailOvation” are:

$$\frac{L_{WL}}{V^{(1/3)}} = 7.2 \qquad \frac{S_A^{(1/2)}}{V^{(1/3)}} = 5.2 \cdot$$

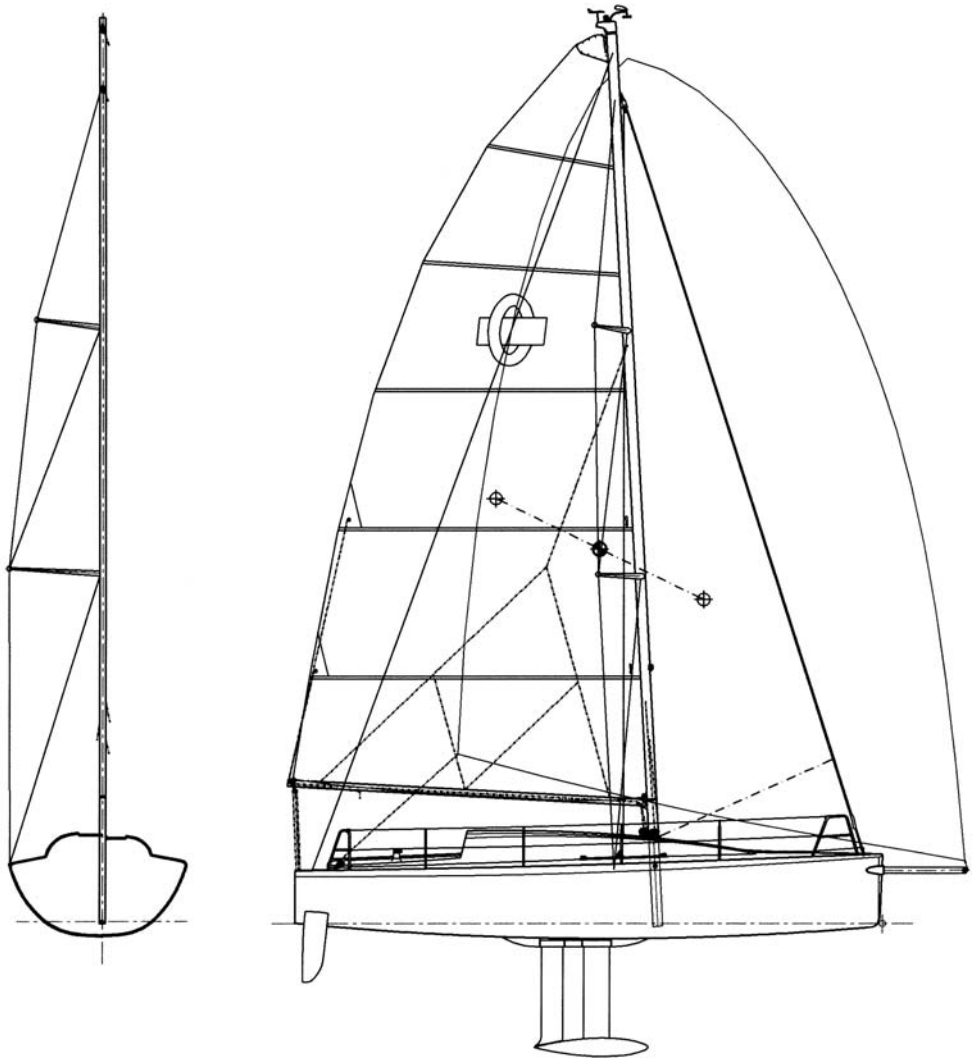

Figure 1: Rig and sail plan

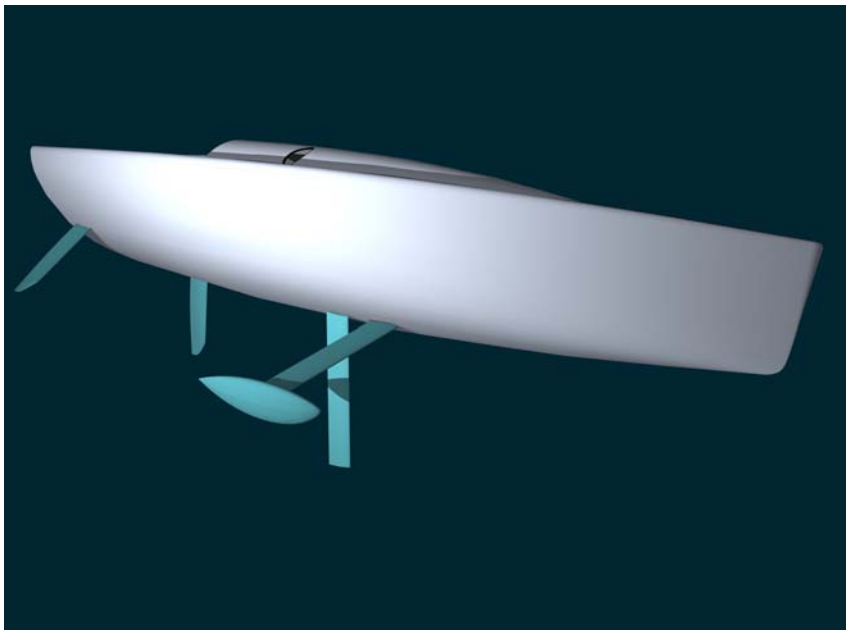

Figure 2: X-keel arrangement

Figure 1 shows the sail and rig plan. The „sailOvation“ has a 9/10 fractional rig with two 25° aft raked spreaders, no backstay and no checkstay for easy handling as a cruiser. The absence of a backstay enables a big roach of the main sail and a low centre of effort. The rig has top runners. For this type of rig the runners are only used for controlling the mast bend and as a mast support when running [1].

The main dimensions of the rig are:

P = 11.760 m	I = 11.960 m
E = 5.420 m	J = 3.160 m.

The main sail has an area of 42 m². It is fully battened and has a big roach for high efficiency. The genoa has an area of 21 m². It has a furler for easy handling. There is no spinnaker but a gennaker with an area of 90 m². The sails were sponsored by elvstrom sobstad.

The rig is constructed by Nordic Mast with a carbon mast tube and after some trouble with aluminium spreaders also carbon spreaders. The use of carbon instead of aluminium reduces the weight of the rig. An aluminium mast tube weighs about 50 % of the whole rig weight. A carbon mast tube weighs again about 50 % of an aluminium mast tube. The weight reduction for the complete rig is accordingly about 25 % choosing carbon for the mast tube instead of aluminium. Carbon for mast tubes is common on racing yachts today and there was no other choice for the “sailOvation” than to choose carbon.

On the search for more weight reduction in the rig there was a look at the shrouds, commonly made out of wire for cruisers and rod for racers. SmartRigging delivered the shrouds for the rig. They are not out of nitronic rod but produced out of PBO-HM (p-phenylene-2,6-benzobisoxazole). That is a new high performance fibre developed by TOYOBO. HM means High Modulus. PBO is still new for the rigging of sailing yachts. Classification companies like the Germanische Lloyd develop Guidelines for type-approvals [2]. PBO is also called Zylon. It has superior tensile strength, elasticity modulus and creep properties than aramid fibres. PBO is suitable for shrouds for it does not creep as much as aramid fibres. The fibres (1.5 denier) have a tensile strength of

5,800 MPa and a tensile modulus of 280 GPa. The density is 1.56 g/cm³. PBO needs a protection cover for it disintegrates after being exposed to sunlight for only a few days, it can chafe and water absorption should be avoided. End terminals for fibre cables have always been a problem. The shrouds of the "sailOvation" are constructed in winding endless fibres round both end fittings. The end fittings are cast in a sturdy poly urethane coating. The custom made PBO shrouds have to be pre stretched with high tension forces to receive their mechanical properties.
The PBO sizes for the standing rigging of the "sailOvation" are not chosen by the equivalent strength but by the equivalent stiffness of rod. The equivalent stiffness is the product of the modulus of elasticity and the cross section area. It should be the same for PBO and rod to get the same stiffness for the rig. The strength of PBO is, when choosing the same stiffness, bigger than that of rod. PBO cables weigh about only one fourth to one third compared to cables out of rod but the diameters of PBO are about 50 % bigger. **Table 1** shows a comparison between rod and PBO for the shrouds of the "sailOvation" neglecting the different terminal weights. The head stay is not changed from rod to PBO to be able to mount a furler and the runners are out of vectran.

Table 1: Comparison between Rod and PBO for the transverse standing rigging of the "sailOvation"

		Rod				PBO			
shroud	length	D	mass/length	mass	area	D	mass/length	mass	area
V1	4.741	6.35	250	1,185	0,030	9,5	80	379	0.045
V2	3.890	5.03	157	611	0,020	7,5	60	233	0.029
D1	4.729	5.03	157	742	0,024	7,5	60	284	0.035
D2	4.053	4.37	118	478	0,018	6,5	50	203	0.026
D3	3.626	5.03	157	569	0,018	7,5	60	218	0.027
	m	mm	g/m	g	m²	mm	g/m	g	m²
			total Rod:	**3,586**	**0.109**		**total PBO:**	**1,317**	**0.163**

The weight of the rigging of the "sailOvation" is reduced by 2.269 kg choosing PBO instead of rod. The PBO rigging has 63 % less mass but 49 % more windage than the rod rigging. The weight reduction of 2.269 kg does not look to be very much on the first view. But the centre of gravity of the rigging is at about 45 % of the height of the mast top. Using PBO instead of rod leads either to bigger righting moments or allows - keeping the righting moment constant - a reduction of the bulb weight of about 3 times of the weight reduction in the rigging. That would be all together 9 kg less weight for the whole yacht. The decision for PBO moves the centre of gravity of the "sailOvation" 60 mm downwards. The righting moment becomes 4 % higher and raises the propulsion force accordingly - one step more to achieve semi-planing on a close reach.

3. Modelling the rig with finite elements

Rigs of sailing yachts are very complicated mechanical structures. They are three dimensional and made of long slim elements. The elements have either 3D bending characteristics of beams (mast, spreaders and boom) or tension only characteristic of cables (shrouds, stays). Cables are non linear elements for they fall slack when compressed. Rigs are pre tensioned like a screw joint but much more complicated three dimensional. Rigs can become instable. They can buckle caused by compression loads acting on the beams. The beams may buckle as a whole. But also the local wall of the beams can buckle. The loading of the rig changes with the deformation of the rig. This is another non linearity called large deformations and has to be considered for the loading becomes bigger with raising deformations. Loadings are caused by the sails depending on wind speeds, apparent wind angles and sail shape. Sail loads depend also on sail trim like mast bend and head stay sag. Sail trim depends again on the deformations of the rig which are caused by the sail loading. And last but not least there are also loadings by inertia forces in a sea way.

When in engineering work something is as complicated as the structure of a rig, a useful way is to combine some simple physics like the Euler buckling formula for beams with a lot of experience and reserve factors. Most spar fabricators go this way and develop their own spread sheets for dimensioning rigs to get numbers for the necessary diameters of standing rigging or moments of inertia for the mast. This way is easy, reproducible and quick. Rules like the Nordic Boat Standard [3] are also based on this procedure.

But if you want to optimize a rig with regard to weight and deformations you have a problem. A spread sheet for rig dimensioning is not an analysis of the rig structure. The spread sheets can't compute deformations or tensions of the rig and it components. You have to choose a more sophisticated "high tech" computation called FEA (**F**inite **E**lement **A**nalysis). Only FEA helps to understand the behaviour of rigs and enables to optimize them.

FEA for rigs is not new. There are several publications [4 – 9] which describe the successful use of FEA for rigs. The Germanische Lloyd has published guidelines [10] for the certification of large modern rigs that are based on FEA.

Important aspects for the simulation of the rig of the "sailOvation" with finite elements are:

- **geometry:** 3D including mast rake, lift and rake of spreaders, load points like halyard sheaves axles
- **elements:** 3D beams for mast, spreaders and boom; nonlinear link elements with the ability to fall slack when compressed for the shrouds, beam elements for the head stay to make visible the sag; bearing element for goose neck of the boom; spring element at the chain plate of the head stay to simulate the hull stiffness
- **real constants:** cross section areas, moments of inertia according to the carbon spars and PBO rigging
- **material properties:** according to laminate plan for carbon, PBO, rod and vectran
- simulation of the **real connecting points** of the elements for example between mast and spreader or tang of a shroud with so called "helping beams" from the centre line of the mast to the outside of the mast tube
- **constraints:** the hull is not modelled, clamping of key points at the connections to the hull like chain plates and mast step, all in x, y, z direction and mast step additional in zz
- consideration of geometrical non linearity, **large deformations**

The computations for the "sailOvation" are performed with the software ANSYS on a PC. The geometry of the modelled rig can be seen in **figure 3**.

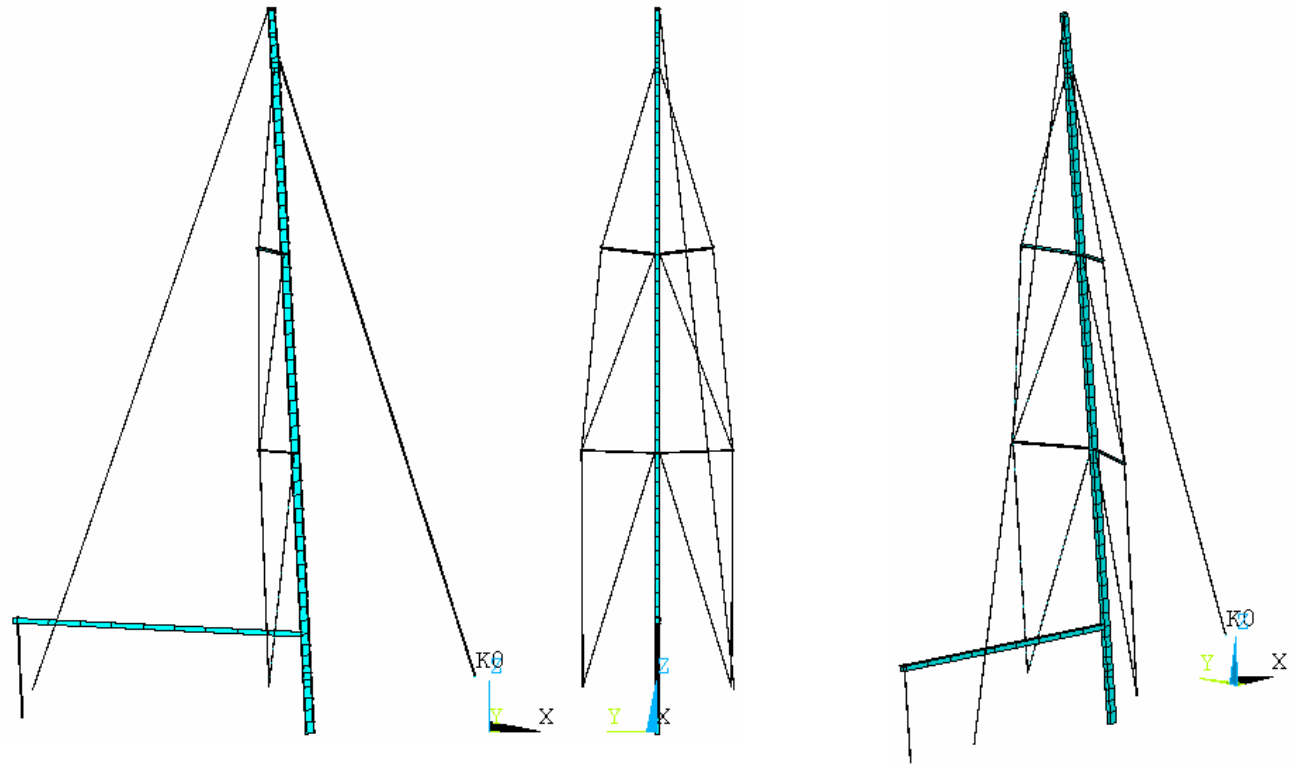

Figure 3: Geometry of FE model, looking from starboard side, astern and 3D

4. Pretensions

There are different ways to tension the standing rigging. To tension it intuitive and adjusting it on the leeward side when sailing may lead to acceptable results only for simple cruising sailboat rigs. A second and more exact method is to measure the elongations of the standing rigging as a percentage of the breaking loads. Typical tension loads are 15 to 20 (25) % of the breaking loads. A limiting factor is, that it may be impossible to achieve the necessary tensions by turning the rigging screws with hand tools. The threads of the rigging screws may also be damaged in the procedure. The third way is to use a hydraulic jack. The principle use of a hydraulic jack is to adjust the rigging screws without tension loads on them and then to lift the mast step with the jack and to set it on shims. Good pretensions can be achieved with some iteration on the length of the rigging screws. This method is much more certain and reliable than the other ones mentioned above. The pretensions of a rig become reproducible. That is very important for racing rigs with different pretensions for different wind speeds and seaways. Hydraulic jacks are today common on racing yachts with a length of 10 m and more. The knowledge about the size of the pretension forces in numbers in the rigging is unfortunately very limited unless there are load cells at the chain plates. This can be changed by using FEA for the rig.

The procedure of tensioning the rig of the “sailOvation” with a hydraulic jack is simulated with FEA. With a FEA the shrouds can be shortened using a function called “initial strain”. To find the right “initial strains” for every shroud and the head stay is an iteration process like in “real live”. It takes some time with FEA especially for rigs with aft swept spreaders. The reason is the interaction between fore/aft and transverse rigging. Four conditions have to be complied. First the mast shall have a pre bend in the dock tune of 0.5 % of the P measurement. Second the head stay sag, when sailing close hauled with 25° heel, must be small. Sag of 1 % of the forestay

length is common on racing yachts to get an effective headsail. Third the cap shrouds are not allowed to fall slack (the D's may fall slack) when sailing close hauled with 25° heel. Otherwise the rig will start to collapse. And fourth the rig has to be able to carry the sail loads without buckling of the mast. The sail loads correspond with the righting moment at 25° heel. The fourth condition may be not fulfilled, when the rig is not stiff enough.

To come back from simulation to "real live" there has to be a way to achieve the computed "initial strains" in the real rig. The way is to subdivide the dock tuning into three steps:

1. tensioning only the cap shrouds (V1, V2, D3) and the head stay,
2. tensioning additional the D1's and
3. tensioning additional the D2's.

For every step the compression forces in the mast foot are computed with FEA and listed in table 2.

Table 2: Jacking up the rig in three steps

step	tension in	hydraulic pressure [bar]	force in mast foot [kN]
1	V1, V2, D3, headstay	75	9,8
2	additional D1	266	34,5
3	additional D2	322	41,9

Now the simulated steps have to be transferred to the real rig. In the first step in "real live" the rigging screws of the V1's and the head stay are iteratively adjusted until the compression force (corresponding with the hydraulic pressure, which could be controlled by a pressure gauge) of the computed first step is achieved. In the second step the D1's are adjusted until the computed compression force for the second step is achieved. The same procedure is performed with the D'2s in the third step.

Figure 4 shows the computed forces and the deformations of the rig for every step. The forces in Newton [N] are made visible with contours and colours. The width of the contour is proportional to the force. The mast bending curve is shown with vectors in meter [m]. The length of the vectors and the colour correspond with the deformation in three dimensions. The length of the vectors is in an enlarged scale to make the small deformations visible.

It is of great importance, that the computations are performed with the non linearity of large deformations. In the first step the mast bends forward a lot by the compression forces of the spreaders. The mast top moves downward. In the second and third step the mast is pulled back by the D1's and the D2's and straightened to the 0.5 % pre bend. The straightening of the mast tensions the cap shrouds for the mast top moves up again. Neglecting large deformations (here specially the bending deformation of the mast) leads to wrong tensions. The cap shrouds would be tensioned too much in the first step.

Hydraulic jacks can produce a lot of force and may overload the rig when used carelessly. It is good engineering to control the stress levels in the rig for the three computed steps jacking up the rig.

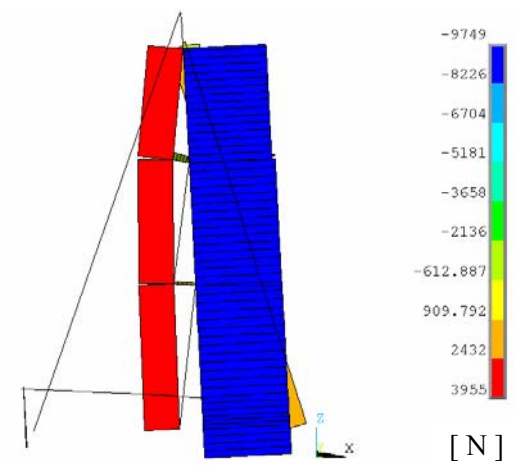

forces – **caps only**

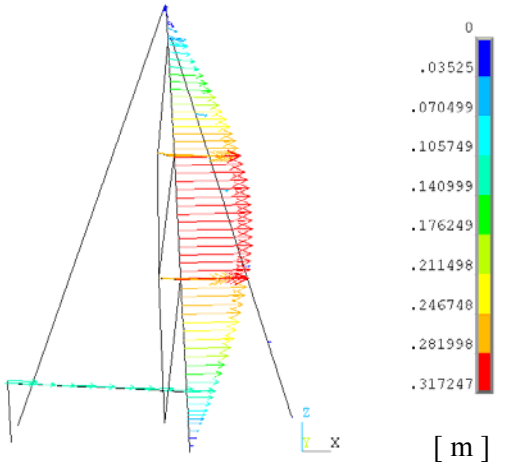

deformations – **caps only**

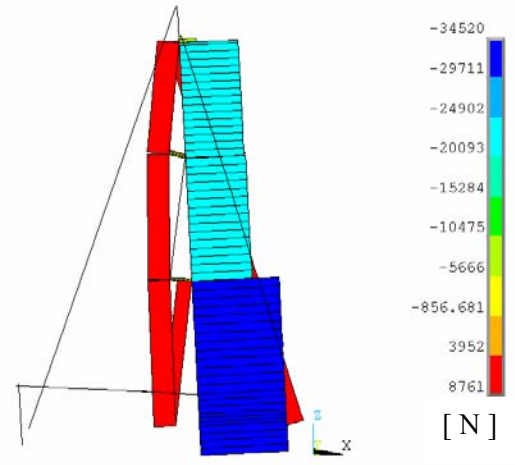

forces – **caps, D1**

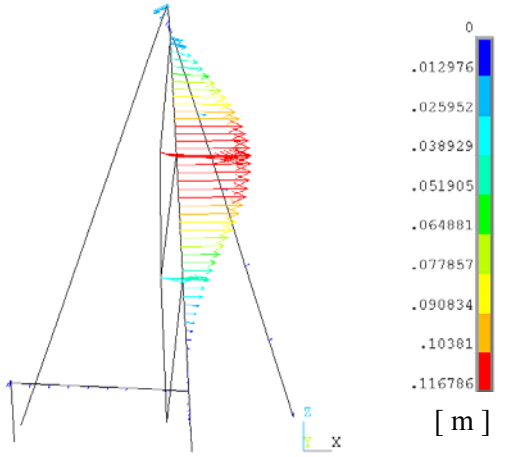

deformations – **caps,**

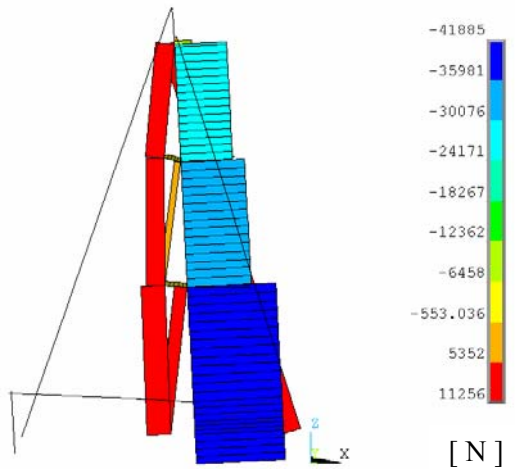

forces – **caps, D1,**

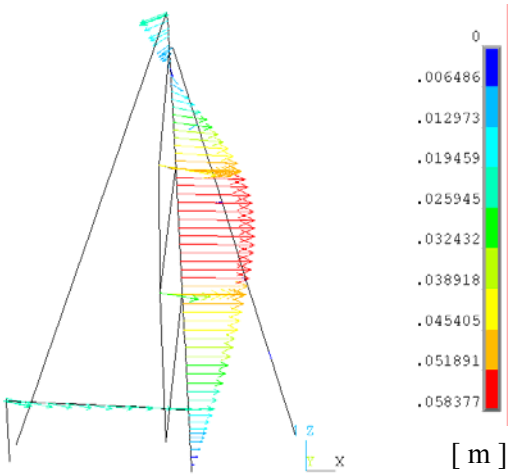

deformations – **caps, D1,**

Figure 4: Forces and deformations jacking up the mast with a hydraulic jack in three steps

5. Sailing close hauled

The forces on the rig sailing close hauled depend on the righting moment. Computations were performed for the righting moments corresponding up to 25° heel with the keel fully canted to windward. The righting moment at 25° heel is 2,750 kgm. The wind in the computations comes from the starboard side.

Forces and line loads acting on the rig are computed on the base of a load model developed by full scale measurements of rigging loads and FEA on the research sailing yacht “DYNA” of the TU-Berlin [5]. **Table 3** shows the forces and line loads for a righting moment of 2,670 kgm. This is the maximal possible righting moment for a mast pre bend of 0.5 % of the P measurement. Computations with higher righting moments did not converge, what means, that the rig in the computations is buckling under the pretension and sail loads. In real live the mast does not buckle completely. The mast helps itself by bending much and this automatically depowers the sails, reducing the sail loads on the rig. The applied forces of the sails in the FEA are independent of the mast bending and the sag of the head sail. The sails always stay full in the computations. This way the computations show the limit of the rig to carry the full power of the sails according to the righting moment of the hull.

A pre bend of 0.5 % of the P measurement is a good standard value. FEA showed, that smaller pre bends allow higher sail loads than bigger pre bends. The reason for this is the different stiffness of the rig. An almost straight mast is stiffer than a mast which is already bent a lot. A less stiff mast has also less tension forces in the head stay. This leads to larger sag of the head stay and poorer performance of the genoa. A complete straight mast would be best for stiffness. But when there is no or a too small pre bend in the mast movements in a seaway like pitching results in inverting and pumping of the rig. This has to be avoided by pre bending the rig a little bit and the 0.5 % pre bend is a good compromise between stiffness and avoiding inverting and pumping of the rig (see also chapter 6).

Table 3: Forces and line loads acting on the rig sailing close hauled with a righting moment of 2,670 kgm

Forces		**Main sail**	**Genoa**	
halyard sheeves	x	-1554	92	N
	y	430	203	N
	z	-7621	-4062	N
boom end, outhaul	x	3201		N
	y	678		N
	z	4103		N
gooseneck boom	x	-402		N
	y	203		N
	z	101		N
Line loads		constant on mast	triangle on fore stay	
x		-140	-247	N/m
y		81	143	N/m

The computed forces, deformations, bending and torsion moments can be found in **figure 5**. The compression force in the mast step raises from 41,885 N for dock tuning to 49,350 N when sailing close hauled. The leeward shrouds are almost slack. The runner is not tensioned. The mast top has a deformation of 267 mm. The sag of the head stay is 94 mm or 0.76 %. That is less than 1 % and a very good value.

The biggest bending moment is 3,163 Nm in the top of the mast at the head stay tang. The halyard of the mainsail pulls at his sheave the mast top backwards. This results in steadily raising bending moments starting from the mast top downwards to the head stay tang. Here counteracting moments from the forestay forces and the halyard forces of the genoa reduce the bending moment with a jump in the bending moment curve. Torsion moments increase from the masthead stepwise with every tang and spreader. They are relatively small.

Figure 6 shows a strength control in the carbon mast with von Mises stress. The biggest value of 180 N/mm² can be found on the leeward aft side of the mast in the height of the forestay tang. This corresponds with the location of the biggest bending moment. At this location there are additional local reinforcements not considered in the global FEA model. The real stresses are smaller. This part of the mast should be evaluated further with a local FEA model.

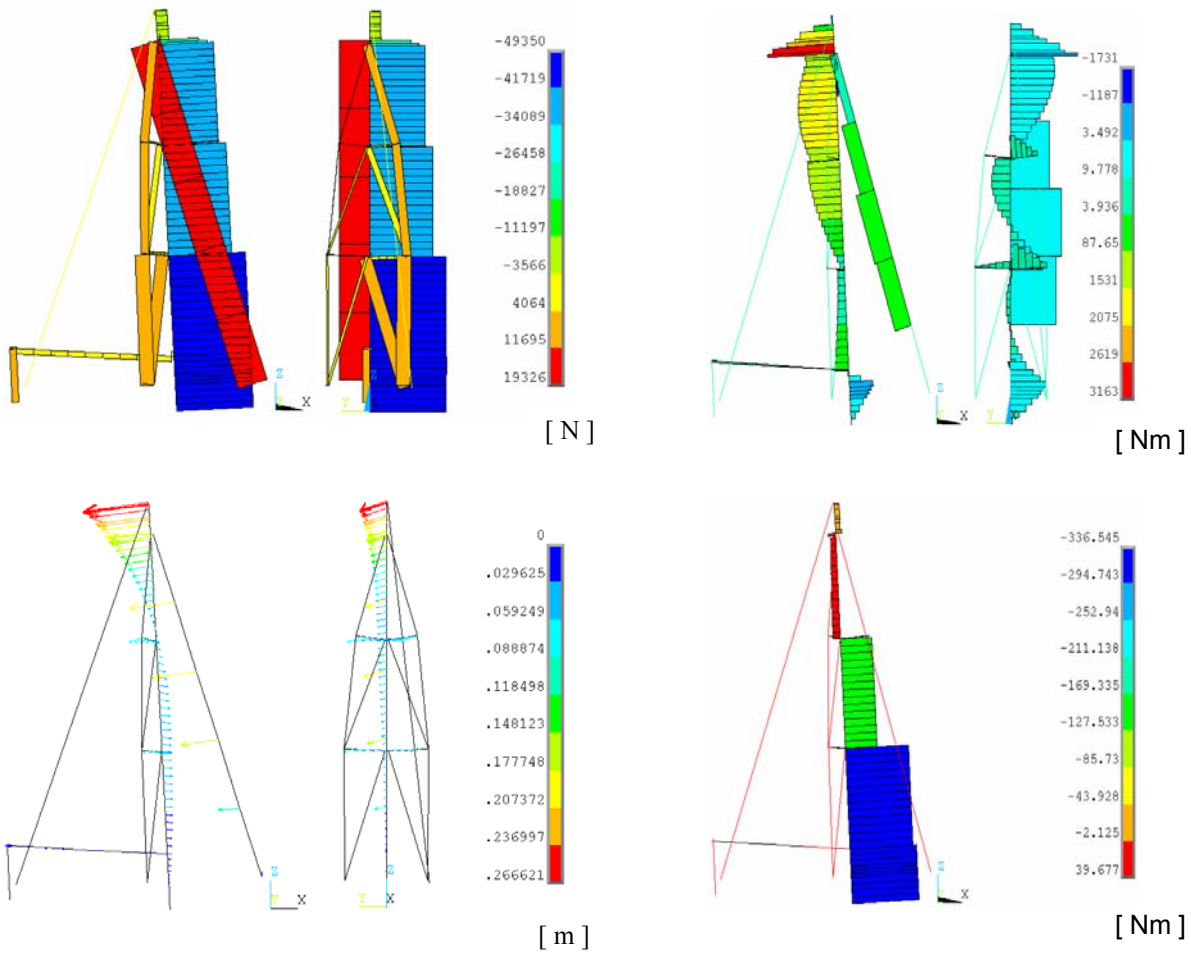

Figure 5: Sailing close hauled: forces, deformations left side – bending and torsion moments right side

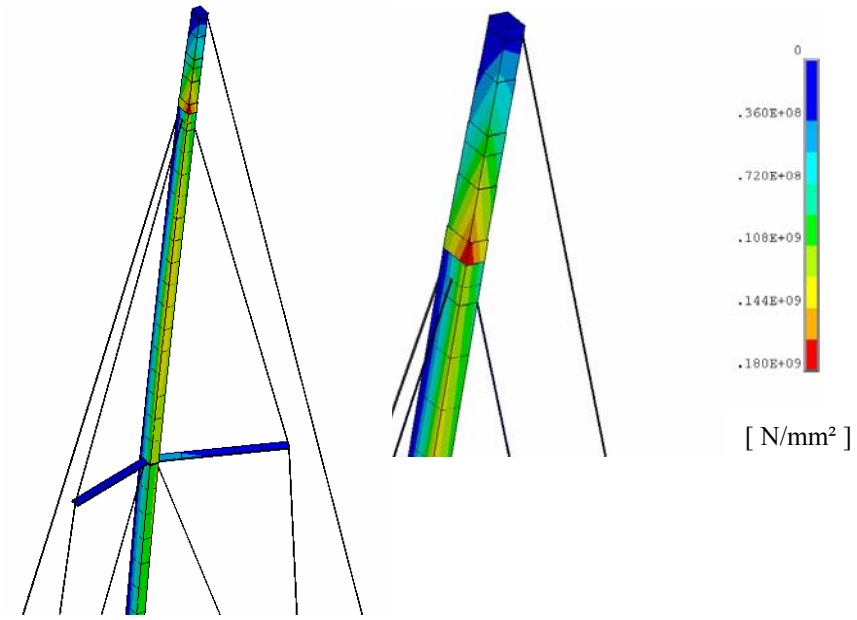

Figure 6: Von Mises stress looking from port side

6. Validation of trial runs, applicability of FEA for rigs

First trial runs started in the summer 2006. The rig was pre tensioned according to the described procedure in three steps on the base of the FEA. The achieved mast compression in the last step corresponded very well with the computed one. The procedure to pretension the rig this way worked very well. It took less than one hour and was very satisfying.

Different pre bends of the mast in the dock tune were examined. First sailing trials with a pre bend of the mast in the size of 0.1 to 0.2 % of the P measurement were disappointing. The rig in this dock tune is very stiff and able to carry a lot of sail power, but the mast started to invert and to pump sailing in a seaway. A pre bend of 0.5 % proved to be enough to avoid inverting of the mast and the rig was still stiff enough to carry the sail loads and the sag of the head stay was very small like computed with FEA.

Higher pre bends of the mast were also examined. The luff curve of the main sail was very rounded and with the almost straight mast the sail chord depth was too big. It was tried to bend the mast round the main sail luff to reduce the chord depth. The tensions in the diagonals (D1's, D2's) were reduced and the mast pre bend in the dock tune was raised up to 2 %. The main sail could now be trimmed very well and the sail chord depth could be adjusted by bending the mast with the runner. But there was a very negative effect for the genoa. The sag of the head stay became too big sailing close hauled. Pulling at the runner only worsened the sag of the head stay. The rig is not stiff enough with 2 % pre bend of the mast. It has already started to buckle. There is no alternative, a new flatter main sail with a less rounded luff is necessary for the rig of the "sailOvation".

Results of FEA performed with different pre bends are in accordance with the results of the sail trials. The pre bend of the “sailOvation” mast has to be small to get a stiff rig. Otherwise the sag of the head stay becomes too big. The sail maker can design his sails much better, if he knows exactly the deformation behavior of the rig. The deformation behavior can be computed with FEA and need not be tested expensively with sets of sails with different luff curves.

The experiences with FEA for the rig of the “sailOvation” are:

- FEA is applicable for rigs very well
- the results of the FEA correspond very well with the experiences in the real world
- FEA helps to understand the structural behavior of rigs
- using FEA for a rig reduces time for trial runs and saves costs.

To perform a FEA for a rig you need a good computer, powerful FEA software and a qualified engineer. FEA is a common tool in the automobile and aircraft industries to optimize structures and to reduce costs. But FEA for rigs is until today only seldom performed. Mast builder usually use self made spreadsheets and experience to dimension the mast tube and the standing rigging. Some sparmakers don’t do any calculation at all to cut costs. Until customers are prepared to pay a proper price for FEA it won’t happen more often. A customer is willing to pay a lot of money for carbon and the combined high tech feeling but not for computations that he cannot understand. Even with full global FEA the rig can fall down. Most errors are in fact associated with fittings and attachments. Global specifications of mast stiffness and rigging sizes are seldom the fault. Local FEA of all that fittings and attachments is an order of magnitude beyond the global FEA. The reasons for sparmakers to go without FEA for rigs are mainly costs but also lacking FEA know how. The costs for a global FEA are almost independent of the size of the rig. For small rigs the percentage of the total costs is prohibitive high. For large rigs, that cost several hundred thousand Euros, a FEA is only a small part in the bill. That is the reason why a FEA is almost only performed for large rigs.

The costs of FEA for rigs are accepted by the customer only when he gets advantages. The advantages are:

- insurance companies **reduce** their **premiums** if a rig is certified for example by the Germanische Lloyd according to his guidelines that are based on 3D FEA computations [10]
- **quickly, reproducible and defined dock tuning** in steps with a hydraulic jack on the base of computed hydraulic pressures
- **optimization** of the behaviour **of the rig** before it is built; much less expensive changes after trial runs with bad results
- data for the deformations of a rig under sail and trim loads like bending curves of the mast and the sag of the head stay; this **data** are important **for the sailmaker**
- **safe weight reduction:** global stress control of the mast tube, the spreaders, the boom and the standing rigging; dimensions of cross sections can be adjusted so that they are safe and not unnecessary heavy
- **3D buckling control** of the rig by computing with large deformations and simulating the buckling process with raising sail loads or alternative and more simple 3D linear “euler buckling”.

The velocity polar diagram of the “sailOvation” can be seen in **figure 7** for a true wind speed of 12 kn. She starts semi-planing (Fn = 0.4) at a wind angle of about 60° on a close reach. The “sailOvation” reacts very sensible to trim changes. She has still a potential for higher velocities in the next summer with a new main sail and a better trim.

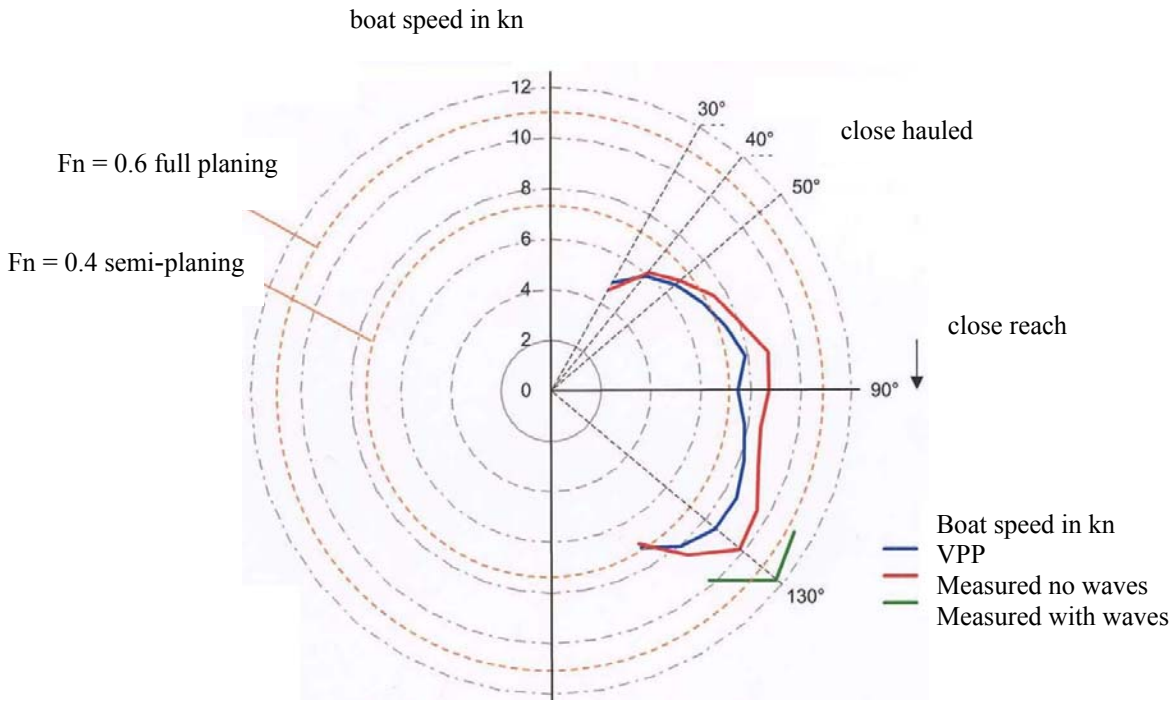

Figure 7: Polares for 12 kn (6 m/s) true wind speed

7. References

[1] Dedekam, I.: „Sail & Rig Tuning“, Fernhurst Books, 2000

[2] Germanischer Lloyd: Draft Guidelines fort the Type-Approval of Carbon Strand and PBO cable rigging for Sailing Yachts

[3] Larsson, L.; Eliasson, R.E.: „Principles of Yacht Design“, Adlard Coles Nautical, London 2000

[4] Jansson, R.: “Best Mast: a new way to design a rig”, The 18th International Symposium on “Yacht Design and Yacht Construction”, Amsterdam, 2004

[5] Grabe, G.: “The Rig of the Research Yacht “DYNA” – Measurement of Forces and FEA”, HP-Yacht, Auckland, 2002

[6] Grabe, G.: ”Downwind Load Model for Rigs of modern Sailing Yachts for Use in FEA”, The 16th Chesapeake Sailing Yacht Symposium, Maryland, 2003

[7] Grabe, G.: “The Rig of the “UCA” – Finite Element Analysis”, The 18th International Symposium on “Yacht Design and Yacht Construction”, Amsterdam, 2004

[8] Roberts, D.; Dijkstra, G.: “The use of fibre optic strain monitoring systems in the design, testing and performance monitoring of the novel freestanding Dynarigs on an 87m Super Yacht by Perini Navi, design by G Dijkstra”, The 18th International Symposium on “Yacht Design and Yacht Construction”, Amsterdam, 2004

[9] Wallace, J.; Philpott, A.; O’Sullivan, M.; Ferris, M.: „Optimal Rig Design Using Mathematical Programming“, 2nd High Performance Yacht Design Conference, Auckland, 2006

[10] Germanischer Lloyd: Rules for Clasification and Construction, Ship Technology, Special Equipment: „Guidelines for Design and Construction of Large Modern Yacht Rigs“

Internet:

www.segeln-magazin.de
www.va-yachtdesign.de
www.janssen-renkhoff.de
www.nordicmast.com
www.smartrigging.com
www.elvstromsobstad.com

Session 6

Ajit Shenoi

Interactions Between Yacht-Crew Systems and Racing Scenarios Combining Behavioural Models with VPPs

Scarponi M[1], Shenoi R A[2], Turnock S R[2], and Conti P[1]
(1) Dipartimento di Ingegneria Industriale
University of Perugia, Italy

(2) s School of Engineering Sciences
University of Southampton, United Kingdom

Abstract

Considerable progress has been made in the development of Velocity Prediction Programs (VPPs) suitable for analysis of racing yacht performance. Similarily, there has been rapid advances in sensor capabilties (smaller mass, lower power consumption, and greater accuracy) and with a resultant increase in use in helping assess and improve racing yacht performance. While these tools and techniques will no doubt be further refined and computations speeded up, there is also a need to assess the performance of the yacht's helm and crew.

The scope of the present study is the prediction of the performances of a yacht-crew system as a whole, by deriving numerical models for human behaviour alongside with those referred to the physics of yacht motion. The latter issue, the mechanical side of the problem, is analysed by solving yacht equations of motions in the time domain; crew inputs in terms of yacht steering and sail trim are considered. The yacht-crew system can sail a racecourse in an arbitrary wind pattern, according to strategic rules and given decision making schemata.

Keywords: decision making, yacht performances, human behavioural models, sports psychology.

Nomenclature

[Symbol]	[Definition]
awa	apparent wind angle
awa_{ref}	reference apparent wind angle
twa	true wind speed
DMG	distance made good

Introduction

The use of Velocity Prediction Programmes, (VPP) to assess yacht performances can be regarded as a well-established technique in yacht design. Considerable improvements were actually carried out in the last decades, in order to achieve a closer modeling of hydrodynamics and aerodynamics of sailing yachts [1]. As a result, designers can now obtain valuable information on the straight-line, equilibrium state of a yacht for each point of sail and wind speed. Screening among a fleet of design candidates is also possible through VPPs: a 'test fleet' can be generated, usually by applying systematic variations to a 'base boat', and the minimum time required to complete a set of racing legs can be predicted. VPPs have also been used in conjunction with weather databases, in order to predict the outcome of races [2]: these are usually identified as Race Modeling Programs (RMPs). It is widely felt that further additions to the traditional models for yacht performance prediction are necessary: as an example, in Keuning *et al.* [3] it is pointed out that aspects of yacht dynamics (namely, the tacking ability) should also be modeled for handicapping purposes.

One of the distinctive features of modern yachting is clearly one-design racing: the attention of either yachtsmen, designers, sponsors and media is actually switching to contexts where the skill of crews and the ability to make the right decisions at the right time are keys to winning races. In the Authors' opinion, any improved approach to performance prediction should therefore aim at taking two factors into account: the racing hardware, the boat, and the software (or wetware!), the sailors. Regrettably, little or no published attention has been paid to the latter issue so far. This seems to be paradoxical, since sailing is a discipline so rich in uncertainty that gambling, taking chances, predicting future scenarios, assessing outcomes of decisions always come heavily into play.

Yacht performance prediction

1. 2.1 Background on VPPs

The goal of VPPs consists in solving iteratively the equilibrium equations of a sailing yacht subject to hydrodynamic loads (hull and appendages) and aerodynamic loads (sailplan). The steady state surge speed of the yacht can therefore be calculated for a range of wind speeds, points of sail and sail inventories, which then gives designers an insight into the overall quality of their yacht design. The reliability of VPP predictions is closely related to the quality of experimental and numerical data upon which the aero-hydrodynamic models are based.
To bear the costs of a close modeling of a sailing yacht, with the purpose of getting accurate VPP predictions, is still far from being an easy task. In fact, access to facilities such as a suitably-sized towing tank and a wind tunnel is required, in order to investigate the hydrodynamic behaviour of appended hulls and to build up the aerodynamic model. A numerical approach in terms of Computational Fluid Dynamics can also be regarded as a valuable source of information, but traditional testing can hardly be avoided, since numerical methods can provide just partial responses to designers.

2. 2.2 Dynamic VPPs

Altough further improvements can still be achieved, VPP technology in itself looks mature enough: research is therefore required to take a step forward and investigate unsteady aspects of sailing yacht motion.
A few attempts to investigate yacht dynamics in the time-domain can be found in recent literature. Some Authors have focused on manoeuvering, in order to evaluate the optimal tacking procedure [3], [4], while others have simulated a yacht racing on an upwind leg, focusing on its motion in a seaway [5] or its interactions with an opponent [6]. A great part of the Authors concentrate on solving simultaneously the set of unsteady non-linear equations of motions, or the use of system identification, based on neural networks, has been investigated as well. Up to six degrees of freedom (DOFs) have been taken into account, but four DOFs (surge, sway, yaw and roll) analyses proved to be adequate for tacking simulations and yielded results whose agreement with full scale trials is reasonable [4]. Therefore, the latter approach has been followed in this work; the non-linear equations of motions are those proposed by Masuyama *et al.* [4]. The yacht reference frame adopted here is the horizontal body axes system.

Features of the sailing simulation

The four equations of motions mentioned in the above Section represent the core of the sailing simulator described herein, whose purpose is to estimate the time a given yacht takes to sail a racecourse. The simulator is composed of three interacting modules:
a physical model of an International America's Cup Class (IACC) yacht;
a visualization module where the yacht motion is shown in a virtual reality context;
a control module, referred to as 'automatic crew'.

The IACC yacht is racing solo, against the clock: this is to show to what extent strategical decisions influence the time required to complete a race. The simulator has been implemented in MATLAB: this choice lead to slower simulation times but, facilitated algorithm development and offered the possibility of interacting with a virtual reality environment, either to model yacht features or to generate animations.

3.1 Physical model of the yacht

The geometry of an IACC hull referred to as 'M566' has been implemented in the present version of the simulator; several towing tank and CFD tests have been carried out on the M566 model so far [7], and a fairly large amount of data is available on its hydrodynamic resistance, sideforce and manoeuvering characteristics. However, data such as added masses and higher order hydrodynamic derivatives for the M566 have not been calculated so far; if the investigation pattern suggested in [4] were followed, full-scale trials such as rolling tests with and without sails would be required, which is well beyond the scope of this paper. So, although the experimental results provided in [4] are not referred to an IACC yacht, some of those data are still used herein, since it is thought they provide a sensible starting place for dynamic analyses.
A mainsail-jib combination only has been implemented here: geometry and further details on this sail inventory are provided in [8]. Lift and drag sail coefficients (C_L and C_D respectively) expressed as a function of true wind angle are available from past wind tunnel tests on IACC sailplans. When model sails are tested, they are usually trimmed in real-time by means of a remote control: aim of the trimming process is to attain the maximum C_L or maximum C_L/C_D ratio at each apparent wind angle of the test matrix. However, when human sail trimmers are modeled, sub-optimal sail performances should be considered as well (i.e. C_L and C_D for under/overtrimmed sails). A sensible way to account for an ill-trimmed sail could be to express sail lift and drag as a function of sail incidence angle (□) instead of apparent wind angle (awa): as a full set of data is not available on this, an estimate had to be made for sail coefficients between □=□, or dead downwind trim, and □=2□, when apparent wind hits the sail leech first, then flows towards the luff.
This approximation, which is deemed reasonable for the purposes of the present paper, is shown in Figs. 1 and 2.

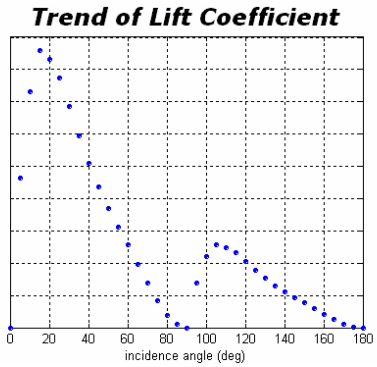

Fig. 1 - lift coefficient C_L as a function of incidence angle (□)

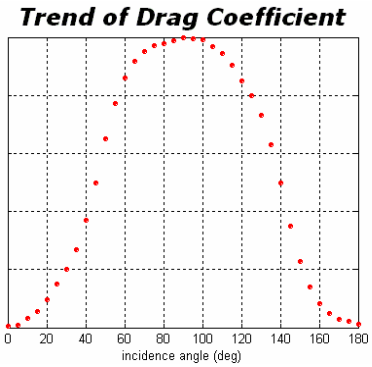

Fig. 2 - drag coefficient C_D as a function of incidence angle (□)

3.2 Simulations and visualization of results

While a simulation is running, a stepwise solution of the four simultaneous equations of motion has to be calculated; a standard fourth order Runge-Kutta solver is used for this purpose. The

CPU time required to simulate a one-mile upwind leg in an arbitrary true wind pattern is approximately 60 seconds on a conventional PC.
At every time-step, the time-histories of state variables (velocities, accelerations, leeway, yacht heading, apparent wind speed and angle), hydrodynamic and aerodynamic forces, rudder angle and sail trim parameters are recorded. This set of data can be supplied to the visualization routine, programmed within Simulink and using the features of MATLAB Virtual Reality Toolbox in order to generate 'offline' animations. Within this context, the use of Virtual Reality Modeling Language (VRML) allowed both the modelling and animation of the yacht motion within a 3D world. From a physical standpoint, this allows the yacht accelerations and heel, rudder movements, and sail trim to be visualized and compared with actual (recorded) values. In addition, positives and negative aspects of the race strategy implemented by the automatic crew can be highlighted as the simulation proceeds on. With this purpose, a one-design fleet implementing different strategies can sail the same course simultaneously (as in Fig. 3): in this case no mutual interactions occur, so that races can only be won thanks to better technical skills (i.e. driving style, sail trim) and a successful race strategy.

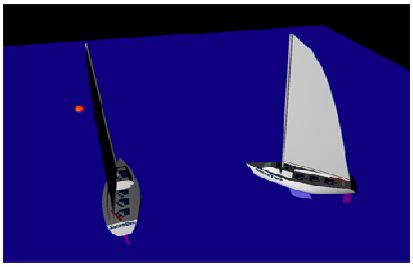
Fig.3 - a screenshot of the animation

Human factor issues in saling

4.1 Sources of uncertainty

As in most outdoor sports, sailing is a discipline rich in uncertainty due to ever-changing environmental conditions. One of the keys to winning races is indeed the ability to predict and to 'play' effectively all weather changes, namely speed and direction of wind and tide.
An extensive analysis on predicting the outcome of match races under weather uncertainty is due to Philpott and Mason [9]: speed and direction of true wind are considered as independent stochastic variables, whose values vary over time and over the racecourse. Changes in wind conditions are supposed to propagate downstream according to Taylor's hypothesis of wind engineering: wind eddies travel down the flow field at a given mean wind speed. The model is based on wind measurements on Hauraki Gulf, New Zealand and can model large shifts in wind direction occurring at random intervals.
Other than weather conditions, many more non-deterministic factors affect the outcome of sail races: insight on opponents behaviour, sailors' self-confidence and personal attitude towards risk (risk-averse or risk-taking), knowledge of racing rules being just a few examples. These factors influence both racing strategy and tactics which, in turns, affect the way a yacht is sailed. Other than technical skills, a wide range of additional abilities are therefore required to win races: assess risks connected to decisions, estimate gain/loss probabilities, predict changes to present race scenario, react to unforeseen events. Personal experience, training and recalling similar situations from the past are therefore key skills to winning races.

4.2 Sailors as decision makers

The factors highlighted above and the role they play in winning or losing races are difficult to quantify and subsequently model within the framework of an 'automatic' yacht crew. However, it is felt that modeling them in general terms can still provide insight to the following questions:
What drives novices and expert athletes' decisions?

- How do athletes assess the risk of their decisions ?
- What gains/losses follow sailors' choices ?
- To what extent can athletes predict changes to racing conditions ?
- Can good technical skills (boatspeed) compensate poor decisions and vice-versa?

Behavioural sciences are underpinning many disciplines such as football, cricket and racquet sports and interesting conclusions can be drawn. Regrettably, only a few behavioural investigations on competitive sailing contexts are available.
Rulence-Paques *et al.* [10] claim that athletes' knowledge base is apparently structured and organized in decision-making schemata, whose 'quality' is likely to affect performance. Recent research by Araujo *et al.* [11] also emphasize the relationship between sailing expertise and decision-making skills, by pointing out that experimental evidence exists that 'best sailors' function 'as better decision-makers'.

4.3 Decision-making in the face of uncertainty

Investigations on decision making have been carried out in a number of fields: from marketing (`how customers choose a product?') to politics (`how voters choose a candidate?'), from warfare to management sciences, from behavioral finance to criminology (`how people decide to commit a crime?'). A decision-making problem under uncertainty, is usually formulated in terms of a decision matrix, whose general features are reported in Tab.1.

Table 1 - Formulation of a Decision Problem

	S_1	S_2	..	S_j	..	S_n
A_1						
A_2						
..						
A_i				$C_{i,j}$		
..						
A_m						

Columns S_j are referred to as 'attributes' or 'outcomes' and represent the possible states of a variable V; rows A_i are referred to as 'alternatives' or 'gambles' and represent the choices available to the decision maker. When A_i is the chosen alternative and outcome S_j occurs, the payoff to the decision maker is $C_{i,j}$. When elements of uncertainty are present, a classical approach is usually followed [12] which assumes that individuals are aware of probability information related to outcomes. A probability distribution $\{ P_1 , P_2 ,..., P_n \}$ therefore exists over $\{ S_1 , S_2 ,..., S_n \}$, such that P_j represents the probability that outcome S_j occurs.
A great part of such research is based on the maximization of expected utility: deciders are supposed to evaluate an alternative by guessing payoffs and probabilities for all the possible outcomes. Each payoff is then multiplied (weighted) by the corresponding probability and the products are summed, obtaining therefore the expected utility of the choice. When a number of alternatives is available, the one that shows the largest expected value is supposed to be selected. The above decision making strategy is usually referred to as 'weighted added'.

4.4 Deciding how to decide: MaxiMin and MaxiMax strategies

When decision-making problems characterized by n-alternatives and m-outcomes are formulated in terms of a payoff matrix, as in Tab. 1, several methods exist to identify the most advantageous choice. Depending on the information available with respect to the outcomes { S_1 , S_2 ,..., S_n }, two categories are usually considered: decision-making under risk and decision-making under ignorance [12]. In the first case, the assumption of probabilistic information about outcomes is supposed to hold: this is to say that decides are aware of a probability distribution { P_1 , P_2 ,..., P_n } over { S_1 , S_2 ,..., S_n }, such that P_j represents the probability that outcome S_j occurs. Firstly, the 'expected payoff' of each alternative has to be calculated as follows:

$$E_i = \sum_{j=1}^{n} P_j C_{i,j} \qquad (1)$$

Eqn.1 can be regarded as a weighted average, where each payoff is weighted by the probability of an outcome to happen. Individuals are then supposed to choose the alternative yielding the highest value of E_i.
Conversely, when deciding under ignorance, no probabilistic information is attached to outcomes and the decision maker is supposed to express a judgement according to his 'attitude' towards risk. Three prototypical attitudes are usually modeled in literature: a pessimistic/conservative, an optimistic/adventurous and a neutral attitude. In the first case, a strategy referred to as MaxiMin is adopted: being afraid of losses, individuals are firstly supposed to consider the minimum payoff for each alternative:

$$EP_i^{(\min)} = \min_j (C_{i,j}) \qquad (2)$$

then choosing the alternative whose $EP_i^{(min)}$ is largest.
When modeling an optimistic attitude, the so-called MaxiMax strategy is used instead: being confident in winning, individuals are firstly supposed to calculate the maximum payoff for each alternative:

$$EP_i^{(\max)} = \max_j (C_{i,j}) \qquad (3)$$

and finally choosing the alternative showing the largest $EP_i^{(max)}$.
Lastly, the strategy expressing a neutral attitude is based upon the evaluation of the mean payoff for each alternative:

$$EP_i^{(mean)} = \frac{1}{n} \sum_{j=1}^{n} C_{i,j} \qquad (4)$$

then, again, the preferred alternative is the one whose $EP_i^{(mean)}$ is largest.

Set-up of an automatic crew

An automatic crew system has been implemented that is composed of three sub-systems, organized as shown in Table 2. The automatic crew has the task of sailing the yacht on a given racecourse, according to a set of basic strategical rules. Details on the sub-systems are provided in the following paragraphs.

Table 2 - Automatic crew system

Sub-system	Input	Output
Helmsman	yacht state variables; navigator decisions (e.g. target heading when sailing in a straight line).	rudder angle δ; rudder rate $\frac{d\delta}{dt}$.
Sail Trimmer	yacht state variables; navigator decisions (e.g. target sheeting angle).	sheeting angle γ; sheeting rate $\frac{d\gamma}{dt}$.
Navigator	yacht state variables;	decisions.

5.1 Helmsman

An attempt of simulating human actions on a yacht rudder can be found in [5], where a proportional-derivative (PD) controller is adopted that controls the error between the actual and target yacht heading. Weather helm effect is accounted for by applying an open-loop rudder offset expressed as a predetermined function of true wind angle (twa). The PD controller is switched off while manoeuvering, when rudder position is being supplied as a function of time.
Two steering modes have been adopted here, in order to allow the yacht to sail a complete racecourse: a 'fixed-awa' mode for upwind and 'dead downwind' legs, when beating is necessary to get to the next mark, and a 'fixed-heading' mode for reaching legs, when it is possible to sail to the next mark in a straight line. Both steering fashions are based on simple PID controllers, whose gains have been adjusted in order to mimic actual time-histories of rudder angle. Upwind steering based on the 'fixed-awa' PID yields a straightforward, yet effective, model for tacking: the sign of target awa is changed and the PID lets the yacht tack around without exibiting unrealistic overshoots.

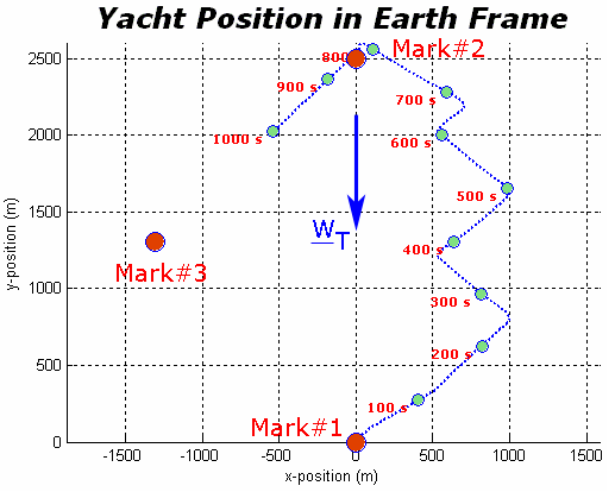

Fig. 4 - yacht reaching (t=1000s) towards Mark #3 at a fixed heading; $\underline{W}_T$ = true wind vector

5.2 Sail trimmer

A mainsail-genoa combination is considered here, whose details can be found in [8]. Two sail trimming modes have been implemented in the simulator: the first one provides 'directly' the sailplan C_L and C_D as a function of awa. Since no human judgement is involved, this can be regarded as the optimal trimming mode. A second trimming mode provides C_L and C_D 'indirectly': the sail trimmer module takes awa as an input and returns the sheeting angle with respect to the yacht centreline. Once is known, the sail angle of attack is calculated out of awa, the yacht leeway and through the formula below, according to Fig. 8

$$\alpha = awa - (\beta + \gamma) \tag{5}$$

C_L and C_D can then be calculated through lookup tables. Linear (awa) trimming 'rules' are adopted here: this is to say that sails are eased off as the helmsman bears away, which is a basic sail trim technique.
A PID controller has been implemented alongside with the latter sail trim sub-system. The PID is required to take over in strong breezes, when the sailplan is overpowered and sails have to be eased off in order to keep the yacht heel angle within acceptable limits. The choice of such a threshold for the heel angle represents a further aspect open to human judgement.

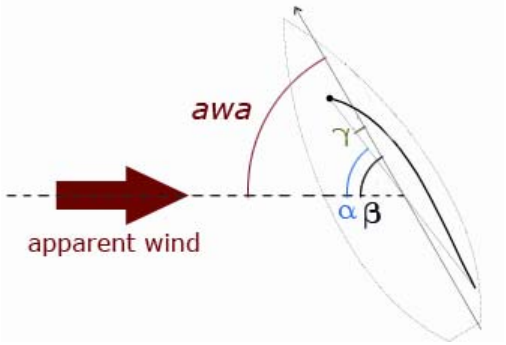

Fig. 5 - Schematic of reference angles for yacht

5.3 Navigator

This represents the core of the control system and, as in real-life sailing, issues decisions that affect both the steering and sail trimming. Firstly, it checks the yacht position at each time-step of the simulation, detecting as an example when a layline is hit or a mark has to be rounded. Secondly, it detects when the weather conditions change and can issue strategical decisions accordingly (e.g. to tack on a windshift). The navigator sub-system also deals with manoeuvres: for instance, it issues the decision of tacking and detects when the boat has recovered from a tack (attainment of surge speed target value) and the next one can take place.
In spite of the basic set of strategic rules implemented so far, broad spaces for simulating human behaviour are present. One example is provided below:
Windshifts: when sailing in shifty wind conditions on upwind or dead-downwind legs, considerable advantage can be obtained by sailing on the 'lifted' tack (i.e. the one that yields the higher boatspeed towards the mark). The decision of tacking when a boat is hit by a windshift is not trivial: the shift should be sufficiently large and stable to be worth the time loss of a tack.

6. Upwind sailing and gambling: a case study

A common decision making problem arising while sailing upwind is considered in the present section. A yacht is supposed to be headed by a 10° windshift, which generates a strategical dilemma: tacking immediately, delaying the tack or waiting for further changes in the true wind direction. The situation described above is investigated in terms of a decision making problem with three alternatives (actions taken by the crew) and four outcomes (possible developments in the weather scenario). Purpose of the study is to quantify gains and losses following given strategical choices. Furthermore, possible decision-making strategies are suggested, in order to choose among alternatives in a context characterized by uncertainty.

6.1 Generalities

A yacht is supposed to sail on port tack, in a Northerly breeze, in equilibrium conditions and towards the upwind mark. At time t_0 = 200s, the True Wind direction is supposed to shift towards East by 10° (+10° header). The alternatives available are then three (m=3 in Tab.1): tacking immediately onto starboard, delaying the tack by 60 seconds or not to tack until further windshifts occur. The navigation stops at t_{end} = 800s.
Four possible weather scenarios or 'outcomes' are set (n=4 in Tab.1):

1) True Wind Speed and True Wind Angle constant from t_0 = 200s onwards;
2) True Wind shifts further right (additional +10° header) at t_1 = 320s;
3) True Wind shifts back North (-10° lift) at t_1 =320s;
4) True Wind shifts back North (-10° lift), at t_1 =320s, then further left by extra -10° at t_2 =440s;

Choices' payoffs $C_{i,j}$ are calculated according to Eqn.6 below, where $DMG_{i,j}$ is the distance sailed towards the mark (equal to zero if the yacht sailed at right angles to the mark itself) when considering the i-th strategical alternative and j-th weather scenario. DMG* is the reference distance sailed in 10 minutes at the initial surge speed u_0 = u(t=0). This yields payoffs within the range [0;1], where higher payoffs correspond to higher levels of 'utility'.

$$C_{i,j} = (100 - \frac{DMG* - DMG_{i,j}}{DMG*}) * 100 \qquad (6)$$

After t_0, when the decision is made, the yacht is always sailed according to a unique set of strategical principles: as an example, the navigator would always call for a tack on 10° headers or more. This propagates to the whole navigation the positive/negative effect of the decision made at t_0.

6.2 Decision tables

In order to investigate the sensitivity to simulation parameters, two factors are considered: awa_{ref} and tws. Each of them is varied at two levels, yielding four factor combinations: these are due to a 2 (awa_{ref}, 25° and 30°) by 2 (tws, 4m/s and 6m/s) factorial. Payoffs are calculated according to Eqn.6, where DMGs were estimated by means of the sailing simulator described in the previous Sections. The case awa_{ref} = 25° and tws = 4m/s is summarized in Tab.3 below; readers are referred to Appendix A for the whole set of payoff matrices.

Table 3 - payoff matrix for awa_{ref} = 25° and tws = 4m/s

	S_1	S_2	S_3	S_4
A_1 - tack	62.47	72,94	51,77	58,77
A_2 - don't tack	34,69	66,67	47,29	55,80
A_3 - delay tack by 60 secs	59,88	69,71	48,43	55,45

Before commenting the simulation results, let us focus our attention to the fact that, owing to the assumptions described in Sect. 6.1, different scenarios involve different number of tacks. As an example, let us consider scenario S_2 (wind veering to East): if alternative A_1 was selected (blue track of Fig.10), the yacht would tack just once (onto starboard) since any subsequent windshift to the right would represent a lift for the starboard tacker, yielding higher VMGs and DMGs. Conversely, if alternative A_2 was chosen (green track of Fig.6), the yacht would still be sailing on port when hit by the subsequent 10° windshift: this would represent a further header for the port-tacker and the navigator would therefore call for a tack onto starboard. In conclusion, the lower payoff ($C_{2,2} < C_{1,2}$) is due to a 120 seconds beat on the headed tack.

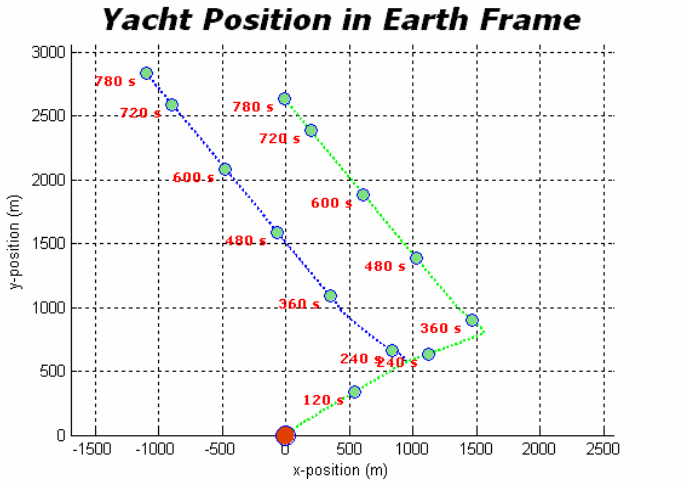

Fig.6 - scenario S_2 : blue track corresponds to choice A_1, green track to choice A_2

Now, let us focus on the simulation results of Tab.3. It can be seen that, when all weather scenarios are equally likely to occur, the most advantageous choice is A_1: tacking as soon as the yacht is headed. Higher payoffs can indeed be obtained when selecting alternative A_1, for any given outcome. Other alternatives (not tacking or delaying the tack) always yield lower payoffs; alternative A_3 is the 'second-best' choice, despite the gap between $C_{2,j}$ and $C_{3,j}$ varies. When the judgement is made across outcomes instead than across alternatives, i.e. choosing an alternative first and then considering all possible outcomes, it can be observed that highest payoffs are always obtained under the outcome S_2.

6.3 Decision making strategies

Two possible approaches to decision making were highlighted in Sect.4.4; their application to the present decision-making problem is investigated in the present Section. Let us consider the payoff matrices of Tab.3 and Appendix A.
When hypothesizing a condition of 'decision-making under ignorance', it can be shown that either an optimistic, a pessimistic and a neutral decider would choose the options of tacking as soon as the yacht is headed (alternative A_1). This is valid irrespectively of the factor combination considered (awa_{ref} and tws). Furthermore, alternative A_3 turns out to be the 'second-best' choice

for all factor combinations. This means that, within the four weather scenarios considered, alternative A_1 is the choice yielding the highest expected utility and therefore represents the most advantageous strategical option when the evolution of the racing scenario is uncertain.
On the other hand, different results can be observed when deciding 'under risk'. As an example, let us consider a possible high-dispersion probability distribution such as { P_1 , P_2 , P_3 , P_4 } = {0.05, 0.12, 0.15, 0.68}. In this case, oscillating wind patterns (outcomes S_3 and S_4) are more likely to occur than veering wind patterns (S_1 and S_2): it can be shown that delaying the decision can yield lower payoffs than deciding not to tack. When tws = 6m/s and awa_{ref} = 25°, if outcome S_4 is considered, the yacht that delays the decision sails a 60s beat while headed and pays the price of two tacks (Fig.7, green track). Conversely, the yacht that does not tack when hit by the first windshift (t_1 =320s) sails a longer beat while headed, but will not tack afterwards (Fig.7, blue track), since it experiences a constant lift after t_2 =440s. Owing to the fact that higher payoffs are weighted by higher probabilities (P_4 = 0.68), alternative A_2 proves to be the 'second-best' choice after A_1.

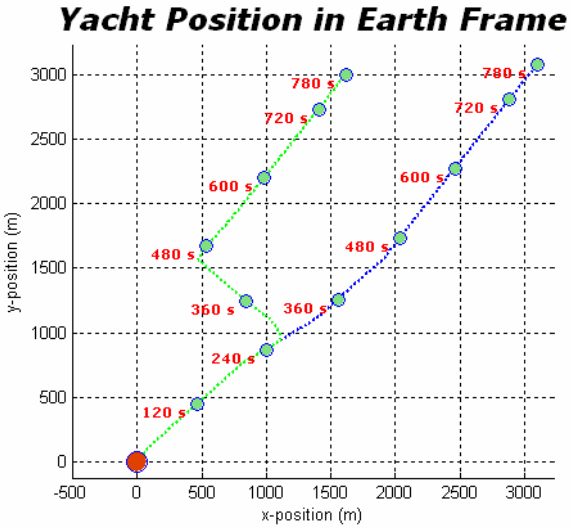

Fig.7 - scenario S_4 : blue track corresponds to choice A_2, green track to choice A_3

3. 7. Conclusions and future work

A four-DOF dynamic VPP has been developed, making it possible to simulate a yacht racing solo on given racecourses and in predetermined wind patterns. The distinctive feature of the present VPP consists in built-in behavioral models, shaped as an 'automatic crew'. The 'crew' is given tasks such as steering the yacht, trimming sails and making strategical decisions, with the purpose of sailing the course efficiently e.g. taking advantage of changes to the weather scenario. The problem of decision-making under uncertainty is addressed and a formulation in terms of payoff matrices is considered. A case study is investigated that involves three strategical alternatives and four possible weather scenarios: gains and losses are assessed through the sailing simulator and payoffs associated with choices are calculated. The most advantageous alternatives is selected through a maximization of expected utility. For this purpose, two possible decision-making contexts are considered: 'decision-making under risk' and 'under ignorance'. In the first case, probabilistic informations associated with outcomes are used, while the latter context involves considerations on the decider 'attitude' towards risk.
Further refinements to the model should undoubtedly be carried out in the future: this refers either to a closer modeling of yacht dynamics (e.g. when sharp course changes occur: quick manoeuvres, mark roundings) and to a refinement of the navigation module. In addition, interaction between yachts should be accounted for, so that decision trees related to racing

tactics (e.g. blanketing, influence of right of way rules), could be investigated alongside with racing strategy.
Nevertheless, several applications can be envisaged for the simulator: as an example, interactive races could be set up and human choices recorded in order to provide a feedback on gains and losses due to personal decision-making schemata.

8. References

13. 1. Claughton A. R., Oliver J. C. III. Developments in hydrodynamic force models for velocity prediction programs. Proc. of RINA Conference 'The Modern Yacht', Southampton (UK), 2003. pp. 67-77

14. 2. Todter C., Pedrick D., Calderon A., Nelson B., Debord F., Dillon D., *Stars and Stripes* Design Program for the 1992 America's Cup. Proc. of The 11th CSYS, pp. 207-222

15. 3. Keuning J.A., Vermeulen K.J., de Ridder E.J., A generic mathematical model for the manoeuvering and tacking of a sailing yacht. Proc. of The 17th CSYS, pp. 143-163

16. 4. Masayuma Y., Fukasawa T., Sasagawa H., Tacking Simulations of Sailing Yachts - Numerical Integration of Equations of Motions and Application of Neural Network Technique, Proc. of The 12th CSYS, pp. 117-131

17. 5. Harris D.H., Time Domain Simulation of a Yacht Sailing Upwind in Waves, Proc. of 17th Chesapeake Sailing Yacht Symposium, pp. 13-32

18. 6. Roncin K., Simulation dynamique de la navigation de deux voiliers en interaction. PhD Thesis, Laboratoire de mécanique des fluides, ECN, 2002

19. 7. Rousselon N. Prediction of hydrodynamic and aerodynamic forces and moments, for use in a 4-DOF simulation tool, using a lifting surface panel code. MSc Thesis, Univ. of Southampton, 2005

20. 8. Le Pelley D.J., Mancebo P., Smith R.P. A technical proposal for the design of an IACC yacht for the Year 2000, Ship Science Group Design Project Report, University of Southampton, 1998

21. 9. Philpott A. and Mason A., Advances in optimization in yacht performance analysis, Proc. of High Performance Yacht Design Conference, Auckland, 2002.

22. 10. Rulence-Paques, P., Fruchart E., Dru V., Mullet E. Cognitive Algebra in Sport Decision Making. Theory and Decision, 58, 387- 406., 2005

23. 11. Saury, J. and Durand, M. Practical Knowledge in Expert Coaches: On-Site Study of Coaching in Sailing. Research Quarterly for Exercise and Sport, 69(3), 254-266, 1998.

24. 12. Luce, R. D. And Raiffa, H., Games and Decisions: Introduction and Critical Survey, Wiley, New York, 1967

Appendix A – Payoff matrices

Table 4 - payoff matrix for awa_{ref} = 25° and tws = 6m/s

	S_1	S_2	S_3	S_4
A_1 - tack	80,84	88,92	70,72	76,56
A_2 - don't tack	55,19	83,04	66,98	74,54
A_3 - delay tack by 60 secs	76,61	84,79	66,40	72,23

Table 5 - payoff matrix for awa_{ref} = 30° and tws = 4m/s

	S_1	S_2	S_3	S_4
A_1 - tack	42,60	55,16	28,95	37,15
A_2 - don't tack	9,67	47,62	24,01	34,25
A_3 - delay tack by 60 secs	38,83	51,42	25,16	33,36

Table 6 - payoff matrix for awa_{ref} = 30° and tws = 6m/s

	S_1	S_2	S_3	S_4
A_1 - tack	69,22	80,38	56,28	63,23
A_2 - don't tack	37,97	72,83	52,26	61,94
A_3 - delay tack by 60 secs	63,70	74,92	50,73	57,67

Session 7

Balázs Hunyadi

"Does it pay to play with the construction material of a sailing yacht?"

by

Hunyadi Balasz and Jan Alexander Keuning

1. Introduction.

Nowadays when one is looking around the boat market to see what kind of materials are being used for hull construction, a wide spectrum can be observed, ranging from traditional boat building materials to space age composite structures. One of the first decisions to be made at the beginning of any new yacht design is to determine the materials of the hull construction. To make the right decision brings many different aspects of the inquiry together: i.e. the cost of the alternative materials that will greatly influence the price of the vessel; the designer's and builder's experience with the construction method; the service cost of the vessel, etc. Of course this will be the customers' choice but the designer's and builder's have to guide the owners with useful and practical information to be able to make the right decision.

To make the right choice the purpose or mission of the vessel should be clear. This will have an important effect on the materials used for the construction. For instance, the weight of a racing yacht hull has to be as low as possible, and the cost of it is not as important a question as the performance. A lighter hull requires less power to drive it, which means the efficiency of a lighter vessel with the same power or sail area will be better than of a heavier one. For vessels which are designed to operate at semi planing or planing speeds, a low weight is also beneficial. Racing yachts are commonly "one-off" projects and therefore made of high tech composite materials. (i.e. America's CUP, Volvo Ocean Race, The Race, etc.) In the case of the cruiser category boats, which are usually more or less standardized production boats, the comfort and the final cost of the yacht have a much greater importance in the decision process and the performance has less than is the case with the racing vessels. In our days these cruising yachts are mostly made of glass FRP in combinations with sandwich construction.

Looking at the "performance cruiser" (as an increasing segment of the yacht market) one sees the selection of the right hull construction to be not so clear and evident. The flavours of this yacht can be described as a "High Performance Sailing Yacht", which means that it has a luxurious inside with all the facilities that one wants onboard. Beside this luxury the yacht requires good sailing performance and must be able to compete in races with her "colleague yachts". Of course the main "driver" in the design again is the light weight of the vessel, but fashion and hypes take this problem sometimes a bit out of hand. Because of the fact that high performance composite materials become nowadays more and more affordable we can see new trends in the construction of these yachts. But most of the time these come from the "owners' fashion" and sometimes these don't know or care about the disadvantages of the chosen materials. Nowadays the trend of these yachts is to be made of light weight high tech composite materials.

The logical task is to formulate the expected advantages when using these high tech hull materials for your next boat. Well, the lightweight is a good choice, and if you se the length-displacement ratio separately -as one index number of the boat performance- you will think this is the best solution. But it is not the only indicator of the yacht's speed prediction.

The aim of the present study was to determine: ***"what are the differences in a sailing yacht performance in different sailing conditions if the building material is changed for the same hull shape, while some selected speed factors are kept the same"?***
Or: ***"how significant is the advantage of weight on the yacht's performance?"***
And: in particular ***"at which cost"***?

2. The approach.

For the present study one particular yacht will be used. This "base yacht" will be the Standfast 64'. It is a design from Frans Maas and was built in 2002 at the Standfast Yachts yard in Breskens, the Netherlands. It is a carbon epoxy sandwich hull construction.
Based on this design three other versions of the same boat have been engineered with different materials for the hull construction. These new designs have been used for a weight estimate based on the new hull construction. With this data a performance analysis has been made at different wind conditions using a state of the art Velocity Prediction Program. (VPP)

The following procedure for the derivation of the new versions of the base design and in agreement with the designer Frans Maas the following "boundary conditions" were considered:

1. The base yacht the Standfast 64 is classed according to Germanischer Lloyd (GL). To make an equal comparison for the alternative versions they also have to comply with the regulations according to GL.
2. At all times the hull geometry of the base yacht will be used for the weight assessments and the following VPP calculations.
3. The main distinction between the different versions of the yacht is the choice of building materials of the hull such as the frames and stiffeners. The considered alternative building constructions are:
   - Carbon fibre reinforced sandwich with foam core (Carbon),
   - Aluminium construction (Aluminium),
   - Glass fibre reinforced sandwich with foam core (Glass),
   - Glass fibre reinforced sandwich with wood core (Wood).
4. For each construction material the weight and the height of the Centre of Gravity of the hull and deck construction has been calculated based on a construction according to GL.
5. For maintaining the sailing performance of the alternative designs the sail area-displacement ratio ($SA/\Delta^{2/3}$) of the various design variations has been maintained
6. For maintaining the sailing performance of the alternative designs also the heeling angle at a given wind speed (Dellenbaugh angle) has been kept the same.
7. This implied for the different building materials used that different amounts of sail area and ballast have been determined in order to yield the required stability moment
8. The VPP calculations have been carried out for light, moderate and heavy air conditions. To take account of the influence of the waves due to wind the typical North Sea wave spectrum has been used.
9. The yachts that are considered are all assumed to be built as a one-off project. This is a boundary condition used, because the original yacht is a one-off product and the continuous produced yachts are really in a different market segment especially concerning moulds costs.

To keep the amount of work within the present study within certain limits some of the items in the design have been kept the same for all versions of the design: i.e. the rudder remains the same, the interior remains the same and the technical installation remains the same. No specific engineering has been put in the design of mast and rigging but instead specific generic design data for these items have been used. This does not imply that at these items no weight benefits may be obtained.

3. The base boat

As base boat the Standfast 64' yacht will be used throughout this study. The yacht has been designed by Frans Maas in 2002 and has been built at the yard Standf Standfast Yachts at Breskens, the Netherlands.

The yacht can be best described as a “High Performance Sailing Yacht”, which means that it has a luxurious accommodation with all the necessary facilities. Beside this luxury the yacht possesses a very good sailing performance and has proven to be quite able to compete in races with her “colleague yachts”. The main particulars are depicted in the Table.

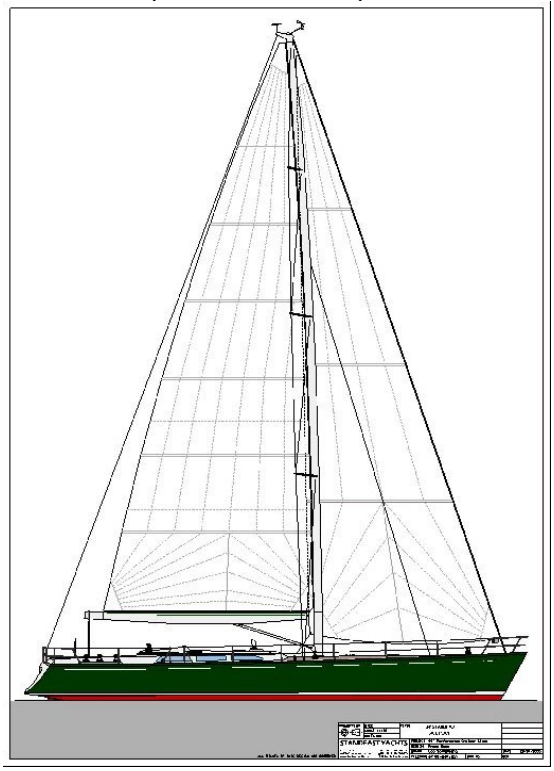

L_{oa}	19.70	[m]
L_{wl}	17.00	[m]
B_{oa}	5.20	[m]
B_{wl}	3.34	[m]
T	2.50	[m]
∇	23.0	[m^3]
Bulb	9240	[kg]

I	24.8	[m]
J	7.1	[m]
P	22.8	[m]
E	8.3	[m]
SF	88	[m^2]
SM	106	[m^2]
SA	194	[m^2]

The yacht has been designed as a sandwich hull with epoxy resin and carbon fibre reinforcement. All construction laminates consist of twill woven carbon (12k T700 600 g/m^2) in epoxy resin (SP Prime 20). The foam core (Core Cell A550 90 kg/m^3) has 25 mm thickness. All interior parts were constructed of fibre/epoxy foam core panels and are glued together with fillet technique, to further minimise the weight. After the hull is turned these interior parts are mounted in.
Thanks to “post curing” construction technique of the complete hull with deck bonded at 55°C for 16 hours, a very strong and stiff but light hull was created. This carbon fibre with epoxy prepreg laminate composition and production method results in an efficient ratio of matrix material (resin) with fibres and extremely low levels of enclosed moist and air in the laminate. The same technique was applied to the fabrication of the Hall Spars mast and “Park Avenue” boom.

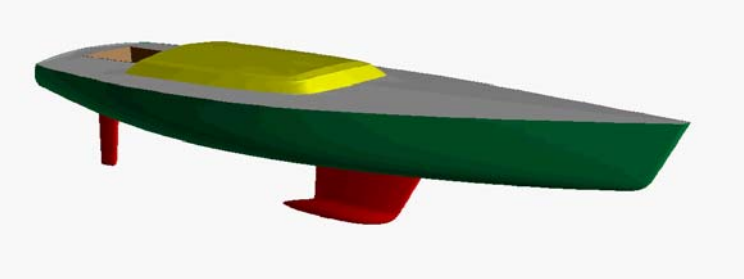

4. The construction and weight assessment.

For engineering the new constructions in the various versions of this design using the four building methods described use has been made of the 3D CAD program DELFTSHIP as developed by the Design Department of Maritime Technology Faculty of the Delft University of Technology. DELFTSHIP is an entirely 3D CAD Design tool for application in the marine industry, best characterized by its ability to create any kind of hull form with high flexibility. A short description will be given here.
At present DELFTSHIP consist of two fully integrated modules: i.e.
1) Using the hull form module, a model of the ship can be modelled either from scratch, by transforming a previous design or by importing it from another program. The hull form is accurately described using the latest surface-modelling techniques. After the body has been made various calculations and transformations can then be performed, such as volumes, centre of buoyancy and mass, moment of inertia around a specific axis etc. Contrary to most other ship design tools, DELFTSHIP does not use stations for the calculation of hydrostatics. Instead the panels obtained by the subdivision surfaces are used. This way more accuracy is obtained in areas such as gondolas and bulbs.
2) Once the shape of the (initial) hull is created the construction-module is used to add all the internal structures in a parametric way. This means that variations in hull form or construction can be explored without having to redefine the construction or hull. The 3D construction model is entirely parametric. This means that after a change of hull form the construction model will be updated to the new state. Also, when for example the tank top height is altered, all plate floors and girders are adapted to the new situation. Further repetitive construction items can be copied to different locations. This reduces the amount of required user input strongly. All parent-descendant relations thus created are maintained and updated by DELFTSHIP and can be disconnected or reconnected when required.

5. Global description of the Germanische Lloyd (GL) method

GL has special regulation for pleasure crafts in general. The regulations which have been used in the present study are: "Rules for Classification and Construction, I – Ship Technology, Part 3 – Special Craft, Chapter 3 – Yachts and Boats up to 24 m, edition 2004". These regulations are generally applicable for recreational motor and sailing crafts with a scantling length $\mathbf{L}^{4}$ between 6 and 24 meters made out of wood, metal and composites.

The hull of a yacht is divided in two areas: a horizontal line separates these areas at 150 mm above the CWL of the yacht. The main dimensions of the yacht, will determine the working loads for the areas of the different hull parts, which are mostly a function of the scantling length, waterline length, operating categories and the expected maximum speed. These loads on the areas are the points of departure for further calculations.

[4] $L = ((L_{WL}+L_{OA})/2)$

5.1 Aluminium configuration

The formulae used for the calculation of the component scantlings embody the mechanical characteristics of ordinary hull structural steel. For the use of different metals a simple formula is present to calculate the material factor 'k':

$$k = \frac{635}{R_{p02} + R_m} \quad [-] \quad \text{, where:}$$

$R_{p0,2}$ = 0,2 % yield strength of the aluminium alloy in [N/mm^2]
R_m = Ultimate tensile strength of the aluminium alloy in [N/mm^2]

This factor will become k = 1.6 due to the aluminium, which will be used linear with the determination of the required section modulus (W) and with the square root for the minimum plate thickness.

The scantlings of the shell (bottom and side) and deck will be determined for various alternatives of the stiffener spacing. These stiffeners may be arranged either on the transverse frame principle or the longitudinal frame principle, or on a mixture of the two. After this the scantling of the bulkheads, the structural members and finally the scantlings of the floor beams will be determined. These contain the required minimum plate thickness and stiffeners section modulus.

Description		Plate [mm]	Frames	
			Transverse	Longitudinal
Shell	Bottom	8	HP 80x6	FB 120x50
	Side	6	HP 80x6	FB 120x50
	Stern	17	-	HP 80x6
Deck	Deck	5	HP 80x5	T 100x11
	Superstructure	5	HP 80x5	T 80x9
	Cockpit	5	HP 80x5	-
Bulkheads	Fore	5	-	HP 80x7
	Midship	5	-	HP 80x7
	Aft	5	-	HP 80x7

Properties of the aluminum construction

The results of the scantlings determination for the aluminium yacht are shown in the Table above. According to the rules the aluminium components do not need any allowances for corrosion. It is assumed that these components will be adequately protected against corrosion by a coating. Non seawater resistant components or coated seawater resistant alloys below water shall be protected against corrosion by zinc galvanic anodes. [GL, 2004]

6. Composite configurations

For the sandwich construction the regulations of GL, as they were in 2004, start with the minimum requirements for the thickness of the solid laminate [Chapter I-3-3, Section 1, B]. The minimum outer skin thickness of a sandwich panel is determined by multiplying with a factor of 0.8 the calculated glass weight per square meter of the solid laminate. Hereafter the calculation, which shall be based on the classic beam/plate and laminate theory, is required for the total sandwich structure with the various design pressures and laminate layers. For the total sandwich structure the following factors of safety (*FoS*) are required for the lay-up and stiffener:

The laminate lay-up has to contain the strain of each individual FRP layer, the shear stress of the core in the case of a sandwich construction and the deflection of the panel. The required *FoS*

between the ultimate strain and the calculated strain of each FRP layer according to the ply analysis must be at least 4.0 In the case of a sandwich construction the *FoS* against core shear failure must be at least 2.0. The standard value taken for the maximum panel deflection is 1% in the case of a sandwich panel.
For stiffeners the factor of safety between the ultimate calculated strain of each FRP layer due to stiffener's bending must be at least 4.0. This holds true also for the ultimate shear stress in stiffener webs and the default value for maximum deflection of stiffeners is 0.5% of their unsupported length.

The Table shows the results of the scantling calculations for the sandwich construction. The properties of the foam used in the shell are: 25mm thickness and 90 kg/m^3 average density, while the red cedar used as core in the wood-core construction is 35mm thick and the mean density is 350 kg/m^3. In the calculations of the deck construction 25mm foam thickness and 110 kg/m^3 average density has been used.
According to the boundary conditions the weight of the keel bolts, rudder and rudder construction, engine, mast and rigging are considered as a given weight on board. The reason for this simplification is found in the assumption that the changes in the weights of these items are considered not to be significant compared to the hull weight. It does not mean that the scantling of these parts is negligible but from in the scope of the present project these do not play a significant role.

Description		Glass Weight [g/m^2]	Thickness [mm]	Section Modulus [cm^3]
Shell	Keel	6800	16	-
	Bottom	3000	7	-
	Side	2300	5,5	-
	Stern	2300	5,5	-
Deck	Deck	1600	4	-
	House	1500	3,5	-
	House side	2200	5	-
Frames	Transverse	1800	-	61
	Longitudinal	2700	-	91
Bulkheads		2400	6	-

Properties of the sandwich laminate

7. Results of the weight calculation

For the weight calculation the previously (Chapter 2.4) presented *DelftShip* CAD program has been used. After the hull shape has been made the internal structure is added to this model. Using the results of the scantling and the structural mass database of this program the weight of the various yachts was determined. The results of the weight calculations based on the scantling calculations as described above are presented below.

Using the structural arrangement of the control yacht the following mass groups have been assumed:

- Construction;
  - Hull
  - Deck
  - Structure (frames, interior walls, keel)
- Insulation;
- Bulb;
- Unchanged mass (wood work, technical installation, deck equipment, rig and sail, electric installation, painting, instruments, inventory, etc.)

The Table shows the calculated mass of the four different constructions:

Yacht	Hull	Deck	Structure	Construction
Carbon	1550	910	1140	3600
Aluminium	3730	1720	3150	8600
Glass	2670	1230	1400	5300
Wood Core	3670	1230	1400	6300

Construction mass in [kg] of the various designs

What is eminent from these results is that the aluminum hull construction leads to an excessive construction weight. This will lead to the introduction of some design alternatives, which will be discussed in more detail further in this report.

So in close consultation with the designer of the Standfast 64, i.e. Frans Maas, it was decided to design also an alternative design for the aluminum construction. First the possibility of a new hull shape was considered. But this would lead to an increased draft over the imposed limit of 2.5 meters. This option therefore was rejected. So the basic yacht hull shape was now “stretched” in the athwart direction in such a way that, by keeping the overall length and the waterline length within the imposed limits, the draft of the canoe body did not change.

Also for the aluminium, the glass and the wood-core versions the “not-watertight” bulkheads are assumed to be constructed from 25.0 mm foam core (ρ=230 kg/m^3) with a 2.5 mm mahogany (ρ=600 kg/m^3) laminate at both sides. The deck sandwich construction of the wood-core yacht is the same as the glass one. This is a commonly used technology for weight saving.

8. Determination of Sail Area and Stability.

Using the results as derived above for the weight of the hull, deck and structure a choice has to be made for the sail area and the ballast, or actually the bulb weight, to go with it.
According to the boundary conditions for the design variations the performance of the yacht using different construction materials should be kept the same as much as feasible.
In consultation with the designer Frans Maas it was decided to focus on the following two design parameters:

- The Sail Area versus Displacement ratio, since this is an important parameter for the performance of the yacht in light air
- The Sail Area versus Wetted Area ratio, since this is an important parameter at higher wind speeds
- The Sail Carrying Ability , the so called Dellenbaugh angle is used, which relates the heeling forces of the sails to the stability moment of the yacht and is an important parameter for the upwind and beam wind conditions.

Through the project the following definition for the relation between sail area and displacement has been used: $10 * \frac{\sqrt[3]{\nabla}}{\sqrt{SA}}$

The sail area used in the expression is the full main sail area and the so called 100% fore triangle in [m^2] and the displacement of the yacht represented in [m^3].
After consultation with the designer, the recommended range for this type of performance cruiser is the sail area displacement ratio to be between 2.0 and 1.9, where the lower value means a better performance ability. However, in the subsequent calculations for the base yacht it turned out to be:

$$10 * \frac{\sqrt[3]{\nabla}}{\sqrt{SA}} = 2{,}04$$

This value was used as the starting point of the further calculations. The relation between the fore and main sails was assumed to be the same so the 'J' and 'E' dimensions had to be considered constant. The results of these calculations are shown in the Table below:

Yacht	SA [m^2]	SF [m^2]	SM [m^2]	I [m]	J [m]	P [m]	E [m]
Carbon	194	88	106	24.8	7.1	22.8	8.3
Aluminium	254	114	140	32.4	7.1	30.4	8.3
Glass	204	93	111	26.2	7.1	24.2	8.3
Wood Core	210	96	114	27	7.1	25	8.3
A5	219	100	119	28	7.1	26	8.3

Sail area and sail dimensions of the various designs

From the results in this Table we may observe that the sail area of the Aluminium yacht has been considerably increased when compared with the other designs due to this applied design rule. It results also in value for *'I'* and so mast height, which is considered highly undesirable. Although this result is in agreement with the imposed boundary conditions it was felt that the feasibility of such a design is doubtful. Therefore, in agreement with the designer Frans Maas, the fifth design variation, nominated A5, was introduced. The basic of this A5 design is the same aluminium construction as the first one with the same shape and calculated weight but the mast height is limited to an *'I'* value of 28m. Thereby the sail area/displacement ratio of her is 2.11 what means the power capacity is slightly worse than with the other four designs.

With the sail area determined the sail carrying capacity may be determined also.
Basis of this assessment is the criterion that all variations should under similar wind condition, i.e. 22 knots of wind in a close hauled condition, have the same heeling angle. This implies that:

$HM_\varphi = RM_\varphi$ Heeling Moment = Righting Moment

or in formula form:

$$FH_\varphi * a = W * GZ_\varphi ,$$

where :
'a' = the vertical distance between the centre of effort of the sails and the centre of lateral pressure on the underwater body,
'W' = the weight of the yacht and
'GZ' = the righting arm of the stability moment.

So we may write the following:

$$\frac{FH_{\varphi} * a}{W} = GZ_{\varphi}$$

The left side in this equation can be seen as the heeling arm (*HA*).

To determine the heeling sail force from 5° to 35° heel angles the following experimental expression has been used:

$$FH = \frac{\rho}{2} * C_H * S_A * V_a^2 ,$$

where

ρ density ofthe air [kg/m^3]
C_H heeling coefficient [-]
S_A the sail area of the main and 100 % fore triangle in [m^2]
V_a apparent wind speed [m/s]

The values of Ch are derived from the so called *Gimcrack* sail coefficients based on a full-scale trials of the *Gimcrack*, a 6-Metre type yacht, supplemented by towing tank model tests to predict yacht performance.[5] The Table below presents these values at different heel angles ranging from 5° to 35°.

Angle of heel (φ)	5°	10°	15°	20°	25°	30°	35°
Heeling coefficient (C_H)	1,54	1,345	1,195	1,045	0,902	0,778	0,666

The Gimcrack sail coefficients

For the *FH* calculation the assumed apparent wind speed is 22 knots. The intersection of the *RM* curve and *HM* curves will determine the heeling angle at which equilibrium is obtained at the used wind speed. The plot of the stability curves of the various designs again was generated using the *DelftShip* program. The result of such an exercise for the base yacht, the carbon Standfast 64, is depicted in the figure below.

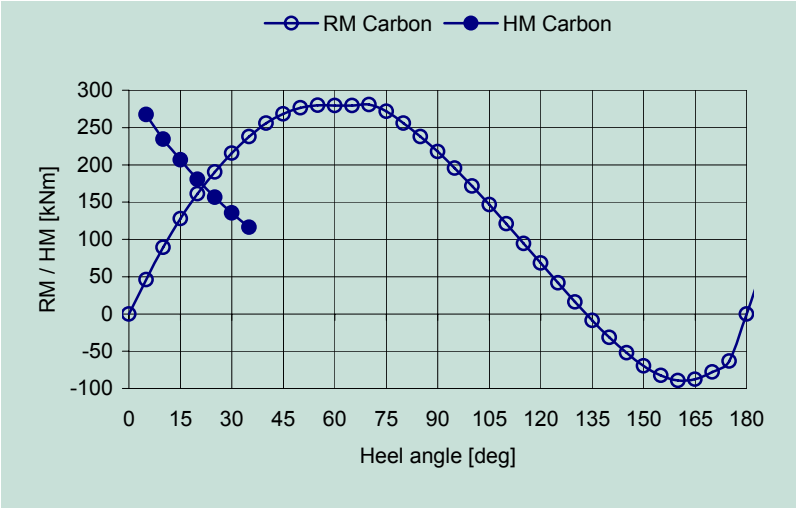

The calculated heel angle of the carbon base yacht is 21.8°. According to the boundary conditions the other versions have to keep the same properties. This requirement is solvable by the systematic changing of the mass and vertical centre of gravity of the ballast (bulb).

The result of this procedure applied to all the other design variations in the project is depicted in the Table below:

Yacht	Mtot [kg]	Zg [m]	Mbulb [kg]	Zg bulb [m]	Heel [deg]
Carbon	23000	-0.23	9240	-2.13	21.8
Aluminium	34500	-0.36	12740	-2.35	22.1
Glass	24700	-0.24	9240	-2.25	22.1
Wood	25700	-0.25	9240	-2.31	22.2
A5	30500	-0.06	8740	-2.18	22.1

Heeling angles at equilibrium of the different yachts

The total mass of the yachts may now be calculated and the results are then presented in the following Table.

Ship	Construction	Insulation	Bulb	Unchanged	Total
Carbon	3600	-	9240	10160	23000
Aluminium	8600	3000	12740	10160	34500
Glass	5300	-	9240	10160	24700
Wood Core	6300	-	9240	10160	25700
A5	8600	3000	8740	10160	30500

Total mass of the different yachts in [kg]

The 5th yacht design variation in the Table above (A5) is an aluminium construction with the same hull as the other ones but with a smaller sail area than the other aluminium yacht. The rationale behind this design variation will be explained in the section about sailing performance. This design variation results in a lower ballast weight, as will also be explained in the section about performance.

9. The Building Cost Assessment.

Comparing costs for alternative materials is rather difficult, since they largely depend on the starting point. A yard specialising in aluminium alloy may find the cost of retooling/retraining to build in composites to be prohibitive. Design costs may also be an issue. Designing an aluminium alloy hull to class rules may be a fraction of the cost of a fully engineered advanced composites solution, albeit that the latter results in a 'better' structure. Alternatively an independent designer/specialist structural design bureau may be able to approach a range of yards and so this issue may not arise. It is generally accepted that comparisons based on raw material cost have limited value. For production craft, it is the overall cost per unit that matters. For racing yachts, cost may be virtually irrelevant in the drive towards the minimum weight solution in order to maximise ballast ratio and hence sail area capacity.

The building cost of a one-off sailing yacht is something that many builders keep as a company secret because the up front costs of the yacht cannot be easily predicted. The determination of the actual cost afterwards, when the yacht is delivered to the customer, is often not fully carried out. However, the aim of this project is to make a comparison of the building costs involved with

the various building materials used. Therefore in the next paragraph the main outline of the cost calculations and the result of this comparison will be introduced.
For the sake of simplicity the expense can be separated in two main groups, namely the costs involved with *building* and the cost involved with *equipment and installation*.

The first part contains the *building* price of the:
- positive mould;
- hull;
- deck construction;
- bulkheads and walls;

the *equipment* part contains the costs of the:
- engines and propulsion line;
- rig and sails (shrouds, mast, etc.);
- deck gear;
- keel (ballast).

Building price:

At the preliminary design stage it is possible to use the following estimation[6] of the building cost:

$$F_c = O_F * H_W(1+S) * [M_R + L_P * W_R + T_C + M$$

F_c	=	fabrication cost;
O_F	=	overhead factor;
H_W	=	hull weight in kg;
S	=	proportional of scrap material;
M_R	=	material rate in Euro/kg;
L_P	=	labour productivity in man-hours/kg;
W_R	=	wage rate in Euro/kg;
T_C	=	tooling cost per kg worked;
M	=	margin.

It is assumed that the composite yachts are all being built at the same yard. Hereby the productivity, the wage rate and the other workshop factors such us the technology will have the same value and by comparing the fabrication costs with each other we can assume that knowledge about the hull weight and material rate is sufficient. The applied technology during the building process will also affect the cost and therefore throughout this project the Vacuum Resin Infusion method was assumed. This method was also used for building the base yacht. The following average material cost values have been used in the calculations:

Carbon	30 € / kg
Glass	6 € / kg

Foam Core	20 € / kg
Red Cedar	6 € / kg
Ayous	2.50 € / kg

The ayous is generally used to positive mould for the hull and the deck. For the wood core construction the assumed core material is the Red Cedar. From a building cost point of view the main advantage of the wood core construction is that you don't have to build complete mould for

the hull. This means that the man-hours can be significantly decreased. It remains necessary however to build the frames to plank the hull on.
The following table shows the result of this comparison where the base of the comparative is the carbon yacht.

Description	Carbon		Glass		Wood	
	work hours	material price	work hours	material price	work hours	material Price
Hull mould	1.00	1.00	1.00	1.00	1.00	0.20
Deck mould	1.00	1.00	1.00	1.00	1.00	1.00
Hull	1.00	1.00	0.90	0.34	0.20	0.14
Deck	1.00	1.00	0.90	0.28	0.30	0.28
Constructions	1.00	1.00	1.00	0.24	1.00	0.24
Summa	1.00	1.00	0.97	0.36	0.78	0.27
Total	1		0.64		0.50	

Comparison of the building cost of the yachts

The comparison of the composite and the aluminium construction remains rather difficult due to the considerably dissimilar construction technology. Hereto ample consultation with builders and designers amongst others with Standfast Yachts (Breskens) and Gerard Dijkstra and Partners (Amsterdam) who are well established in the composite and aluminium yacht construction lead to the following assumptions used: the determination of the building costs for the aluminium yacht largely depends on the number of bulkheads, tanks, complexity of the cockpit and keel, incorporated deck fittings, foundations etc. Nevertheless it is possible to use a range of €/kg value for the estimation of the building cost including the price of the material and working hours.

For the aluminium building price the following items have to be taken in consideration:

- Hull and deck construction
- Insulation
- Bulkheads and walls

The following table shows the comparison between the carbon and aluminium yachts.

Description	Carbon price	Aluminium price
Building	1.00	0.76

Equipment price:

The comparison of these groups is a little easier than the previous because we can use the same man-hours and the price of the equipments can be estimated as a function of the weight or the sail area. The next table shows the comparison of the equipment prices for the five yachts:

Description	Carbon	Aluminium	Glass	Wood Core	A5
Main engine + Propulsion line	1	1.5	1.08	1.12	1.33
Rigging (carbon)	1	1.3	1.05	1.08	1.13
Sails	1	1.3	1.05	1.08	1.13
Deck gear	1	1.3	1.05	1.08	1.13
Keel (ballast)	1	1.5	1	1	0.95

Total	1.00	1.32	1.05	1.08	1.14

Equipment cost relation

The rate of the final results is shown in the following figure where the basic of the comparison is the Carbon yacht.

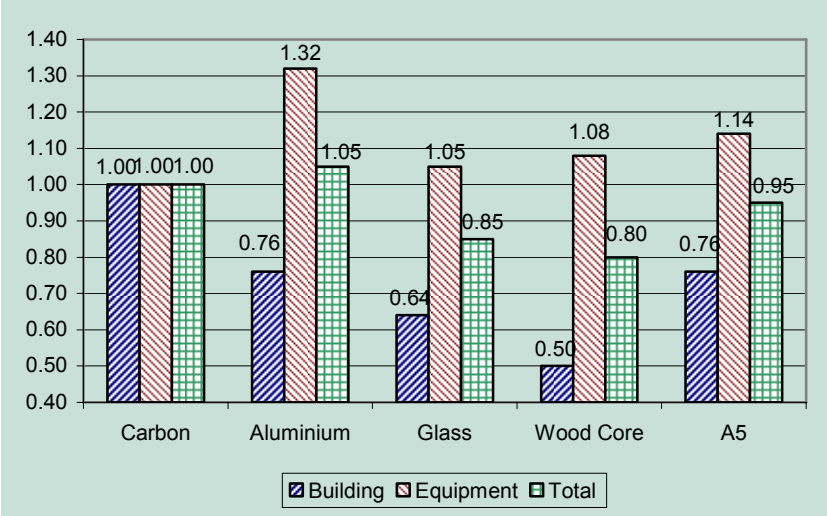

Figure: Overall cost relation of the yachts

The results in this figure clearly shows that although the material rate for example the glass to the carbon is about 20% the building cost changing to about 64% and finally the total cost of the yacht is about 85%. So comparing only the prices of the materials separately is rather inaccurate and the change of the equipment prices due to the increasing loads have to be taken in to account also in the yacht overall price comparison.

10. The Performance Assessment

In order to assess the performance differences between the various realizations of the same design (the base boat) build in different materials use has been made of a Velocity Prediction Program, i.e. “Windesign”. The formulations used for the assessment of the hydrodynamic and aerodynamic forces involved use has been made of those expressions derived from the results of the Delft Systematic Yacht Hull Series (DSYHS).
The performance of these boats has been compared in different environmental conditions, i.e.:

Light air 5 knots true wind
Moderate air 10 & 14 knots true wind
Heavy air 20 & 25 knots true wind

To calculate the influence of wind-waves on the performances the North Sea conditions have been taken into consideration. The Table below shows the characteristics of the wave spectra used at the different wind speeds.

Wind speed [kn]	Wave height [m]	Period time [s]
1,6	0,50	3,25
3,9	0,65	3,65
7,4	0,80	3,90
12,0	1,10	4,30
17,5	1,65	4,75

22,0	2,50	5,30
25,0	3,50	6,00

North Sea wind-wave conditions

In the calculations for the sake of comparison the following sail sets have been applied:
Sail set with the true wind direction between 0 – 130 degrees: Main and Jib and with the true wind direction from 80 to180 degrees: Main and Spinakker.
The sail dimensions used in the VPP calculations are depicted in the table below:

Yacht	Main			Fore				Spin				
	P	E	BAD	IG	J	LP	HBI	ISP	SPL	SMW	SLU	SLE
	[m]	[m]	[m]	[m]	[m]	[m]	[m]	[m]	[m]	[m]	[m]	[m]
Carbon	22,8	8,3	1,98	24,8	7,1	7,9	1,650	24,8	7,1	12,78	25,80	25,80
Aluminium	30,7	8,3	1,98	32,4	7,1	7,9	1,623	32,4	7,1	12,78	33,17	33,17
Glass	24,2	8,3	1,98	26,2	7,1	7,9	1,618	26,2	7,1	12,78	27,14	27,14
Wood	25,0	8,3	1,98	27,0	7,1	7,9	1,599	27,0	7,1	12,78	27,92	27,92
A5	26,0	8,3	1,98	28,0	7,1	7,9	1,575	28,0	7,1	12,78	28,87	28,87

Sail dimensions of the various designs as used in the VPP

The following Table shows the mast dimensions which were used to determine the mast and rigging drag. These were the same at every version.

MDT1 [m]	MDL1 [m]	MDT2 [m]	MDL2 [m]	TL [m]
0,22	0,35	0,22	0,25	5,13

Mast dimensions

The following Table depicts the flotation data of the various designs as used in the VPP calculations:

Yacht	Dsplt	Dsplc	Lwl	Bwl	Tc	Tmax	Awp	Cp	LCB	LCF	Mlong
	[kg]	[kg]	[m]	[m]	[m]	[m]	[m^2]	[-]	[%]	[%]	[m]
Carbon	23081	21775	16,901	4,350	0,740	2,500	51,16	0,564	-5,18	-7,09	34,581
Alu	34520	33320	17,106	4,838	0,951	2,527	58,24	0,563	-4,40	-7,41	27,315
Glass	24739	23432	17,094	4,399	0,772	2,532	52,39	0,565	-4,70	-6,80	33,810
Wood	25742	24434	17,208	4,427	0,791	2,551	53,10	0,566	-4,43	-6,63	33,360
A5	30518	29330	16,729	4,756	0,881	2,457	55,85	0,560	-5,25	-7,95	28,017

Flotation data as used in the VPP calculations.

For the ease of assessment only the optimal performances of the various designs are listed. First the results for the upwind conditions will be presented.

Yacht	Wind speed (Vt) in knots				
	5	10	14	20	25
Carbon	2,882	5,101	5,788	5,847	5,688
Aluminium	3,360	5,491	6,013	6,126	5,928
Glass	2,992	5,192	5,833	5,895	5,727
Wood	3,052	5,241	5,859	5,961	5,750

A5	2,982	5,151	5,595	5,629	5,395

Optimal upwind performance in Speed made good (knots)

The differences in delta's and percentages with the carbon base boat are presented in the Table below:

Wind speed (Vt) in knots				
5	10	14	20	25
0,00	0,00	0,00	0,00	0,00
0,48 16.59%	0,39 7.65%	0,23 3.89%	0,28 4.77%	0,24 4.22%
0,11 3.82%	0,09 1.78%	0,04 0.78%	0,05 0.82%	0,04 0.69%
0,17 5.90%	0,14 2.74%	0,07 1.23%	0,11 1.95%	0,06 1.09%
0,10 3.47%	0,05 0.98%	-0,19 3.33%	-0,22 3.73%	-0,29 5.15%

Delta Vmg in knots and in %

When considering the different performances of the various designs it should be noted first that only those characteristics of the boats are visible in the results that are actually accounted for in the VPP. This implies amongst others that performance improvements associated by boat stiffness are not found in these results. This is one of the reasons for designers to choose for a carbon construction.

What becomes obvious from these results is that in the light conditions the advantage of the wood core boat over the carbon boat is close to 6%, while in heavy air this is about 1%. Something similar is seen with the modified aluminium boat A5 which performs circa 3.5% better in light air when compared with the base boat but 5% worse in heavy air.
To a large content these differences may be attributed to the differences in sail area versus wetted surface ratio, as demonstrated in the table below:

Yacht	Sail Area [m^2]	Wetted surface [m^2]	SA / Ws [-]
Carbon	194	56,01	3,464
Aluminium	254	66,38	3,826
Glass	204	57,78	3,531
Wood	210	58,80	3,571
A5	219	62,68	3,494

Sail area versus wetted area ratio's

The last table shows the heeling angle of the boats at their optimal performance upwind. It clearly demonstrates the validity of the design rules used as all the heeling angles are close. The carbon boat is the stiffest after the A5 variant, which has less sail then it should have.

Yacht	Wind speed (Vt) in knots

	5	10	14	20	25
Carbon	3,3	12,8	19,1	20,3	21,0
Aluminium	4,6	16,2	21,4	22,0	22,2
Glass	3,6	13,7	19,7	20,5	21,3
Wood	3,7	14,2	20,0	21,4	21,5
A5	3,7	15,2	18,9	19,3	20,4

Heeling angles at optimal speed made good

Another possibility to compare the different performances is by sailing different course types with the boats and compare their average time needed over one mile of such a course. This procedure is similar to the standard course types used in the International Measurement System handicap options.
The course types used are:

- Windward – Leeward consist of one track upwind and one track downwind of the same length(WL)
- Olympic Triangle consist of the classical Olympic track two windward tracks, one down wind track and two reaching tracks (OLY)
- Linear Random which is a straight track with systematically varying wind direction over the entire length (LR)

The results for these tracks are:

Yacht	Wind speed (Vt) in knots				
	5	10	14	20	25
Carbon	1116	629	529	485	473
Aluminium	989	594	515	472	465
Glass	1085	620	526	482	471
Wood	1068	615	524	479	470
A5	1086	626	543	501	496

WL course times in seconds per mile

Yacht	Wind speed (Vt) in knots				
	5	10	14	20	25
Carbon	1057	600	516	484	477
Aluminium	929	567	503	472	470
Glass	1025	591	513	481	475
Wood	1008	587	511	478	474
A5	1026	597	531	503	504

OLY course times in seconds per mile

Yacht	Wind speed (Vt) in knots				
	5	10	14	20	25
Carbon	748	455	396	356	335
Aluminium	678	443	395	361	345
Glass	732	451	395	357	336
Wood	723	449	394	356	336
A5	729	458	408	373	356

LR course times in seconds per mile

The general conclusion that may be drawn from these results can be summarized as follows

- At light wind conditions the yachts with bigger sail area has better performance due to the better SA/Ws ratio.

- At medium and heavy air conditions the effect of the L_{wl} is determine the performance because the SA/∇ ratio are equal.
- At the angel of stability the yachts have the same property.
- Differences between the comparable performances at light wind are not bigger than 6%. At moderate wind this gap is decreasing to 3% while at heavy weather this is more or less balanced (1%).
- Although the first aluminium version is matching with the precept it can be seen that her performance is incomparable due to the disproportionate huge sail area.

11. Conclusions

In this study the Standfast 64' yacht has been used as a base boat for comparising the building price and performance differences that arise when the same yacht is build in different materials.
The base yacht was designed as a carbon epoxy sandwich construction and the considered other building materials are aluminium, glass epoxy sandwich and wood-core.
The main boundary conditions used are that the hull shape remains the same, an equal SA/∇ ratio and the same stability at a given wind speed. It was necessary however to make another hull shape for the aluminium version, because when the design rules were strictly applied the weight and the draught increased too much. Due to this large weight difference the sail area of this yacht became impractical when the SA/∇ ratio had to be kept constant. This yacht does not seem to be feasible and therefore the fifth yacht A5 was presented in to this study. This design has the same hull and construction weight as the aluminium one but the sail area is limited by the value of the mast height.

As an overall result the following table which contains the condensed differences between the various designs is presented. The data in the figure are derived from the building cost, the overall cost relation and the average speed prediction. The last column is the price-performance ratio relative to the carbon yacht.

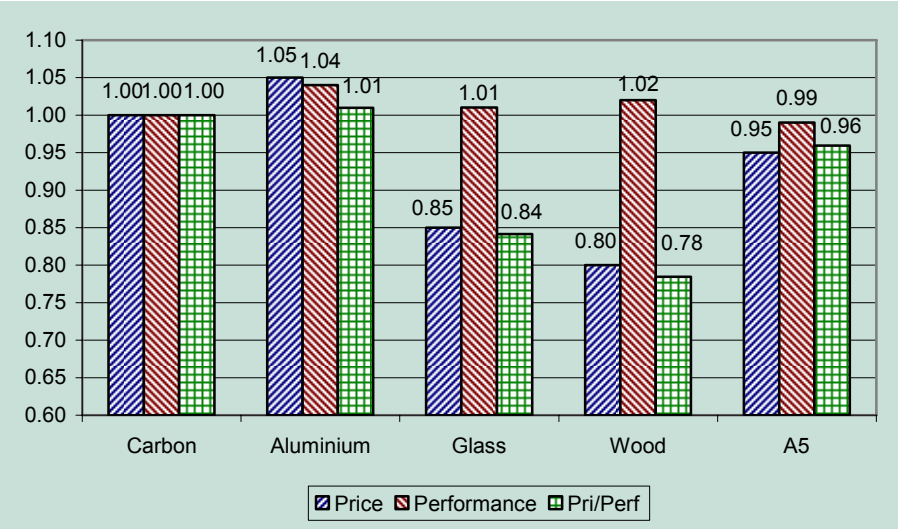

Price-Performance comparison

From this figure we can see the yacht's performances are close to each other therefore the price-performance relation is mostly depends on the building cost discrepancy in this situation. While the performance difference is about 5% the building cost diverge to 20%. Seen like this the cheaper building construction seems to be a profitable choice. On the other hand, the rate of the design attributes for a performance cruiser such us safety, cost, comfort, beauty, etc. are usually

have major angle than the cruising speed but this is mostly the owner's task to determine this weighted rating.

List of symbols

Basic

L_{oa}	[m]	Length over all		I, IG	[m]	Vertical dimension of fore triangle
L_{wl}	[m]	Waterline length		J	[m]	Longitudinal dimension of fore triangle
B_{oa}	[m]	Beam over all		P	[m]	Vertical dimension of main triangle
B_{wl}	[m]	Waterline beam		E	[m]	Longitudinal dimension of main triangle
T	[m]	Draught		SM	[m^2]	Main sail area
Disp, ∇	[m^3]	Volume displacement		SF	[m^2]	Fore sail area
Bulb	[kg]	Mass of the ballast		SA	[m^2]	Total Sail area

Symbols used in the VPP

Rig parameters

BAD	[m]	Vertical distance from HBI to bottom of P		MDT1	[m]	Mast Section Transverse Dimension
HBI	[m]	Height of base if I above sailing water plane		MDL1	[m]	Mast Section Longitudinal Dimension
SPL	[m]	Spinnaker pole length		MDT2	[m]	Topmast Section Transverse Dimension
SMW	[m]	Spinnaker mid width		MDL2	[m]	Topmast Section Longitudinal Dimension
SLU	[m]	Spinnaker luff length		TL	[m]	Length of mast Taper
SLE	[m]	Spinnaker leach length				
ISP	[m]	Vertical height of spinnaker halyard sheave				

Hull parameters

Dsplt	[kg]	Total Displacement		Awp	[m^2]	Water plane area
Dsplc	[kg]	Canoe Body displacement		Cp	[-]	Prismatic Coefficient of canoe body
Lwl	[m]	Waterline length		LCB[1]	[%]	Longitudinal centre of buoyancy
Bwl	[m]	Waterline beam		LCF[1]	[%]	Longitudinal centre of flotation
Tc	[m]	Canoe body draft		Mlong	[m]	Something
Tmax	[m]	Maximum draft of keel				

[1] - % of Lwl - relative to Lwl/2 - aft is negative
[2] - for 0,2,10,25 & 40° heel

References:

1. Claughton, Wellicome & Shenoi, *Sailing Yacht Design: Theory,* Addison Wesley Longman Limited 1998.

2. Germanischer Lloyd AG, *Rules and Guidelines 2004,* Hamburg,

3. John S. Letcher, Jr., *Handicapping Rules and Performance of Sailing Yachts,* Chesapeake Sailing Yacht Symposium, 1974

4. Journee, J.M.J and Massie, W.W., *Offshore hydromechanics Lecture Notes, Delft University of Technology,* 2001

5. Keuning, J.A., Sonnenberg, U.B., *Approximation of the Hydrodynamic Forces on a Sailing Yacht based on the 'Delft Systematic Yacht Hull Series',* International HISWA Symposium on Yacht Design and Construction, Amsterdam, 1998

6. Larson, L., *Principles of Yacht Design,* Adlard Coles Nautical, London 2000.

7. Marchaj, C.A., *Aero-Hydrodynamics of Sailing,* Adlard Coles, Great Britain 1990

Session 8

Ian Campbell

DEVELOPMENT OF THE STRUCTURAL REQUIREMENTS IN THE VOLVO OPEN 70 RULE VERSION 2

Ian M. C. Campbell , imc@soton.ac.uk

1 INTRODUCTION

The Volvo Open 60 Rule was used as the class rule for yachts eligible to enter the 2001/02 Volvo Ocean Race. This rule was developed from the Whitbread 60 Class Rule, used in 1993/94 and 1997/98 Whitbread Round the World Races and over a span of 12 years these rules produced yachts that survived record-breaking ocean racing.

During 2003 the Volvo Ocean 70 Rule was developed for a new class of 70-foot yachts eligible for the current 2005/06 Volvo Ocean Race. These boats were intended to be faster than their predecessors and differed by permitting canting keels, which had been proven in ocean races by the IMOCA Open60 monohulls, but for safety reasons the development of the rule drew on the experience embodied in the Volvo Open 60 Rule.

This paper deals with the development of the new rule rather than the performance of the boats built to it. The Volvo Ocean 70 Rule was reviewed following the conclusion of the 2005/06 Volvo Ocean Race and a number of changes were introduced into Version 2 of the Rule to address significant structural problems that occurred in some of the yachts.

2 BACKGROUND TO STRUCTURAL REQUIREMENTS

2.1 Volvo Open 60 basic rule principles

The Volvo Open 60 Rule (V.O.60) contained three main requirements to regulate the structures: permitted materials, minimum panel weights and compliance with the American Bureau of Shipping “Guide for Building and Classing Offshore Racing Yachts”.

These requirements were complementary since hull shells could be designed to the minimum panel weights in the permitted materials such that they would also comply with the requirements of the ABS Guide, which further provided the requirements for the internal members of the structure, e.g. frames, and for the keel fin and its attachments.

2.2 Changes for the Volvo Ocean 70 Rule

It was decided early in the development of the new V.O. 70 Rule to permit the use of carbon fibres and honeycomb cores in the hull construction, which, together with the anticipated performance increase, necessitated a review of the minimum panel weights.

Meanwhile, during the life of the Whitbread 60 and V.O.60 rules there had been changes to the associated regulations. The Council of European Communities Recreational Craft Directive 94/25/EC, commonly known as the RCD, came into force for vessels up to 24 metres in length and the ABS effectively withdrew the use of their Guide for yachts of less than 24 metres in length.

Other Classification Societies had also withdrawn their scantling rules for yachts in anticipation of the new harmonised ISO/CEN Standard 12215-5 “Small craft — Hull construction/scantlings — Part 5: Design pressures, design stresses, scantling determination” but unfortunately this had an extremely long gestation and was only in draft form at the time the new Volvo Ocean 70 Rule was being written and was untested for use in racing yacht design.

Some new requirements entered the 1994 Version of the ABS Guide and Notice #1 provided further changes before the ABS withdrew it’s publication. The existing V.O.60 Rule managed to continue to apply these requirements, using the Wolfson Unit MTIA as an independent

organisation to check conformity of designs with the published requirements. It was, however, unclear whether there was a legitimate basis for making reference to the ABS Guide in a new rule. Attention was therefore directed towards the RCD even though racing yachts could be excluded from its scope.

2.3 Rationale for structural requirements

Det Norske Veritas (DNV) were consulted during the V.O.70 Rule development and although they did not become fully involved they provided an interesting rationale by distinguishing between the three aspects of the rules:

Fitness for purpose requirements, to ensure that important matters are addressed regarding structural integrity, e.g. structural arrangements and load cases.

Equal racing requirements, to ensure that matters are addressed on a common basis with appropriate measurements etc. so hull weights were similar.

Safety requirements, to ensure the safety for the people onboard, not necessarily the structural integrity of the yacht.

2.4 IMOCA Class Rules

The International Monohull Open Classes Association (IMOCA) was responsible for the Open 60 ISAF International Class, which had developed independently of the V.O.60 class and used the canting keel arrangement that was to be adopted in the new V.O.70 class.

Rule C-5 stated “The boat shall be constructed in such a way as to be able to stand, without irreparable damage, the forces of nature, which it is intended to have to face in the course of races classified by the ORC in category0…..”

This was non-prescriptive and left the designers with the responsibility of producing adequate structural arrangements but was considered to be too open to be adopted in the new V.O.70 Rule.

2.5 Fundamental Rule Policy

It is worth noting here the Fundamental Rule Policy that is stated at the beginning of theV.O.70 Rule:

“The Volvo Open 70 Rule is intended to produce fast, single mast monohull keelboats of similar performance, suitable for long distance racing offshore at the highest level of the sport. The need for safety and self-sufficiency is paramount. The Rule is intended to foster gradual design development leading to easily driven, seaworthy yachts of high stability, requiring moderate crew numbers. Any development that is contrary to this policy may give rise to Rule change.”

This also embodies the three rule aspects identified by DNV; safety; self-sufficiency, which is dependent upon fitness for purpose; and similar performance, which is partly achieved through equal racing requirements.

2.6 Safety and risk assessment

Failures continue to occur in racing yachts despite best attempts by regulators, designers and builders to ensure structural integrity so the risk of failure needs to be assessed to improve safety for the sailors. Table 1 was prepared during the development of the V.O.70 Rule and was used to identify the important safety requirements to be incorporated into the Rule.

Further details about the risk assessment can be found in reference 6 and a full study was conducted into the buoyancy subdivision requirements with regard to flooding and stability.

A major concern was the risk of failure of the fin or bulb leading to capsize of the yacht with no prospect of self-righting. Therefore it was considered important to include in the Rule load cases, material properties and factors of safety for the ballast keel to try and ensure that the keels were adequately strong and to ensure “similar performance”.

2.7 Concepts for the V.O.70 Rule

Seahorse Rating Limited put together the V.O.70 Rule for the Volvo Ocean Race organisation and together they consulted with a number of designers and other organisations and held a series of meetings. One of the issues was the degree of openness allowed by the Rule and the scope for design. A balance had to be struck between rule prescriptions and designer’s responsibilities and also between the dichotomy of intent expressed in the Fundamental Rule Policy for both similar performance and design development.

Perhaps surprisingly, the consensus view amongst designers consulted during the Rule development was a preference for some prescription within the Rule.

3 SAFETY RULES

The concept of safety was widely accepted but it is difficult to define in a rule so to avoid semantic problems reference was made to the Essential Safety Requirement given in the RCD. The hope was that the Directive had already been well drafted and would gain international recognition.

3.1 Essential safety requirement

The essential safety requirement 3.1, “Structure” given in the RCD states:

“The choice and combination of materials and its construction shall ensure that the craft is strong enough in all respects. Special attention shall be paid to the design category according to section 1, and the manufacturer's maximum recommended load in accordance with section 3.6.”

This is similar to the IMOCA Open 60 Class Rule C-5, quoted earlier in this paper but has a more formal status – being part of the RCD. It is a non-prescriptive statement so required reinforcing for incorporation into the V.O.70 Rule.

3.2 Conformity assessment

The RCD is a complex document consisting of 15 Articles and 15 Annexes with cross referencing between them. Full conformity is required for production yachts built and sold within the EU and it was within the bounds of possibility that a V.O.70 yacht could achieve this.

Instead the V.O.70 Rule merely refers to Annex VII (EC Type-examination Module B), which applies to ocean sailing yachts between 12m and 24m in length and for full CE Marking would involve a Notified Body, some of which are Classification Societies, checking the technical documentation. An exception was written in the Rule to the requirement to use a Notified Body but for the 2005/6 race the Volvo Ocean 70 Rule Management Group (RMG) invoked the Rules requiring designers to make their technical documentation available and sought the assistance of the Wolfson Unit MTIA to check this – a task that the Wolfson Unit thought it had relinquished when it consulted on the change from the V.O.60 Rule to the V.O.70 Rule.

Annex VII of the RCD refers to relevant standards and to Article 5, which also relates to standards and this is perhaps the part of the conformity assessment with the least clarity, due to the transition between Classification Societies rules and guides that had been withdrawn and the new harmonised ISO standard that was in draft form. It was assumed that designers would select the standard they would work to and it would be their responsibility to conform to its requirements. In practice most designers continue to work informally to the requirements of the ABS Guide. It would seem difficult for the ABS to withdraw existing knowledge from prior application of their Guide even if its status is withdrawn.

4 STRUCTURAL DESIGN

The new V.O.70 Rule embodied the principles of the three main structural requirements in the V.O.60 Rule but with different applications. The permitted materials had changed, new panel weights were specified and the conformity assessment was less prescriptive.

4.1 ISO/CEN Standard 12215-5

This standard was published in draft DIS form and a final draft FDIS was circulated to the Working Group in September 2005, after the current fleet of V.O.70 yachts had been designed, and was embodied in the new Wolfson Unit HullScant program. It is anticipated that the Standard will be published in 2007. The HullScant program was developed to aid the conformity assessment of the V.O.70 yachts and simplifies the input of material properties and layups and comparison with the ISO Standard requirements. A simple example of the associated graphical output is in Figure 1. The program was based on an earlier version, used within the Wolfson Unit for assessment of the V.O.60 yachts to the ABS Guide, and not commercially available because of Copyright and Intellectual Property Rights held by the ABS.

4.2 Application to V.O.70 yachts

The technical documentation and hull scantlings of the V.O.70 yachts were compared with the requirements of both the ABS Guide and the DIS ISO standard.

There are several points of note with regard to the application of the ISO Standard:

The introduction to the Standard states: “The working group considers this International Standard to have been developed applying present practice and sound engineering principles. The design pressures of this International Standard shall be used only with the equations of this International Standard.” This means that the pressures should not be taken as reliable values to be used in Finite Element Analysis.

There is no “Alternatives” clause in the Standard, such as found in Classification Society rules. Its requirements therefore have to be followed strictly according to the published text.

Part 5 of the ISO Standard does not include structural requirements for the ballast keel, reinforcing the need to have included these within the V.O.70 Rule, and Part 6 is still in draft.

Round bilges and hard chines can be considered as natural stiffeners for panels, enabling large panels to be sub-divided for structural calculations. This is somewhat different to the curvature correction within the ABS Guide and can lead to different panel sizes with the same strength limitations.

4.3 Design of the hull shell

The minimum panel weights specified in the V.O.70 Rule were derived following comparative calculations based on the requirements of the ABS Guide and a consultation process with designers, with responses based on their experience with other successful racing yacht designs.

The Rule panel weights oscillated during the consultation but ended up being within 7% of the values in the V.O.60 Rule, heavier in the bottom forward and generally lighter elsewhere. This took account of the higher strength of carbon fibre, the lighter displacement and greater length of the V.O 70 yachts and an expectation of higher loading due to the anticipated increase in performance, which may have been underestimated given reports from the sailors.

An intention in setting the minimum panel weights was to allow designers to opt for single skin in parts of the bottom without incurring a weight penalty, to avoid the possibility of core shear in areas notorious for damage due to slamming.

Aramid fibres, used in the construction of the V.O.60 yachts, have relatively poor compressive strength and were a ruling property in the scantling determination for these boats. By comparison, carbon fibres are significantly stronger in compression, so there were generally few problems in designing a sandwich hull shell to the minimum panel weights that complied with the conformity assessment standards.

Providing adequate core thickness to meet shear strength requirements remained the main design issue. It is recognised that, in practice, material choice and construction methods and standards are also very important in maintaining structural integrity.

4.4 Design of internals, including stiffeners

Both the ABS Guide and the ISO Standard deal with the requirements for internal structural components. The watertight sub-division requirements of the V.O.70 Rule placed bulkheads that also provided structural support for the hull shell. Core shear requirements then determined panel sizes and the placement of intermediate internals, although, as previously discussed, there were differences depending on the chosen standard.

It was, however, considered that a more formal requirement should be written into the Rule, in lieu of the requirement in the ABS Guide for stringers in the slamming area, so maximum panel dimensions were specified. This resulted in duplicity of requirements and it is not uncommon in such instances to find one of the requirements becomes effectively redundant.

5 STRUCTURAL REQUIREMENTS FOR BALLAST KEELS

The ABS Guide contained specific requirements for the design of ballast keels or fins and their attachments. These had been strictly applied to the V.O.60 yachts; according to the published text of the Guide and not the alternatives that some design offices had approved by the ABS. Despite their slender appearance V.O.60 fins had proved to be robust. Whilst the need to comply with the essential safety requirement should have ensured that the V.O.70 ballast keels would also be robust, the consensus view from designers and the rule makers was that some prescription should be provided. The absence of reference to the ABS Guide in the V.O.70 Rule meant that the structural requirements for ballast keels had to be incorporated into the Rule.

5.1 Load cases

The sailing and grounding load cases were based on those formerly published the ABS Guide. They used the yacht's displacement including the bulb, as applied to the V.O.60 yachts, not excluding the bulb, as used by some design offices according to "alternatives" previously accepted by the ABS.

The grounding load cases are notional and are assessed using a quasi-static analysis, which will not represent actual dynamic behaviour in real instances. Nevertheless they provide a useful method for ensuring that the ballast keel is designed to cope with impact loads and the high accelerations associated with the performance of canting keel yachts in ocean racing conditions. V.O.60 yachts have been reported to survive grounding on rocks, so their experience was embodied in the Rule, and one of the V.O.70 yachts was reported to have grounded during the Cape Town port race.

5.2 Design stresses and factors of safety

It is the keel scantlings that are important when comparing strength and these are determined from the combination loads, stresses and factors of safety.

There was a general opinion that the factor of safety needed to be higher for a canting keel than for a fixed fin, because the canting keel generally operates at higher angles. Sailors' reports of high vertical accelerations due to the speed of the V.O.70 yachts sailing over waves also confirm the need to consider higher fin loadings.

The V.O.60 Rule and the ABS Guide included maximum strength values for design purposes. Higher strength steels could be used in the construction but the increased strength added to factor of safety and could not be used to reduce the keel scantlings. This strength was included in the V.O.70 Rule. Care was taken to ensure that the overall design of the ballast keel would be relatively stronger than the V.O.60 keel, taking account of the different bulb weights and leaving designers with the choice of construction and materials.

6 STRUCTURAL PROBLEMS REPORTED DURING THE 2005/06 VOLVO OCEAN RACE.

A number of problems were reported in the media and on the Volvo Ocean Race website. Many of these were subject to further examination but confidential reports were not available for this paper. The media reports mainly concerned problems that led to obvious issues that affected the race, such as the retirement of yachts from legs of the race, sudden speed loss or, sadly, *Movistar's* abandonment. Some less obvious problems remained largely unreported, although word spread within the race community.

The obvious structural problems for the hull and canting keel were:

i) Loss of keel fairings, the so called bomb doors, which led to pressurisation of the keel compartment when the yachts were sailing at speed.

ii) Hydraulic ram rod end failures, which led to loss of control of the keel cant angle.

iii) Damage and failures within the structure associated with the canting keel, which could progressively worsen.

iv) Failure of a deck structure, which restricted the sail loads that could be applied. This was an isolated incident attributed to construction problems

Notable absences from this list were:

a) Failures of the canting fin, so there were no incidents of catastrophic loss of stability.

b) Breaches of the hull shell, so there were no major incidents of flooding.

Nevertheless, the reported problems gave rise at the time to concerns about the integrity of the yachts and good seamanship was displayed in the incidents to ensure the safety of the crew by their self-sufficiency.

The hydrodynamic pressurisation of the keel compartment, caused by high speed water entering when the fairings were lost, exceeded the normal hydrostatic pressures and probably exceeded the hydrodynamic pressures for the bottom shell of the hull, such as those given in the ABS Guide, reference 3, and the ISO Standard 12215-5, reference 4. The effective remedy was to slow the boat but if the fairing loss remained undetected the keel compartment could be breached leading to flooding of the central hull compartment. The watertight bulkheads and sub-divisions were designed to keep the yacht afloat in such an incident but the crew's concerns were expressed in the regular reports on the website.

The ram rod end failures were potentially serious since an uncontrolled keel and bulb, the so called "free-Willy" problem, leaves the hull and rig free to roll and could potentially break-up the internal structure. There was the safeguard of having two rams for redundancy but when one failed there were concerns because the other was either similarly loaded or twice as loaded so likely to also fail.

In the event the crews managed to contain the ram failure problems, which began in leg 1 on *Ericsson Racing Team*, and it was not damage to the rams but rather their associated structure that led to *Movistar's* abandonment during leg 7.

It was clear from the Volvo Ocean Race reports following leg 2 that the rod end failure on *Pirates of the Caribbean* involved fatigue and by then crew reports were widespread about the high dynamic loading compared to other racing yachts, although experience from the IMOCA Open 60 yachts had been taken into account when drafting the Volvo Open 70 rule and ram failure had not been raised as a particular problem.

Dynamic loading remains a difficult issue to address within the Volvo Open 70 rule since even scantling rules such as the former ABS Guide and the recent ISO Standard only use quasi-static loads and pressures in their scantling calculations. Section 8 of this paper describes tank tests in waves that illustrate the complex nature of the dynamic loading on a canting keel.

There were also some mast structural problems that arose during the race but these were outside the scope of the structural requirements of the rule and this paper.

7 CHANGES TO THE STRUCTURAL REQUIREMENTS FOR VERSION 2 OF THE VOLVO OPEN 70 RULE.

Following the 2005/06 Volvo Ocean Race the Rule Management Group sought opinions on the development of Version 2 of the Rule. These were generally in favour of developing the requirements from the original rule rather than introducing new requirements.

A number of changes were, however, introduced partly to clarify the Rule:

i) Specific reference was made to ISO 12215-5 for conformity assessment

ii) The requirement for ring frames was removed, leaving intermediate internal structural arrangements between bulkheads up to designers but within the conformity assessment requirements.

i) Load cases for keel design were explicitly applied to the canting mechanism and associated structure

iii) The terms sailing and grounding were deleted from the load cases and the horizontal load in case 2 is to be considered in both fore and aft directions.

7.1 Discussion of the changes

It was suggested that reference to the Recreational Craft Directive was unjustified because the RCD states that craft solely intended for racing shall be excluded from its scope. It is perhaps a little strange that the Volvo Open 70 Rule opts into certain aspects of the RCD however the UK Marine and Coast Guard Agency (MCGA) published comments on the RCD indicating that it is the manufacturer's choice to seek exclusion.

Reference was made to the RCD because it provided definitions of safety requirements and specified requirements for conformity assessment so avoided the need for these to be redefined within the Volvo Open 70 Rule. There was not strong opposition to reference to the RCD and its removal would necessitate the addition of equivalent rules.

Reference to ISO 12215 was included although it is currently only issued as an FDIS and it is unclear whether it is yet accepted as a harmonised standard, however its status has risen since the original Volvo Open 70 Rule was written and it is referred to in the MCGA comments on the

RCD. It was also used in the previous conformity assessment of the existing boats so its inclusion clarifies the status quo.

8 TANK TESTS TO INVESTIGATE THE DYNAMIC LOADING ON A CANTING KEEL IN WAVES.

In order to investigate further the nature of the dynamic loading that caused fatigue problems in the hydraulic rams, tank tests were performed in waves on a model with a separate dynamometer attached to the keel. An existing model was available at short notice that had been used previously for University of Southampton School of Engineering Science student projects and represented a 6.5m LOA Mini Transat, not a Volvo Open 70, however this class pioneered the use of canting keels and the results can be scaled from the model to represent a 70ft yacht. The Mini Transat boat was of lighter displacement/length ratio than a Volvo Open 70 so there were options in the selection of a representative scale.

8.1 Model and scaling

The model was 2.17m LOA and is shown under test in Figure 2. It represented the length of a Volvo Open 70 yacht at 1:10 scale and the keel fin, bulb and attached dynamometer then had a scale mass of 7.3t compared to approximately 6t for the yacht. The displacement, however, corresponded to 35t at this scale compared to 14t for a Volvo Open 70 but for the tests in waves it was probably better to scale the length and keel mass than the overall displacement, which would have required the use of 1:7.5 scale.

8.2 Tests and results

Tests were conducted in irregular head seas at the GKN/WAL No. 3 towing tank on the Isle of Wight at scale speeds between 10 and 27 knots and significant wave heights between Hs=1-2m. The lateral force was measured together with the motions and vertical accelerations of the boat. Due to model limitations the keel was canted to the maximum angle of 30 degrees and most of the tests were run with the hull at zero angle of heel.

Results from a typical time history are shown in Figures 3 and 4 and reveal some interesting characteristics. The run corresponded to a scaled speed of 27 knots into 2m significant wave height and the pitch motion, shown in Figure 3, was relatively large with a range of 10 degrees and high accelerations were also measured. The keel lateral force, shown in Figure 4, showed positive peaks that corresponded to the troughs in the motion, where the boat was pitching down into the waves and slamming on occasion.

A positive keel lateral force was associated with loading from the downward gravitational direction acting normal to the canted keel and also corresponded to the righting moment produced by the keel and bulb. The peaks in the loading shown in Figure 4 correspond to slam loading on the keel. It can be seen that the mean keel lateral force is, however, negative and this corresponds to the hydrodynamic lift, which is necessary to react against the sail force but produces a destabilising moment.

8.2 Force components

The loading on the keel therefore consists of several components: gravitational, due to the cant angle; hydrostatic, due to the buoyancy; hydrodynamic, due to the varying lift force; and inertial, due to the pitch motions. In addition higher frequency components than those in the pitch motions can be seen in the keel lateral force record and these represent the dynamic response of the keel and dynamometer mounting arrangement and were of smaller magnitude than the general wave induced loads. The net result of these components is the record shown in Figure 4 and it can be seen that in this test the lateral force was generally less than the keel weight except following a slam at 65 seconds.

The dynamic component of the keel lateral force is shown in Figure 5 for various runs in different sea-states and at different speeds. The root mean square (rms) value for the force was normalised using the keel weight and the results show its variation with the rms acceleration measured above the keel. It is noted that significant values are approximately twice the rms values and the peak acceleration exceeded 1g in some runs. The acceleration was also recorded near the bow, at station 1 on the model, and was generally a factor of 1.7 greater than at the keel. It can be seen from Figure 5 that there is good correlation between the acceleration and keel force so onboard acceleration measurements, taken whilst racing, can be used to indicate keel loading.

8.2 Correlation

Pressure measurements in the canting keel hydraulic system on racing yachts had previously indicated that the 90 degree heel load was occasionally exceeded, see reference 7. The force measurements from the tank tests shown in Figure 4 were also consistent with this. In the Volvo Open 70 Rule the sailing load case, or load case 1 in version 2 is concerned with this condition and includes a minimum safety factor of 3. It is clear from the tests that this factor of safety is necessary, not only to ensure that overloads can be tolerated but also to ensure adequate fatigue life, which was not the case for some of the hydraulic rams on the Volvo Open 70 yachts in the 2005/06 Volvo Ocean Race.

9 CONCLUSIONS

Drafting a new rule for a faster class of ocean racing yachts is a difficult task and designing to it is also difficult because of the higher speeds and absence of any prior boats for experience. Record breaking performances were achieved by the new Volvo Open 70 yachts during the 2005/06 Volvo Ocean Race and a new Version 2 of the Rule was developed based on experience from the problems encountered during the race. Time will reveal whether the issues were correctly addressed.

10 ACKNOWLEDGEMENTS

The Volvo Ocean Race organisation and Seahorse Rating Ltd. led the development of the V.O.70 Rule and this paper represents just part of their development process. The author thanks both organisations for their invitation to be part of the process and their permission to publish this paper and colleagues at the Wolfson Unit MTIA for their work on the Rule and assistance with the tests.

11 REFERENCES

1. Royal Ocean Racing Club Rating Office, (1999), Volvo Ocean 60 Rule, Seahorse Rating Ltd., UK.
2. Royal Ocean Racing Club Rating Office, (2003), Volvo Open 70 Rule, Seahorse Rating Ltd., UK.
3. American Bureau of Shipping. (1994), Guide for Building and Classing Offshore Racing Yachts, ABS, New York USA.
4. ISO (2005), Standard 12215-5, Small craft — Hull construction/scantlings — Part 5: Design pressures, design stresses, scantling determination, ISO, Geneva.
5. The Council of European Communities, (1994), Recreational Craft Directive 94/25/EC, Brussels.
6. Safety considerations in developing the stability and structural requirements in the Volvo Open 70 Rule, I.M. Campbell, A. R. Claughton, B. Deakin, (2006) RINA High Performance Yacht Design Conference, Auckland NZ.
7. Practical aspects of canting keel design, construction and analysis, L. Tier, M. Owen, T. Sadler, (2006) RINA High Performance Yacht Design Conference, Auckland NZ.

DEVELOPMENT OF THE STRUCTURAL REQUIREMENTS IN THE VOLVO OPEN 70 RULE VERSION 2

Figures

Ian M. C. Campbell , imc@soton.ac.uk

Item	Requirement	Safety issues	Safety backup	Compliance
Hull plating	Minimum weight/m^2 Maximum span	Watertight integrity Global hull strength	Buoyancy subdivision	Core sample
Deck plating	Minimum weight/m^2	Watertight integrity	Buoyancy subdivision	Core sample
Bulkhead plating	Minimum weight/m^2	Maintain intact compartments	Life rafts	Core sample Flooding test
Fin	Minimum strength	Essential for stability	Habitability when Inverted	Calculation
Bulb	Minimum strength	Essential for stability	Habitability when inverted	Calculation
Dagger board	None	Related damage to hull	Fin and rudder	N/A
Rudder	Minimum weight Half the weight for 2	Need to reach port	Emergency rudder	Weigh rudder
Mast and rigging	Minimum weight	Need to reach port	Jury rig Engine	Weigh

Table 4. Risk assessment for construction requirements

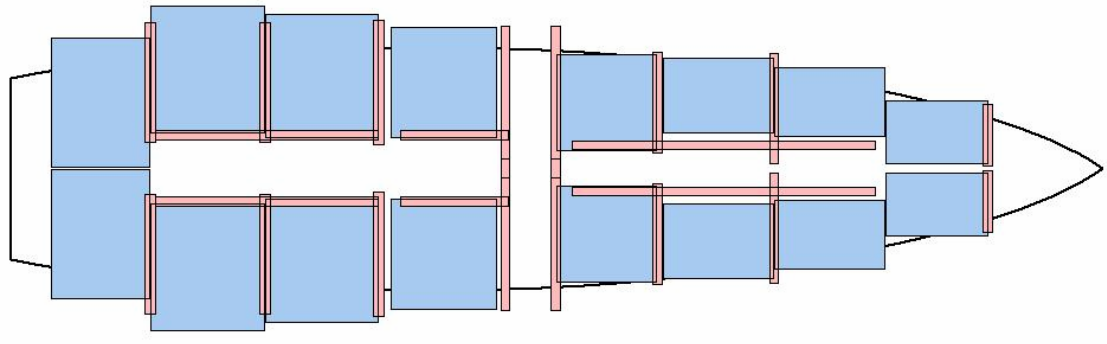

Figure 1. HullScant output showing panel layout

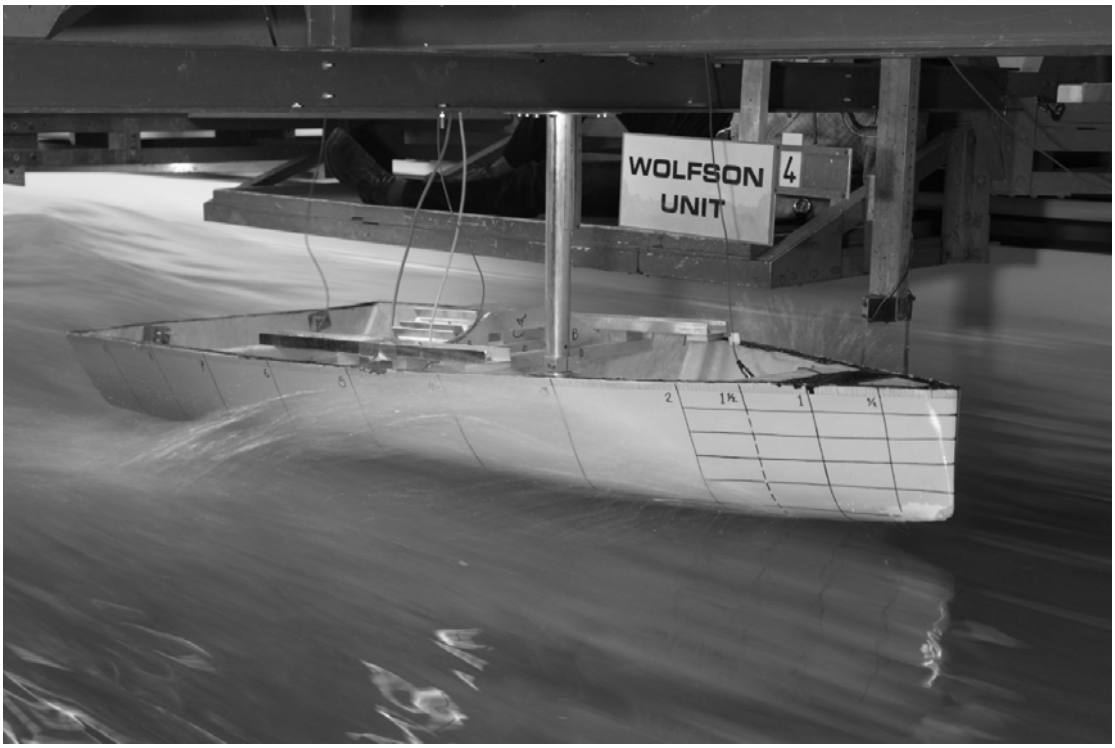

Figure 2. Model under tests in waves

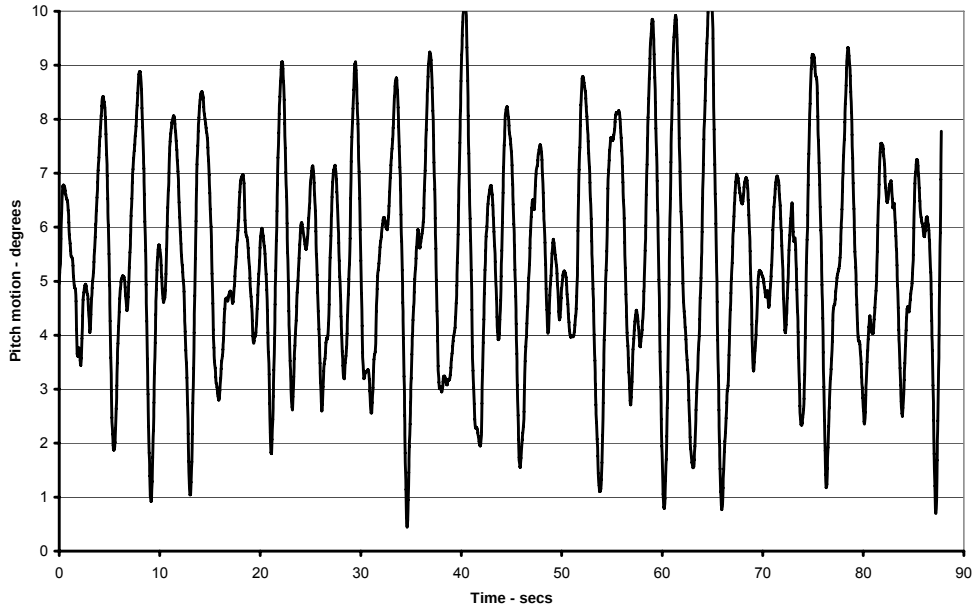

Figure 3. Pitch motion in waves

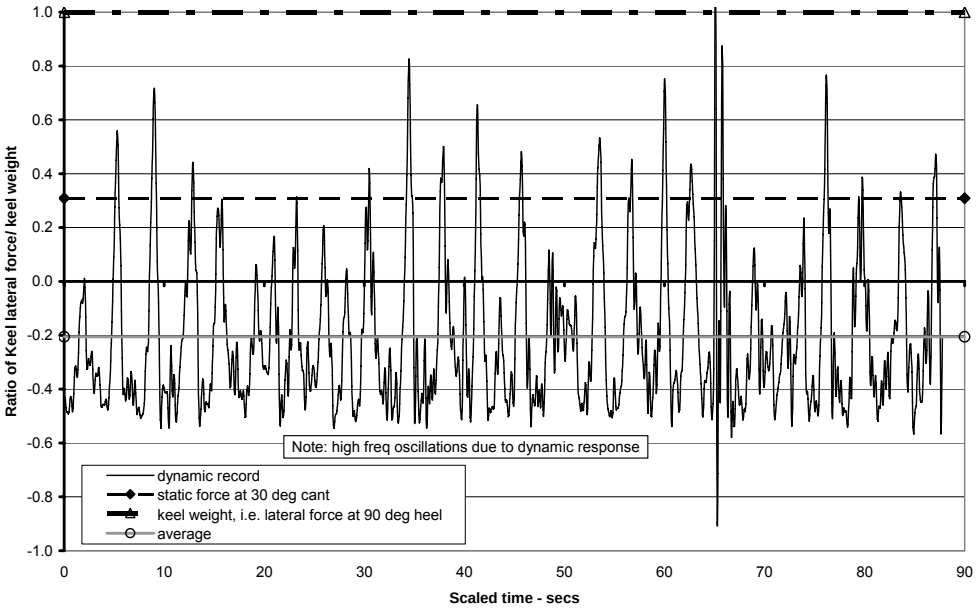

Figure 4. Corresponding keel lateral force record in irregular waves

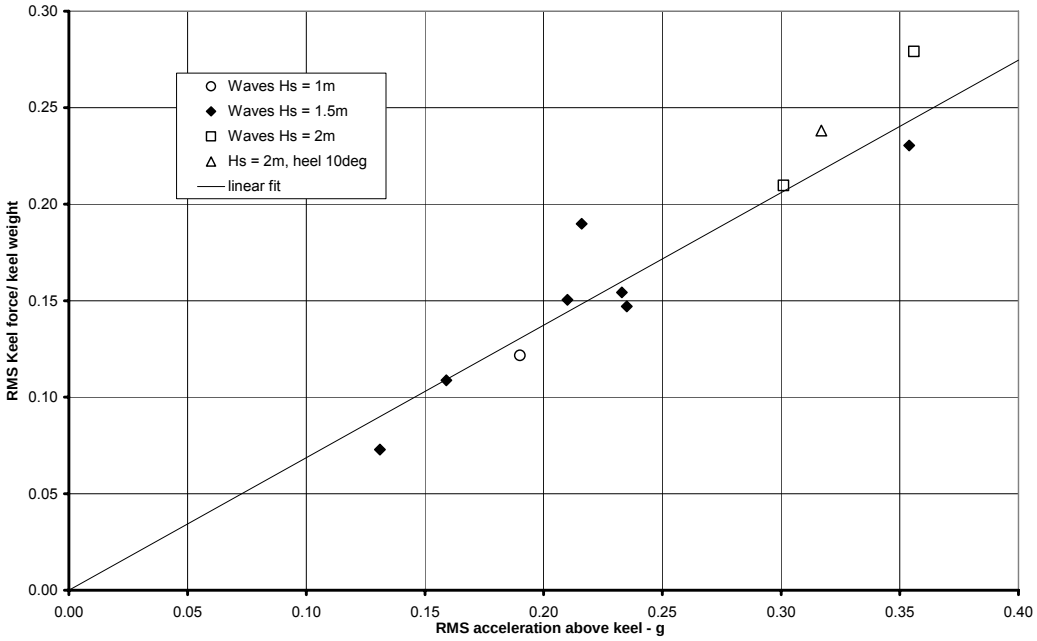

Figure 5. Variation of dynamic keel force component with acceleration for various speeds and wave periods

Session 9

Florent Maes

19th International HISWA Symposium on Yacht Design and Yacht Construction
13 and 14 November 2006, Amsterdam, The Netherlands, Amsterdam RAI Convention Centre

"An experimental study of the hydrodynamics of a yacht with a canting keel and forward rudder"

by Florent Maes

NOMENCLATURE

A_w = waterplane area at design waterline
A_{ws} = wetted surface area
C_K = canting keel
C_{K_angle} = angle of the canting keel
F_n = Froude number
F_R = forward rudder
L = lift force
L_{WL} = waterline length of canoe body
S_F = side force
T_{cb} = draft of the canoe body
T_{ck} = draft of the bulb tip
V = forward speed
V_F = vertical lift force

β = leeway angle
φ = heeling angle
ρ = density of water in the tank

1. INTRODUCTION

The canting keel was introduced in 1991. Today it is installed on most new-built offshore racing yachts and is even beginning to make an entry to the cruising yacht market. The concept uses a swinging mechanism to bring a leaden bulb to the windward side of the yacht which increases its righting moment. The increased transverse stability can then be used to enhance the performance of the boat by increasing the sail area or reducing the ballast weight. However, a sailing yacht keel is required not only to provide a righting moment but also a hydrodynamic side force balancing the aerodynamic side force generated by the sails. It is in this respect that the canting keel displays a significant drawback. By swinging the keel sideways, its lateral area is reduced which leads to a reduced side force.

In the early days of canting keel design, sailing at a higher leeway or drift angle was considered sufficient compensation for the loss of side force. Today more advanced appendage systems are being installed that are designed to decouple the production of side force from the generation of a righting moment, but very little can be found on the topic in the open literature. One such appendage configuration is the canting keel with forward rudder, otherwise referred to as CBTF™ technology.

One of the main benefits of the turning forward rudder is the fact that the side force produced is independent of the leeway angle. The optimal lift distribution on the two rudders can be determined using the biplane theory, originally developed for the aeronautical industry. This approach was first used to describe the benefits of the twin rudder configuration for a sailing yacht by Claughton et al. [1]. In the present study, tests were undertaken in a towing tank to determine whether sailing with the optimal rudder loading at several leeway angles had a significant benefit on the resistance and side force production of the yacht.

In 2004, Pavon et al. [2] conducted a brief study on the hydrodynamics of the CBTF™ configuration. They investigated the effects of the canting keel angle on the yacht's resistance and the drag reduction caused by the turning forward rudder, but a number of aspects of the subject remain unaddressed.

The starting point of the present study also involved model tests carried out in a towing tank with a view to exploring the influence of the canting keel angle on resistance, vertical lift and side force. Its purpose, in addition to obtaining this basic data, was to address a number of issues concerning the hydrodynamic performance of canting keels that have not been dealt with elsewhere in the public domain.

The canting keel contributes to all aspects of yacht resistance. As the keel angle increases, the interaction with the free surface, and hence the wave resistance, become increasingly significant. The contributions of the different components of resistance to the total resistance is one of the issues that has been considered. Swinging the keel sideways gives rise to a vertical lift component. The influence of this component on the viscous resistance has also been investigated. The addition of the forward rudder introduces further levels of complexity as interaction effects between it and the canting keel come into play. The effect of this third appendage on the resistance, vertical lift and side force characteristics has also been closely examined.

2. BACKGROUND THEORY

2.1 THE LOSS OF SIDE FORCE

When sailing at constant speed in a given direction all the forces acting on the yacht are in equilibrium. The driving force, produced by the sails balances the resistance and the aerodynamic lateral force is balanced by a hydrodynamic side force. The latter is provided by the canoe body and appendages.

In order to develop a lift force by a symmetrical keel, which plays the major role in the side force production of a conventional keel and rudder configuration, a leeway angle is needed. The analogy with aeronautical theory is direct and the keel, rudder and canoe body can be thought of as wings which need a given angle of attack (the leeway angle) to produce a corresponding lift or side force.

When a canting keel is installed the situation becomes more complex. By canting the keel, the lateral projected area is reduced which has a negative effect on the side force production because part of the total lift is now directed vertically. The situation is illustrated in Figure 1.

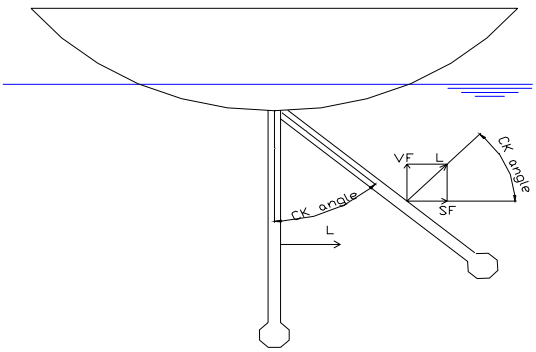

Figure 35: Force components acting on canting keel

In the configuration analysed in this paper, the loss of side force is compensated for by the forward rudder.

2.2 THE CALM WATER RESISTANCE COMPONENTS

The total calm water resistance of a sailing yacht can be written as:

$$R_T = R_V + R_W + R_H + R_I$$

R_V : viscous resistance
R_W : wave resistance
R_H : heel resistance
R_I : induced resistance

These components and their relevance to the analysed appendage configuration are now looked at in more detail.

2.2(a) The viscous resistance

This component is made up of frictional drag and the resistance caused by the pressure imbalance between the fore- and after body (3D-effect) due to viscous effects such as boundary layer development and flow separation.

The viscous resistance can be subdivided into two major components, one associated with the canoe body, and the second with the appendages. For both components the viscous resistance can be determined using:

$$R_v = (1+k)C_f \frac{1}{2}\rho V^2 A_{ws} \qquad (1)$$

where C_f is the frictional resistance coefficient of the body or appendage, determined from the ITTC '57 extrapolation line and k is the form factor, accounting for velocity augmentation and the other viscous effects apart from friction.

When the keel is canted sideways and a leeway angle is adopted, a vertical lift component is produced (figure 1). This vertical lifting reduces the wetted surface of the hull and thus the viscous and total resistance (equation (1)).

When sailing at a realistic leeway angle (4°) and canting the keel sideways, the effect of interaction between the different appendages on their viscous resistance has been assumed to be negligible compared to the influence of other drag components. This simplification appears to be borne out from the results of a CFD analysis carried out by McKee [3], who looked at 2D horizontal slices of the flow around a canting keel configuration. However, when a zero leeway angle is adopted, the effect of an increased angle of attack of the forward rudder on the downstream appendages' viscous resistance might be significant [3].

2.2(b) The wave resistance

When a body moves with forward speed at or near the free surface it generates waves that manifest themselves as drag, usually referred to as wave resistance. Not only is the hull producing wave resistance, but the addition of extra appendages will also increase the wave drag [4]. Adding a forward rudder will thus increase the wave resistance.

2.2(c) The heel resistance

The heel resistance can also be subdivided in two parts associated with the canoe body, and with the appendages. The first is caused by a change in wetted surface area and a change in the

three dimensional shape of the submerged part of the hull. These changes influence both the viscous resistance and wave resistance.
The heeling of the yacht appears to have no influence on the viscous resistance of its appendages [5]. However, the wave making drag of the appendages is strongly dependent on the heeling angle by the fact that the volume of the appendages is brought closer to the free surface. This effect, which is not related to lift production by the appendage, has been proven by experiments and has been reported by Beukelman and Keuning [6]. When the keel is canted, a submerged volume is brought even closer to the free surface and an additional change in resistance is to be expected.

2.2(d) The induced resistance

The induced resistance can be regarded as being resistance associated with the generation of lift by the hull and its appendages. The generation of waves on the free surface, caused by the low pressure zone at the windward side of the appendages when they are brought closer to the surface, is directly linked with the lift generation on these foils. On the basis of the above definition, this wave pattern will interact with the waves generated by the hull and will increase the (induced) resistance. For the present purpose, the latter part of the induced resistance defined in this way will be called the “free surface” induced resistance.

Induced resistance is more commonly associated with the induced angle of attack of a wing in a fluid flow. The induced angle of attack is a result of the downwash which is created by a lift producing foil. It should be appreciated that because of the downwash effect, the angle of attack of the appendages downstream of a lift producing foil are reduced. The angle of attack could be reduced by as much as one half [7].

As a first approximation, the canting keel with a twin rudder configuration can be regarded as a biplane, whose induced resistance Claughton et al. [1] have reported takes the form of equation (2). It should be noted that this expression ignores the interaction effects introduced by the canting keel and is only valid for ideal flows and elliptical rudder loading.

$$R_I = \frac{\frac{L_1^2}{b_1^2} + 2\sigma\frac{L_1 L_2}{b_1 b_2} + \frac{L_2^2}{b_2^2}}{4\pi\frac{\rho}{2}V^2} \qquad (2)$$

In which: L_1 is the lift produced by the forward rudder; L_2 is the lift produced by the aft rudder; b_1 is the span of the forward rudder; b_2: is the span of the aft rudder; and, σ is the interference factor.

The interference factor σ depends on the span ratio ($\frac{b_2}{b_1}$) and on $\frac{2z}{(b_1+b_2)}$, in which z is the distance between the trailing vortices of the two rudders in a direction vertical to the flow direction. This distance is also known as “the gap”. For a yacht, the gap can be approximated [1] using

$$z = s \cdot \sin(\beta - downwash\_angle) \qquad (3)$$

where s is the distance between the two rudders along the axis of symmetry and the downwash angle refers to the forward appendage

Equation (3) shows how the induced resistance can be lowered by reducing the interference between the two trailing vortices. This can be achieved by increasing the leeway angle or the distance along the centreline between the two foils and thus increasing the gap.

The theoretical optimal load distribution between two wings can be derived from equation (4):

$$\frac{L_2}{L_1} = \frac{\frac{b_2}{b_1} - \sigma}{\frac{b_1}{b_2} - \sigma} \qquad (4)$$

In theory, the induced drag of a biplane (twin rudders) should always be smaller than or equal to that of a monoplane of the same span and producing the same total lift if the load is distributed in an optimal way [1]. Since the induced resistance is quadratically dependent on the side force (equation (2)), plotting the total resistance against the side force squared for a given heeling angle and forward speed should result in a straight (R_T-S_F^2) line. Furthermore, as stated by van Oossanen [7], the induced resistance for a given speed and heeling angle is the difference between the straight line and the resistance due to heel. The resistance due to heel, therefore, can be obtained by extrapolation of the line to the point of zero side force.

A convenient method of quantifying the induced drag is provided by the effective draft principle. A higher effective draft means that a better induced resistance characteristic for a certain appendage setup is obtained. If the slope of the R_T-S_F^2 line is known, the effective draft can be determined [4] using:

$$T_e = \sqrt{\frac{1}{\left(\frac{dR}{dS_F^2}\right)\rho\pi V^2 \cos^2\varphi}} \qquad (5)$$

in which dR/dS_F^2 is the slope of the straight line on the R_T-S_F^2 graph.

3. THE EXPERIMENTS

3.1 EXPERIMENTAL FACILITIES

The towing tank used for this project is located in the School of Marine Science and Technology (MAST) at the University of Newcastle upon Tyne. It is 40 metres long, 3.75 metres wide and was filled with fresh water of 1.2 metres deep.

3.2 THE MODEL

The model hull used in the experiments was an existing conventional 1:6.4 scale model of a half tonne displacement yacht designed by Ed Dubois Naval Architects LTD.

The model was fitted with a tripwire to trigger turbulent boundary layer flow over the whole wetted surface. Its main hull dimensions are summarised in the table below:

L_{WL}:	1.129 m
T_{cb}:	0.072 m
k:	0.077 m
A_{ws}:	0.340 m^2
A_w:	0.294 m
Waterline perimeter:	2.339 m

Table 5: Model principal dimensions

The original aft model rudder was used for the experiment and has the following dimensions:

Span:	0.206 m
Tip chord:	0.051 m
Root chord:	0.079 m

Table 6: Details of aft rudder

The forward rudder was designed by one of the authors specifically for the experiment and was constructed in the MAST workshops. It consisted of a very high aspect ratio aluminium foil with a uniform NACA 0012 section profile. Its details are given in the table 3.

Span:	0.240	m
Tip chord:	0.060	m
Root chord:	0.060	m
Maximum thickness:	0.007	m

Table 7: Details of forward rudder

The position of the forward rudder on the hull was located halfway between the keel and the forward perpendicular.

A canting keel with bulb was also manufactured for the experiments. The strut of the new keel was designed with the same profile section as the forward rudder and had a span of 0.24m. At the tip of the keel strut, an aluminium bulb was fitted. It was not optimised for minimal drag but was designed to simulate a representative canting keel bulb.

4. DISCUSSION OF EXPERIMENTAL RESULTS

4.1 VERTICAL LIFT PRODUCTION BY THE CANTED KEEL

The vertical lift caused by the canting keel while sailing with a leeway angle reduces the wetted surface area of the hull and affects the viscous resistance of the yacht. The question is whether this effect has a significant influence on the total resistance.

During a test where the upright model was towed at four degrees leeway at several speeds, the change in heave motion was measured, with the keel successively at a zero and forty degree canting angles.
It was noted that at slow speeds the vertical lift force was negative (table 4). This is not expected when looking at the theory (figure 1).

Multiplying this heave difference with the value of the waterplane perimeter (table 1) allows for the calculation of the new wetted surface area to be made. The perimeter is assumed to be constant over the speed range. With the new value for the wetted surface area for different speeds, the change in viscous resistance can be determined using formula (1) in conjunction with the ITTC ’57 formula.

Fn[-]	V[m/s]	Δheave[mm]	ΔRVhull[%]
0,208	0,691	-0,07	-0,212
0,260	0,866	-0,11	0,007
0,312	1,038	0,07	0,030
0,364	1,212	0,15	-0,118
0,417	1,455	0,62	-0,161

Table 4: Relative change in viscous resistance for keel canted to forty degrees.

The change in viscous resistance when the keel is swung sideways from zero to forty degrees as a fraction of the total resistance with the non-canted keel is given for different Froude numbers in Table 4. The viscous resistance change due to vertical lift generated by the canted keel is thus smaller than 0.22% of the total resistance even for a relatively high speed. This lift effect and its influence on the viscous resistance of the yacht were therefore assumed to be negligible for any further resistance calculations.

4.2 SIDE FORCE LOSS WITH A CANTED KEEL

The model was towed with six different canting keel angles, including zero degrees, at a fixed speed (Fn = 0.364). Zero heeling and a four degree leeway angle were adopted. The forward rudder was removed.

The theoretical side force reduction for a canted keel can be determined as a fraction of the side force produced by the non - canted keel alone (figure 1):

$$\Delta SF_{theory} = \frac{SF\_onCK_{CK=angle} - SF\_onCK_{CK=0^\circ}}{SF\_onCK_{CK=0^\circ}} = \cos(CK\_angle) - 1 \qquad (6)$$

To be able to compare the experimental values with the theory, the measured change of side force is also represented by a value in percentage:

$$\Delta SF_{\exp} = \frac{SF\_total_{CK=angle} - SF\_total_{CK=0^\circ}}{SF\_total_{CK=0^\circ}} \qquad (7)$$

Thus, the experimental loss of side force is expressed as a percentage of the total side force instead of the side force on the non-canted keel alone in the theoretical case. The reason for this is that during the experiment only the total side force could be measured.

When the values for both curves are compared in the Figure 2, one must be aware that the theoretical loss is thus relatively overestimated (SF_onCK < SF_total at same speed and leeway angle).

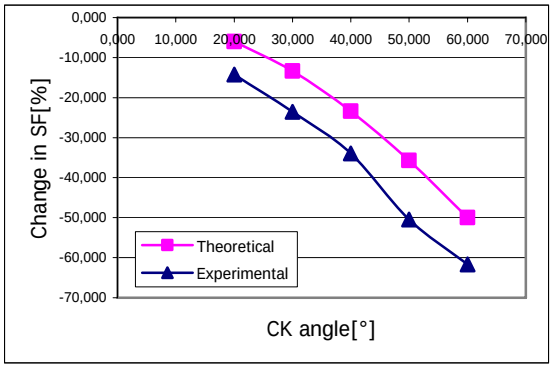

Figure 2: Change in side force as a function of the canting keel angle

Even with the theoretical loss being overestimated, the experimental values on the graph are still higher than theory predicted. This means that the side force is reduced more than theoretically expected. This result can now be considered together with the findings from the previous section, where the vertical force was found to be negative at slow speeds.
The results indicate external vertical force acting downwards on the canting keel, reducing the vertical lift and the side force. This adverse effect could be explained by a relative flow around the hull having a vertical downward component due to the negative pressure at the keel's windward side.

4.3 RESISTANCE CHANGE WITH A CANTED KEEL

The total resistance change at a four degree leeway angle between a zero and forty degree C_K angle at several speeds is given in Figure 3. The model was towed without heel for this test and the forward rudder was installed.

When the keel is canted sideways from zero to forty degrees, the heel and induced resistance are the only varying components. As was stated before, the viscous resistance change due to varying appendage interaction can be neglected at four degrees leeway. The heel resistance is augmented due to the bulb which is brought closer to the surface, as was stated in the theory chapter. The induced drag is changed in two different ways. Bringing the low pressure zone at the windward side of the keel closer to the free surface, changes the wave pattern of the free surface. The "free surface" induced drag is thus increased. On the other hand, the interaction of the trailing vortices is reduced due to a greater gap when the keel is canted. The induced resistance associated with vortex generation is thus decreasing.

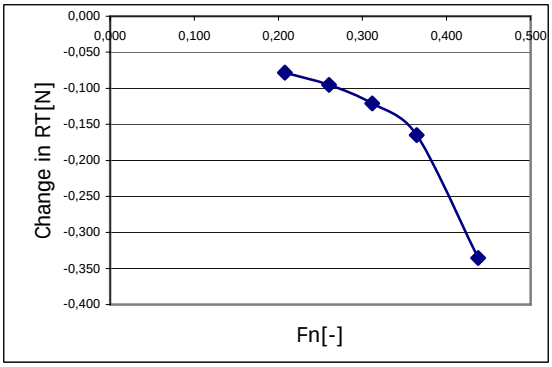

Figure 3: Change in total resistance for change of forty degree canting keel angle as a function of F_n.

Because the trend in figure 3 is negative for the whole speed range, the results indicate that the induced resistance reduction due to the trailing vortex separation is the most significant effect.

To investigate what happens to the induced resistance when the keel is canted to higher angles the upright model was towed at a fixed four degrees leeway angle, at a fixed speed, with varying canting keel angle. By subtracting the upright resistance (total resistance with zero heeling, leeway and canting keel angle) from the measured total resistance, the induced resistance can be calculated for this specific speed (bearing in mind that the induced resistance was defined as the resistance components associated with the production of lift). For this theory to valid, the increase in heel resistance, due to the keel which is brought closer to the free surface, has to be neglected. This is reasonable on the basis of Figure 3, which shows that for a forty degree canting angle the change in induced resistance components are dominant. The results of this calculation are shown in Figure 6.

It is clear that the induced resistance is reducing with increasing canting keel angle. The total lift produced by the canting keel strut and thus the induced resistance due to vortex generation remains constant when the keel is canted. This could not be the reason for the drag reduction.

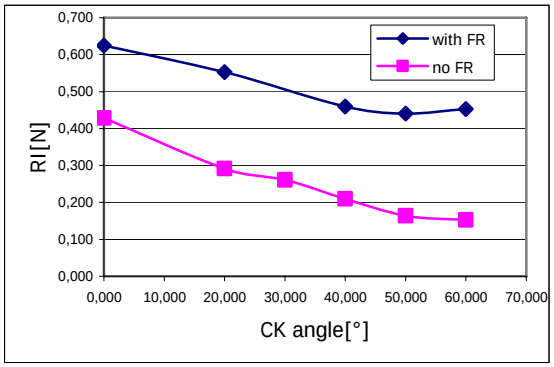

Figure 4: Variation of induced resistance as a function of the canting keel angle.

Because the trend is also negative without the forward rudder attached, downwash effects between the forward appendage and the keel can't be the reason either. The only explanation left for the negative trends is the increasing vertical distance between the trailing vortices with increasing canting keel angle. The resulting drag reduction is much more significant than the increase in "free surface" induced drag due to bringing the keel to higher angles.

When analysing the Figure 4, one can see that the curve levels off from a certain canting angle onwards. This effect could be explained by the increase of the "free surface" induced resistance when the low pressure system is brought closer to the free surface at higher canting angles.

4.4 INFLUENCE OF THE FORWARD RUDDER

It is interesting to examine table 5 for the upright model at four degrees leeway with different canting keel angles with and without forward rudder at a fixed speed (Fn=0,364).

CKangle[°]	Δheave with FR[mm]	Δheave no FR[mm]
20,000	0,4	0,559
30,000	x	0,601
40,000	0,2	0,501
50,000	1,1	0,484
60,000	0,0	0,247

Table 5: Heave change with and without FR fro different CK angles

All the values of the change in heave relative to the upright case are higher without the forward rudder installed than with it. These results indicate that a forward rudder generate a vertical force acting downwards. Because the canting keel is working in the forward rudder's downwash, the angle of attack of the flow on the canting strut is reduced. This results in a smaller total lift on this appendage.

Because the canting keel is the only upward lift producer, the forward rudder has a negative effect on the heave motion.

To analyse the interaction effects of the forward rudder in more detail it is useful to plot the reduction of side force when the keel is canted relative to the upright case both with and without the forward rudder. The same test setup was used that led to the values in table 5 and the results are displayed in Figure 5.

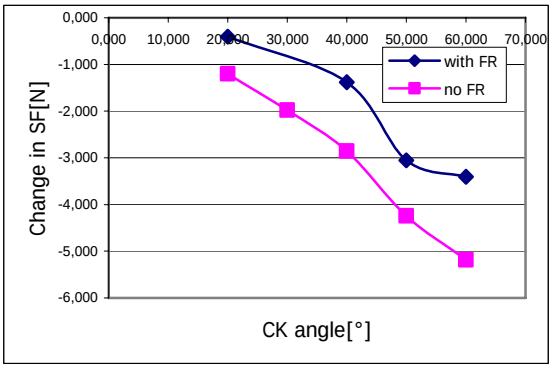

Figure 5: Change in side force as a function of canting keel angle

When the keel is canted sideways, the loss of side force should in theory be equal for both cases if there were no interaction effects, but this is not reflected in the two experimental curves. The results indicate that the difference is due to the changing interference between the forward rudder and the canting keel.
When the keel is swung sideways from zero to twenty degrees for example, the side force drops less when the forward rudder is fitted. The same is true for higher canting angles.

This situation could be explained by the downwash effect of the forward rudder, reducing the angle of attack of the canting strut, which is less significant at higher canting angles. This way the angle of attack would slowly increase compared to the zero canting angle case, generating a greater total lift and thus side force.

Looking back at the graph in Figure 4 it should be appreciated that the two curves seem to diverge at the higher canting keel angles. They both level off, but with the forward rudder the

curve does so more. This trend could also be explained by downwash effects. A relative increase in the angle of attack of the canting strut at higher canting angles when a forward rudder is fitted increases the lift and thus the induced resistance.

4.5 A BROADER PICTURE: RESISTANCE VERSUS SIDE FORCE

In this section the effects of the canting keel and forward rudder on resistance, side force and heave motion, which have so far been discussed separately, will be considered in combination. To compare different appendage setups the effective draft principle (equation (5)) has been used together with total resistance versus side force squared plots.

The effective draft ratio for a test where the speed of the upright yacht was fixed (Fn = 0.364), the leeway angle constant (4 degrees) and the forward rudder fitted, is given below. The maximum draft ($T = T_{cb} + T_{ck}$) is constant and equals 0.334m. For the calculation of the effective draft, equation (5) can be rewritten as:

$$T_e = \sqrt{\frac{SF^2}{R_I \rho \pi V^2 \cos^2 \varphi}} \qquad (8)$$

in which R_I is the induced resistance calculated by subtracting the upright resistance from the measured total resistance.

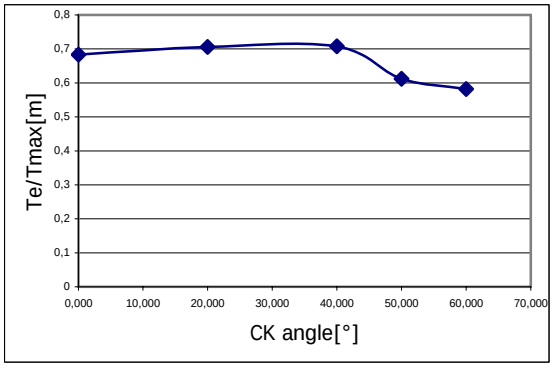

Figure 6: Variation of effective draft to maximum draft as a function of canting keel angle.

When the keel is canted up to forty degrees, the induced resistance for a given amount of produced side force is lower than in the upright case. Canting the keel to higher angles shows an adverse effect. At higher canting angles the assumed external force reduces the side force significantly and the reduction of induced resistance levels off, as discussed previously. Thus, sailing with a canting angle greater than forty degrees, for this model at Fn = 0.365 and four degrees leeway leads to a significantly sub-optimal performance.

4.7 SIDE FORCE PRODUCTION BY THE TWO RUDDERS AND CANTING KEEL

A major benefit of the forward rudder configuration is the fact that lift production is independent of leeway.

In the configuration considered, the canting keel was installed and canted sideways over forty degrees to represent a realistic sailing condition. With this third appendage, the biplane theory is assumed to be still applicable, although errors will be introduced due to extra interference effects.

The conventional keel case, plotted on the R_T-S_F^2 graph for the purposes of comparison, have been calculated by generating all the required side force through leeway without the canting keel and leaving the rudders unturned. It should be kept in mind that the drag for an equal amount of side force is higher for a real monoplane because splitting the lift over more than one appendage reduces the induced resistance.

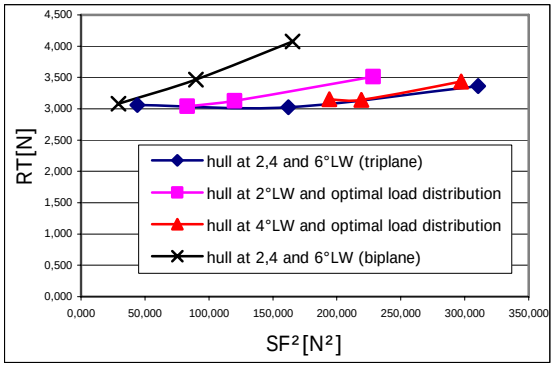

Figure 7: R_T-S_F^2 curves for the different configurations with the canting keel included.

The results show that there is a significant drag reduction for an equal amount of produced side force when the rudders are turned compared to the conventional keel setup (biplane vs hull at 2 and 4° leeway). There is also a significant induced drag reduction when the biplane is compared with the triplane case. This is due to the distribution of the total lift over three instead of two appendages.

It can also be seen that there is a significant difference between the resistance curves for the two and four degree leeway case.
The results show that from a pure resistance point of view it is better to choose a greater leeway angle and to get more trailing vortex separation.

For practical purposes, a trade off should be made between sailing at a higher leeway angle with less drag, and sailing with a more optimal course and hence resistance surplus at a smaller drift angle.

5. CONCLUSIONS

A number of conclusions relating to the hydrodynamic performance of a canting keel in the presence of a forward rudder can be drawn from the data generated by the experiments set in the context of biplane theory and using the effective draft concept.

Sailing at a realistic leeway angle and forward speed and canting the keel sideways reduces the induced and total resistance.

When the keel is swung to higher angles at a realistic drift angle, the side force and vertical lift force are found to decrease more rapidly than might be expected from theoretical considerations. This could be explained by a downward acting force generated by the relative flow around the hull due to the negative pressure at the keel's windward side.

The hydrodynamic characteristics of the canting keel and forward rudder configuration, with respect to the side force and resistance generated, are such that there is an optimal canting keel angle for a given speed and leeway angle.

The addition of a forward rudder to the canting keel configuration introduces severe interaction effects. The downwash of the forward appendage causes a reduction of the angle of attack of the appendages downstream. This interference effect between the forward rudder and canting keel is reduced with increasing canting keel angle.

A more realistic situation, with the canting keel at forty degrees to windward and the rudders optimally loaded using the biplane theory, was also tested. In this case it was also found that having the rudders at their optimal angles of attack had a major drag benefit over the fixed, conventional keel case.

In reality, the situation is more complex because the rudders ought to balance the yacht as well. In many cases it might thus not be possible to achieve the optimal rudder load distribution.

6. REFERENCES

[1.] CLAUGHTON, A., OLIVER, C., Design considerations for canting keels, *The International HISWA Symposium on Yacht Design and Yacht Construction*, 2004

[2] PAVON,C.L., RODRIGUEZ,R.Z., AND ROJAS,L.P., Hydrodynamic study of a canting keel based appendage configuration, *Simposio Internacional de diseno y produccion de yates de motor y Vela*, 2004

[3] MCKEE, C., A CFD Analysis of a Canting Keel Forward Rudder Configuration, *MEng thesis, University of Newcastle upon Tyne*, 2006

[4] CLAUGHTON, WELLICOME, SHENOI, Sailing yacht design; theory, *Addison Wesley Longman Limited*, 1998

[5] KEUNING, J.A., SONNENBERG,U.B., Approximation of the Calm Water Resistance on a Sailing Yacht Based on the Delft Systematic Yacht Hull Series, *14th Chesapeake Sailing Yacht Symposium, SNAME,* 1999

[6] BEUKELMAN,W., KEUNING,J.A., The influence of Fin Keel Sweep-back on the Performance of Sailing Yachts, *5th HISWA Symposium,* 1975, Amsterdam

[7] VAN OOSSANEN, P., Predicting the speed of sailing yachts, SNAME Transactions vol. 101, pp. 337-397, 1993

Session 10

Jan Alexander Keuning

"Keel – Rudder Interaction on a Sailing Yacht"

by:

J. A. Keuning, M. Katgert and K. J. Vermeulen
Delft University of Technology, Shiphydromechanics Department

1 Introduction

In their earlier publications on "the yaw balance of sailing yachts" (Keuning and Vermeulen, Ref [1] 2003) and "the mathematical model for the maneuvering of a sailing yacht" (De Ridder, Keuning and Vermeulen, Ref [2] 2005) an assessment method has been presented for determining the force distribution in yaw and sway over the hull, keel and rudder. In Ref [1] it was used to deal with the yaw balance of a sailing yacht on a straight course and in Ref [2] the similar approach was used to determine the necessary forces and moments on a maneuvering sailing yacht.
In this assessment method use was made of what is called: the Extended Keel Method (EKM) as introduced by Gerritsma in 1971, Ref [3] for calculating the side force on the keel and rudder (and hull) of a sailing yacht.
This EKM yielded very good results for the total side force of the hull, keel and rudder together in the upright condition, indicating that the mayor part of the side force is produced by the appendages, in particular for boats with average to high aspect ratio keels and rudders. In assessing the yaw moment it turned out that the canoe body of the hull has a significant contribution not accounted for with the EKM. A modified approach to the correction method as introduced by Nomoto in 1975, Ref [4] yields good results for the yaw moment as well.
In the calculation procedure used for the yaw moment the side force of the keel and the side force on the rudder with their respective distances to the Center of Gravity play an important role. So the actual side force distribution between the keel and the rudder is of significant importance in assessing the yaw moment. This distribution however is strongly influenced by the underlying assumptions made in the EKM on the influence of the keel on the rudder. This influence makes itself felt through:

- a reduction in "free stream" velocity of the incoming fluid on the rudder (since it operates in the wake of the keel) and
- a reduction of the effective angle of attack on the rudder through the vorticity shed off by the keel caused by the lift generated on the keel, i.e. the down wash.

In order to account for the effect of the keel on the rudder a correction of the effective angle of attack on the rudder of 50% of the leeway angle was suggested by Gerritsma as well as a reduction of the velocity by 10%. Overall this yields a reduction of the side force on the rudder by some 60%.Other formulations as those formulated by S F Hoerner, Ref [5] have also been used.
It was felt however that some more information on the downwash angle was asked for. In particular more information on the influence of the aspect ratio of the keel and the rudder on this downwash was needed because Gerritsma's approach does not account for different aspect ratios.
So it was decided to carry out a series of dedicated experiments to determine the down wash angle of a series of different keels on one particular rudder. To be able to "blend" these results into a larger database it was decided to make use of one of the models of the Delft Systematic Keel Series (DSKS) as well as three of the keels used in that series. This procedure also allowed for the re-evaluation of the expressions presented in the past on keel residuary resistance and side force production of a sailing boat.
The results will be presented in this paper.

2 The approach

The approach that has been followed in the present study is as follows.
A sailing yacht model has been equipped with a keel and a rudder, which are both connected to the model by means of separate dynamometers. The rudder was connected in such a way that a positive and negative rudder angle could be applied. The model as a whole could be heeled, trimmed, heaved and yawed.
By taking measurements with a series of yaw (leeway) angles applied to the model the side force on the keel could be varied. At each yaw angle the rudder angle has been varied with 10 different rudder angles from 15 degrees to starboard till 15 degrees to port. This whole series of conditions has been repeated with 0 and 15 degrees of heel applied to the model. This procedure in the end has been repeated with all different keels.
By interpolation between the tests the rudder angle, at which the side force on the rudder is equal to zero has been determined and comparing this with the leeway angle of the model as a whole, the downwash angle on the rudder could be determined. It should be noted that this downwash angle is therefore the “averaged” downwash angle over the entire rudder span.

3 The Measurements

3.1 The model

The model which has been used for the measurements, is hull number # 366, which is a lower beam/draft ratio version of parent hull # 329, a 1992 vintage America’s Cup class model. The lines plan of this hull is presented in figure 2.1.

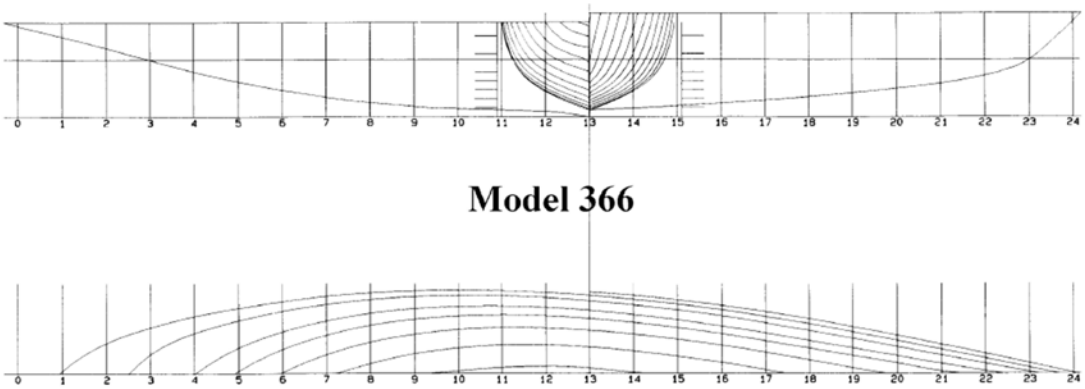

Figure 1: Lines plan of the model hull #366 used for the experiments

Four different keels have been used for this study, varying in aspect ratio and thickness/chord ratio. These keels are denoted #1, #3, #4 and #5. The principal dimensions are presented in Table 1 and the lateral views of the keels can be found in Figure 2. Furthermore one rudder, of which the principal dimensions are also presented in Table 1, has been used for the measurements.

			Keel 1	Keel 3	Keel 4	Keel 5	Rudder
Lateral Area	A_{lat}	[m2]	0.086	0.086	0.086	0.086	0.066
Wetted Area	S	[m2]	0.176	0.177	0.189	0.177	0.321
Aspect Ratio	AR	[−]	1.623	0.696	0.696	3.769	0.115
Span	b	[m]	0.374	0.245	0.245	0.57	0.321
Mean chord	c_{mean}	[m]	0.231	0.352	0.352	0.15125	0.115
Sweepback angle	Λ	[◦]	9.85	14.42	14.42	3	18
Volume	□k	[m3]	0.00155	0.0016	0.00305	0.000853	
Thickness/chord ratio	t/c	[−]	0.1	0.066	0.15	0.1	

Table 1: Main particulars of the various keels and the rudder

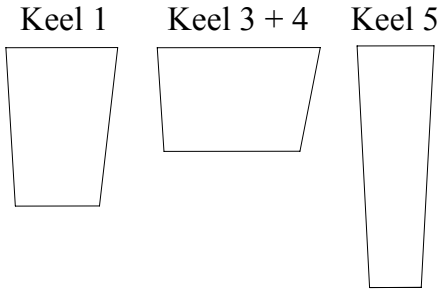

Figure 2: Lateral plan view of the four keels used in the experiment.

3.2 The Measurement Setup

The tests have been carried out in the #1 towing tank of the Delft Shiphydromechanics Laboratory. This tank has a length of 145 meter, a width of 4.5 meter and a maximum attainable water depth of 2.5 meter. The model has been fitted to the towing carriage by means of the so called 'Hexamove'. This is a hydraulic activated system capable of controlling the positioning and movement of the model in 6 degrees of freedom. This system was used for the sake of absolute controllability of the model during the tests and it guaranteed that during each comparable test condition (with the different keels) the attitude of the model in the water with respect to sinkage, trim, heel and leeway was always exactly the same. For every run, the model was heeled and yawed as required. The sinkage and trim values were taken from earlier measurements carried out with the same model and were as reported by R. Meulemans, Ref [6] and B.J.B. Binkhorst, Ref [7].
The forces and moments on the hull, the keel and the rudder were measured by means of a set of five 6 DOF dynamometers: three fixed to the hull, one for the keel and one for the rudder. Keel and rudder were attached to their respective dynamometer in such a way, that all the forces and moments on these appendages were absorbed only by the dynamometer, and not by the hull.
During the tests the following quantities were measured:

- Forward speed of the model
- The position of the model in surge, sway, heave, roll, pitch and yaw
- The forces and moments in x, y and z-direction of the 5 pick-ups

The reference coordinate system is as shown in Figure 3, in which:
β = Leeway angle
φ = Heel angle
θ = Trim angle
δ = Rudder angle

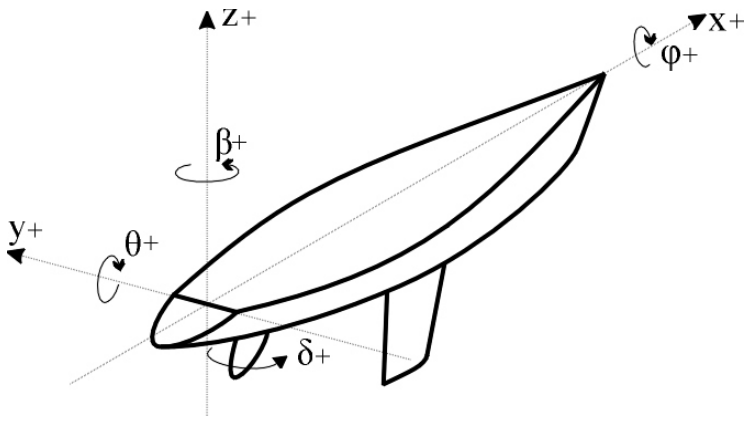

Figure 3: Coordinate system used during the experiments.

3.3 The Measurement Program

An identical series of tests (with respect to forward speed, rudder angle and leeway angle) has been carried out with the model equipped with each of the four different keels. The rudder was present in all tests.
A series of additional runs has also been carried out with the model without any keel but with only the rudder fitted. The tests have been carried out with the model both in the upright condition and in the heeled condition (15 degrees), as mentioned before. So the following tests were carried out:

- **Upright condition**
  Used for the determination of the total resistance of the hull and four different keels in a large speed range. The residual resistance of the appendages has been determined in this upright condition in the speed range from Fn.= 0.10 up to Fn.= 0.60.
- **Leeway without rudder angle**
  For three forward speeds (Fn.= 0.27, = 0.35 and = 0.38) and four leeway angles (-3°, +3°, +6° and +9°) tests have been carried out with heel φ = 0° and φ = 15° with a fixed rudder angle δ=0°.
- **Leeway with varying rudder angle**
  For one speed (Fn.= 0.35) and four leeway angles (-3°, +3°, +6° and +9°) tests have been carried out with rudder angles varying between δ = -15° to δ = +15° with heel angle φ = 0° and φ = 15°.
- **Rudder performance**
  To measure the rudder performance on its own without the presence of the keel, tests have been carried out without keel at one speed (Fn. = 0.35) with varying rudder angles between 5° and 20°.

3.4 The Elaboration Procedure

During the tests the model and the keels and rudder were fitted with carborundum strips for turbulence stimulation according to the standard procedure of the Delft Shiphydromechanics Laboratory. On the hull three strips have been used which were 40 mm. wide. On the keel and rudder one single strip was placed at roughly 5% of the chord length from the leading edge of the profile. On the keel the strip was 30 mm and on the rudder 20 mm wide. The added resistance from these turbulence strips was corrected for by carrying out all upright resistance tests twice: once with half width of the strips and once with full width strips. The difference between these two measurements was used to determine the specific resistance of the turbulence strips. The model resistance was then calculated by subtracting the strip resistance from the measured total resistance.

4 The Results

4.1 Keel resistance

To determine the residual resistance of the appendages, the viscous resistance of the appendages has to be known. This is acquired by calculating the frictional resistance coefficient of both keel and rudder according to the ITTC '57 formulation and using the form factor of the appendages as expressed by the empirical formulations as given by Hoerner, Ref [5]:

$$(1+k)_{hoerner} = 1 + 2 \cdot \left(\frac{t}{c}\right) + 60 \cdot \left(\frac{t}{c}\right)^4$$

The added fin tip drag coefficient is calculated using the following expression:

$$C_{Dv,\text{fintip}} = 0.01875 \cdot \left(\frac{t}{c}\right)^2_{tip}$$

The residual resistance of the appendages is then acquired by subtracting these components from the total measured appendage resistance, i.e. :

$$R_{res} = \left(C_t - C_f \cdot (1+k) - C_{Dv,\text{fintip}}\right) \cdot \tfrac{1}{2} \rho V^2 S$$

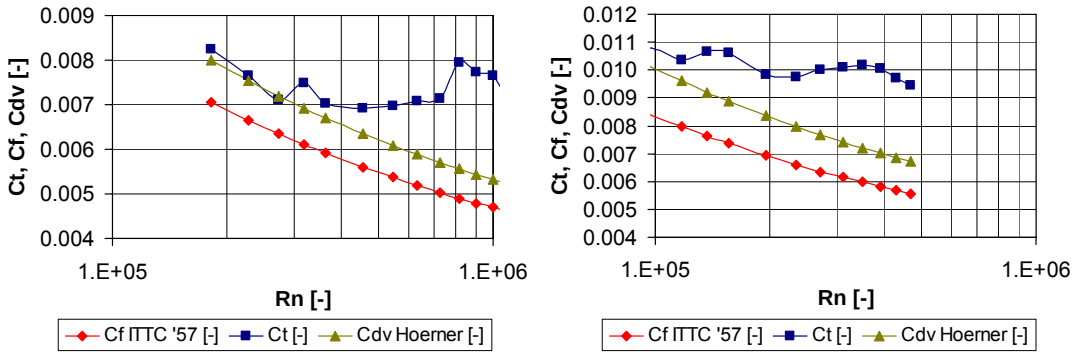

Figure 4: Resistance coefficients keel 3 (left) and keel 5 (right)

As an example of these resistance coefficients the results for keel 3 and 5 are presented in Figure 4. In this figure *Cdv Hoerner* is the added viscous drag of the fin tip together with the viscous drag of the keel, or:

$$C_{DvHoerner} = C_f \cdot (1+k) + C_{Dv,\text{fintip}}$$

Just as in the previous publications by Binkhorst, Ref [7], the existence of a residuary resistance component in the upright keel (appendage) resistance is evident from these results. It shows in the plots as an abrupt (upwards) deviation of the total resistance coefficient of the appendage from the viscous coefficients with increasing forward speed. This trend proved to be true for all the four different keels tested, albeit to different extents.

The measured total resistance of the keels is used to determine the residual resistance of the appendages. The research carried out by B. J. Binkhorst, Ref [7], showed a clear relationship between the distance of the vertical center of buoyancy of the keel volume from the free surface (Z_{cbk}) and the magnitude of this residual resistance of the keel. A larger distance from the free surface yields a higher residual resistance. The current measurement data has been used to further check and verify this trend.
In Figure 5 the results for all 4 keels are presented of this "specific residual resistance" versus the "relative depth of the center of buoyancy of the keel volume". The aforementioned trend as formulated by Binkhorst in Ref [7] is clearly also present in the present measurements, i.e. the residuary resistance increases with increasing separation between the center of buoyancy of the keel volume to the free surface. The increase however appears to be less pronounced for the larger distances.

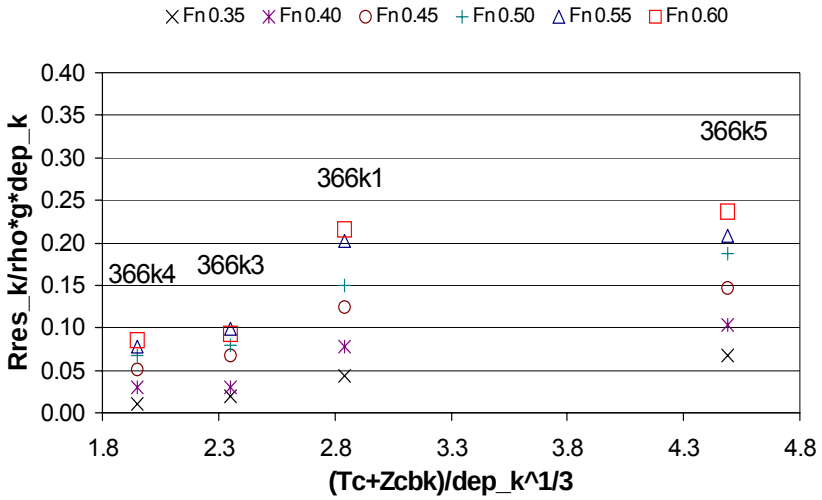

Figure 5: Residuary Resistance of the keels as function of immersed volume depth

4.2 The Rudder Resistance and "Keel Wake" or "Velocity Reduction Factor"

The resistance data of the rudder has been used to calculate the residual resistance of the rudder as with the keels. In addition to this, the measured data has been used to asses the free flow velocity reduction over the rudder.
Gerritsma, Ref [3], measured this reduction of the free flow velocity in the rudder plane due to the presence of the keel in the zero leeway and upright condition. He found a 'free flow velocity reduction' of some 10% when compared with the undisturbed free flow velocity. With the present measured data these values may now be verified.

Both the resistance of the rudder in free flow without the presence of the keel in front of it and the resistance of the rudder in the wake of all the four different keels has been measured. By relating the resistance measured behind a keel to the resistance of the rudder measured with no keel present a "change" in resistance could be determined. This "change" has to be attributed to the influence of the wake of the keel on the rudder.
In Figure 6 this "change in the measured rudder resistance" in the upright condition without leeway due to the presence of the keel in front of it is presented for all four different keels.
Although some scatter exists it appears that in general a fraction of $\frac{Rr_{wake}}{Rr_{free}} \approx 0.9$ may be found.
This implies a free flow velocity reduction fraction $\frac{V_{wake}}{V_0} \approx 0.95$, assuming that the rudder residual resistance has been subtracted and the viscous resistance, by nature, is grossly dependent on the flow velocity squared. If considered in more detail however there appears to be a significant forward speed influence with a peak in the Froude numbers which come close to the so called "hull speed". This may imply that other effects such as wave generation may also play a role.
However, when the boat has a small leeway angle this "change" in resistance or resistance reduction (and thus the velocity reduction) becomes much smaller or even almost zero. This may be seen from the results as presented in Figure 7 in which the same fraction as in Figure 6 is presented but now with the boat yawed from 3 to 9 degrees. For the larger leeway angles the reduction fraction becomes very close to 1.0.
This implies that in normal sailing conditions the flow velocity over the rudder will not be influenced too much by the presence of the keel.

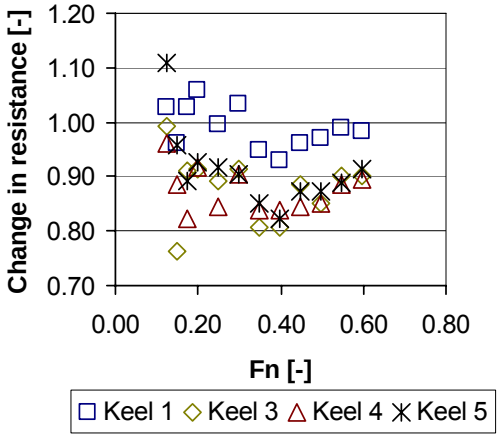

Figure 6: Change in rudder resistance in the upright condition without leeway angle

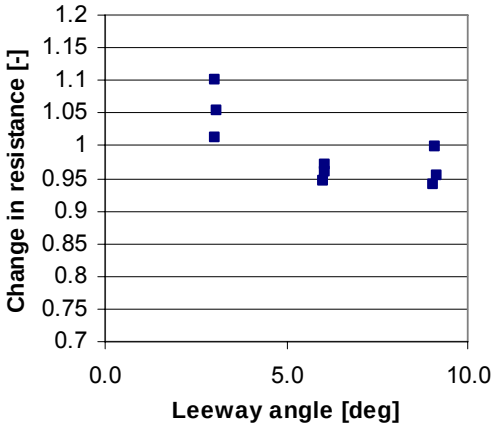

Figure 7: Change in rudder resistance in the upright condition for keel 3 with leeway angle

4.3 The Downwash Angle or Rudder Lift

The keel has another effect on the performance of the rudder as well: the downwash. Keel downwash will cause a change in the effective angle of attack of the rudder. The magnitude of this downwash has been determined by the procedure described in the "approach chapter": i.e. tests have been carried out with the hull in yawed condition, while the rudder angle has been varied. The lift generated by the rudder can then be plotted against the rudder angle δ. The difference between the leeway angle β and the rudder angle at which rudder lift becomes zero δ_0 maybe considered to be equal to the averaged downwash angle Φ. In formula (see Figure 8):

$$\Phi = \beta + \delta_0$$

In Figure 9 the lift curve of the rudder as function of the rudder angle when placed behind the keel, in this figure it is keel #1, is presented for various leeway angles.
This procedure has been applied for all four keels and for both the upright and the heeled condition applied during the tests. For all four keels the downwash angle has been determined.
The resulting downwash angles as a function of the leeway angle and thus of the loading on the keels, are depicted for the four different keel in Figure 10 and Figure 11.
The influence of the aspect ratio of the keel on the downwash on the rudder is obvious from these results. The higher aspect ratio keels, i.e. #1 and #5, produce the least downwash. In general the assumption that the downwash is half the leeway seems only valid for the lower aspect ratio keels, i.e. the keels #3 and #4. What is also evident from these results is that the absolute magnitude of the downwash angle related to the leeway angle on the keel diminishes with increasing leeway angle. This may be due to the fact that at the higher leeway angles the flow is relatively more diverted past the rudder in those conditions. It should be remembered that the separation between the keels and the rudder on this particular model is reasonably large for all the keels tested. It would therefore be of interest to gather some additional experimental results from lower aspect keels and smaller keel-rudder separations also.

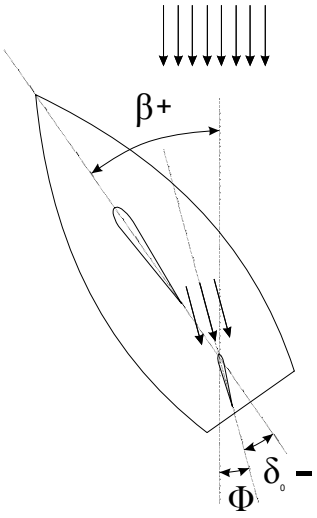

Figure 8: Determination of the downwash angle Φ

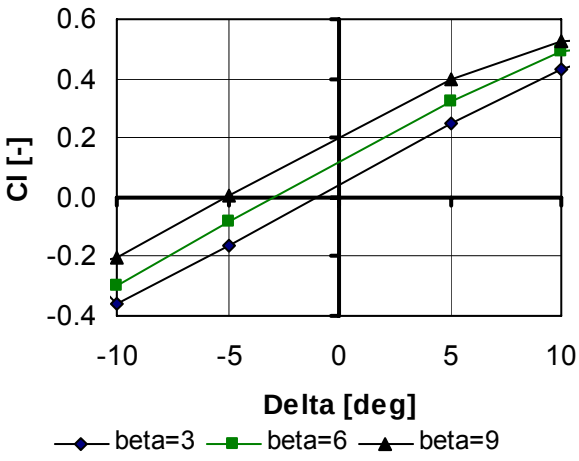

Figure 9: Lift curve of the rudder behind keel #1 for various leeway angles at heel = 0°

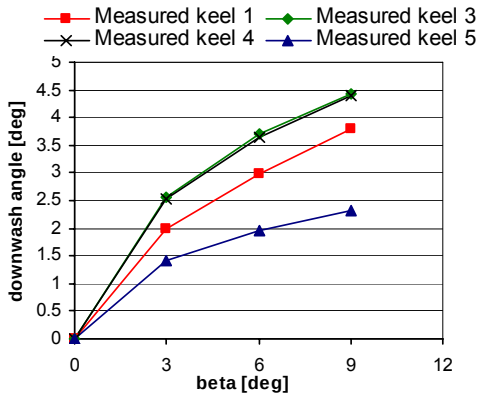

Figure 10: Downwash angle versus leeway angle for heel = 0°

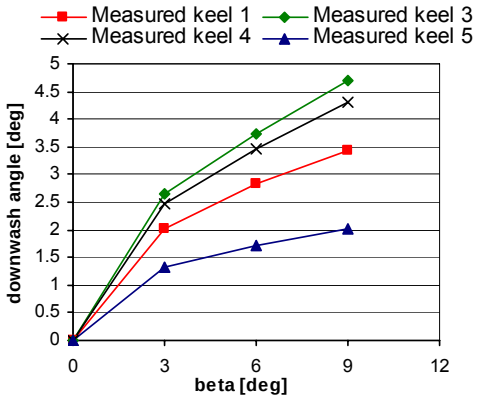

Figure 11: Downwash angle versus leeway angle for heel = 15°

4.4 The Free Flow Velocity Reduction over the Rudder Due to the Hull Presence

The measured lift on the rudder has been compared with the available theoretical predictions for the lift. To this aim use has been made of the well known formulations as presented by Whicker and Fehlner, Ref [8] for the lift curve slope, i.e.:

$$\frac{dC_L}{d\beta} = \frac{5.7 \cdot ARe}{1.8 + \cos\Lambda\sqrt{\frac{ARe^2}{\cos^4\Lambda} + 4}}$$

in which:

$\frac{dC_L}{d\beta}$ = Lift curve slope

ARe = Effective Aspect Ratio = 2 * Geometric Aspect Ratio for the keel and rudder

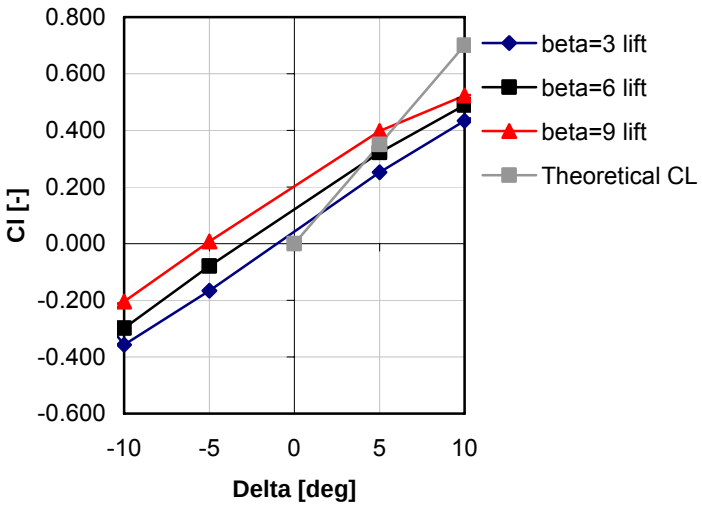

Figure 12: Theoretical lift coefficient curve of the rudder versus the measured one

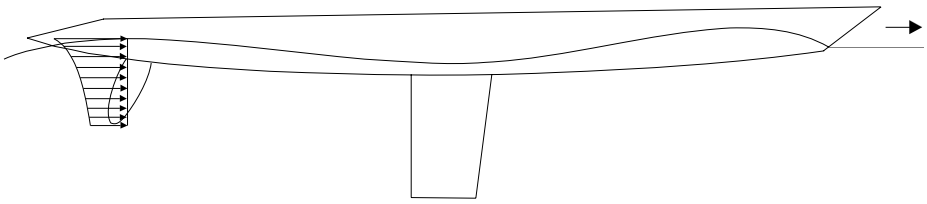

Figure 13: Wave generated velocity component near rudder

In Figure 12 the theoretical derived lift coefficient of the rudder is presented together with the lift coefficients as derived from the measured lift results. There is an apparent deviation between these lift coefficients. A possible explanation for this difference may be found in the difference between the supposed water flow velocity in the rudder plane (as used to calculate the measured lift coefficient) and the actual flow velocity. If this difference really exists, this supposed water velocity appears to be taken too high.
Different from the earlier analysis about the free flow reduction factor this speed difference can not be caused by the wake of the keel. This is so because the results of the lift on the rudder are compared in absence of the keel. The only constant factor in all these measurements on the rudder forces (both with and without the keel present) is the presence of the hull. So the difference should originate from the hull's presence. This leads to the wave system generated by the hull. The orbital velocity of the stern wave generated by the hull generates a velocity component opposite to the boat's forward direction and leads to a reduction of the free flow velocity also. If the properties of this bow wave are known, this velocity component could be calculated using regular deep water wave theory to assess the validity of this assumption.
Using the results as obtained by K. Audenaert in the framework of his master's thesis research, the wave height at the required speed is known; in addition the wave crest is visually confirmed to be at the rudder position. The wave length follows from the boat speed.

For the horizontal orbital velocity in the wave crest the formulation is:

$$u = \zeta \frac{g}{c} e^{kz}$$

in which:

ζ	=	wave amplitude
g	=	9,81 m/s^2
c	=	wave speed (here equal to the boat speed)
k	=	wave number = $\frac{2\pi}{\lambda}$
λ	=	wave length
z	=	distance from (below) the free surface

Calculating this horizontal velocity for the tip and the root of the rudder and subsequently integrating this velocity over the depth (span) of the rudder yields a mean velocity reduction in the rudder plane of some 20%. The reduction of the velocity required to fit the measured lift curve slope to the theoretical lift curve slope is 22%.

The orbital velocity in the stern wave may therefore very well be the cause of the decrease in rudder performance. It should be noticed that this velocity reduction determined for these calculations is only valid for this particular hull.

5 Downwash formulations

Hoerner, Ref [5] presented a formulation for the angle of downwash behind an arbitrary wing:

$$\Phi = \frac{1.6 \cdot C_L}{\pi \cdot A\mathrm{Re}_k}$$

This formulation has been compared with the present measurements. This comparison is presented in Figure 14. This comparison revealed a significant difference between measured and calculated values.

.

Regression analysis of the new data as presented in the Figures 10 and 11 has therefore been applied to yield new formulations for the downwash angle for an arbitrary keel. Important parameters for the magnitude of this downwash angle are the lift coefficient and the aspect ratio of the keel. Another variable which has been assessed also in the present measurements is the thickness/chord length ratio of sections of the keel. This variable however also makes itself felt in the loading or the lift coefficient of the keel so it has been implicitly incorporated in the formulation.

The following formulation for the total downwash angle yielded the best fit trough the available data:

$$\Phi = a_0 \cdot \sqrt{\frac{C_{Lk}}{A\mathrm{Re}_k}}$$

with:

φ	0 °	15 °
a_0	0.136	0.137

The fit of this regression formulation through the original measured data is presented in the Figure 15 and 16.

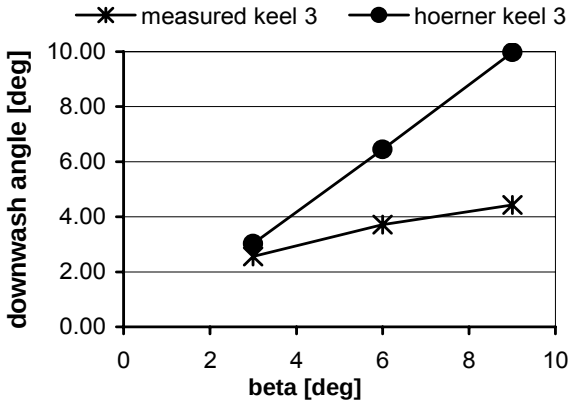

Figure 14: Downwash angle for keel #3 measured and calculated with Hoerner

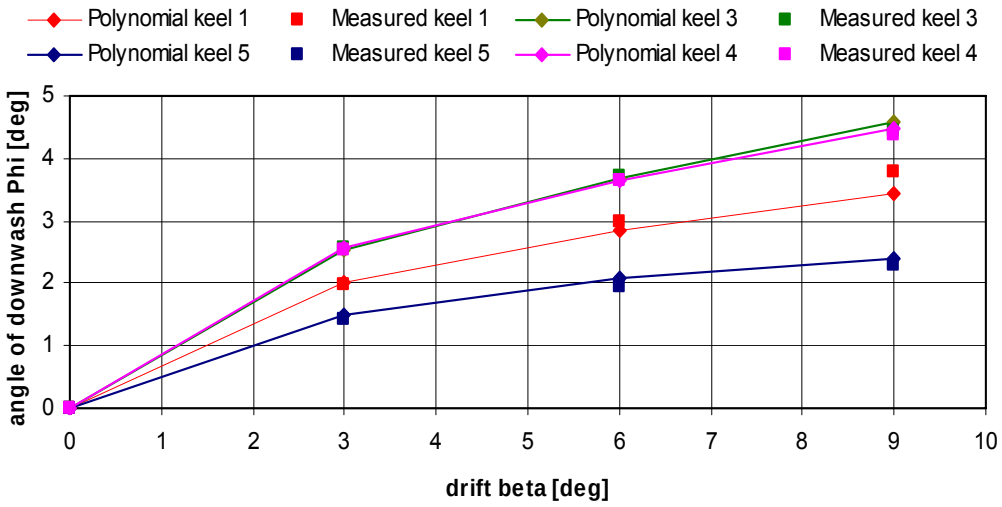

Figure 15: Downwash angle measured and approximated at heeling angle φ = 0°

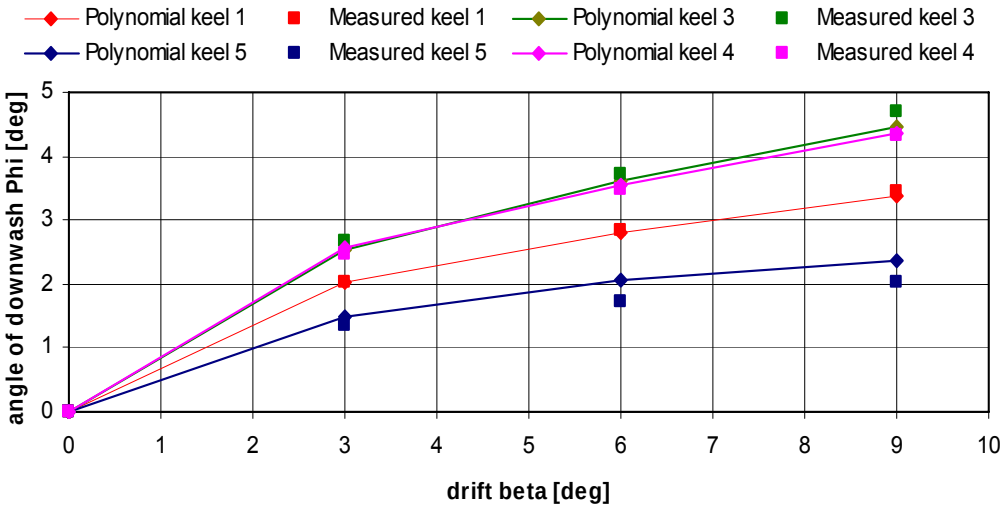

Figure 16: Downwash angle measured and approximated at heeling angle φ = 15°

6 Side force production

The side force measurements carried out within the scope of the present study on a wide variety of keels made it possible to re-assess the polynomial expression formulated with the DSYHS results on the side force production of a sailing yacht upright. The polynomial for the heeled side force is still under scrutiny because the heeling angles used in the DSYHS and the earlier DSKS tests were different. It was known from comparison with measured data that this expression lacked sufficient accuracy for keels with high aspect ratios.
This formulation is also of importance for the assessment of the yaw balance. For the yaw balance the distribution of the side force over the keel and rudder is determined using a procedure as described in Ref [1] making use of both the polynomial expression for the side force as of the EKM. In the maneuvering model of a sailing yacht (as presented by Keuning, Vermeulen and De Ridder, Ref [2]) use is also being made of this polynomial expression. So improvement on any flaws in this expression would mean a significant benefit in many applications.

The previous expression was derived for the side force production for the hull, keel and rudder together and based on the results of the DSYHS and the Delft Systematic Keel Series (DSKS). But the results within the DSKS were only used as available at that time. This implies that no really high aspect ratio results were present in the data base used for the regression. The formulation was presented in various publications about the Delft Systematic Yacht Hull Series (DSYHS), by amongst others by Gerritsma, Keuning and Onnink in 1993, Ref [10] and by Keuning and Sonnenberg in 1998, Ref [11].
Due to the fact that the polynomial expression is based on measurement data from mainly the standard keel used within the DSYHS and a limited number of different keels at that time available within the DSKS, the lower aspect ratio keels dominate the data base.
With the current set of measurement data on higher aspect ratio keels the data base is significantly extended and a new regression using the same polynomial expression for the side force production at zero heeling angle can be carried out now.
The original polynomial expression reads:

$$\frac{Fh \cdot \cos(\varphi)}{\beta \cdot \tfrac{1}{2} \cdot \rho V^2 S_c} = b_1 \cdot \frac{T^2}{S_c} + b_2 \cdot \left(\frac{T^2}{S_c}\right)^2 + b_3 \cdot \frac{T_c}{T} + b_4 \cdot \frac{T_c}{T} \cdot \frac{T^2}{S_c}$$

In which:
Fh = Side force [N]
φ = Heel [rad]
β = Leeway [rad]
T = Total draft [m]
S_c = Wetted surface canoe body [m^2]
T_c = Draft canoe body [m]

The coefficients for this polynomial have now been recalculated based on original DSYHS measurements augmented with the results of the extended DSKS obtained from the present measurements. The new coefficients for the polynomial for side force production at zero heeling angle are presented in Table 2:

φ	0 °
b_1	3.213
b_2	-3.462
b_3	0.438
b_4	-2.790

Table 2: New coefficients for the side force polynomial

In figure 17 and figure 18 a comparison of the polynomial using both the old and the new coefficients versus the measured values for keel 1 and 5 are presented.

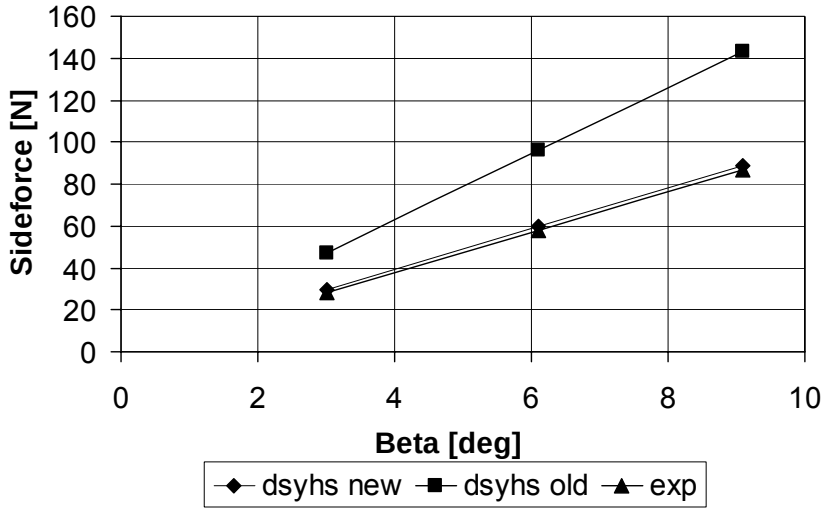

Figure 17: Comparison of old and new polynomial versus experiments for keel 1

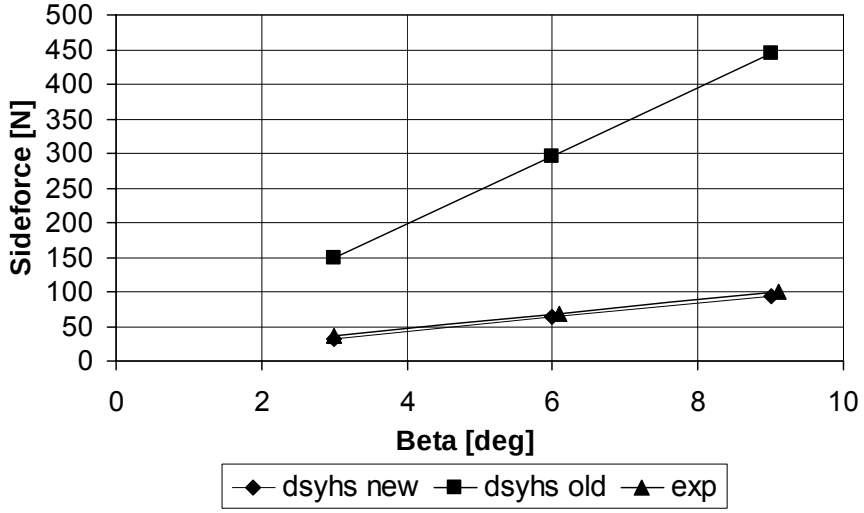

Figure 18: Comparison of old and new polynomial versus experiments for keel 5

7 Conclusions

Based on the results of the present study the following conclusions may be drawn:

- The aspect ratio of the keel has a significant influence on the downwash angle as experienced by the rudder.
- The downwash angle on the rudder does not increase linearly with the loading (C_L) on the keel but it depends also on the leeway angle. This is probably due to the change in the keel-rudder positioning with respect to each other with increasing leeway.
- A better formulation than the one presented by Hoerner for the downwash angle behind a keel with variable aspect ratio and leeway angle has been found which takes these effects into account. This should make the assessment of the yaw balance more reliable.
- On a straight course and without leeway the resistance of the rudder is influenced by the wake of the keel and the wave forming around the stern of the ship.
- At present in the DSYHS results the change in the rudder resistance between the upright condition with no leeway and the heeled and yawed condition is assessed as “induced resistance” although from this study that is not entirely correct.
- New regression through an extended data base yields a better fit of the polynomial expression for the side force production of a sailing yacht in the upright condition with the measured data for high aspect ratio keels. This is of importance when dealing with the yaw balance of a sailing yacht.

Recommendations:

- Similar tests as described in the present report should be carried out with low aspect ratio keels and should include variable keel-rudder separation.
- The tests should be repeated with more heeling angles to suit the DSKS data base.

References

[1]
Keuning, J.A. and Vermeulen, K.J.
The yaw balance of sailing yachts upright and heeled
Chesapeake Sailing Yacht Symposium, 2003

[2]
Keuning, J.A., Vermeulen, K.J. and de Ridder, E.J.
A generic mathematical model for the maneuvring and tacking of a sailing yacht.
Chesapeake Sailing Yacht Symposium, 2005

[3]
Gerritsma, J.
Course keeping qualities and motions in waves of a sailing yacht.
Technical Report, Delft University of Technology
May 1971

[4]
Nomoto, K. and Tatano, H.
Balance of helm of sailing yachts, a shiphydromechanics approach on the problem
HISWA 1979

[5]
Hoerner, S.F.
Fluid Dynamic Drag.
1965

[6]
Meulemans, R.W.M.
Benaderingsmethoden voor de hydrodynamische dwarskracht en geïnduceerde weerstand van een zeiljacht.
Delft University of Technology, Master's Thesis (in Dutch)
November 1998

[7]
Keuning, J.A. and Binkhorst, B.J.
Appendage resistance of a sailing yacht hull
Chesapeake Sailing Yacht Symposium, 1997

[8]
Whicker, L.F. and Fehlner, L.F.
Free-stream characteristics of a family of low-aspect ratio control surfaces.
Technical report 933
David Taylor Model Basin, 1958

[9]
Gerritsma, J., Keuning, J.A. and Onnink, R.
Sailing yacht performance in calm water and in waves
HISWA 1992

[10]
Keuning, J.A. and Sonnenberg, U.B.
Approximation of the hydrodynamic forces on a sailing yacht based on the Delft Systematic Yacht Hull Series.
HISWA 1998